FOOD EMULSIFIERS INCREASE TOXICITY OF FOOD CONTAMINANTS

WU MANHUI

PhD

The Hong Kong Polytechnic University

2023

The Hong Kong Polytechnic University

Department of Applied Biology and Chemical Technology

Food Emulsifiers increase toxicity of food contaminants

WU MANHUI

A thesis submitted in partial fulfilment of the requirements for
the degree of Doctor of Philosophy

May 2023

CERTIFICATE OF ORIGINALITY

I hereby declare that this thesis is my own work and that, to the best of my knowledge and belief, it reproduces no material previously published or written, nor material that has been accepted for the award of any other degree or diploma, except where due acknowledgement has been made in the text.

_____

(Signed)

WU ManHui

(Name of student)

ABSTRACT

Emulsifiers are used extensively in processed food to enhance product stability while emulsifiers mostly have low toxicity, recent studies have found that they could lead to alteration of gut microbiota community and subsequently gut inflammation. Such effects opened up further questions as to whether emulsifiers could lead to higher sensitivity of the individual due to higher chemical uptake and/or increased toxicity as a result of impaired gut lining integrity. Importantly, food emulsifiers are typically used in food products containing other food additives and contaminants. For example, food emulsifiers are used in baked products which also contain process contaminant acrylamide. We performed a local survey of over 100 baked products (e.g. bread, cookies, etc.) and all contains at least one food emulsifier. Therefore in this study we hypothesized that toxicity of two food contaminants of opposite spectrum of water solubility, namely acrylamide (**AA**) and benzo[a]pyrene (**BAP**), will be increased in the presence of two food emulsifiers of opposite spectrum of hydrophilic–lipophilic balance (HLB) values, namely polyoxyethylene sorbitan monooleate (Tween80; **TW**) and glycerol monostearate (**G**).

The hypothesis was first tested using three human cell lines (liver carcinoma cell line HepG2, small intestine epithelial cell HIEC-6, colorectal adenocarcinoma cell Caco-2), representing three organs of the GI tract. When AA or BAP was combined with low concentration of TW, toxicity significantly increased and decrease in cell viability compared to treatments without TW. When Tween80 was added, IC50 value of AA decreased by 56.1 % in HepG2, 20.4 % in HIEC-6 and 50 % in Caco-2 at 72h. Co-exposure of TW led to significant different expression of inflammation and redox related genes compared with AA or BAP alone. Investigating with Caco-2 cells, uptake of contaminants and cell membrane permeability were enhanced by TW. Tight junction proteins expressions of Caco-2 monolayer also be influenced by TW. There was no

significant effect caused by the addition of G. Our results suggested that TW have the ability to increase uptake and aggravate the inflammatory, oxidate stress and toxicity of AA and BAP.

Mixtures of emulsifiers (TW and G) and food contaminants (AA and BAP) were also tested using zebrafish via dietary exposure. In this whole animal model, both food emulsifiers increased the toxic effect of both food contaminants and significantly increased biomarkers expression related oxidative stress, inflammation, and cell death. Ingestion of AA and BAP contaminated diets with emulsifiers induced more severe damages to the liver and gut than the AA and BAP treatments alone, including fusion of villi, change in cell populations, inflammation and infiltration of immune cells, and foci of necrosis. Acute uptake of AA and BAP in liver and gut were also increased after emulsifiers addition.

To better understand the interaction of the mixtures to human, C57BL/6J mice were given AA and emulsifiers by oral gavage for 2 weeks. BAP was not carried out in this study due to the weaker effect of BAP. Similar to earlier chapters, AA combined with either emulsifier was found to have significantly higher expression pro-inflammatory cytokines and obesity biomarker of ileum than AA alone treatment. Moreover, the intestine barriers were more attenuated by AA in the presences of emulsifiers. Interestingly, AA and emulsifier mixture led to significant increase in mice weight but AA or either emulsifier alone had no significant effect on weight. Acute uptake experiment in SD rats showed that when co-exposed with TW or G, glycidamide, the primary metabolite of acrylamide, was significantly higher in the liver and gut. Transcriptome analysis of mice ileum carried out by RNAseq confirmed our findings by indicating lipid metabolic pathways, nervous system and immune pathways were more disrupted after addition of emulsifiers. The behavior test confirmed the higher

neurotoxicity. Microbiota community analyzed through 16s sequencing of mice fecal pellets also showed addition of emulsifiers aggravated microbiota dysbiosis by increasing abundance of harmful bacteria that are associated with inflammation and obesity and decreased in bacteria that are associated with weight-loss.

Effects of this mixture on human microbiota were investigated using *in vitro* fermentation and an *ex vivo* gastro-intestinal simulator SHIME for 1 day and 21 days respectively. 16S sequencing of microbial community data showed that emulsifiers aggravate effect of AA-induced gut dysbiosis which are associated with increased permeability, Crohn's disease, metabolic disorders and obesity. Results supported that effects observed in previous chapters have high potential to occur in humans.

Lastly, study was concluded by giving a general discussion of all results and their implications on human health. Limitations of this study and potential further research were also discussed.

In conclusion, exposure of emulsifiers and food contaminants caused leaky gut by disrupt gut barriers to increase absorption of food contaminants, followed by over-absorption of contaminants and their mixtures, contributing to activate inflammation, weigh gain and microbiota dysbiosis. The propose of subject is to draw the attention of risk assessors to make an adequate evaluation of emulsifiers and improve the toxicity assessment of mixtures of food contaminants and emulsifiers.

ACKNOWLEDGEMENTS

Throughout my four years as a PhD student, although Covid 19 held for over three years, I have been fortunate to receive a lot of assistance and support from many people. It is with gratitude and appreciation that I would first like to acknowledge my supervisor Dr. Kevin Wing-hin Kwok, for his continuous guidance and encouragement during study. I am deeply impressed by his patience and profession. He will be the role model in my future profession. The existence of this doctoral thesis will last longer than mine in this world. I am grateful to Dr. Kwok for teaching me how to write.

My appreciation also goes to Dr. Ka-Hing Wong and his staff Dr. Peter Luk, for shared the laboratory and their helpful guidance on my thesis project. I thank profusely to my seniors and lab mates: Dr. Hang-Kin Kong, Dr. Huan Zhang, Dr. Fan Xia, Kwong-Sen Wong, BaoShan Liao, Dr. Ka-Chai Siu, Ye Yang, Chong Li, Huan Li, Jonh Kwok, YingLun Wang, Dr. Samunel Gnanamuthu and Dr. ZhiWen Liu for their generous help. I also would like to thank my external and internal examiners for their valuable comments on my thesis.

I also thank all the technical support and comprehensive training from the technical support team in department of Applied Biology and Chemical Technology, and the staff in the University Research Facility in Life Sciences, Chemical and Environmental Analysis and Centralised Animal Facilities.

I am extremely thankful to my friends XiaoChun Su, Dr. WenXuan Yu, HeTing Hou, YinNan Lei, YePing Ma and Dr. WenQin Sun for their listening and support. XiaoChun and WenXuan gave me enormous help in animals studies and LCMS/MS analysis.

Finally, I owe a deep sense of gratitude to my family for their constant love, care, support and motivation.

May peace prevail on earth.

Table of Contents

Certification of orginality ii
Abstract iii
Acknowledgements vi
Table of Contents vii
List of Figures ix
List of Tables xiv
List of Abbreviations xvi

General introduction 1

1.1 Emulsifiers 2
1.2 Food contaminants 7
1.3 Association of food contaminants and emulsifiers 9
1.4 Research hypotheses 11
1.5 Research objectives 12
1.6 Thesis structure 12

Food emulsifiers increase toxicity of food contaminants *in vitro* 15

2.1 Introduction 15
2.2 Methodology 18
2.3 Results 26
2.4 Discussion 36

Food emulsifiers aggravates inflammation and oxidative stress induced by food contaminants in zebrafish 40

3.1 Introduction 40
3.2 Methodology 41
3.3 Results 45
3.4 Discussion 57

Dietary emulsifiers tween 80 and glycerol monostearate increased absorption of acrylamide and exacerbates inflammation, microbiota dysbiosis and metabolic symptom in mice 60

4.1 Introduction 60
4.2 Methodology 62
4.3 Results 71

4.4 Discussion 94

Effect of acrylamide and in combination with emulsifiers on human fecal microbiota 103

5.1 Introduction 103
5.2 Materials and methods 104
5.3 Results and discussion 110
5.4 Conclusion 138

General Discussion 139

6.1 Co-exposure with emulsifiers increased toxicity of process contaminants 139
6.2 Co-exposure with emulsifiers increased the uptake of food contaminants 139
6.3 Co-exposure with emulsifiers increased gut inflammation 140
6.4 Potential effects of emulsifier co-exposure on metabolism and obesity 141
6.5 Co-exposure with emulsifiers increased alteration of gut microbiome 142
6.6 Co-exposure with emulsifiers increased neurotoxicity 143
6.7 Limitations and recommendations for further research 144

Supplementary data 146
References 152

List of Figures

Chapter 1

Figure 1.1 Illustration of emulsifiers orientation in oil-in-water emulsion and water-in-oil emulsion.

Chapter 2

Figure 2.1 Cell viability after treating HepG2, HIEC6, Caco-2 cell lines with different dose of AA and TW (80 μM) or G (3.5 μM) for 48 h, 72 h.

Figure 2.2 Cell viability after treating HepG2, HIEC6, Caco-2 cell lines with different dose of BAP and TW (80 μM) or G (3.5 μM) for 48 h, 72 h.

Figure 2.3 Gene expression of HepG2, HIEC6 and Caco-2 exposed to AA alone or in combination with TW or G for 72 h.

Figure 2.4 Gene expression of HepG2, HIEC6 and Caco-2 exposed to BAP alone or in combination with TW or G for 72 h.

Figure 2.5 Cellular uptake of AA and BAP after co-treated with TW or G in HepG2, HIEC6 and Caco-2 cell lines for 2 h.

Figure 2.6 Effects of emulsifiers on cell membrane permeability of HepG2, HIEC6, and Caco-2 in 2 h.

Figure 2.7 Rate of increase of intracellular Calcein AM fluorescence intensity and representative images in HepG2, HIEC6 and Caco-2 cells exposed to food emulsifiers.

Figure 2.8 Relative gene expression of ZO-1, claudin-1 and occluding in differentiated Caco-2 cells exposed to TW or G for 2 h.

Chapter 3

Figure 3.1 Gene expression in the liver and gut of adult zebrafish after 7 days emulsifiers, AA and the co-exposure of emulsifiers and AA treatment.

Figure 3.2 Gene expression in the liver and gut of adult zebrafish after 7 days emulsifiers, BAP and the co-exposure of emulsifiers and BAP treatment.

Figure 3.3 Activities of SOD and ROS level in the liver and gut of adult zebrafish after 7 days emulsifiers, AA and the co-exposure of emulsifiers and AA treatment.

Figure 3.4 Activities of SOD and ROS level in the liver and gut of adult zebrafish after 7 days emulsifiers, BAP and the co-exposure of emulsifiers and BAP treatment.

Figure 3.5 Photomicrographs H&E-stained paraffin sections showing liver pathology in adult zebrafish after exposure to different fish feeds.

Figure 3.6 Photomicrographs H&E-stained paraffin sections showing gut pathology in adult zebrafish after exposure to different fish feeds.

Figure 3.7 Quantification of the goblet cell number.

Figure 3.8 Accumulation of AA in livers and guts of zebrafish after 2 h or 7 days exposure.

Figure 3.9 Accumulation of BAP in livers and guts of zebrafish after 2 h or 7 days exposure.

Chapter 4

Figure 4.1 Experimental treatments and design.

Figure 4.2 Concentration of AA and its metabolite glycidamide after a single dose of gavage of AA (24 mg/kg) with or without emulsifiers in plasma and liver respectively.

Figure 4.3 Expression of genes related to inflammation and gut barrier integrity in mice ileum after exposure to AA, AA_{TW} and AA_{G}.

Figure 4.4 Expression of phospho-p38 and phospho-ERK.

Figure 4.5 Plasma MCP-1 and Fabp2 levels in mice after 14 days oral administration of emulsifiers, AA, AA_{TW} and AA_{G}.

Figure 4.6 Representative images of mice liver after 14 days oral administration of emulsifiers, AA, AA_{TW} and AA_{G}.

Figure 4.7 Representative images of mice ileum after 14 days oral administration of emulsifiers, AA, AA_{TW} and AA_{G}.

Figure 4.8 FITC-dextran concentration of serum in the mice after 3 h and 14 days oral administration of emulsifiers.

Figure 4.9 Identification of the differentially expressed genes (DEGs).

Figure 4.10 Biological processes of GO Ontology.

Figure 4.11 KEGG pathway enrichment analysis of DEGs between Control and AA in ileum.

Figure 4.12 KEGG pathway enrichment analysis of DEGs between AA and AA_{TW} in ileum.

Figure 4.13 KEGG pathway enrichment analysis of DEGs between AA and AA_{G} in ileum.

Figure 4.14 Comparison of α-diversity analysis of intestinal microbiota.

Figure 4.15 Gut microbiota communities of various treatments at phylum level.

Figure 4.16 Gut microbiota communities of various treatments at family level.

Figure 4.17 Cumulative change in percentage body weight over experimental period and net change; liver/body weight ratio and colon weight/length ratio.

Figure 4.18 Fine motor coordination comparison between mice of different treatments as indicated by measurements of time to fall on rotor rod and landing hindlimb foot spread.

Chapter 5

Figure 5.1 SHIME design.

Figure 5.2 Minimum inhibitory concentration after AA and emulsifiers co-exposure treatments.

Figure 5.3 Changes of concentrations of acetic acid, propionic acid, N-butyric acid and total SCFAs during 24 h fermentation of fecal samples with different treatments.

Figure 5.4 Comparison of fecal microbiota after 24 hours emulsifiers alone, 25 mM AA alone and co-exposure of emulsifiers and 25 mM AA.

Figure 5.5 Taxonomic distribution of fecal microflora at phylum, family, and genus level in 25 mM AA alone or in combination with TW, low G or High G treatment.

Figure 5.6 Comparison of relative abundance of *Firmicutes*, *Lachnospiraceae*, *Ruminococcaceae*, *Gemmiger*, *Blautia* and *Collinsella* in 25 mM AA alone or in combination with TW, low G or High G.

Figure 5.7 Comparison of fecal microbiota after 24 hours emulsifiers alone, 200 mM AA alone and co-exposure of emulsifiers and 200 mM AA.

Figure 5.8 Taxonomic distribution of fecal microflora at phylum, family, and genus level in 200 mM AA alone or in combination with TW, low G or High G treatment.

Figure 5.9 Comparison of relative abundance of *Firmicutes*, *Lachnospiraceae*, *Ruminococcaceae*, *Gemmiger*, *Blautia* and *Collinsella* in 200 mM AA alone or in combination with TW, low G or High G.

Figure 5.10 Short chain fatty acid levels during and after treatment in PC and DC chambers from AA, TW, AA_{TW} treatment in terms of total SCFA, acetic acid, propionic acid, butyric acid and valeric acid.

Figure 5.11 Boxplots of total observed species, Chao index and Shannon diversity index in PC on day 3, day 7 and day 21.

Figure 5.12 Boxplots of total observed species, Chao index and Shannon diversity index in DC on day 3, day 7 and day 21.

Figure 5.13 Comparison of fecal microbiota after 3 days AA alone, TW alone and co-exposure of AA and TW in PC and DC chambers.

Figure 5.14 Comparison of fecal microbiota after 7 days AA alone, TW alone and co-exposure of AA and TW in PC and DC chambers.

Figure 5.15 Comparison of fecal microbiota after 21 days AA alone, TW alone and co-exposure of AA and TW in PC and DC chambers.

Figure 5.16 Relative abundance of selected phyla on day 3, day 7 and day 21 of exposure in PC and DC chambers.

Figure 5.17 Relative abundance of selected genera on day 3, day 7 and day 21 of exposure in PC and DC chambers.

Supplemental data

Figure S 1 Effects of TW on cell viability.

Figure S 2 Effects of G on cell viability.

Figure S 3 Photomicrographs H&E-stained paraffin sections showing liver and gut pathology in adult zebrafish after exposure to DMSO fish feeds.

Figure S 4 Minimum inhibitory concentration after 24 hours emulsifiers treatment.

List of Tables

Chapter 1

Table 1.1 Examples of food products and emulsifiers.

Table 1.2 Different phase mixtures in food products.

Table 1.3 Examples of food product contain process contaminants.

Table 1.4 Examples of food product contain process contaminants and emulsifiers.

Chapter 2

Table 2.1 List of primer sequences used for qPCR.

Table 2.2 IC 10 values of AA alone and combined with emulsifiers.

Table 2.3 IC 10 values of BAP alone and combined with emulsifiers.

Chapter 3

Table 3.1 List of primer sequences used for qPCR.

Chapter 4

Table 4.1 List of primer sequences used for q-PCR.

Table 4.2 The top three molecular networks based on differentially expressed genes (DEGs) between Control and AA, AA and AA_{TW}, and AA and AA_{G}.

Chapter 5

Table 5.1 List of primer sequences used for q-PCR.

Supplemental data

Table S 1 Classification of top 30 KEGG-enriched pathways between Control and AA in ileum.

Table S 2 Classification of top 30 KEGG-enriched pathways between AA and AA_{TW} in ileum.

Table S 3 Classification of top 30 KEGG-enriched pathways between AA and AA_{G} in ileum.

List of Abbreviations

3-MCPDE	3-monochloropropane-1,2-diol
4-MEI	4-methylimidazole
5-HT	Serotonin
AA	Acrylamide
ACN	Acetonitrile
AhR	Aryl hydrocarbon receptor
ALP	Alkaline phosphatase
ANOVA	Analysis of variance
APCI	Atmospheric pressure chemical ionization
ARNT	Aryl hydrocarbon receptor nuclear translocator
ATF3	Activating transcription factor 3
BAP	Benzo[a]pyrene
BCA	Bicinchoninic Acid
BCA	Bicinchoninic acid assay
CLDN1	Claudin-1
CMC	Carboxy methyl cellulose
CNS	Central nervous system
CYP1A1	Cytochrome P450 Family 1 Subfamily A Member 1

CYP2E1	Cytochrome P450 Family 2 Subfamily E Member 1
DC	Distal colon
DCF-DA	2,7-diacetyl dichlorofluorescein diacetate
DCs	Dendritic cells
DEGs	Differentially expressed genes
ENS	Enteric nervous system
ERK	Extracellular signal-regulated kinase.
F/B	*Firmicutes* to *Bacteroidetes*
FABP2	Fatty acid-binding protein 2
FXR	Farnesoid X receptor
G	Glycerol monostearate
GA	Glycidamide
HDL	High-density lipoprotein
HLB value	Hydrophilic to lipophilic balance
HPLC	High performance liquid chromatography
IBD	Inflammatory bowel disease
IL-1β	Interleukin 1 beta
IL-8	Interleukin 8
iNOS	Inducible nitric oxide synthase

IPA	Ingenuity Pathway Analysis
KEGG	Kyoto Encyclopedia of Genes and Genomes
MCP-1	Monocyte chemoattractant protein
MIC	Minimum inhibitory concentration
MPEs	A phthalate mixture
MS-222	Tricaine methanesulfonate
O/W	Oil in water
OCLN	Occluding
OTU	Optical transform unit
p38	Mitogen-activated protein kinase (MAPK)
PAEs	Phthalic acid esters
PAHs	Polycyclic aromatic hydrocarbons
PC	Proximal colon
PCA	Principal component analysis
PPAR**γ**	Peroxisome proliferator-activated receptor gamma
RA	Retinoic acid
ROI	Regions of interest
ROS	Reactive Oxygen Species
SCFA	Short chain fatty acids

SD	Standard deviation
SHIME	Simulator of Human Intestinal Microbial Ecosystem
SOD	Superoxide Dismutase
TEER	Transepithelial electrical resistance
TLR	Toll-like receptors
Tnfα	Tumor necrosis factor alpha
TW	Tween80; ppolyoxyethylene sorbitan monooleate
VLDL	Very low density lipoprotein
W/O	Water in oil
ZO-1	Zonula occludens-1

CHAPTER 1

General introduction

Traditional toxicology focused on effects of single chemical (Kortenkamp et al., 2009). This is, however, never the case for chemical exposure. Exposure always encompass multiple exposure routes and complex chemical mixtures recognizing these lead to the development of the exposome concept (Vineis et al., 2020). Dietary exposure is one of the primary pathways of human chemical exposure (Domingo, 2012; Domingo and Nadal, 2015; World Health Organization, 2009). Food, in particular, are complex chemical mixture themselves. Of all chemicals present in food, most are beneficial, such as various macro and micronutrients, some are nutritively neutral such as food additives, but some are potentially harmful, such as food contaminants and natural toxins. Food additives are substances added to food to preserve flavor or enhance taste, appearance, or other sensory qualities and have important applications for processed food products (Branen et al., 2001). This is further complicated by large number of ways food could be prepared and processed, and certain preparation procedures can lead to formation of secondary process contaminants. Process contaminants refers to undesired chemical by-products that can be formed during food processing, especially under heating, drying, or fermenting foods (Bonwick and Birch, 2019).

There are currently more than 10,000 food additives approved by the US FDA for application in food (Neltner et al., 2011). Food additives are classified into five major categories based on their functions: 1) taste enhancers, 2) preservatives, 3) antioxidants, 4) stabilizers and emulsifiers, and 5) coloring (Rangan and Barceloux, 2009). Responsible use of food additives can help provide more nutritious and cheaper food to the general public (Branen et al., 2001). There has long been public concerns on safety of certain food additives, but many of such perceived risks had no scientific basis (Florença et al., 2021). However, there are also opposite scenarios where seemingly

harmless food additives were found to have potential adverse health effects. Emulsifiers were one of such. They were recently reported to be able induce intestinal and metabolic disorders indirectly through changing gut microbiome composition (Chassaing et al., 2017).

1.1 Emulsifiers

1.1.1 Types and applications of emulsifiers

Emulsifiers were widely utilized as food additives to enhance formation and stability of emulsions. Further advantages of emulsifiers include viscosity reduction, starch complexation, and crystallization suppression (Garti, 2002). Emulsifiers such as glycerol monostearate and polysorbates contribute in development of stable oil/water emulsions required for dressings, bread, desserts, and sauces, as well as in delay of fat bloom in chocolate and the retention of fat in ice creams (Partridge et al., 2019). Some examples of common processed foods products and emulsifiers applied are listed in Table 1.1 (European Commission, 2008; US Food Drug and Administration, 2013).

Table 1.1 Examples of food products and emulsifiers.

Food products	Emulsifiers
Bread	Sodium or calcium stearoly-2-lactylate (481, 482); Glycerol monostearate (471); Diacetyl tartaric acid esters (472e).
Margarine	Polyglycerol eaters and lactic acid esters (477); Lecithin (322); Glycerol monostearate (471); Citric acid eaters of mono and diglycerides (472c).
Chocolate	Sorbitan tristearate (492); Lecithin (322) or ammonium phosphatide (422).
Ice-cream/Sorbet/Frozen Yogurt	Lecithin (322); Glycerol monostearate (471); Polysorbates (432, 436); Polyoxyethylene sorbitan monooleate (433).
Processed Meat	Citric acid esters of mono and diglycerides (472c); Glycerol monostearate (471).

Emulsifiers operate through a lipophilic tail that is attracted to the oil phase, and a hydrophilic head group that prefers to be in the aqueous phase (Fig. 1.1). Lipophilic part of the emulsifiers often originates from hydrocarbon chains of fatty acids, and the hydrophilic moiety consists of polar functional groups such as hydroxyl, amino and carboxylic or phosphoric acids groups (Friberg et al., 2003). Respective types and sizes of hydrophilic heads and lipophilic tails determine the functional behavior of the emulsifiers. Emulsifiers are amphiphilic molecules which have two or more immiscible phases and an interface. Food emulsions encountered in food are gas-in-liquid, solid-in-oil, solid-, gas, or oil-in-water and so on (Table 1.2).

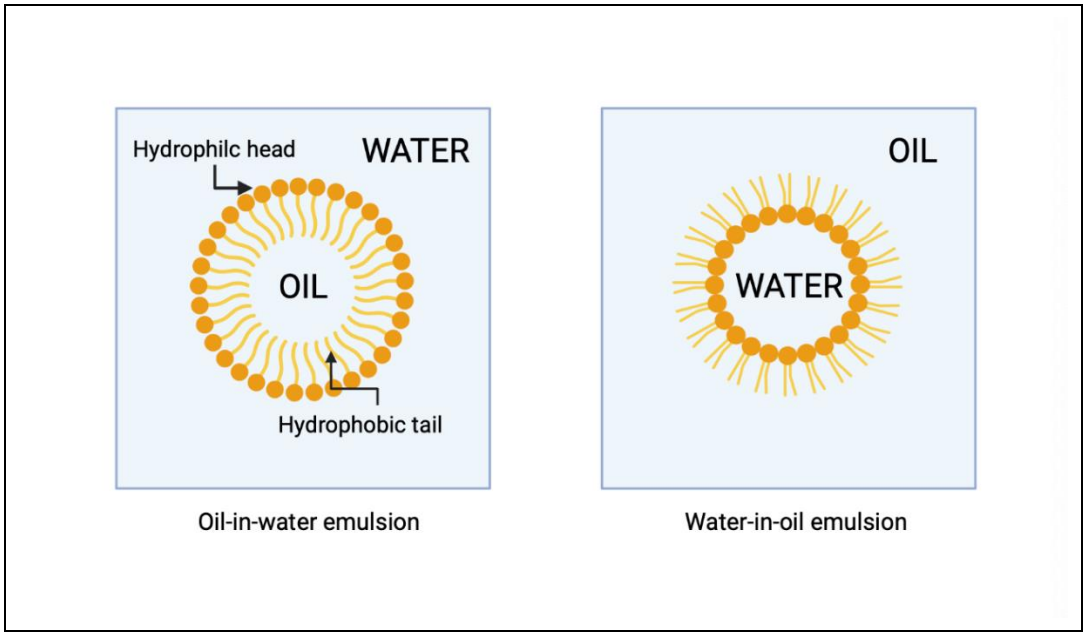

Figure 1.1 *Illustration of emulsifiers orientation in oil-in-water emulsion (left) and water-in-oil emulsion(right). Oil-in-water emulsion (left): amphiphilic emulsifier molecules spontaneously surround the oil droplets, directing their heads outwards into the continuous polar phase while their non-polar tails extend into the droplet. Water-in-oil emulsion(right): polar heads point toward the center of water droplets, while non-polar tails point to the oil phase.*

Table 1.2 Different phase mixtures in food products.

		Continuous phase		
	Phases	**Liquid**	**Gas**	**Solid**
Dispersed phase	**Liquid**	Emulsion E.g. Creamy dressing	Liquid aerosol E.g. Spray oil	Semi-solid emulsion E.g. Margarine
	Gas	Gas dispersion E.g. Carbonated beverage	N/A	Foam E.g. Whipped topping
	Solid	Dispersion E.g. Hot Chocolate	Solid aerosol E.g. Spray icings	Alloy/solid solution E.g. Chocolate

Food emulsifiers is often classified according to their hydrophilic to lipophilic balance (HLB value) which can be calculated by a formula based on chemical structure and molecular weight (Becher, 1965). The HLB value represent whether the hydrophilic or lipophilic moiety are dominant, where HLB values smaller than 10 are considered lipophilic and that larger than 10 are hydrophilic (Pomeranz, 2012). A low HLB value means that the emulsifier is good for preparing water in oil (W/O) emulsions and readily dissolve in oil. A high HLB emulsifier can easily dissolve in water and is useful for oil in water (O/W) emulsions (Hasenhuettl and Hartel, 2008).

Food emulsifiers can also be classified according to their polar functional groups as they have different mechanisms of action in forming emulsions. Emulsifiers are divided into four categories on the basis of their overall charges: nonionic (no formal charged), cationic (positively charged), anionic (negatively charged), or amphoteric (simultaneously positively and negatively charged) (Fitzgerald, 2015; Whitehurst, 2008). Common nonionic surfactants such as mono-/di-glycerides and distilled monoglycerides contained glycerol as the hydrophilic moiety and longer hydrocarbon chain of the fatty acid as the lipophilic moiety. For ionic emulsifiers, anionic emulsifiers are the prevailing type used in food application and they tend to be more hydrophilic due to its charged nature (Marhamati et al., 2021). For example, calcium or sodium

stearoyl-2-layctylate, and diacetyl tartaric acid esters of monoglycerides are anionic emulsifiers commonly used in bread (Kohajdová et al., 2009). Amphoteric food emulsifiers contain anionic and cationic groups can shift its function depending on the pH of the food product and are particularly useful in bread, frozen dessert and oil (Kohajdová et al., 2009). Lecithin, a by-product of fat is a good example of this category of emulsifier (Kohajdová et al., 2009; McClements and Gumus, 2016; Stampfli and Nersten, 1995).

1.1.2 Studies on indirect impact of emulsifiers

Most governments regulate food additives application and their maximum use concentrations. Food emulsifiers were generally regarded as harmless or of low direct toxicity. For example, emulsifier glycerol monostearate is classified as a safe additive (GRAS) by the FDA and the body intake is not regulated (US Food and Drug Administration, 2018). Emulsifier sucrose fatty acid esters is also qualify as 'general recognition' of safety by JECFA (Joint FAO/WHO Expert Committee on Food Additives, 1996).

Recent research on indirect effect of food emulsifiers revealed a different story. Emulsifiers were reported to disrupt gut barriers by increasing permeability (Lerner and Matthias, 2015). For example, polysorbate was reported to increase permeability of Caco-2 cell monolayers because of cell membrane solubilization (Dimitrijevic et al., 2000). Synthetic polyoxyethylene sorbitan monooleate, also known as Tween80 (TW), and lecithin were also shown to alter tight junction proteins expression and increased absorption of known allergens (Khuda et al., 2022). At just 0.2 % TW, monolayer integrity decreased by 20 % as determined by higher lucifer yellow influx and transport of allergens through monolayers were found to increase by 2-fold. Similar effects had been reported on bacteria translocation. Translocation of *E. coli* was increased by 0.1 % TW across M-cells and Caco2-cl 1 cells (Roberts et al., 2010). Another emulsifier

Polysorbate-60 was also shown to have similar effect on *E. coli* translocation but the effect was less pronounced (Roberts et al., 2010).

Emulsifiers exposure can lead to shift in microbiota composition and subsequently trigger inflammation. Studies on short-term effect of soy lecithin, TW, rhamnolipids, carboxymethylcellulose and sophorolipids on human microbiota showed that except for soy lecithin other emulsifiers decreased microbiota diversity (Miclotte et al., 2020). Emulsifiers rhamnolipids and sophorolipids exposure led to increase in *Fusobacterium* and pathogenic *Escherichia sp.* and *Shigella sp.* but decreased in *Bacteroidetes* (Miclotte et al., 2020). Exposure to an anionic dietary emulsifier sodium stearoyl lactylate was reported to increase the abundance of *Bacteroidaceae* and proinflammatory *Enterobacteriaceae* families, and levels of lipopolysaccharide and flagellin in fecal bacterial culture medium (Elmén et al., 2020).

Such changes in gut microbiota caused by emulsifiers were believed to be associated with Crohn's disease, metabolic disorders, obesity, and intestine barrier disruption (Viennois and Chassaing, 2018). Naimi *et al.* investigated analysis of 20 common dietary emulsifiers on human gut microbiota using *ex vivo* bioreactor and found 8 out of 20 emulsifiers have significant impact on microbiota community diversity but effect of each emulsifier was different (Naimi et al., 2021b). The authors also suggested that wide application of food emulsifiers maybe related increasing incidence of gut inflammation (e.g. colitis, irritation bowel syndrome), metabolic syndrome and possibly obesity. In mice, TW and carboxymethylcellulose (CMC) have been shown to cause changes in microbiota composition and low-grade inflammation and metabolic syndrome (Chassaing et al., 2015; Chassaing et al., 2017; Naimi et al., 2021a). Interestingly TW and CMC did not trigger inflammation in germ-free mice (Chassaing et al., 2017). However, after transfer of CMC- and TW-treated mice microbiota to germ-free mice, the germ-free mice developed low-grade inflammatory

and metabolic syndrome (Chassaing et al., 2017). These findings demonstrated the key roles of microbiota in gut inflammation induced by food emulsifiers.

1.2 Food contaminants

Food contaminants refers to chemical substances that do not naturally exist in food (Hussain, 2016). Contaminants have three pathways to enter food: firstly, food may take up contaminants from external environmental exposure during production. Secondly, food can be contaminated during transportation, processing, cleaning, packing and disinfecting. Thirdly, intrinsic substances in food may be transformed into harmful contaminants during thermal processing (Nerin et al., 2016). While food contaminants in the first two categories can be effectively controlled through better agricultural methods and processing technology, contaminants in the third category are difficult to control or eliminate in the food system (Nerin et al., 2016). Process contaminants are chemicals that form in food when they undergo chemical reactions during processing. Processing methods include heat treatment such as cooking, as well as baking, frying, grilling or barbecuing (Bonwick and Birch, 2019). It was estimated 80-90 % of food consumed by humans had underwent some form of thermal processing to ensure food safety and produce attractive flavor (Nerin et al., 2016). Examples of common process contaminants includes acrylamide (AA), 3-monochloropropane-1,2-diol (3-MCPDE), glycidyl esters, polycyclic aromatic hydrocarbons (PAHs), 4-methylimidazole (4-MEI), furans and ethyl carbamate (Bonwick and Birch, 2019; Folmer et al., 2018). Foods associated with these process contaminants are listed in Table 1.3.

Table 1.3 Examples of food product contain process contaminants.

Process contaminants	Food categories
AA	Baked/fried potato products, fine bakery products, bread, breakfast cereals, coffee, chocolate, baby biscuits and infant cereals, baby jar foods.
3-MCPDE	Soy sauce, oyster sauce, broths and soups, savoury snacks, gravy mix, stock cubes.
Glycidyl Esters	Vegetable fats and oils, margarines, infant formula and follow-on formula, medical foods intended for infants and young children, products containing refined vegetable oils.
PAHs	Oils and fats, cocoa beans and derived products, smoked/dried meat, fish and shellfish and derived products, dried herbs and spices, processed cereal-based foods and baby foods, infant formula and follow-on formula, food supplements.
4-MEI	Roasted coffee beans, roasted/grilled meats, caramel coloring used in foods.
Furan	Coffee, canned and jarred foods, baby food.
Ethyl carbamate	Spirits, wine and beer, fermented foods and beverages, soy sauce, yoghurt.

1.3 Association of food contaminants and emulsifiers

A survey on food additives was conducted on all available processed food products in supermarkets/grocery store and convenient stores in Hong Kong based on food ingredient labels (click to see survey results). Of 1380 types of locally available processed food, 524 products contained at least one emulsifier, including all baked products (98 out of 98), majority of noodles (66 out of 74), and dairy products (90 out of 173). Based on literature review on food products containing process contaminants, we found that they often co-exist with food emulsifiers in the same food item. Some common examples of pairing of food emulsifier and process contaminants are provided in Table 1.4.

This high degree of association led us to question if the presence of emulsifiers can increase chemical toxicity. Although limited, there were evidence that glycerol monostearate (G) increased the internal exposure concentration of phthalic acid esters (PAEs) in mice (Gao et al., 2016) and TW enhanced the absorption and bioavailability of mono-2-ethylhexyl phthalate in both rats and mice (Zhu et al., 2021). Previous studies have also found that emulsifiers could lead to alteration of gut microbiota community and subsequently gut inflammation. Such effects opened up further questions as to whether emulsifiers could lead to higher sensitivity of the individual due to higher chemical uptake and/or increased toxicity as a result of impaired gut lining integrity.

Table 1.4 Examples of food product contain process contaminants and emulsifiers.

Food categories	Process contaminants	HK local food products and their emulsifiers
Snacks - potato, cereal, flour or starch-based	AA	Lay's Swiss Cheese Flavored Potato Chips (471); Brilliant Indonesia Shrimp Chips (Cheese Flavour, 471); Orion Choco Boy (476).
Heat-treated processed comminuted (minced) meat, poultry, and game products	AA, PAHs, 4-MEI, Furan	Sealect Tuna in Tomato Sauce Dressing (Tuna with Baby Corn Peas and Onion in Tomato Sauce, 412); Ma Ling Pork Luncheon Meat (407, 451 (i)); Sky Dragon Chopped Pork and Ham (451 (i), 452 (i)).
Instant noodle	3-MCPDE, Glycidyl Esters	Nissin Cup Noddles Demae Iccho Sesame Oil Flavour Instant Noodle (471, 452, 412); Nissin Cup Noddles Thai Crab Curry Flavour Instant Noodle (471, 452, 412, 466); Nissin Cup Noodles Shrimp and Salt Flavour Instant Noodle (471, 452, 401, 466).
Bread and cake	AA, Glycidyl Esters	Orion Fish Shaped Cake (471, 473, 491, 492, 493, 494, 495, 410, 415); Garden Blueberry Cake (475, 471, 435); Yamazaki Raisin Finger Cake (472 b, 473, 477, 471).
Beverages	AA, PAHs, 4-MEI, Furan, Ethyl carbamate	Bundaberg Diet Ginger Beer (412); Nescafe Cold Brew Marble Latte (460, 466, 471, 452, 472 e, 407); UCC Blended Coffee (473, 475).

In this study we selected two nonionic emulsifiers: a high HLB value TW (HLB=15.4) and a low HLB value G (HLB=3-4) (Campbell et al., 2002; Kamel and Stauffer, 2013) to study the combined effect with process contaminants. TW is water-soluble and composed of polyoxyethylene group (hydrophilic) and oleic acid

(lipophilic) (Hasenhuettl and Hartel, 2008). G is a non-ionic oil-soluble surfactant. The mono glycerol constituted the hydrophilic part, and the lipophilic part formed from the hydrocarbon chain of the fatty acid radical. The US Food and Drug Administration (FDA) maximum use level of TW in selected foods is up to 1 % and the acceptable daily intake of TW is 25 mg/kg body weight (Chassaing et al., 2015). The emulsifiers G is classified as a safe additive (GRAS) by the US FDA and daily intake is not limited by regulation (US Food and Drug Administration, 2018). Suggested use level of G in food products ranged from 0.3 % to 3.5 %.

Two process contaminants that were likely co-occurring with food emulsifiers were selected for the study, namely water-soluble contaminant acrylamide (AA) and oil-soluble contaminants benzo[a]pyrene (BAP). AA is produced in food by Maillard reaction between amino acid asparagine and reducing carbohydrates (Halford and Curtis, 2019). Concentration of AA can be as high as 5849 µg/kg in biscuits, 7095 µg/kg in coffee, and up to 10722 µg/kg in potato crisps (Dunovská et al., 2004; European Food Safety Authority, 2012). BAP is one common member of the PAHs family which can be formed during incomplete combustion of carbon and are present on food processed by high temperature such as barbequing, roasting and drying. Concentration of BAP in food vary greatly. For example, concentration of Bap in meat products ranged from 0.03 to 100 µg/kg depending on the cooking method (World Health Organization, 2006).

1.4 Research hypotheses

I hypothesize the presence of food emulsifiers TW and G can increase toxicity of AA and BAP. Specifically, we hypothesize that 1) presence of food emulsifiers will increase absorption of AA and BAP; 2) food emulsifiers can interact with AA and BAP synergistically can lead to gut inflammation and redox damage; 3) food emulsifiers and AA can alter gut microbiota associated with gut inflammation.

1.5 Research objectives

Objective 1: To test whether uptake of acrylamide or benzo[a]pyrene would be altered by presence of low concentration of emulsifiers

Objective 2: To test whether toxicity related to oxidative stress and inflammation caused by acrylamide or benzo[a]pyrene would be altered by presence of low concentration of emulsifiers

Objective 3: To test how mechanism of toxicity of acrylamide would be changed in the presence of low concentrations of emulsifiers

Objective 4: To investigate the impact of acrylamide on gut microbiota would be altered by presence of low concentration of emulsifiers

1.6 Thesis structure

This thesis is divided into six chapters. The first chapter act as a general introduction to the study (**Chapter 1**), followed by four experimental chapters (i.e. **Chapters 2-5**), and a concluding general discussion (**Chapter 6**).

In **Chapter 2**, we have chosen three cell lines representing three different organs of the human GI tract as model: human liver carcinoma cell line HepG2, human fetal small intestine cryptlike HIEC-6 cells, and human colon enterocyte-like cell line Caco-2. Toxicity of selected food emulsifiers and food contaminants were tested individually and in combination. Cellular uptake, cell membrane permeability, inflammation and oxidative stress related biomarkers were studied in this chapter. Findings confirmed that food emulsifiers had very low toxicity on its own, but when in combination they decreased 72 h IC 50 values of AA 56.1 % in HepG2, 20.4 % in HIEC-6 and 50 % in Caco-2 respectively. Emulsifiers also changed expression of genes related to inflammation and oxidative stress caused by AA and BAP. They also increased cellular uptake of AA and BAP. These findings were consistent in all three cell lines, suggesting that this is a universal biological phenomenon and not unique to certain organ or cell type.

In **Chapter 3**, combined effects of emulsifiers and food contaminants were tested with zebrafish. Zebrafish is a widely accepted model in molecular biology and toxicology. Similar effects of emulsifiers were detected in zebrafish, increasing uptake and toxicity of AA and BAP. Effects including increased inflammation and oxidative damage. The increased toxicity was not only detectable in the gut but also found in the liver. Toxicity of AA was much more pronounced than BAP.

In **Chapter 4**, effect of the mixtures were investigated with C57BL/6 mice with additional objectives to understand how the mixture interact with the gut microbiota using 16S sequencing and subsequent toxicity using transcriptome analysis. Due to low toxicity of BAP found in chapter 2 and 3, experiment in this chapter only focused on AA. Results showed that AA in combination with emulsifiers, compared with AA alone, led to significantly increased AA metabolite glycidamide concentration, increased weight gain, decreased in motor coordination, increased expression of genes related to inflammation and obesity, decreased expression of genes related to tight junction protein, and increased kinase protein expression. Microbiota composition changed by AA in combination with emulsifiers was minor, with changes in minor phyla such as *Verrucomicrobiota* and *Proteobacteria*. Transcriptome analysis showed that molecular pathways related to inflammation and fatty acid synthesis were more perturbed in when AA is combined with emulsifier. Our results demonstrated that emulsifiers increased known toxicity of AA (e.g. neural toxicity) and created new toxicity (e.g. fatty acid synthesis and weight gain), and microbiota changes may be playing a minor role.

In **Chapter 5**, effect of the mixtures on human microbiota was explored. To test our hypothesis, a traditional *in vitro* fermentation batch for 1 day and an *ex vivo* gastro-intestinal simulator SHIME for 21 days was used. Due to limitation of time and space, only effects of TW and AA were studied in SHIME. Changes in microbiota caused by the combined treatment were significantly different from AA or TW alone. Short chain fatty acids production was increased in the combined treatment in 1day fermentation but there were no significant change in SHIME. Notably, *Escherichia* abundance were

increased by the combined treatment by 5-83 fold, suggesting that the combined treatment may lead to increased risk of gut inflammation.

Lastly, **Chapter 6** summarizes the findings from the previous chapters and discusses the synergistic toxic effect and mechanisms of emulsifiers and food contaminants. The limitations and future research plan of this study were also discussed.

CHAPTER 2

Food emulsifiers increase toxicity of food contaminants *in vitro*

2.1 Introduction

Food is a necessity of life. However, food is also a major exposure route to chemical contaminants (Nerin et al., 2016). Food contaminants refers to chemical substances that do not naturally exist in food. Contaminants have three pathways to enter food: firstly, food may take up contaminants from external environmental exposure during production. Secondly, food can be exposed to contaminants during transportation, processing, cleaning, and disinfecting. Thirdly, intrinsic substances in food may be transformed into harmful contaminants during thermal processing, such as polyaromatic hydrocarbons (PAHs) and acrylamide (AA) (Nerin et al., 2016). While food contaminants in the first two categories can be effectively controlled through better agricultural methods and processing technology, contaminants in the third category are difficult to control. It was estimated 80-90 % of food consumed by humans had underwent some form of thermal processing to ensure food safety and produce attractive flavor (Nerin et al., 2016). During cooking, chemical reactions between food components occur, such as degradation and oxidation of oil and Maillard reactions between amino acids and reducing sugars (Zhao et al., 2017). However, some food contaminants can also form during these processes. For example, AA is formed from the reaction between sugars and amino acids, particular asparagine. PAHs can be formed during incomplete combustion of carbon and are present on food processed by high temperature such as barbeque. New formed food contaminants were demonstrated to induce carcinogenesis and toxicity (Zhao et al., 2017).

Emulsifiers as food additives were used extensively in food industry. Emulsifiers are used in food to promote the formation and enhance the stability of emulsions to ensure the processed food under overall quality (Garti, 2002). In the intestine,

emulsifiers could decrease the hydrophobicity of phospholipid layer (primarily-phosphatidylcholine) and lead to easier penetration of water-soluble food contaminants through cell barrier (Qin et al., 2008). Emulsifiers have weak mucolytic activity and could break non-covalent bonds of mucus gel of the mucosal layer (Sood and Panchagnula, 2001). This enhances the permeability of the gut as well as harmful luminal components exposure (Lugea et al., 2000; Qin et al., 2008). Emulsifiers can also interact with similar amphipathic phospholipid bilayer of cell membranes and led to easier diffusion across cell membranes (Csáki, 2011). When emulsifiers are below critical micelle concentration, they can penetrate into the phospholipid bilayer of cell membrane and change lipids fluidity; when present above the critical micelle concentration, they further interact with phospholipid bilayer and form a mixed micelle and facilitating uptake (Ahyayauch et al., 2010; Xia and Onyuksel, 2000). Some transport proteins can be interfered with by emulsifiers and food contaminants. P-glycoprotein is the product of the MDR1 gene and well known for limiting permeability in drug absorption process (Ayrton and Morgan, 2001). It was found that P-glycoprotein as a transport protein can transport harmful substances from enterocytes into the intestinal lumen. Emulsifiers glycerol monostearate (Barta et al., 2008; Shah et al., 2006) and polyoxyethylene sorbitan monooleate (Cornaire et al., 2004; Zhang et al., 2003) have been shown to inhibit the P-glycoprotein activity, indirectly increasing uptake if substances in food, including contaminants.

Based on the above reasoning, although emulsifiers in food are present at low concentration and themselves are not likely to cause toxicity, they have potential to increase uptake and thus toxicity of food contaminants. In this study we select two nonionic emulsifiers: a high HLB value polyoxyethylene sorbitan monooleate (TW, HLB=15.4) and a low HLB value glycerol monostearate (G, HLB=3-4) to study the combined effect of food contaminant (Kamel and Stauffer, 2013). TW is water-soluble and composed of polyoxyethylene group (hydrophilic) and oleic acid (lipophilic) (Hasenhuettl and Hartel, 2008). G is a non-ionic oil-soluble surfactant. The mono

glycerol constituted the hydrophilic part, and the lipophilic part formed from the hydrocarbon chain of the fatty acid radical. The US Food and Drug Administration regulates food additives and regulates the amount that can be added to certain foods. The use level of TW has been approved in select foods up to 1 % and the acceptable daily intake of TW was 25 mg/kg body weight (Chassaing et al., 2015). The emulsifiers G is classified as a safe additive (GRAS) by the FDA and the body intake is not limited (US Food and Drug Administration, 2018). The suggested dosage of G ranged from 0.3 % to 3.5 % in a various food product.

In our daily diets, emulsifiers and food contaminants often co-exist in the same food item. For example, baked products such as bread and biscuits will simultaneously contain both emulsifiers and AA. Although low concentration of emulsifiers addition maybe not obvious increase the toxicity, it would more conform to the daily intake. Both toxicity and permeability enhancement rely on the frequency and duration of the exposure. The acute intestine damage induced by emulsifiers can be recovery after stopping the exposure in 1-2 h in healthy people (Touitou and Barry, 2006). The main problem is not the temporary enhanced intestinal permeability of the GI tract but the food they digested together every day. The harmful substances in intestinal lumen enter the mucosa and induce inflammation in a short time but frequently and exactly. The potential co-carcnogenic effect is not clear because the mixture toxcity study were not investigated. This led us to question if the present of emulsifiers can increase chemical toxicity.

In this chapter this hypothesis was tested with three human cell lines. In vitro toxicological models, carcinogenic cell cells are widely utilized as they can be maintained easily and stable during long-term passage (Trapecar and Cencic, 2012). Therefore human hepatoma cell line HepG2 and colon carcinoma cell line Caco-2 were used in this experiment. Besides, normal small intestinal epithelial cell line HIEC6 were also used in this experiment. The xenobiotic-metabolizing properties as well as most

cellular features of HepG2 and normal human hepatocytes are similar and it is widely used as a liver model for research of hepatocytes metabolism and toxicity of xenobiotics (Bouma et al., 1989; Mersch-Sundermann et al., 2004). The human colon enterocyte-like cell line Caco-2, a widely used model of intestinal cell maturation and functions, would develop in mature enterocytes which show brush-border membrane enzymes and morphological polarity 21 days post-confluent culture (Gauthier et al., 2001). The normal human fetal small intestine cryptlike HIEC-6 cells have been shown to express stable specific cytokeratins and intestinal cell markers during the passages (Perreault and Beaulieu, 1996).

2.2 Methodology

2.2.1 Cell culture and maintenance

The human hepatoma cell line HepG2, colon carcinoma cell line Caco-2 and small intestinal epithelial cell line HIEC6 were obtained from American Type Culture Collection (ATCC, USA). HepG2 cells were maintained in Dulbecco's modified Eagle's medium (Gibco) containing 10 % fetal bovine serum (Gibco). Caco-2 cells were maintained in EMEM (ATCC) with 20 % fetal bovine serum (Gibco). HIEC6 cells were maintained in Opti-MEM medium supplemented with 10 ng/ml recombinant epidermal growth factor, 20 mM HEPES, 10 mM glutamine (all obtained from Gibco) and 4 % fetal bovine serum.

All the cell culture mediums contained with 100 U/ml penicillin and 100 μg/ml streptomycin. Cell cultures were incubated at 37 °C in humidified air (95 % humidity) and CO_2 (5 %). Cell culture medium was changed every second or third day. Cells were passaged at when they reached approximately 80 % confluence. Experiments were conducted using cells of less than 10 passages.

2.2.2 Cell culture exposure

Based on preliminary toxicity tests of TW and G, concentrations below NOAEL of cell viability: TW 80 µM and G 3.5 µM, were chosen for subsequent co-exposure experiments (see supplementary data). Eight concentrations of AA (0.6-80 mM) and BAP (1-12 µM) were exposed individually or in combination with TW and G to the three cell lines for 72 h. Exposure conditions were identical to that described in section 2.2.1. Cell viability were determined at 48 h and 72 h of exposure by MTS assay.

Based on results of cell viability tests, low toxic concentrations of AA (0.6 mM and 1.2 mM) and BAP (1 µM and 2 µM) with and without the presence of TW or G were selected for study of gene expression for a number of genes of interest (Table 2.1) at 72 h using RT-qPCR. Cellular uptake of AA and BAP were measured at 2 h by HPLC-MS. Effects of emulsifiers on cell membrane permeability at 2 h as accessed by flow cytometry and confocal microscope. Effects of emulsifiers on tight junction proteins genes of Caco-2 monolayers at 2 h as determined by RT-qPCR.

2.2.3 Determination of cell viability

Cell viability was assessed by MTS assay (Promega, USA). MTS assay is a colorimetric method that uses a novel tetrazolium compound (3-(4,5-dimethylthiazol-2-yl)-5-(3-carboxymethox-pyphenyl)-2-(4-sulfophenyl)-2H-tetrazolium, inner salt; MTS) and an electron-coupling reagent, phenazine methosulfate (PMS). HepG2 (5,000/well), Caco-2 (8,000/well) and HIEC6 (8,000/well) were plated in a sterile flat bottom 96-well plate in a final volume of 100 µL complete culture medium and stabilized by incubation for 48 h and 72 h at 37 °C. After exposure, the cells were incubated with 20 µL MTS solution per well for 2 h at 37 °C. Absorbance of the mixture measured at 490 nm by a microplate reader. The blank only contained cell culture medium as a control. Results were expressed relative to the control group. Results were obtained by six replicate wells of each concentration and three experimental repeats.

2.2.4 Total RNA extraction and RT-qPCR

RNA was isolated from the cells using Trizol reagent (Takara, Japan) according to manufacturer's instructions. Extracted RNA was quantified using Nanodrop Lite Spectrophotometer (Thermo Fisher Scientific, US). Only RNA samples with 260/280 ratio between 1.9 and 2.1 and 260/230 ratio greater than 2.0 were used for RT-PCR analysis. For each RT-PCR reaction, 500 ng of RNA were added for the 10 µL transcription reaction by using Takara PrimeScript™ RT Master Mix (Takara, Japan) according to the manufacturer's instructions. PCR primers were adopted from published sequences or designed using RTprimerDB and described in Table 2.1. RT-PCR was performed on Applied Biosystems QuantStudio 7 Flex Real-Time PCR System using Power-up SYBR Green Master Mix (Applied Biosystems). Every reaction consisted of 0.5 µL of cDNA, 1 µL of forward and reverse primers, 5 µL Power-up SYBR Green Master Mix and 3.5 µL DNA template nuclear-free water. The PCR reaction was processed as a single cycle of UDG activation (50 °C, 2 min) and Dual-Lock DNA polymerase activation (95 °C, 2 min), and then amplification cycles (40 x) consist of denaturation (95 °C, 15 s) and annealing and elongation (60 °C, 1 min). A single cycle of melting process that consisted of an increase temperature from 65 °C to 95 °C for 10 min was performed at the end. A single peak in all melting curves verified the generation of a single amplicon for each primer pair. Results were normalized to GADPH expression. Gene expression was calculated using the $2^{-\Delta\Delta CT}$ method.

CYP2E1 is the primary enzyme for metabolizing AA into glycidamide (GA) (Settels et al., 2008), which could cause to inflammation and oxidative damage (Chen et al., 2018; Pan et al., 2018). This include promotion of inflammatory cytokines (e.g. IL-1β and IL-8) and generation of free radicals, activating protective enzymes such as superoxide dismutase (SOD). (Yousef and El-Demerdash, 2006). Besides, ATF3 was involved in the oxidative stress and inflammation in response to AA treatment (Kim et al., 2015). Therefore, we measured the level of the CYP2E1, IL-1β, IL-8, SOD, and

ATF3 after AA treatment. It has been shown that CYP1A1, which is regulated by aryl hydrocarbon receptor (AhR) and AhR nuclear translocator (ARNT), bio-transformed BAP into its metabolites, which then lead to oxidative stress and inflammation (Shi et al., 2021). Therefore BAP-induced inflammation (IL-1β, IL-8 and ATF3), oxidative stress (SOD) and metabolism (CYP1A1, AhR and ARNT) related genes were measured in this chapter. Real-time PCR was used to measure gene expression in the three cell lines after exposure 72 h.

Real-time PCR was used to assess the effects of the emulsifier on the tight junction proteins ZO-1 (TJP1), claudin-1 (CLDN1), and occludin (OCLN) after the emulsifier treated Caco-2 monolayer for 2 h (Ding et al., 2021).

Table 2.1 List of primer sequences used for qPCR.

Gene	Forward (5'-3')	Reverse (5'-3')	References
ATF3	GGAGTGCCTGCAGAAAGAGT	CCATTCTGAGCCCGGACAAT	(Edagawa et al., 2014)
IL-1β	TCCCCAGCCCTTTTGTTGA	TTAGAACCAAATGTGGCCGTG	(Liu et al., 2015)
IL-8	ACTGAGAGTGATTGAGAGTG GAC	AACCCTCTGCACCCAGTTTTC	(Fu et al., 2016)
SOD	ACAAAGATGGTGTGGCCGAT	TCTGGATCTTTAGAAACCGCG A	(Huang et al., 2021)
CYP2E1	GGGAAACAGGGCAATGAGAG	GGAAGGTGGGGTCGAAAGG	(Huang et al., 2018)
CYP1A1	CTATCTGGGCTGTGGGCAA	CTGGCTCAAGCACAACTTGG	(Ma et al., 2019)
AHR	ACATCACCTACGCCAGTCGC	TCTATGCCGCTTGGAAGGAT	(Pappas et al., 2018)
ARNT	CTGCCAACCCCGAAATGACAT	CGCCGCTTAATAGCCCTCTG	(Zhang et al., 2021)
TJP1	CAAGATAGTTTGGCAGCAAG AGATG	ATCAGGGACATTCAATAGCGT AGC	(Putt et al., 2017)
CLDN1	TGGTGGTTGGCATCCTCCTG	AATTCGTACCTGGCATTGACT GG	(Putt et al., 2017)
OCLN	CCAATGTCGAGGAGTGGG	CGCTGCTGTAACGAGGCT	(Putt et al., 2017)
GADPH	GCACCGTCAAGGCTGAGAAC	TGGTGAAGACGCCAGTGGA	(Li et al., 2016b)

2.2.5 Effect of emulsifiers on permeability of Caco-2 monolayer

Caco-2 cells were seeded on pore Polyester filters (24 mm diameter, 0.4 µM pore diameter Transwell, Corning Inc. Lowell, MA, USA) at a density of 4.5 x 10^4 cells/cm^2 in complete medium supplemented with 10 % fetal bovine serum in both apical and basal compartments. In the setup, 2 ml of the above cell solution was aliquoted into the apical chamber of the transwell insert and 3ml into the basal chamber. Cells were maintained in this setting for 21 days at 37 °C, 5 % CO_2 and 95 % humidity, with medium replaced in both chambers every two days for the first week and then everyday up to 21 days. Morphology of differentiated Caco-2 was verified at day 21 under light microscope to be tight and polarized enterocyte-like epithelial cell layers with brusher border and tight junction formation.

Alkaline phosphatase (ALP) activity in Caco-2 monolayer were performed to confirm differentiation (Li et al., 2015). ALP activity was determined spectrophotometrically using p-nitrophenyl-phosphate-disodium as substrate according to the manufacturer's protocol (Yeasan company, China). Cell monolayer integrity and permeability of the differentiated Caco-2 cell monolayer were examined by transepithelial electrical resistance (TEER) measurements with Ag–AgCl electrodes and voltmeter (Millicell ERS; Millipore Co., Bedford, MA) between the apical and basal compartment of the bicameral chamber, according to manufacturer's instructions. The final values are expressed as $\Omega \times cm^2$ based on the following equation: TEER = $(R-Rb)\times A$, where R is the resistance of filter insert with Caco-2 cells, Rb is the background resistance of the filter alone and A is the surface area. Transepithelial electrical resistance was higher than 600 Ωcm^2 in all our trials. Caco-2 monolayer were exposed to emulsifiers for 2 h and TEER were measured again. The monolayer were collected after exposure to measure gene expression of tight junction proteins.

2.2.6 Determination of cell membrane permeability

Effect of emulsifiers on cell membrane permeability of the three cell lines was investigated by determining the changes in fluorescence intensity of cells stained with propidium iodide (PI, BD Pharmingen) using a BD C6 Accuri Flowcytometry (BD Bioscience). PI is a nucleic acid dye can only pass dead cells or compromised membrane (Rosenberg et al., 2019). After 2 h exposure to emulsifiers, 1×10^6 cells were stained with 500 µl PI at room temperature and stored in the dark for 15min. Samples were then washed three times and fluorescence intensity were detected by flow cytometry in the orange range of the spectrum using a 562-588 band pass filter.

Cell membrane permeability rate of live cells were also measured by confocal microscope (Leica TCS SP8) using Calcein AM stain (Bischof et al., 1995). This stain would be metabolized by which enzyme in live cells and generate fluorescent Calcein molecules. Change in intensity of intracellular Calcein AM fluorescence in 18 min was recorded by the confocal instruments. Cell were excited at 494 nm and fluorescence collected at 517 nm. For each treatment, 10 individual cells images and the mean fluorescence of 2-3 regions of interest (ROI) of each cell were collected and calculated by ImageJ software.

2.2.7 Cellular uptake

For the three cell lines, 1×10^6 cells for cell line were incubated with the same treatments in section 2.2.2 on a shaker at 200 rpm and 37 °C in the dark for 2 h. After exposure cells were centrifuged down and put on ice for 5 min. Cells were then washed third times with ice-cold PBS, and centrifuged at 2,500 rpm, for 3 min. 100 µl MiliQ-H_2O and 100 µl methanol (for AA) or 100 µl acetonitrile (for BAP) was added to the cells. After three cycles of freezing and thawing, pooled mixtures were sonicated three times in an ice-cold bath for 3 min then centrifuged at 13,000 rpm for 10 min at 4 °C. Then supernatants were collected and AA/BAP concentrations were measured as outlined in sections 2.2.8 and 2.2.9.

2.2.8 Quantification of acrylamide

Supernatants collected in section 2.2.7 were filtered by 0.2 µm PTFE syringe filters. To measure acrylamide concentration, supernatant was injected into Agilent 6460 liquid chromatography electrospray ionization triple quadrupole mass spectrometer with an ACQUITY UPLC HSS T3 Column (1.8 µm, 2.1 x 100 mm, Waters Corporation, Milford, USA), and the flow rate was 0.2 mL/min. The mobile phase was composed of water (A) and methanol (B) both containing 0.1 % (v/v) formic acid. The injection volume was 2 µL. The linear elution gradient program was used as follows: 0-7 min, 97 % A; 7-9 min, 10 % A; and 9-12.5 min, 97 % A. AA was detected as a single peak with an m/z ratio of 72 ($[M+H]^+$) and compared with standard curve constructed using AA in the range of 5 ppb to 250 ppb (Sigma Aldrich Chemical Co, USA).

2.2.9 Quantification of benzo[a]pyrene

Supernatants were collected in the section 2.2.7 were filtered by 0.2 µm PTFE syringe filters. To measure BAP concentration, supernatant was injected into 6500 Qtrap liquid chromatography-tandem mass spectrometry system (AB Sciex, Concord, ON, Canada) equipped with an atmospheric pressure chemical ionization (APCI) source (AB Sciex, Concord, Ontario, Canada), with an Agilent SB–C18 column (2.1 mm × 100 m), and the flow rate was 0.5 mL/min. The mobile phase was solvents A (5 mM ammonium acetate in water containing 0.1 % (v/v) formic acid) and B (acetonitrile). Sample injection volume was 5 µL. Linear elution gradient program was used as follows: 0-3 min, 50 % B; 3-17 min, 99 % B; and 17-20 min, 50 % B. The ion transitions monitored were m/z 253 → 250 and 253 → 224. Sample concentration was estimated based on standard curve of BAP (Sigma Aldrich Chemical Co, USA) constructed in the range of 5 ppb to 250 ppb.

2.2.10 Statistical analyses

All results are expressed as mean ± standard deviation (SD). Analysis of variance (ANOVA) and Tukey's multiple-comparison test was used to evaluate statistical differences between biological endpoints of different treatments. All other analyses were performed using GraphPad Prism 8.0 (GraphPad Software, San Diego, CA).

2.3 Results

2.3.1 Co-treatment with TW and food contaminants reduced cell viability synergistically

The three cell lines were exposed to a range of AA with and without the presence of emulsifiers (Fig. 2.1). AA caused a dose-dependent decrease of viability in all cell lines and toxicity were similar at 48 h and 72 h (Fig. 2.1). HIEC6 and Caco-2 cell lines showed similar sensitivities to AA and HepG2 was slightly more resistant. This was more noticeable for HIEC6 and Caco-2 cell lines and a reduction of 20 % cell viability was observed with TW was added. Addition of G did not significantly change toxicity of AA. Smaller of IC 50 values was observed for AA + TW treatments while IC 50 of AA alone and AA+G treatments were similar. At 72 h, IC 50 values of AA+TW treatments were about half of that of AA for HepG2 and Caco-2 cells and 80 % for HIEC6 (Fig. 2.1).

This trend was more significant at low toxicity scenarios. IC 10 values confirmed this observation where those of AA+ TW were significantly smaller than that of AA alone (Table 2.2).

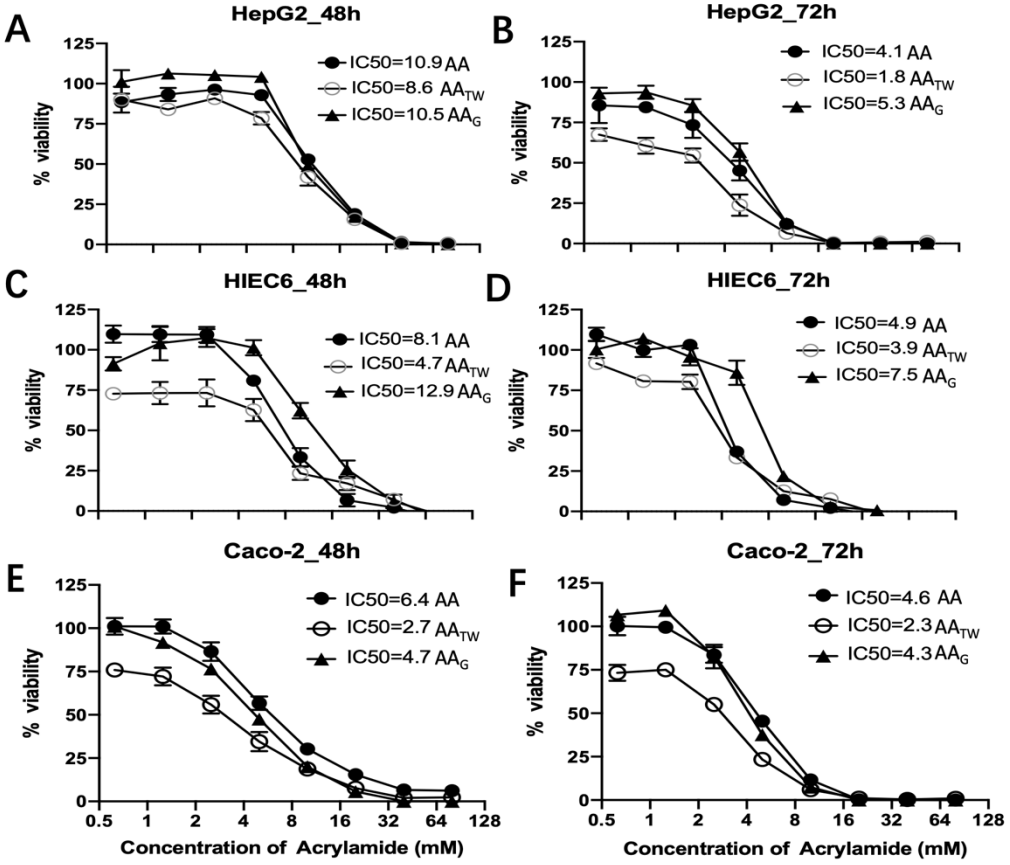

Figure 2.1 *Cell viability after treating HepG2 (A-B), HIEC6 (C-D), Caco-2 (E-F) cell lines with different dose of AA and TW (80 µM) or G (3.5 µM) for 48 h, 72 h was evaluated by MTS assay.*

Table 2.2 IC 10 values (mM) of AA alone and combined with emulsifiers. 95% CI of each IC 10 is presented in the bracket. **Bold** text indicates significant difference as indicated by non-overlapping 95 % CI.

Cell line	**Time**	**AA**		**AA$_{TW}$**		**AA$_G$**	
HepG2	48 h	4.8	(3.4-6.8)	2.8	(1.7-4.6)	5.8	(4.1-8.0)
	72 h	1.2	(0.7-1.9)	**0.3**	**ND**	2.3	(1.8-2.9)
HIEC6	48 h	4.2	(2.9-6.3)	**0.5**	**ND**	5.9	(4.1-8.7)
	72 h	4.3	(2.5-8.4)	**1.3**	**(0.8-2.1)**	4.5	(3.8-5.5)
Caco-2	48 h	1.8	(1.3-2.6)	**0.4**	**ND**	1.5	(1.3-1.7)
	72 h	2.1	(1.9-2.3)	**0.5**	**ND**	2.2	(1.6-2.9)

In general, BAP had little effect on cell viability (Fig. 2.2). For most treatments, more than 70 % of cells remained viable by the end of 72 h exposure, therefore IC 50 of BAP cannot be determined. Co-treatment with emulsifiers did not change cell viability of HepG2 (Figs. 2.2 A and B) cell lines. After 48 h incubation, presence of TW decreased viability of HIEC6 (Figs. 2.2 C and D). Similarly, TW could enhance cytotoxicity of BAP in Caco-2 cells at 48 h, but not at 72 h. G did not significantly alter the cytotoxicity of BAP in the three cell lines. Most of IC 10 of three cell lines also could not be determined due to the low toxicity (Table 2.3). Although some export IC 10 values are extrapolated beyond test concentration, the values for of BAP_{TW} is still lower than that of BAP and BAP_G.

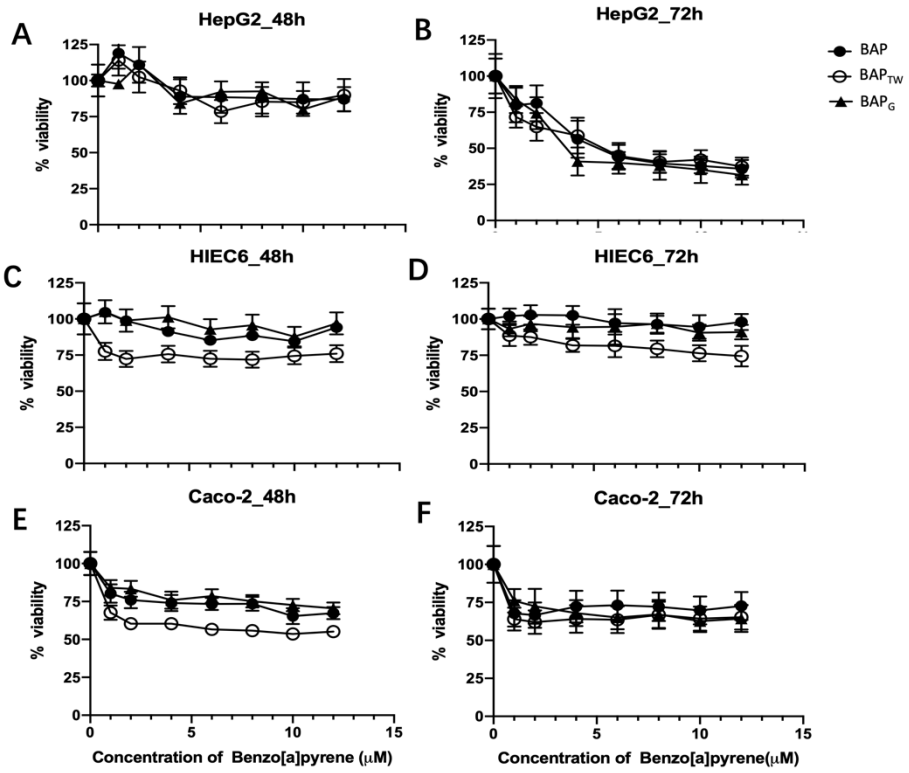

Figure 2.2 *Cell viability after treating HepG2 (A-B), HIEC6 (C-D), Caco-2 (E-F) cell lines with different dose of BAP and TW (80 µM) or G (3.5 µM) for 48 h, 72 h was evaluated by MTS assay.*

Table 2.3 IC 10 values (μM) of BAP alone and combined with emulsifiers. 95% CI of each IC 10 is presented in the bracket. **Bold** text indicates significant difference as indicated by non-overlapping 95 % CI.

Cell line	Time	BAP		BAP_{TW}		BAP_{G}	
HepG2	48 h	8.1	(1.6-ND)	6.6	ND	7.4	(1.3-ND)
	72 h	>12	ND	>12	ND	>12	ND
HIEC6	48 h	>12	ND	1	ND	14.8	ND
	72 h	>12	ND	>12	ND	>12	ND
Caco-2	48 h	>12	ND	1	ND	>12	ND
	72 h	>12	ND	>12	ND	>12	ND

2.3.2 Addition of TW alter gene expression caused by food contaminants

Exposure to low concentration emulsifiers lead to some changes in gene expression (Fig. 2.3). TW had stronger effect on gene expression compared to G. Expression of IL-1β, IL-8, SOD, ATF3 and CYP2E1 were significantly increased by TW. Gene expression pattern also changed when emulsifiers was added to AA exposure, and the changes appeared to be largely additive.

In HepG2, TW increased expressions of ATF3, IL-1β and CYP2E1 but decreased expression IL-8. When co-exposed to AA and TW, resultant gene expression was additive of that caused by the two compounds alone. TW alone had strong effect on HIEC6 cell line, affecting ATF3, IL-1β, IL-8 and SOD. Combined effect of TW and AA again was largely additive. For Caco-2 TW alone had strong effect on IL-1β expression. The combined effect of TW and AA was not largely additive such as IL-1β, CYP2E1 and SOD.

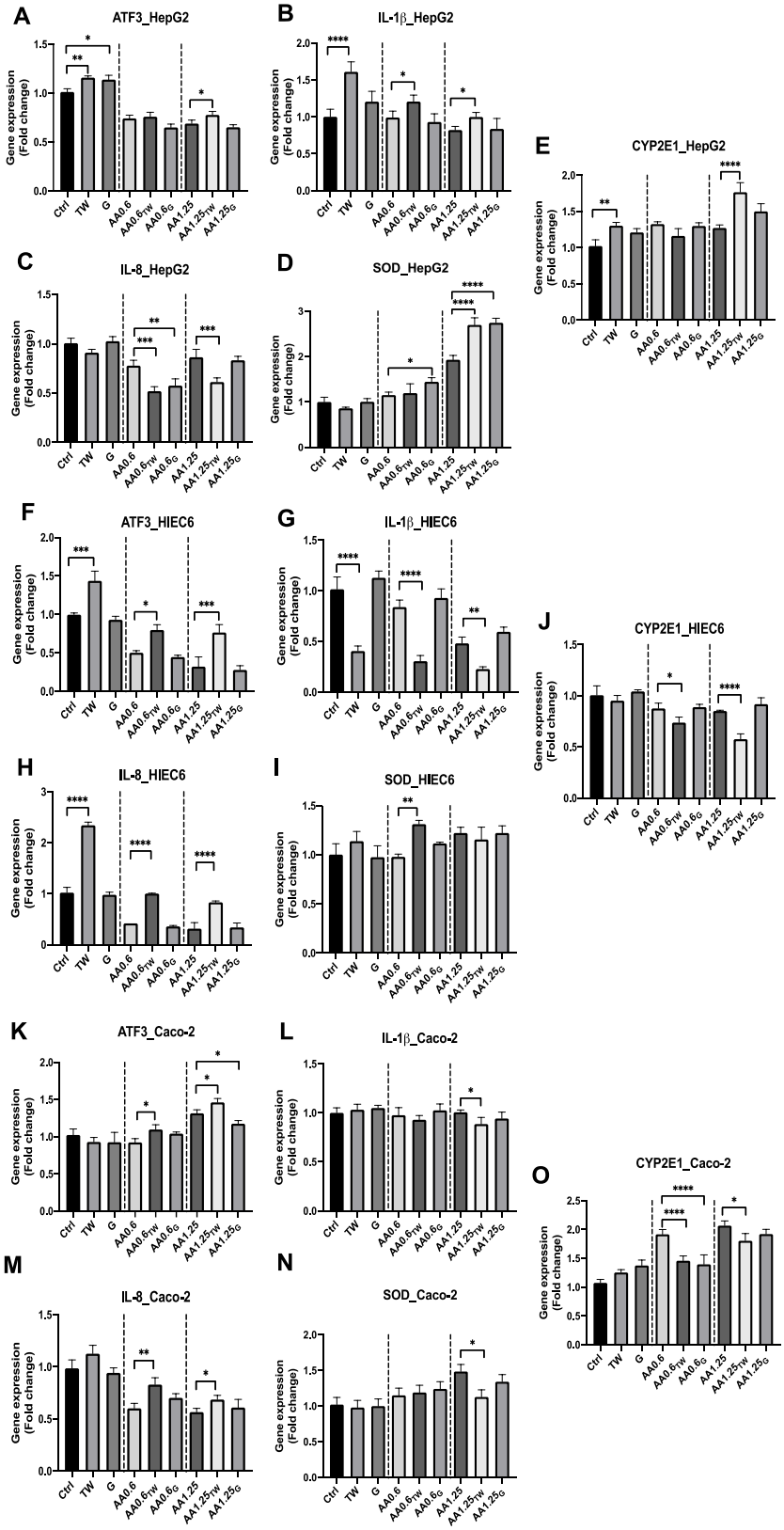

Figure 2.3 *Gene expression (-ΔΔCT) of HepG2 (A-E), HIEC6 (F-J) and Caco-2 (K-O) exposed to AA alone or in combination with TW or G for 72 h, asterisks indicate statistical significance between the treatment pair (n=3).*

Effect of BAP on gene expression was different from that of AA (Fig. 2.4). In HepG2 cell line, TW alone significantly up-regulated ATF3. When BAP was combined with TW, resulted in higher expression of ATF3, IL-1β, AhR, ARNT and CYP1A1 than BAP alone. When BAP was combined with G, IL-1β, SOD and CYP1A1 also changed their expression. For HIEC6, TW influenced the expression of ATF3, IL-1β, IL-8 and CYP1A1 while G alone had minor effect on gene expression. When TW was mixed with BAP, synergistic effect on ATF3, IL-8 and CYP1A1 expressions were observed. For Caco-2, emulsifiers caused significant up-regulation of SOD. When cells were exposed to BAP and TW, they changed ATF3, IL-1β, IL-8, SOD and CYP1A1 except for AhR and ARNT.

Increased up-regulation of CYP1A1 and AhR suggested TW increased toxicity of BAP in the three cell lines. BAP as dietary activators were described to activate the CYP1A1 and AhR activity which also impact the gut immunity (Rannug, 2020). On the basis of previous observations of gene expression, some inflammatory cytokines and SOD were triggered by BAP. After treatment with TW together altered expression more significantly.

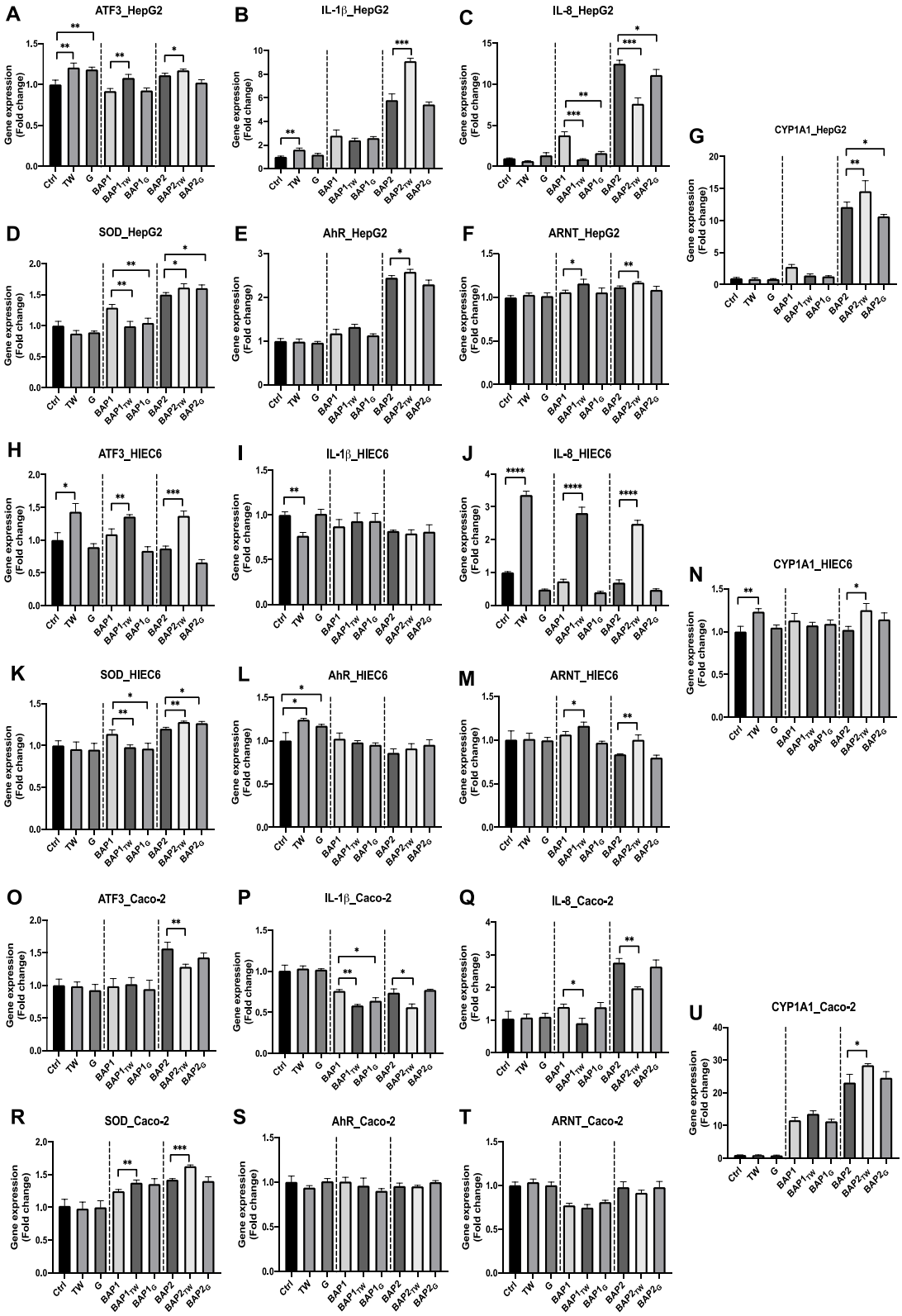

Figure 2.4 *Gene expression (-ΔΔCT) of HepG2 (A-G), HIEC6 (H-N) and Caco-2 (O-U) exposed to AA alone or in combination with TW or G for 72 h, asterisks indicate statistical significance between the treatment pair (n=3).*

2.3.3 TW can increase cellular uptake of acrylamide and benzo[a]pyrene

Effect of emulsifier on cellular uptake of AA was cell type and emulsifier dependent (Fig. 2.5). G had no effect on cellular uptake of AA in all cell types. Cellular uptake was increased for both concentrations in HepG2 by TW. In HIEC6 cell, TW significantly increased cellular uptake at 1.25 mM AA but not at 0.6 mM. TW increased AA uptake significantly only at 1.25 mM in Caco-2.

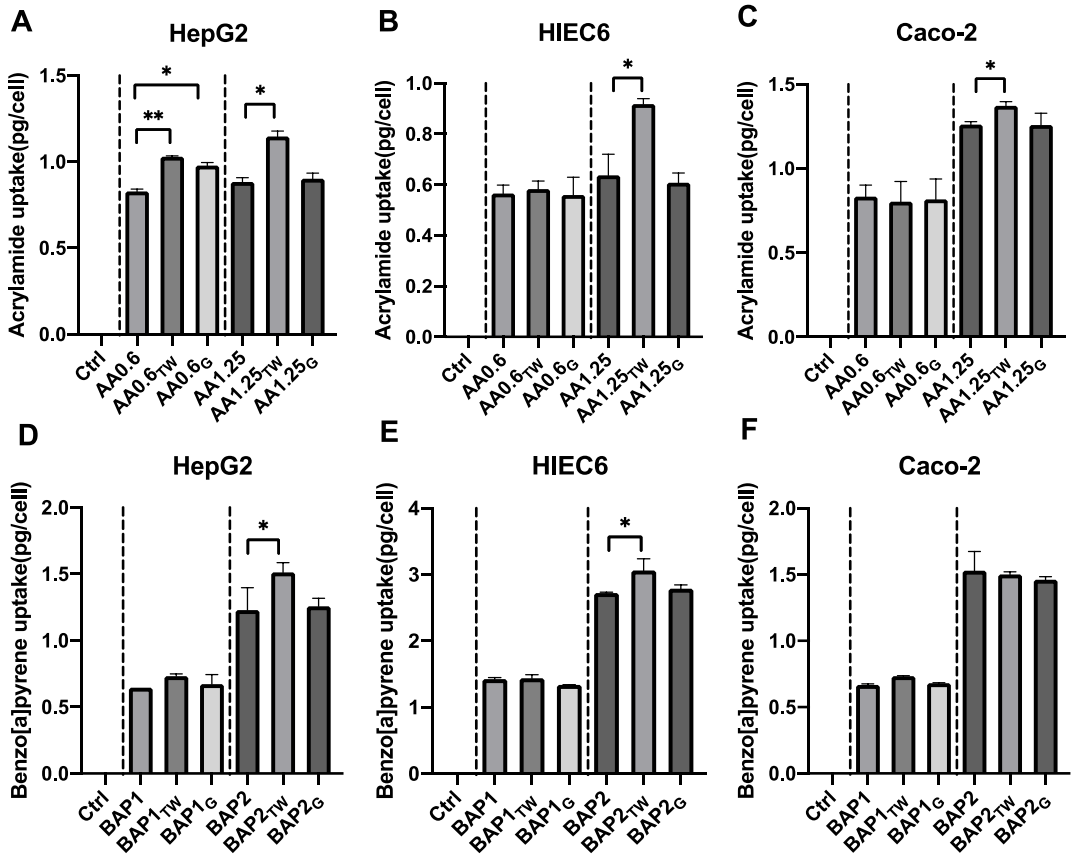

Figure 2.5 *Cellular uptake of AA and BAP after co-treated with TW or G in HepG2, HIEC6 and Caco-2 cell lines. Cells were treated with AA alone, BAP alone or in combination of either TW or G for 2 h at 37 °C. The concentration of AA and BAP in three cell lines were measured by HPLC-MS/MS.*

Similarly, G had no effect on the uptake of BAP. For TW, uptake was significantly increased at 2 μM for HepG2 and HIEC6 cells. For Caco-2, TW had no effect on uptake of BAP as shown in AA treatment group.

2.3.4 TW can increase cell membrane permeability

PI is a nucleic acid dye can only pass dead cells or compromised membrane (Rosenberg et al., 2019). G did not have any effect of PI influx (Fig. 2.6). However, after 2 h exposure to TW, PI influx increased significantly in HepG2 and HIEC6. Therefore, TW may change the membrane of HepG2 and HIEC6 acutely. Based on our previously cell viability results of Caco-2, Caco-2 was less sensitive to TW than the other 2 cell lines (Figs. S 1- S 2). Higher concentration or longer exposure may be required for TW to elicit significant effect on cell membrane permeability in Caco-2.

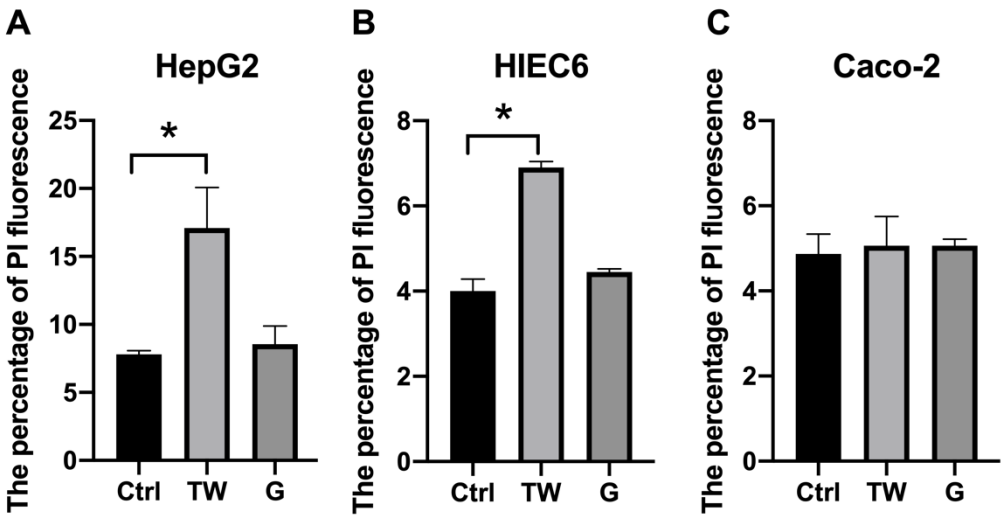

Figure 2.6 *Effects of emulsifiers on cell membrane permeability of (A) HepG2, (B) HIEC6, and (C) Caco-2 in 2 h as accessed by flow cytometry.*

The acetoxymethyl ester of nonfluorescent Calcein AM could permeate a phospholipid membrane by passive diffusion and would be hydrolyzed into fluorescent Calcein AM by intracellular esterases (Bischof et al., 1995). Fluorescence intensity of increased as a steeper slope when TW or G was added (Fig. 2.7). The slope of TW and G were much higher than control, which meant that emulsifiers accelerated the absorption of Calcein AM, particularly TW.

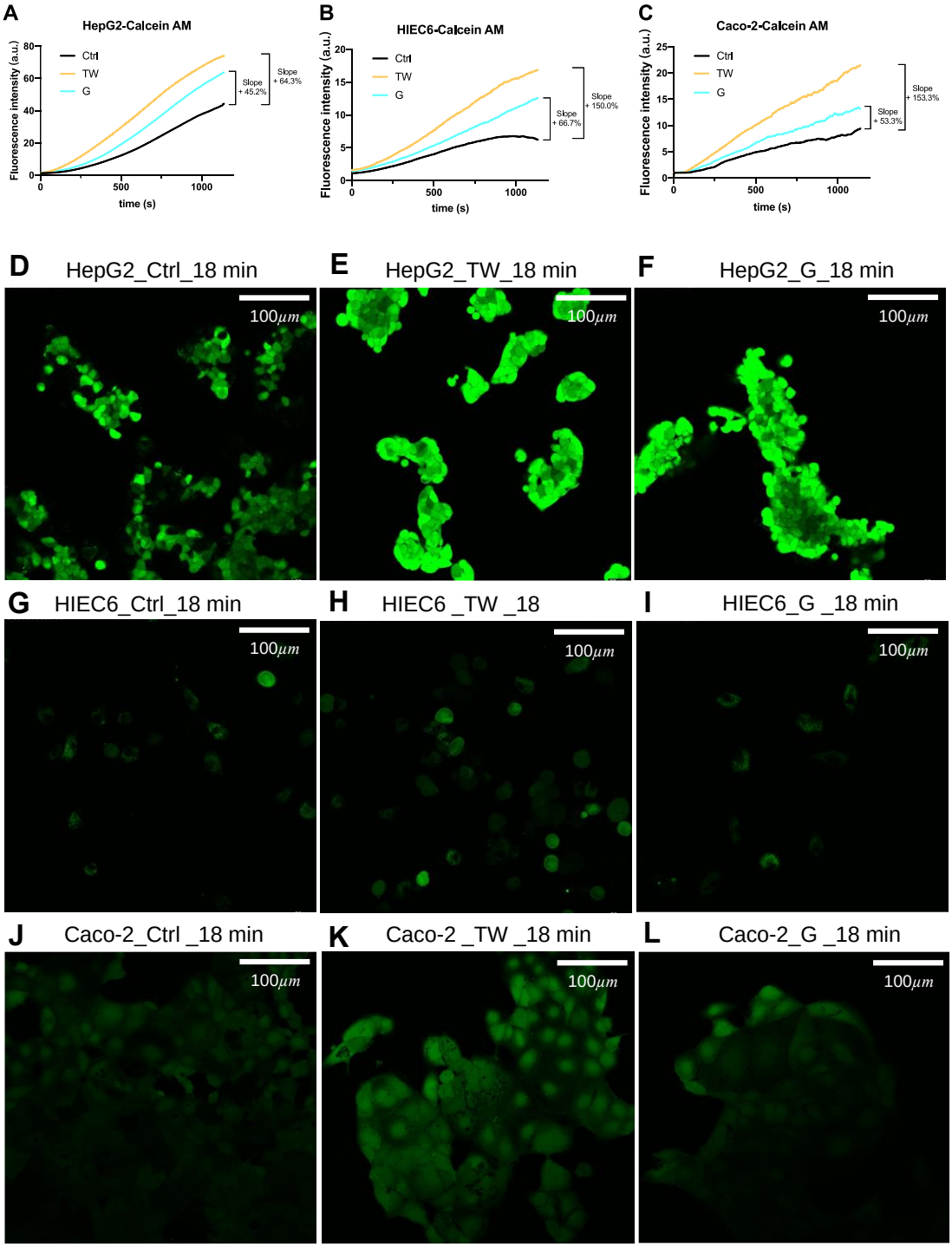

Figure 2.7 *Rate of increase of intracellular Calcein AM fluorescence intensity in (A) HepG2, (B) HIEC6 and (C) Caco-2 cells exposed to food emulsifiers. Representative images of (D-F) HepG2, (G-I) HIEC6, (J-L) Caco-2 cells after exposure to emulsifiers for 18 min. Scale bar is 100 μm.*

2.3.5 Emulsifiers can reduce gene expression of tight junction protein

Because TJP1, CLDN1 and OCLN play an importance role in regulating paracellular permeability, RT-qPCR was used to determine if emulsifiers affect the tight junction proteins gene expression.

After exposure to the emulsifiers for 2 h, expression of TJP1 and CLDN1 were significantly lower than the control, while OCLN was not affected. Both emulsifiers led to similar magnitude of down-regulation of TJP1 and CLDN1.

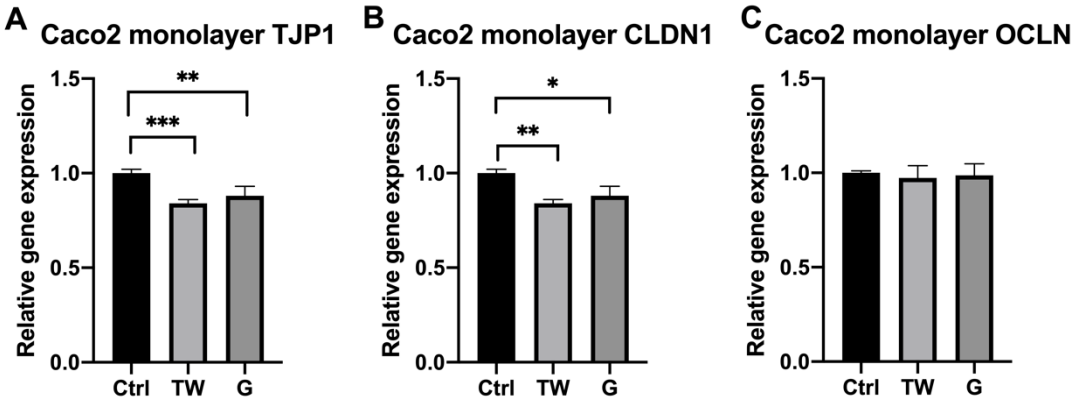

Figure 2.8 *Relative gene expression of A. ZO-1 (TJP1); B. claudin-1 (CLDN1) and C. occluding (OCLN) in differentiated Caco-2 cells exposed to TW or G for 2 h, asterisks indicate statistical significance between the treatment pair (n=3).*

2.4 Discussion

In this study, we found that TW could increase contaminants uptake and enhance inflammation and oxidate stress related gene expressions caused by AA and BAP. Combining emulsifiers with AA or BAP resulted in lower cell viability than just the contaminant alone, and the trend was more obvious for AA as BAP had little effect on cell viability.

Emulsifiers or surfactants have been used to increase drug and nutrients uptake (Hsu et al., 2019; Partridge et al., 2019) and with the same mechanisms they could increase contaminant uptake. We found that TW was able to increase uptake of AA in all three tested cell lines and BAP in two cell lines (Fig. 2.5). The intestinal mucosal epithelium barrier consisted of two barriers: transcellular and paracellular barriers (Turner, 2009). Transcellular barrier is mainly controlled by permeability across cell membrane while paracellular barrier is largely because of tight junction proteins between adjacent cells. TW could potentially impact both barriers adversely. Firstly, it increased cell membrane permeability as it significantly increased cellular uptake PI and Calcein AM by almost 2-folds (Figs. 2.6 and 2.7). Secondly, Caco-2 cells exhibited decreased genes expression of tight junction proteins CLDN1 and ZO-1 after TW exposure (Fig. 2.8). This is complementary to reports that TW exposure decreased CLDN1 and OCLN protein expression together with the modification of protein immunostaining after 24 h and 48 h (Zhu et al., 2021). Tight junction proteins redistribution from continuous to punctate or decrease in expression of tight junction proteins can result in intestinal barrier disruption (Farshori and Kachar, 1999; Putt et al., 2017). It was also reported that increased paracellular permeability is related to chronic intestinal inflammation even increase inflammatory response in rodent (Cani et al., 2009; Schepens et al., 2009), suggesting changes caused by emulsifiers may have more chronic implications.

Emulsifier TW did not only increase contaminant uptake, it also interacted synergistically to increase toxicity of AA and BAP. The IC 10 and IC 50 values of AA and BAP were decreased when TW was present (Tables 2.2 and 2.3). Studies combining emulsifiers and food contaminants are rare. A previous study has shown that treatment with TW (25 mg/kg/day) increased the absorption of DEHP and disturbed mitochondrial respiration (Lu et al., 2014). In another study, it was found that G (200 mg/kg/day) enhanced reproductive toxicity of phthalates in rats (Gao et al., 2016). Combining of TW (15-25 mg/L) and phthalates led to increased bioavailability and

absorption of phthalates, and thus toxicity to rats (Zhu et al., 2021). Glycerin monostearate was also found to increase phthalates testicular toxicity in rats (Xia et al., 2021). However, emulsifier concentration used in this study (80 μM TW and 3.5 μM G) were much lower than these studies and still could enhance toxicity of AA and BAP, suggesting that potential of emulsifiers could be higher than previously thought.

Even at concentrations well below cell viability NOAEL, emulsifiers have significant effect on expression of some gene (e.g. ATF3 and IL-8 in HIEC6, Fig. 2.3). There were cases where emulsifiers have larger effect on gene expression than AA or the combined treatment (e.g. ATF3 and IL-1β in HepG2), suggesting that emulsifiers may not be as benign as reported in food safety analysis reports (US Food and Drug Administration, 2018). Additive effect of emulsifiers and AA was observed for some genes (e.g. ATF3, IL-8 and IL-1β) in HIEC6 while synergistic effect was observed in others (e.g. CYP2E1, IL-8 in HepG2). Even though emulsifiers alone tend to increase expression of genes tested, it was difficult to predict the manner of which emulsifiers impact expression direction (i.e. up or down-regulation) in the combined treatments as there were cases for both types of impact. There were examples where combination with emulsifiers resulted in decreased expression (IL-8 in HepG2 and Caco-2, CYP2E1 in HIEC6 and Caco-2, IL-1β in Caco-2). There were also examples where combination increased expression (SOD in HepG2 and HIEC6, CYP2E1 and CYP1A1 in HepG2).

Impact of the mixtures on gene expression were also different for the three cell lines, confirming our initial hypothesis that different physiology of different cell types may result in different impact of emulsifiers. In HepG2, it was observed that cytokines and oxidative stress markers were highly modified by the combined treatments. Inflammation and oxidative stress have been proposed to be part of the toxic mechanism of both AA (Chen et al., 2018; Pan et al., 2018) and BAP (Shi et al., 2021). Increased expression of these genes could explain how emulsifiers increased toxicity of both compounds and decreasing the IC 10 and IC 50 values. The HIEC6 cells

appeared to be highly sensitive to the presence of emulsifiers and almost all genes tested showed large significant changes in the combined treatments. Caco-2 cells responded to the combined treatments more mildly but the effects were still significant.

Effect of emulsifiers were also dependent on contaminant. For example, in HepG2, combination with AA resulted in increase in SOD expression (Fig. 2.3 D) but decrease in SOD expression when combined in low BAP and increase in high BAP concentrations (Fig. 2.4 D). Similarly, in HIEC6 and Caco-2, emulsifiers increased expression of SOD when combined with AA but decreased expression of SOD when combined in BAP. All these results suggested that interaction of emulsifiers and contaminants are highly complex and could not be easily predicted.

In conclusion, combining low concentrations of emulsifiers could increase toxicity of both process contaminants tested as demonstrated by the decrease in IC 10 and IC 50 values (Tables 2.2-2.3). Cellular uptake of both contaminants were also increased by the emulsifiers (Fig. 2.5), which may be partially explained by the increase in cell membrane permeability caused by the emulsifiers (Figs. 2.6-2.7). This effect may in part be due to decreased expression of tight junction proteins (Fig. 2.8). Gene expression patterns were used to provide insight into the mechanism of which emulsifiers alter toxicity of contaminants. Results showed that while effect of emulsifiers was significant in altering gene expression caused by the contaminants, no generalizable pattern was observed, suggesting that there was no universal response to combined exposure of emulsifiers and contaminants. The effects were also highly dependent on cell line, suggesting that emulsifiers may alter toxicity differently in different organs. Therefore, the effect of emulsifiers on chemical toxicity should be investigated in animal models to better understand its overall effect on individual health.

CHAPTER 3

Food emulsifiers aggravates inflammation and oxidative stress induced by food contaminants in zebrafish

3.1 Introduction

Based on results in Chapter 2, it was observed that food emulsifiers could increase uptake and toxicity of both AA and BAP. The underlying mechanism appeared to be complex based on analysis of gene expression. Zebrafish is a common model in developmental biology, neuroscience, molecular biology and toxicology (Kinth et al., 2013). Zebrafish has many advantages such as high fecundity, rapid development and low maintenance cost (Nusslein-Volhard and Dahm, 2002). It shares around 70% of genes with humans as a vertebrate model (Howe et al., 2013). Therefore in this chapter the zebrafish model was used to verify these findings.

Adult zebrafish were exposed to emulsifiers, contaminants, or co-expose diets for 7 days and some oxidative stress and inflammation makers were determined. The alternations of histology and morphology induced by the mixtures of emulsifiers and food contaminants on liver and gut damage were evaluated. Furthermore, the accumulation of contaminants after emulsifiers addition was also measured by high performance liquid chromatography equipped with mass spectrometry (HPLC-MS) after 7 days or 2 hours of the exposures. This paper evaluated how low-toxic or non-toxic emulsifiers influence the toxicity of food contaminants in adult zebrafish.

3.2 Methodology

3.2.1 Zebrafish maintenance

Wild type adult zebrafish (Danio rerio) were maintained at the Hong Kong Polytechnic University under standard recirculating water conditions. Tanks kept at 28 ±1 °C, pH 7.0-7.4, and 14 h: 10 h light: dark cycle. Fish were fed with Otohime B1 dry diet (Pentair Aquatic Eco-Systems, USA) three times per day and Artemia nauplii once per day. Animal care and maintenance protocols were, approved by the Hong Kong Polytechnic University Institutional Animal Care and Use Committee were followed (19-20/70-ABCT-R-GRF).

3.2.2 Experimental diet preparation

Experimental diet was made by mixing base dry diet (Otohime B1) with different concentrations of AA or BAP and emulsifiers TW or G. Appropriate amount of food contaminants and emulsifiers were dissolved in 10 mL MilliQ water (Millipore, USA). Then this solution was mixed thoroughly with 10 g fish diets to make sure the liquid was evenly distributed and well incorporated. The fish diets frozen at -80 °C and subsequently freeze-dried for 48 h. The mixture fish feed was broken apart gently and stored in 50 mL centrifuge tubes at 4 °C until the experiment was done.

AA exposure group was prepared 9 diets such as solvent group (DMSO), TW (1 g/kg), G (10 g/kg), AAL (3 mg/kg), AAL_{TW} (3 mg/kg AA + 1 g/kg TW), AA_G (3 mg/kg AA + 10 g/kg G), AAH (10 mg/kg), AAH_{TW} (10 mg/kg AA + 1 g/kg TW), AAH_G (10 mg/kg AA+ 10 g/kg G).

BAP exposure group was prepared 9 diets such as solvent group (DMSO), TW (1 g/kg), G (10 g/kg), BAPL (20 µg/kg), $BAPL_{TW}$ (20 µg/kg BAP+ 1 g/kg TW), BAP_G (20 µg/kg BAP+ 10 g/kg G), BAPH (200 µg/kg), $BAPH_{TW}$ (200 µg/kg BAP+ 1 g/kg TW), $BAPH_G$ (200 µg/kg BAP + 10 g/kg G).

3.2.3 Exposure regime

The following exposure regime was repeated for AA and BAP treatment. 6 months old adult zebrafish were randomly divided into groups of 26 in 3 L water tanks and exposed to one of nine dietary treatments for 7 days. The fish were fed at a daily ration of 1 %~1.5 % of their body weight. Water from each tank was completely renewed every day. After 7 days, all individuals were euthanized by using cold tricaine methanesulfonate (MS-222) bath (100 mg/100 ml). Liver and gut of each individual were collected after necropsy for subsequent biomarker measurements and histology.

3.2.4 Total RNA extraction and RT-qPCR

RNA were extracted from liver and gut from six individuals per treatment by Trizol reagent (Takara, Japan) according to manufacturer's instructions. Extracted RNA was quantified using Nanodrop Lite Spectrophotometer (Thermo Fisher Scientific, USA). Only RNA samples with 260/280 ratio between 1.9 and 2.1 and 260/230 ratio greater than 2.0 were used for RT-qPCR analysis. For each RT-qPCR reaction, 500 ng of RNA were added for the 10 µL transcription reaction by using Takara PrimeScript™ RT Master Mix (Takara, Japan) according to the manufacturer's instructions. PCR primers were adopted from published sequences or designed using Primer 3 and described in Table 3.1. RT-qPCR was performed on Applied Biosystems QuantStudio 7 Flex Real-Time PCR System using Power-up SYBR Green Master Mix (Thermo Fisher Scientific, USA). Every reaction consisted of 0.5 µL of cDNA, 1 µL of forward and reverse primers, 5 µL Power-up SYBR Green Master Mix and 3.5 µL DNA template nuclear-free water. The PCR reaction were processed as a single cycle of UDG activation (50 °C, 2 min) and Dual-Lock DNA polymerase activation (95 °C, 2 min), and then amplification cycles (40 x) consist of denaturation (95 °C, 15 s) and annealing and elongation (60 °C, 1 min). A single cycle of melting process that consisted of an increased temperature from 65 °C to 95 °C for 10 min was performed at the end. A single peak in all melting curves verified the generation of a single amplicon for each primer pair. Results were normalized to β-actin expression. Gene expression was

calculated using the $2^{-\Delta\Delta CT}$ method.

Table 3.1 List of primer sequences used for qPCR.

Gene	Forward (5'-3')	Reverse (5'-3')	Reference
ahr	CTACTTGGGCTTCCATCAGTCG	GTCACTTGAGGGATTGAGAGCG	(Roy, 2021)
arnt	TTTGTCAGACCGCGGCGAAT	GTCCTCGTCGTCAAAATCCA	(Wang et al., 2000)
bax	AGTGTTTGCAGCAGATCGGA	GAAGATCTCACGGGCCACTC	This study
il-1β	CGTCATCCAAGAGCGTGAAG	TGCGCACCAGAGACTTCTTA	(Hong et al., 2021)
sod	GGCCAACCGATAGTGTTAGA	CCAGCGTTGCCAGTTTTTAG	This study
β-actin	TCAACACCCCTGCCATGTAT	TCACACCATCACCAGAGTCC	This study

3.2.5 Histopathological evaluation

Livers and guts of the six individual fish in each treatment were collected after exposure and immediately fixed in 4 % paraformaldehyde at room temperature overnight. Tissues were then dehydrated with a graded series of ethanol and cleared through xylene before infiltration and embedment in paraffin wax overnight at 59 °C. Tissues in paraffin wax were sectioned on a microtome at a thickness of 5 μm and mounted onto glass slides. Sections were stained with hematoxylin and eosin and examined under the light microscope.

3.2.6 Measurement of Reactive Oxygen Species (ROS) and Superoxide Dismutase (SOD) Activity

Liver and gut samples from eight individuals from each treatment were homogenized in 1 mL of PBS on ice and incubated with redox sensitive dye 2,7-diacetyl dichlorofluorescein diacetate (DCF-DA) (Nanjing Jianchen Bioengineering Institute, China) on 96-well plate in a dark humidified chamber for 30 min at 28 °C. After

incubation, ROS concentration was measured by fluorescence plate reader at Ex/Em = 502/530 nm. The ROS concentration was normalized against protein concentration by BCA method. SOD activities were detected by using commercial kit (Nanjing Jianchen Bioengineering Institute, China) according to the manufacturer's instruction. Activity of SOD was determined by measuring the inhabitation of tetrazolium salt reduction (WST-1). The liver and intestine were homogenized and incubated with WST-1 solution for 30 min. The SOD activity was measured spectrophotometrically using absorbance levels of 512 and 450 nm. The SOD activity was normalized against protein concentration measured by the BCA (Bicinchoninic Acid) protein assay method.

3.2.7 Acute and sub-acute accumulation of food contaminants in liver and gut of zebrafish

Six fish per treatment were harvested after 2 h and 7 d exposure to measure uptake of food contaminants. Liver and gut were collected, homogenized in MiliQ grade water, and frozen immediately at -80 °C until processing. Acetonitrile was added to precipitate proteins and the solution was put on vertex mixer for 30 s and then centrifuged at 13,000 rpm at 4 °C for 10 min. The supernatant was collected and passed through 0.2 µm PTFE syringe filters. To measure acrylamide concentration, supernatant was injected into Agilent 6460 Liquid chromatography (Electrospray Ionization Triple Quadrupole Mass Spectrometer, USA) with an ACQUITY UPLC HSS T3 Column (1.8 µm, 2.1 x 100 mm, Waters Corporation, Milford, USA), and the flow rate was 0.2 mL/min. The mobile phase was composed of water (A) and methanol (B) both containing 0.1 % (v/v) formic acid. The injection volume was 2 µL. The linear elution gradient program was used as follows: 0-7 min, 97 % A; 7-9 min, 10 % A; and 9-12.5 min, 97 % A. AA was detected as a single peak with an m/z ratio of 72 ($[M+H]^+$) and compared with standard curve constructed using AA (Sigma Aldrich Chemical Co, USA). To measure BAP concentration, supernatant was injected into 6500 Qtrap LC-MS/MS system (AB Sciex, Concord, ON, Canada) equipped with an atmospheric pressure chemical ionization (APCI) source (AB Sciex, Concord, Ontario, Canada), with an Agilent SB–C18 column

(2.1 mm × 100 m), and the flow rate was 0.5 mL/min. The mobile phase was solvents A (5 mM ammonium acetate in water containing 0.1 % (v/v) formic acid) and B (acetonitrile). The injection volume was 5 µL. The linear elution gradient program was used as follows: 0-3 min, 50 % B; 3-17 min, 99 % B; and 17-20 min, 50 % B. The ion transitions monitored were m/z 253 → 250 and 253 → 224. Sample concentration was estimated based on standard curve of BAP (Sigma Aldrich Chemical Co, USA) constructed in the range of 5 ppb to 250 ppb.

3.2.8 Statistical analyses

All results were expressed as mean ± standard deviation (SD). Analysis of variance (ANOVA) and Tukey's multiple-comparison test was used to evaluate statistical differences between biological endpoints of different treatments. All other analyses were performed using GraphPad Prism 8.0 (GraphPad Software, San Diego, CA).

3.3 Results

3.3.1 Addition of emulsifiers alter gene expression caused by food contaminants

There were no mortality and no signs of severe stress in fish throughout the exposure. However, when emulsifiers were added to AA exposure, there were changes to gene expression and the changes were largely additive (Fig. 3.1). Expression pattern of il-1β in the liver and gut was similar. Expression of il-1β was not affected by DMSO, TW or G alone. When emulsifiers added to low or high AA, the expression of il-1β was significantly increased but the increase was not dose-dependent. For example, when low AA was combined with TW or G, il-1β expression of liver increased significantly by 97.5 % and 75.9 % respectively. Expression of sod1 was also unaffected by DMSO, TW or G alone. Significant increases was observed in low AA but not high AA. Addition of TW or G led to significant increase of sod1 in low AA by 218.3 % and 183.5 % respectively but not high AA in the gut. Expression of bax were increased by

TW or G in the gut. Similarly addition of TW or G led to significant increase of bax. This was observed in the liver at the high AA concentration and in the gut at low AA concentration.

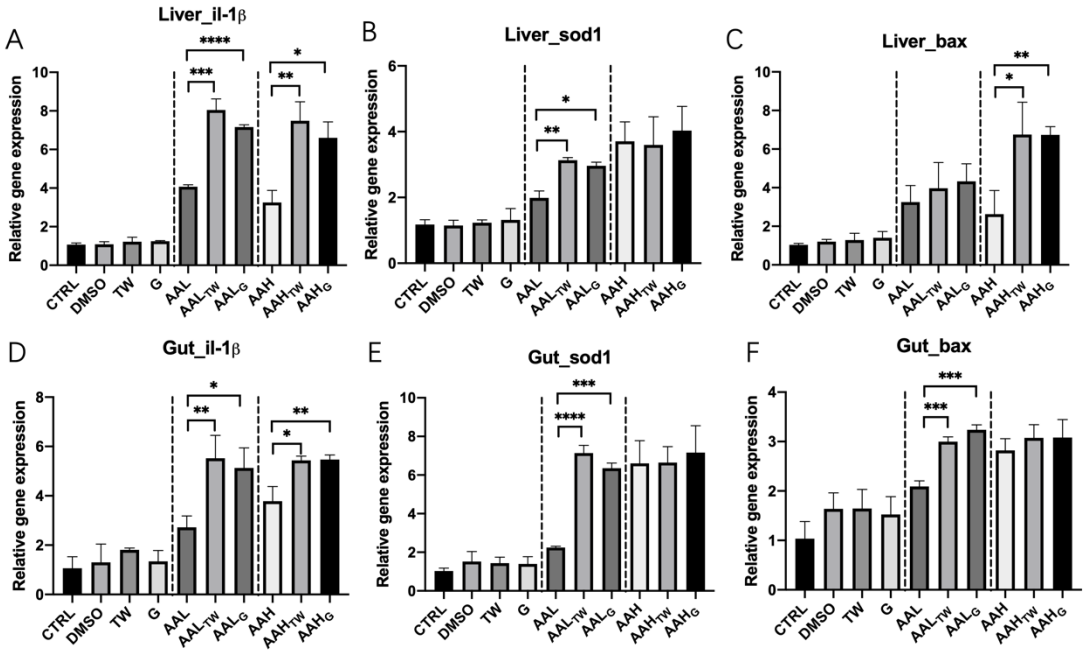

Figure 3.1 *Gene expression in the liver (A-C) and gut (D -F) of adult zebrafish after 7 days emulsifiers, AA and the co-exposure of emulsifiers and AA treatment. β-actin was used as an internal control. Each value represents the mean ± SD (n=6). Asterisk denotes statistical significance, * p<0.05, ** p<0.01, ***p<0.001.*

Effect of emulsifiers on BAP toxicity was largely insignificant in the liver but significant effect was observed in the gut (Fig. 3.2). Both emulsifiers did not elicit significant change in gene expression in both liver and gut. In the gut, expression of both ahr and arnt were induced by BAP and co-exposure to G significantly increased their expression levels (Figs. 3.2 F-G). Expression of il-1β was significantly increased by both emulsifiers at low BAP level but not at high BAP level. Expressions of sod1 and bax were significantly increased by both emulsifiers but G elicited a significantly larger response. In the liver, only significant effect of emulsifier was TW on low dose BAP (Fig. 3.2 E).

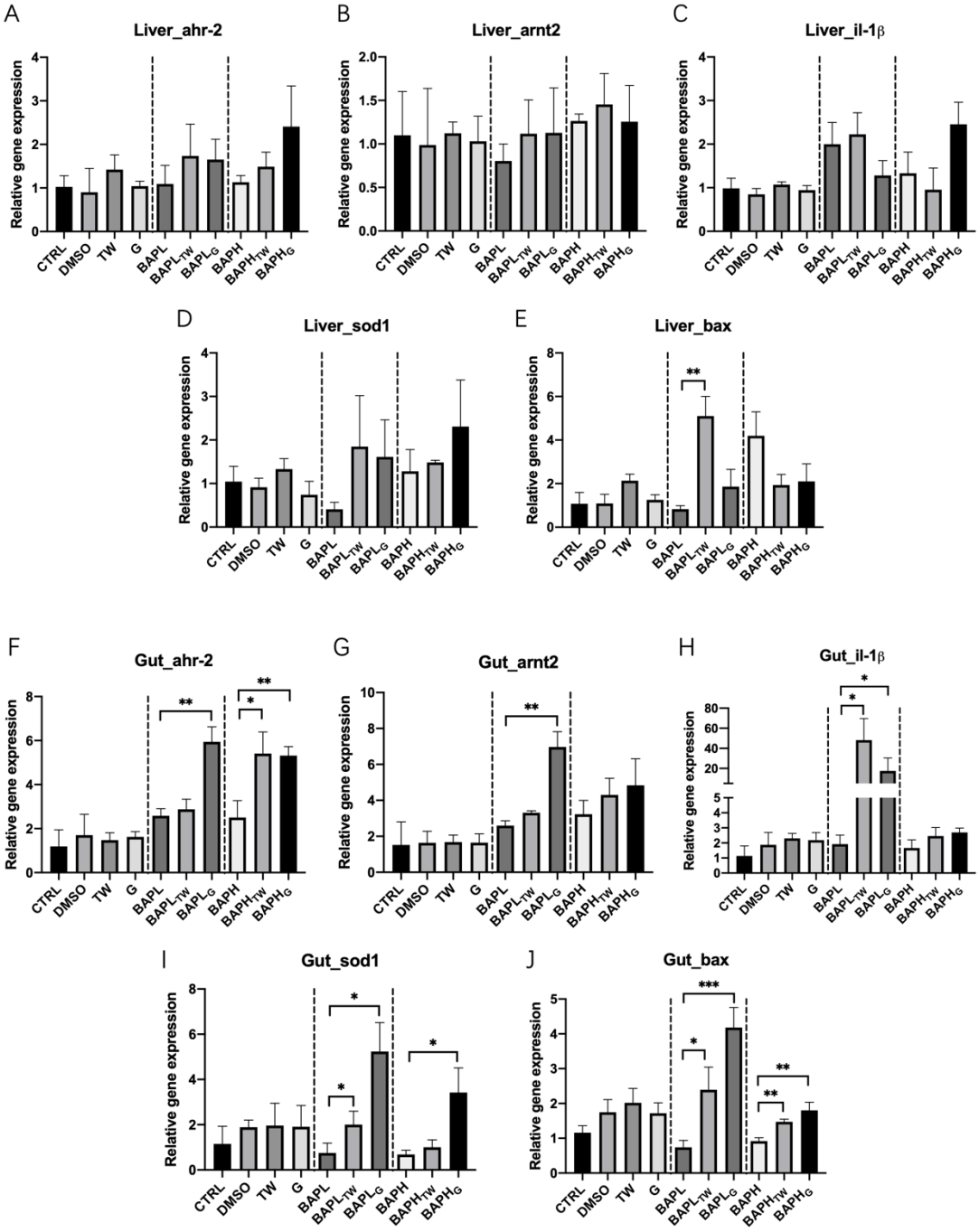

Figure 3.2 *Gene expression in the liver (A-E) and gut(F-J) of adult zebrafish after 7 days emulsifiers, BAP and the co-exposure of emulsifiers and BAP treatment. β-actin was used as an internal control. Each value represents the mean ± SD (n=6). Asterisk denotes statistical significance, * p<0.05, ** p<0.01, ***p<0.001.*

3.3.2 Addition of emulsifiers aggravates oxidative stress caused by food contaminants

Food emulsifiers alone and DMSO did not create oxidative stress and had no effect on SOD activity (Fig. 3.3). Acrylamide significantly increased SOD activity compared with control but the presence of TW or G the effect was reversed and SOD activity was suppressed. This agreed with significant increase in total ROS concentration in the liver of co-exposure treatments. Similar effects of emulsifiers were observed in the gut, where it significantly suppressed SOD activity more than acrylamide treatment. However this was not reflected on the total ROS concentration.

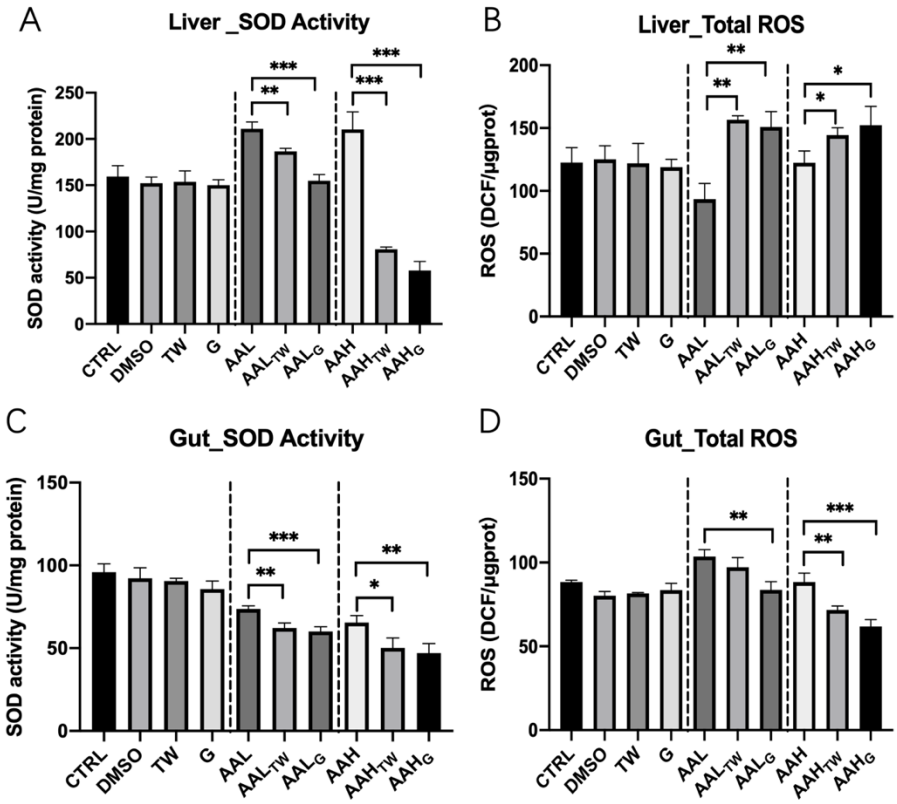

Figure 3.3 *Activities of SOD and ROS level in the liver (A, B) and gut (C, D) of adult zebrafish after 7 days emulsifiers, AA and the co-exposure of emulsifiers and AA treatment. Each value represents the mean ± SD (n=8). Asterisk denotes statistical significance, * p<0.05, ** p<0.01, ***p<0.001.*

Effects of emulsifiers were observed in BAP co-exposure where SOD activity was suppressed and ROS concentration was increased in the liver. Similar effect of emulsifiers was observed in the gut, where it significantly raised total ROS level more than BAP treatment. However, the SOD activity was increased by co-exposure of BAP and G.

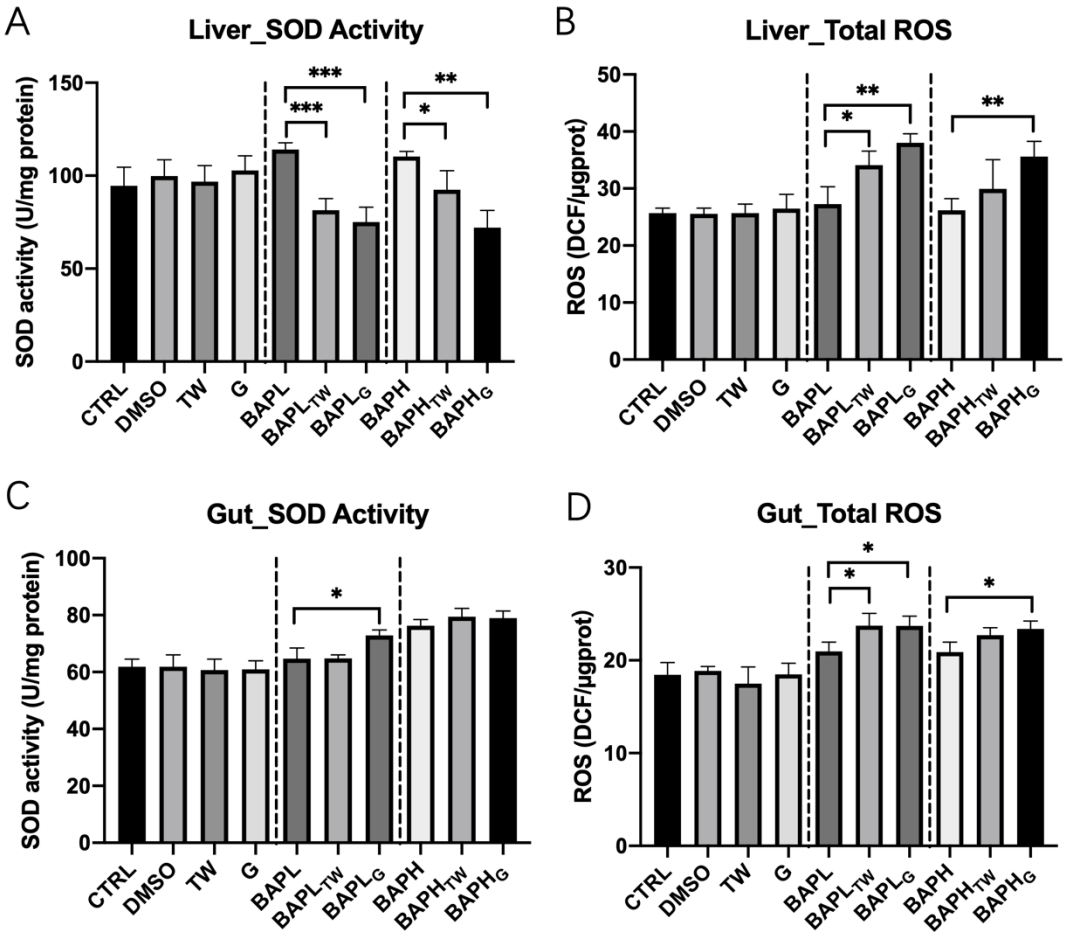

Figure 3.4 *Activities of SOD and ROS level in the liver (A, B) and gut (C, D) of adult zebrafish after 7 days emulsifiers, BAP and the co-exposure of emulsifiers and BAP treatment. Each value represents the mean ± SD (n=8). Asterisk denotes statistical significance, * p<0.05, ** p<0.01, ***p<0.001.*

3.3.3 Emulsifiers aggravates histological changes induced by food contaminants

No changes in the liver were observed in the emulsifier only treatments (Fig. 3.5). There were signs of lipid accumulation in the liver in low AA treatment (Fig. 3.5 D, red arrows) and similar, but more pronounced changes were observed in the AA + emulsifier treatments. Infiltration of immune cells was also observed in the AAL_G treatment. In the high AA treatment, more severe changes were observed, including multiple sites of lesions (Fig. 3.5 G). In AAH_{TW} treatment, large area of degradation and infiltration of hepatocytes was observed (Fig. 3.5 H). In AAH_G treatment, large area of necrotic cells was also observed (Fig. 3.5 I).

BAP treatments did not cause changes to the liver (Figs. 3.5 J and M). At high BAP + emulsifier treatments there were minor lipid accumulation in the liver (Figs. 3.5 L and O, red arrows).

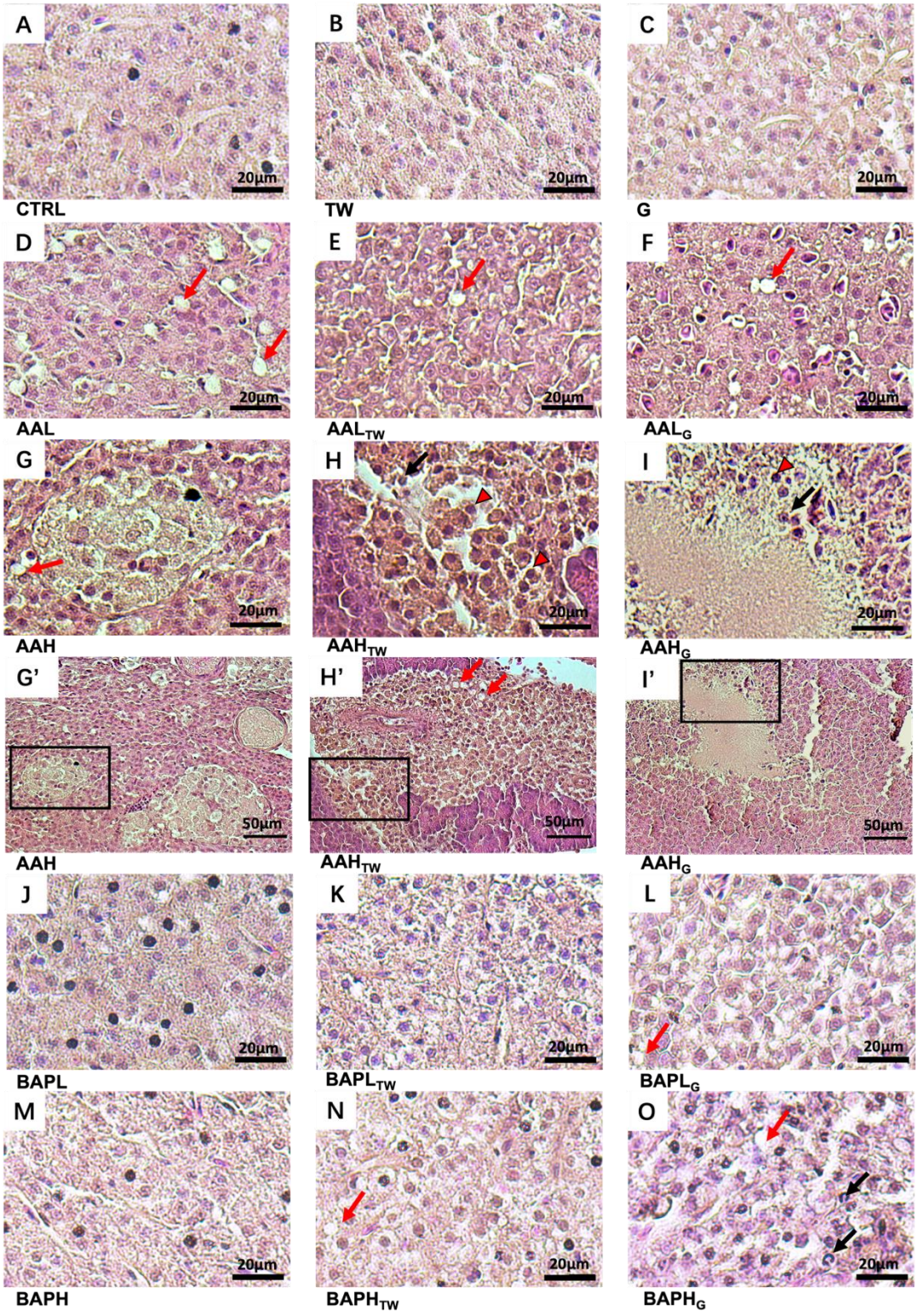

Figure 3.5 *Photomicrographs H&E-stained paraffin sections showing liver pathology in adult zebrafish after exposure to different fish feeds for 7 days: CTRL (A), TW (B), G (C), AAL (D), AAL_{TW} (E), AAL_G (F),AAH (G), AAH_{TW} (H), AAH_G (I) , BAPL (J),$BAPL_{TW}$ (K), $BAPL_G$ (L), BAPH (M), $BAPH_{TW}$ (N), $BAPH_G$ (O), Bars = 20 µm, AAH (G'), AAH_{TW} (H'), AAH_G (I') ,Bars = 50*

μm. The red arrows indicate the deposition of intracellular lipid droplets. The red arrow heads indicate glycogen reduction. The black arrows indicate the existence of some immune cells in the liver.

Emulsifiers alone did not lead to changes in both gut (Fig. 3.6). In low AA treatment (Fig. 3.6 D), there were no changes on villi arrangement, but the staining of cells became more eosinophilic, which might suggest inflammation. When co-exposed with emulsifiers, fusing of villi was observed (Figs. 3.6 E and F). For high AA treatment (Fig. 3.6 G), fusing of villi structures were observed and villi appeared very short. These changes were exacerbated in the emulsifier co-exposure and number of goblet cells were also significantly increased (Fig. 3.7). No significant change was observed in all low BAP treatments (Fig. 3.6 J). In high BAP treatment, there were some fusion of villi and significant increase of goblet cells was observed in the G co-exposure (Fig. 3.7).

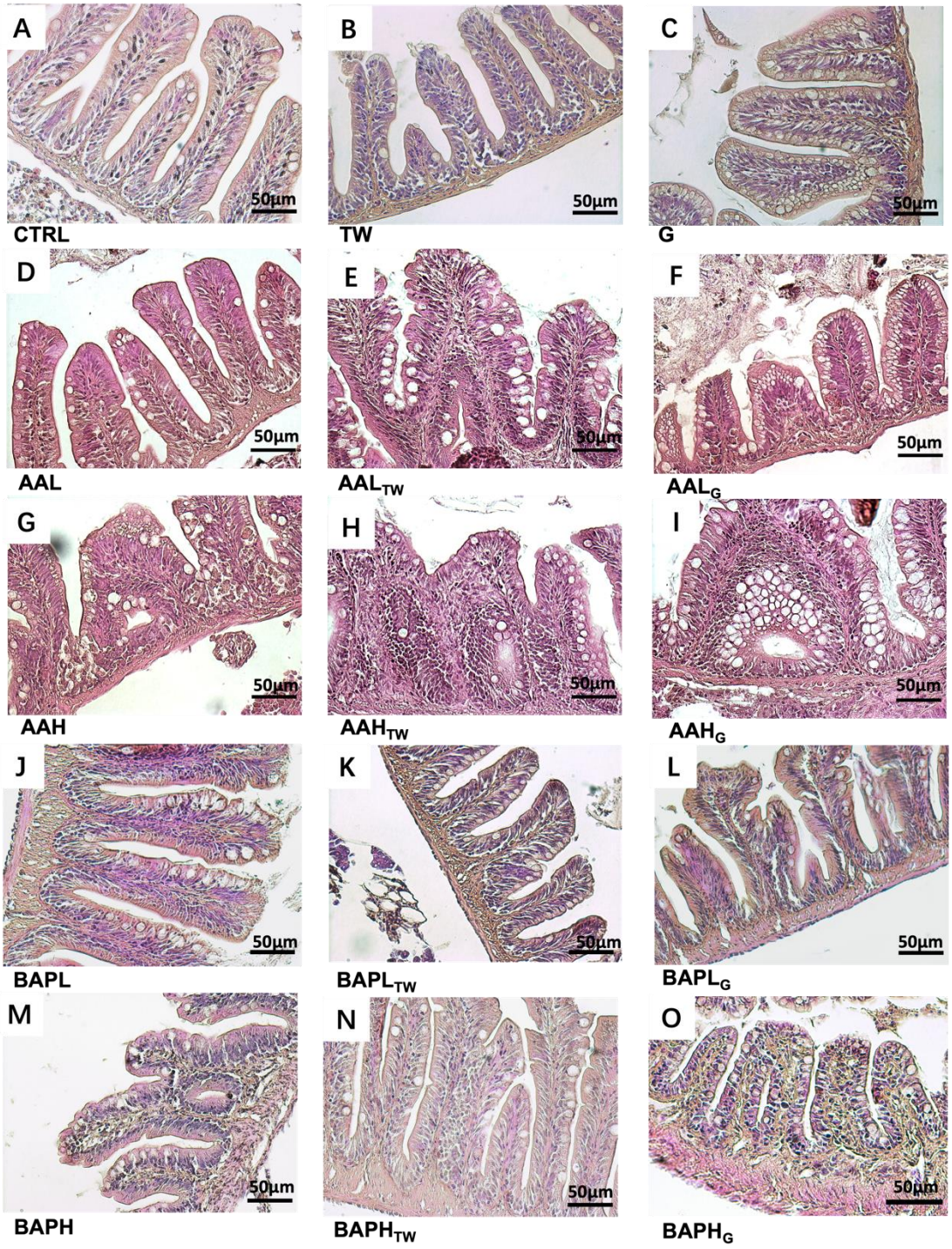

Figure 3.6 *Photomicrographs H&E-stained paraffin sections showing gut pathology in adult zebrafish after exposure to different fish feeds for 7 days: normal CTRL (A), TW (B), G (C), AAL (D), AAL_{TW} (E), AAL_{G} (F),AAH (G), AAH_{TW} (H), AAH_{G} (I) , BAPL (J),$BAPL_{TW}$ (K), $BAPL_{G}$ (L), BAPH (M), $BAPH_{TW}$ (N), $BAPH_{G}$ (O), Bars = 50 µm.*

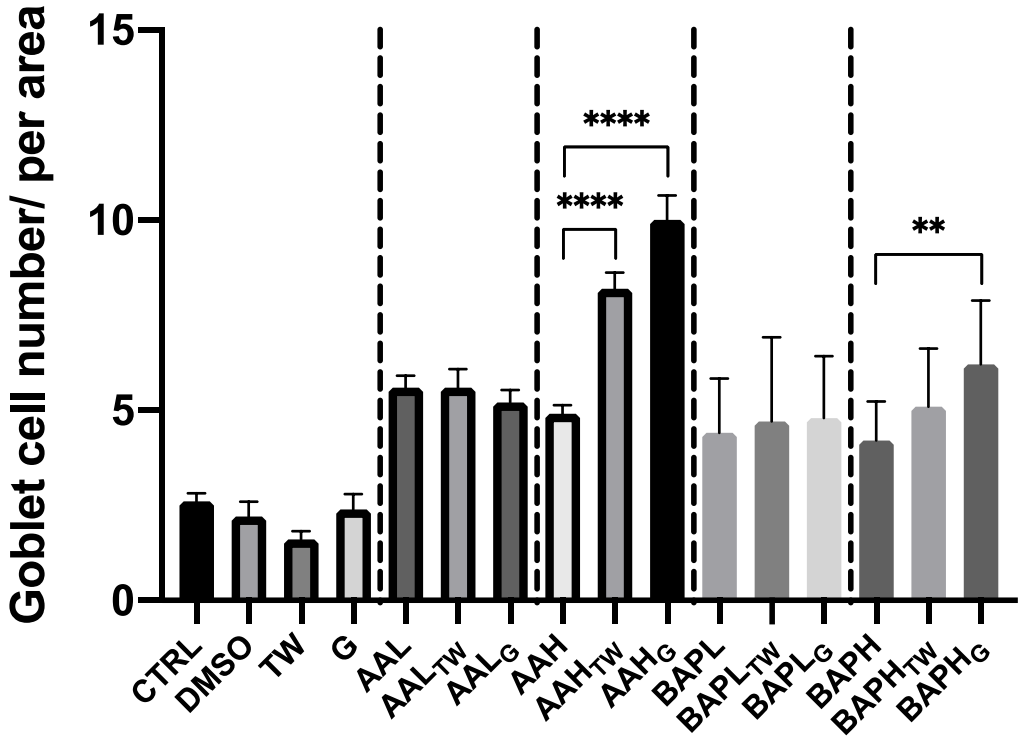

Figure 3.7 *Quantification of the goblet cell number. Values shown are goblet cell density of randomly selected villus (10 villi) per treatment after 7 days of feeding. Asterisk denotes statistical significance, * p<0.05, ** p<0.01, ***p<0.001.*

3.3.4 Emulsifiers increase accumulation of food contaminants in liver and gut

Food emulsifiers increased accumulation of acrylamide in both gut and liver just after 2h of exposure and G had higher effect than TW at low AA concentration. After 7d, this effect was observed only in the liver at the low AA concentration.

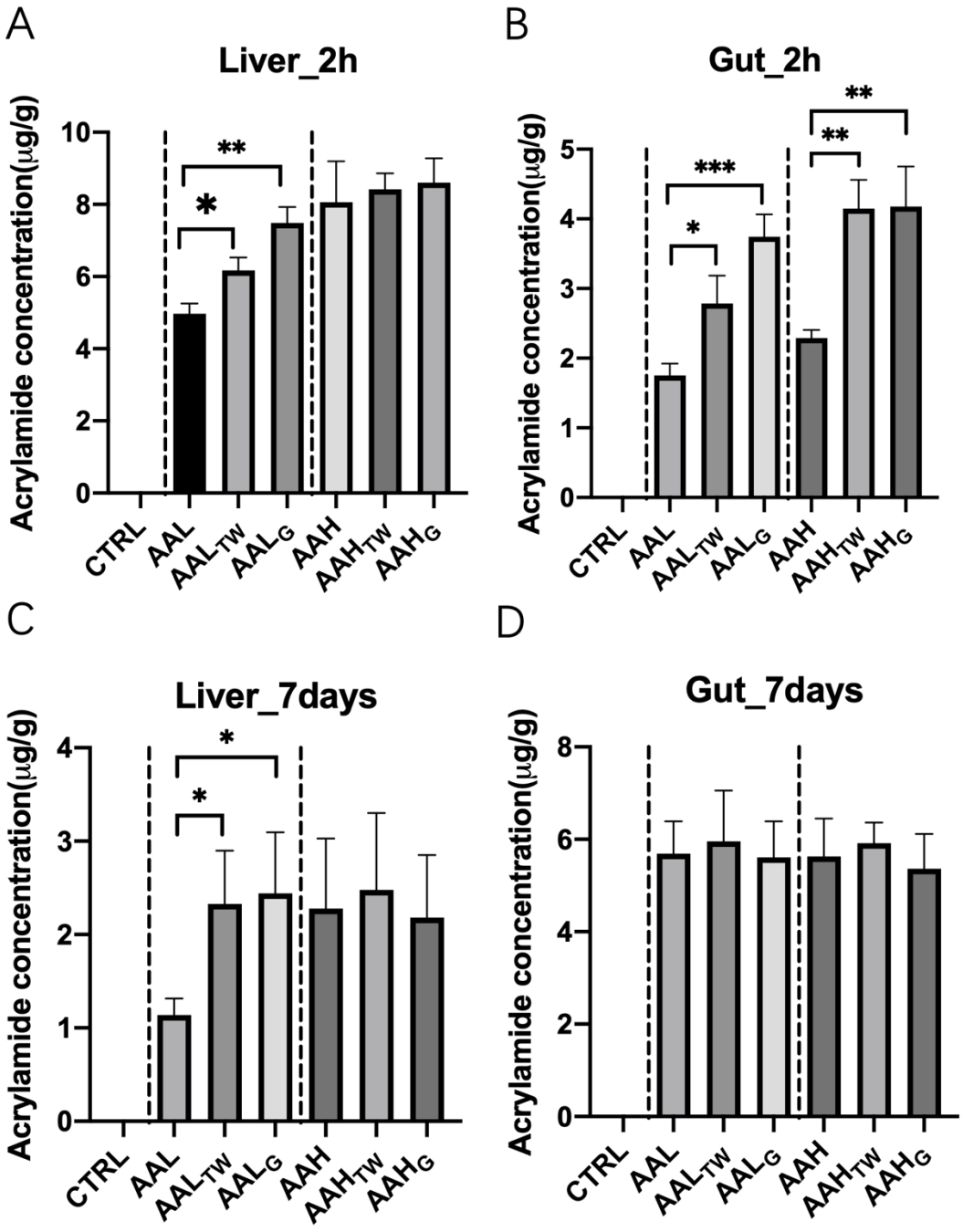

Figure 3.8 *Accumulation of AA in livers and guts of zebrafish after 2 h or 7 d exposure. Zebrafish were administered AA (3 mg/kg or 10 mg/kg) with and without emulsifiers, asterisks show the difference between AA and the co-exposure of AA and emulsifiers according to T-test. Asterisk denotes statistical significance, * p<0.05, ** p<0.01, ***p<0.001.*

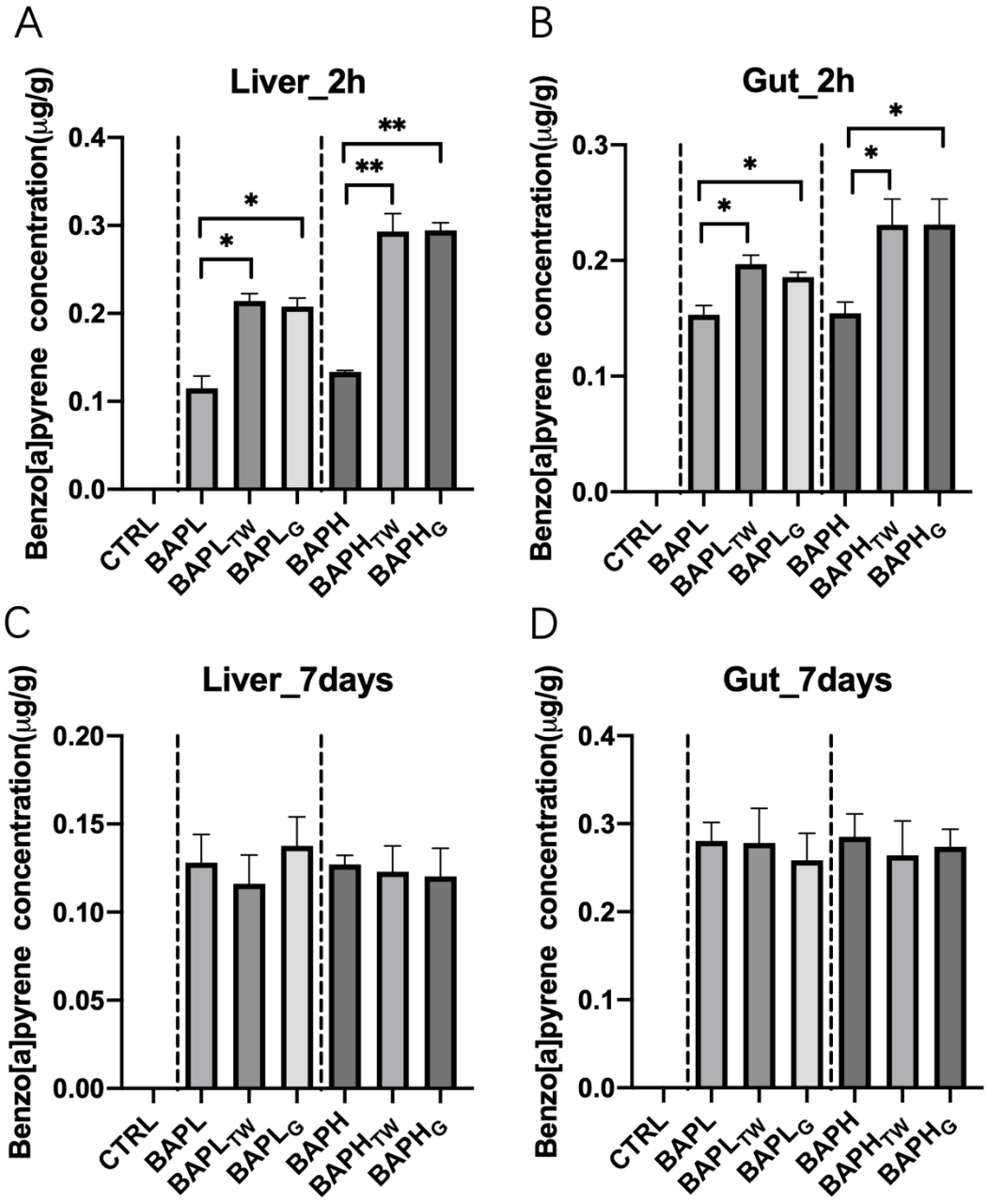

Figure 3.9 *Accumulation of BAP in livers and guts of zebrafish after 2 h or 7 d exposure. Zebrafish were administered BAP (20 μg/kg or 200 μg/kg) with and without emulsifiers, asterisks show the difference between BAP and the co-exposure of BAP and emulsifiers according to T-test. Asterisk denotes statistical significance, * $p<0.05$, ** $p<0.01$, *** $p<0.001$.*

For BAP, emulsifiers also have significant impact on increasing BAP accumulation at 2 h in the liver and gut. Unlike for acrylamide, both emulsifiers had similar effects

for BAP. There was no significant effect of emulsifiers on accumulation of BAP in liver or gut after 7 d.

3.4 Discussion

Our data demonstrated that uptake of food contaminants such as AA and BAP were facilitated by food emulsifiers (Figs. 3.8 and 9). Increase of uptake was observed as quickly as 2 h after ingestion and can be found in both liver and gut. This effect might have plateaued after 7 d as emulsifiers only increased uptake of low dose acrylamide in the liver. Emulsifier-enhanced chemical uptake had been reported in studies looking at drug (Friedl et al., 2020) and contaminant uptake (Gao et al., 2016). There were reports that G increased the internal exposure concentration of phthalic acid esters (PAEs) in urine of mice (Gao et al., 2016) and TW increased the absorption and bioavailability of mono-2-ethylhexyl phthalate in both rats and mice (Zhu et al., 2021). One possibility was emulsifiers decrease hydrophobicity of phospholipid bilayer of cell membranes thus increasing transportation of soluble contaminants (Qin et al., 2008). Mucus gel on the mucosal layer of the gut also help prevent harmful components in gut lumen entering the body (Lugea et al., 2000; Qin et al., 2008). However, emulsifiers were reported to weaken mucolytic activity and further increase gut permeability (Sood and Panchagnula, 2001). This might be the reason that water soluble AA ($\log K_{ow}$ = -0.67) were taken up more readily in this study. Harris *et al*. reported that dietary fat with hydrophobic domains not easily lipolyzed could be a carrier to accelerate the transport of polycyclic aromatic hydrocarbons (PAHs) (Harris et al., 2013). G could be found in the intestinal lumen as micelles or aggregates (Harris et al., 2013), which in turn can enhance solubility and bioavailability of contaminants (Francis et al., 2004).

Biomarkers indicated that toxicity of AA and BAP increased in the presence of emulsifiers. Both TW and G had no significant effect on expression of the genes studied, confirmed emulsifiers concentration used in this study is low-toxic or non-toxic. However they exacerbated the effect of AA and BAP. There is a growing body of

literature that demonstrating AA and BAP toxicities in relation to oxidate stress (Cui et al., 2019; Komoike and Matsuoka, 2019) and inflammation (Santhanasabapathy et al., 2015; Shi et al., 2021). A dose of 20 mg/kg AA administrated for 30 days resulted in significant decrease of GSH, SOD and CAT activities, induced intestine damages such as shorter and wider villi, and the presence of inflammatory cells and ulcerations in SD male rat (Yang et al., 2019). Increased expression of these genes (Fig. 3.1) and some histopathological changes (Figs. 3.5 G) also confirmed AA increased inflammation and oxidative stress. Additive effect was observed in both liver and gut on il-1β, sod1 and bax, which are biomarkers for inflammation, oxidative stress and apoptosis respectively. Increased genes expression and increased SOD activity explain how emulsifiers increased the toxicity of AA in zebrafish. The increased toxicity also brought about histopathological changes (Figs. 3.5 and 3.6). Co-exposure AA and emulsifiers led to more inflammation and necrotic lesions in the liver as well as fused villi and increase in goblet cells in the gut. Increased in goblet cells could be interpreted as increased gastrointestinal toxicity (Rubinstein, 2006; Zheng et al., 2019). BAP have a slight effect on gene expression. But with emulsifiers significant effect was observed for il-1β, sod1 and bax, as well as biomarkers of PAHs exposure ahr and arnt (Fig. 3.2). Similarly, elevated genes expression and total ROS level (Fig. 3.4) indicated emulsifiers could increase toxicity induced by BAP. Histopathological changes also confirmed addition of emulsifiers led to higher toxicity such as higher lipid accumulation in the liver, and more pronounced fusion and shortening of villi in the gut (Figs. 3.5 and 3.6). These changes showed that emulsifiers increased toxicity of AA and BAP through inflammation and other damages.

Impact of the mixtures on gene expression and oxidative stress were also different for different organs. Addition of emulsifiers, BAP elevated most genes expression in gut, while only elevated bax in liver (Fig. 3.2). When emulsifiers were added into AA, total ROS level increased in liver while decreased in gut (Fig. 3.3). Similarly, the accumulation of AA in the liver was enhanced by emulsifiers after 7 days, while there

was no difference in the gut (Fig. 3.8).

Recently several studies reported that the high concentrations of dietary emulsifiers used as a safe food additive can alter intestinal microbiota composition and promote its pro-inflammatory and mucolytic potential (Chassaing et al., 2017; Elmén et al., 2020). Miclotte *et al.* investigated 5 emulsifiers on fecal samples of 10 human individuals for 48 h fermentation. Except soy lecithin, TW, rhamnolipids, carboxymethylcellulose and sophorolipids decreased the microbiota diversity. Therefore, such a co-exposure might induce potential toxicity moderated through changes in gut microbiota composition. But due to large biological differences between zebrafish and human gut microbiota community, the effect of mixtures on microbiota community was not explored in this chapter.

We explored the possible combinations of emulsifiers of high HLB value (TW) and low HLB value (G) and contaminants that are water soluble (AA) and hydrophobic (BAP). Our study showed that regardless of the combination there was synergistic effect on chemical toxicity, suggesting that this phenomenon might be more widespread than the four cases explored. It is important to note that the emulsifier used in this study did not elicit significant response in all the biomarkers tested, confirming that they are safe and with extremely low toxicity food additives. In this study, they interact synergistically to increase toxicity of common food contaminants AA and BAP. Even at concentrations where BAP did not cause toxicity, co-exposure with emulsifiers can led to observable toxicity. These findings are highly relevant to real life as food emulsifiers and these two food contaminants are co-occurring in many processed food including baked products and many drink product. Safety evaluation for food additives and food contaminants may need to bear in mind of potential synergistic interactions in the future.

CHAPTER 4

Dietary emulsifiers tween 80 and glycerol monostearate increased absorption of acrylamide and exacerbates inflammation, microbiota dysbiosis and metabolic symptom in mice

4.1 Introduction

In Chapters 2 and 3, strong evidence were presented that food emulsifiers and AA co-exposure could lead to higher toxicity and more inflammation of the GI tract. However, due to limitations of the models (i.e. cells and zebrafish), other effects of AA and emulsifiers could not be tested. In this chapter, rodents were used to address those effects. Mice is a mature model to study human biology (Bedell et al., 1997). As reported, mice and human have a similar genetic background which have around 90 % of genome could be partitioned into conserved syntenic regions (Breschi et al., 2017).

AA is responsible for neurotoxicity, which has been confirmed by animals and human studies (Exon, 2006). Studies of mechanisms suggests that AA induced neurotoxicity may be associated with nerve cell apoptosis, axonal degeneration of the nervous system, inflammatory response, oxidative stress and gut-brain axis homeostasis (Zhao et al., 2022). Since other toxicities have been observed in earlier chapters to increase with co-exposed with emulsifiers, I hypothesize that emulsifiers may increase neurotoxicity of AA.

Role of gut microbiota is also anticipated to be important. Gut microbiota has been reported to play crucial role in inflammation caused by emulsifiers. Germ-free mice did not develop inflammation when exposed to TW and carboxy methyl cellulose (CMC) but inflammation was developed after transplantation of emulsifier exposed fecal microbiota (Chassaing et al., 2017). Food emulsifiers have been reported to increase GI

tract inflammatory mediated through altered intestinal microbiota composition (Csáki, 2011; Lerner and Matthias, 2015). The hypothesized effect of AA-induced microbiota-gut-brain axis signaling is to induce intestinal bacterial metabolites to enter the damaged intestinal barrier, leading to systemic inflammatory responses. This process compromises the blood-brain barrier and eventually leads to nerve damage and deterioration (Zhao et al., 2022). Therefore I hypothesize that gut microbiota could be one toxicity target of combined toxicity of AA and emulsifiers.

Rodents are the most often used animal model for studying the correlation between gut microbiota and health and illness (Krych et al., 2013). Human and rodents gut microbiota share 90 % and 85 % similarities in phyla and genera, respectively (Park and Im, 2020). The mammalian digestive system is highly conserved, and differences between species are mainly due to diets. Humans and rodents are both omnivores, which makes them comparable in many ways, such as gut physiology and anatomy (Nguyen et al., 2015). Therefore rodent microbiota can be used to test effects of chemicals mixtures on human.

We seek to test whether the transcriptome data would reveal other pathways in addition to confirming the inflammatory-related biomarker that was mentioned before and understand the combined toxicity of acrylamide and food emulsifiers on changes in gut microbiota community. As far as we know, no previous research has investigated the mixture toxicity of food contaminant AA and food emulsifiers. Emulsifiers also used to improve the oral bioavailability of drug in pharmaceutical industry, so it is possible to increase the absorption of contaminant. It is of interest to know how emulsifiers change the toxicity of AA in mice, which will provide evidence for risk assessors to make an adequate evaluation of emulsifiers and improve the toxicity assessment of mixtures of food contaminants and emulsifiers.

4.2 Methodology

4.2.1 Animals maintain and experimental design

All animal experiments were performed in accordance with the regulations of the Animal Ethics Committee of The Hong Kong Polytechnic University and the Hong Kong legislation on animal studies. Male C57BL/6 mice (6-8 weeks of age; body weight, 20-25 g) and male SD rat (body weigh 200-250 g) were purchased from The Hong Kong Chinese University. Animals were acclimatized in a temperature-controlled and germ-free university animal facility with a 12-hour light/dark cycle and unlimited supply of sterilized food and water for 2 weeks before experimentation in The Hong Kong Polytechnic University. All experiments were carried out under animal ethics 21-22/140-ABCT-R-STUDENT and 16-17/33-ABCT-R-GRF. Three experiments were conducted in total (Fig. 4.1).

In the first experiment, 21 male SD rats were divided into two groups of 9 (for chemical uptake of plasma) and 12 (for chemical uptake of liver). All individuals were gavage with a single dose of either (1) AA (24 mg/kg), (2) AA (24 mg/kg) + TW (25 mg/kg.), or (3) AA (24 mg/kg) + G (200 mg/kg). AA or/and emulsifiers were dissolved in the solvent (90% corn oil+ 10% DMSO) before administration. Animals were anesthetized by an intraperitoneal injection of ketamine (100 mg/kg) and xylazine (10 mg/kg). The plasma and liver were collected for chemical uptake using HPLC-MS/MS. Animals were anesthetized by an intraperitoneal injection of ketamine (100 mg/kg) and xylazine (10 mg/kg). Blood was collected from retro-orbital arteries at four time points (0.5, 1, 3, and 6 h) after anesthesia. Blood in heparin lithium-anticoagulant tubes was centrifuged at 6,000 g for 10 mins at 4 °C to obtain plasma. 100 µl of Samples (plasma and liver homogenates) were then deproteinized by adding 300 µl of acetonitrile (ACN). After vortex-mixing for 30 s, samples were centrifuged at 13,000 rpm for 10 mins at 4 °C. The supernatants were filtered through a 0.2 µM PTFE syringe filter and then transferred to glass vials with micro-volume inserts. AA concentration was quantified using same methods described in previous chapters.

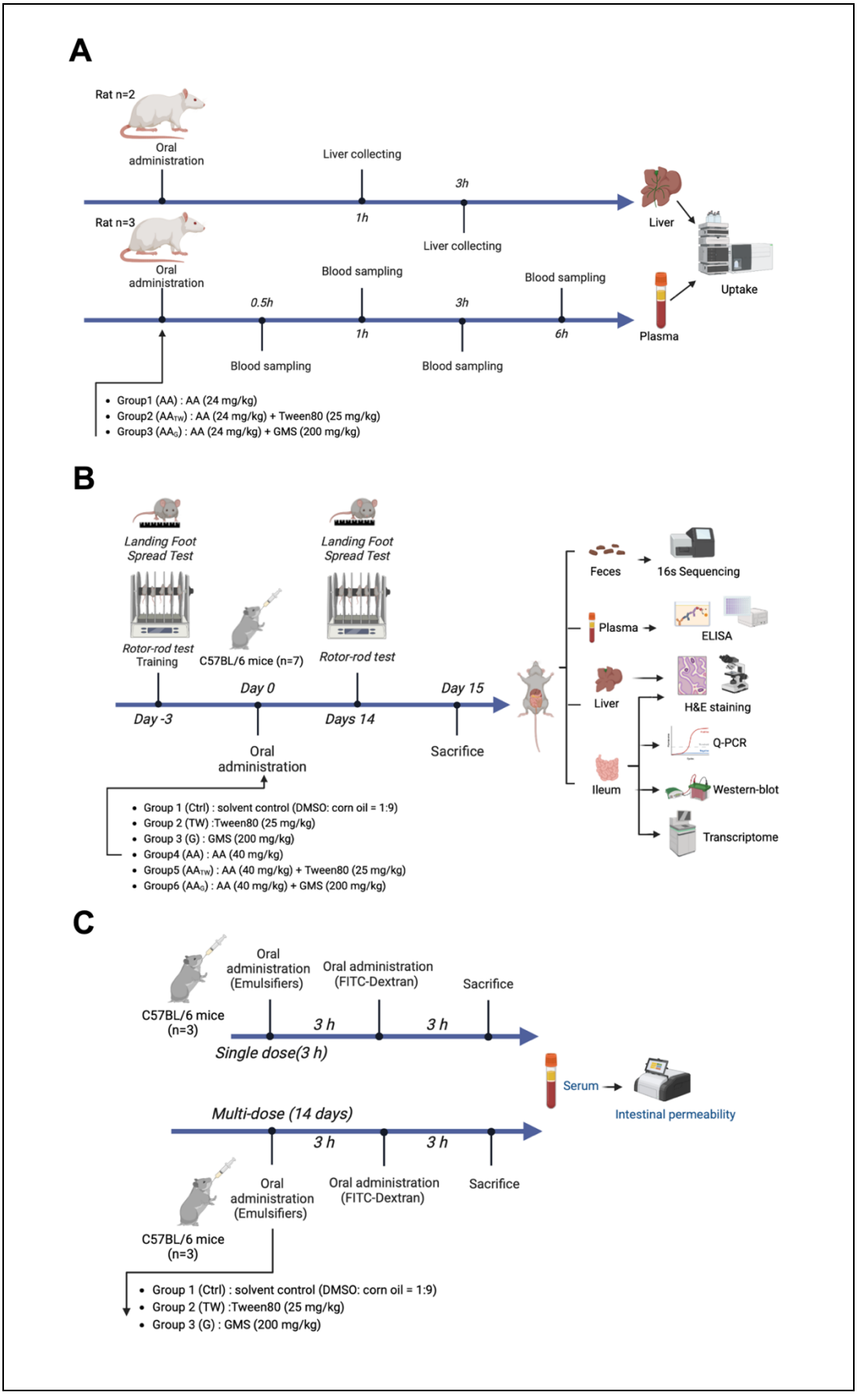

Figure 4.1 Experimental treatments and design.

In the second experiment, 42 male C57BL/6 mice were divided amongst 6 treatments in groups of 7. All individuals were exposed via daily gavage for 14 consecutive days (Fig. 4.1). Plasma of mice were extracted for ELISA assays. Liver were collected for histopathological evaluation. Ileum were collected for RT-PCR, western blot, histopathological evaluation and transcriptome analysis. Fecal sample of mice were collected for 16s sequencing of microbiota. Details of methods used are described in subsequent sections of 4.2.2 – 4.2.6 and 4.2.8-4.2.10.

In the third experiment, 18 male C5BL/6 mice were randomly divided into groups of three. Nine male mice were exposed via gavage for a single dose and sacrifices after 3h and 9 male mice were exposed via daily gavage for 14 consecutive days. Serum were collected to detect the fluorescence of FITC-Dextran and details are provided in 4.2.7.

4.2.2 Necropsy and Sample collection

After 14 days gavage exposure and behavioral test, C57BL/6 mice were euthanized by an intraperitoneal injection of ketamine (300 mg/kg) and xylazine (30 mg/kg), and blood of each mouse was collected by cardiac puncture. Blood in heparin lithium-anticoagulant tubes was centrifuged for 10 mins at 6000 g at 4 °C to collect plasma and stored at -80 °C for further experiments. Ileum from mice were removed, flushed well with cold PBS (10mL syringe with blunt needle), weighed, and snap-frozen in liquid nitrogen and then stored at -80 °C. Fresh feces samples of mice were harvested in a germ-free tube a week before exposure and at day 1, day 6 and day 14 of exposure. They were stored at -80 °C until processed for 16s sequencing.

4.2.3 Ileum gene expression (Quantitative real-time PCR)

Total RNA of samples were extracted with Trizol reagent (Takara, Japan) according to manufacturer's protocol. RNA concentrations were determined by a Nanodrop Lite Spectrophotometer (Thermo Fisher Scientific, US). Synthesis of cDNA

was carried out using Takara PrimeScript™ RT Master Mix (Takara, Japan) on total RNA according to the manufacturer's instructions. The q-PCR was performed on Applied Biosystems QuantStudio 7 Flex Real-Time PCR System using Power-up SYBR Green Master Mix (Applied Biosystems). The thermal cycler parameters were 95 °C for 120 s, 40 cycles of 95 °C for 15 s, and 60 °C for 60 s. Results were normalized to housekeeping gene GADPH expression. Gene expression was calculated using the $2^{-\Delta\Delta CT}$ method. The primers used in this chapter were outlined in Table 4.1.

Table 4.1 List of primer sequences used for qPCR.

Gene	Forward (5'-3')	Reverse (5'-3')	References
iNOS	AGACCTCAACAGCCCTCA	GCAGCCTCTTGTCTTTGACC	(Johnston et al., 2010)
il-1β	TCCAGGATGAGGACATGAGCAC	GAACGTCACACACCAGCAGGTTA	(Kumagai et al., 2015)
Tnfα	CCTGTAGCCCACGTCGTAG	GGGAGTAGACAAGGTACAACCC	(Li et al., 2013)
Fabp2	CTGATTGCTGTCCGAGAGGTT	AGAATCGCTTGGCCTCAACTC	(Shen et al., 2022)
Tlr4	AGCTTCTCCAATTTTTCAGAACTTC	TGAGAGGTGGTGTAAGCCATGC	(Pan et al., 2022)
Occludin	TACTGGTCTCTACGTGGATCAAT	TTCTTCGGGTTTTCACAGCAA	(Ridder et al., 2015)
Claudin1	GGGGACAACATCGTGACCG	AGGAGTCGAAGACTTTGCACT	(Eissa et al., 2018)
Zo-1	CCACCTCTGTCCAGCTCTTC	CACCGGAGTGATGGTTTTCT	(Tsai et al., 2019)
Tlr2	TCTAAAGTCGATCCGCGACAT	CTACGGGCAGTGGTGAAAACT	(Shinji et al., 2021)
Pparγ	AGGACATCCAAGACAACCTGC	TCTGCCTGAGGTCTGTCATC	(Hu et al., 2013)
GADPH	TGTGTCCGTCGTGGATCTGA	TTGCTGTTGAAGTCGCAGGAG	(Ebrahimi et al., 2018)

The ileum samples were weighed, homogenized, and lysed in RIPA buffer with 1 % PMSF and 1 % Protease/Phosphatase Inhibitor Cocktail (Cell Signaling Technologies, USA). The homogenate was centrifuged at 13,000 rpm for 30 min at 4 °C. The supernatant was collected, and concentration of protein was measured by BCA assay (Thermo scientific, USA). Equal amounts of protein were electrophoresed on 12% SDS-PAGE gels. Protein gels were dry blotted onto PVDF membranes with iBlot transfer stacks on the iBlot®2 gel transfer device (Thermo scientific, USA). The PVDF membranes with proteins were blocked with 5 % skimmed milk solution (Bio-Rad, USA) for 1 h at room temperature and followed by incubation with primary antibody targeting p38 MAPK, phospho-specific p38 MAPK, ERK, phospho-specific ERK, Claudin-1, Occludin, and β-actin at 4 °C overnight. After washed with TBST 3 times for 10 mins, the membranes were incubated with secondary antibody for 60 mins. Western ECL substrate reagents (Bio-Rad, USA) will be applied at PVDF membrane. Equal volumes of ECL A and B were fully mixed and added to the membrane and then scanned by BioRad ChemiDoc Touch Imaging System. The protein bands density were quantified using Image J.

4.2.5 Plasma proteins measurements

Levels of pro-inflammatory cytokines monocyte chemoattractant protein (MCP-1) and fatty acid-binding protein 2 (Fabp 2) in plasma were determined by mouse ELISA kits according to the manufacturer's instructions, purchased from Invitrogen Co. (Invitrogen, US) and Novus Biologicals Co. (Novus Biologicals, US) respectively. Expressions were measured using colorimetric peroxidase substrate tetramethylbenzidine, and optical density was read at 450 nm (Thermo Scientific Varioskan LUX Multimode Microplate Reader).

4.2.6 Histopathological evaluation

Following euthanasia, ileum and liver were collected, and fixed in 10 % buffered formalin for 24 h at room temperature. Tissues were then dehydrated with a graded

series of ethanol and cleared through xylene before infiltration and embedment in paraffin wax overnight at 59 °C. Tissues in paraffin wax were sectioned on a microtome at a thickness of 5 µm and mounted onto glass slides. Sections were stained with hematoxylin and eosin and examined under the light microscope.

4.2.7 Intestinal permeability

FITC-dextran intestinal permeability was performed as reported previously (Chassaing et al., 2015; Sharon et al., 2019; Snelson et al., 2021). Animals were randomly assigned and 9 male mice were exposed via gavage of a single dose and 9 male mice were exposed via daily gavage for 14 consecutive days. Each study divided in to three groups (control, TW and G, n=3/ group).

Briefly, mice were individually weighed and fasted for 6 h, and then oral administration of control or emulsifiers. After 3 h, mice were gavaged with 0.1 ml PBS containing 4 KDa FITC-Dextran at 600 mg/kg body weight (Sigma, US). 3 h after gavage of containing FITC-Detran PBS, blood was collected via cardiac puncture and centrifuged at 3000 rpm for 15 mins. C57BL/6 mice were euthanized by an intraperitoneal injection of ketamine (300 mg/kg) and xylazine (30 mg/kg). Fluorescence of FITC-Dextran in serum was determined by Thermo Scientific Varioskan LUX Multimode Microplate Reader (excitation: 488 nm; emission: 520 nm).

4.2.8 mRNA library construction and transcriptomic analysis

RNA was extracted from mice ileum using the RNeasy Mini Kit (Qiagen, Netherlands) according to manufacturer's instruction. RNA concentrations and purity were determined by using a Nanodrop Lite Spectrophotometer (Thermo Fisher Scientific, US). The OD 260/280 value of RNA samples for sequencing ranged from 1.8 to 2.2. For each sample 1µg RNA was used for library construction.

Divalent cations and high temperatures were used to fragment mRNA and poly(A) mRNA was isolated using Oligo (dT) beads (Thermo Fisher Scientific, US). Random primers were used for priming and create first and second strands of cDNA. Purified double-stranded cDNA was treated to repair both ends and add dA-tailing, accompanied by a T-A ligation to add adaptors to both ends. Size of the adaptor-ligated DNA was then selected using DNA Clean Beads. After that, each sample was amplified by PCR with P5 and P7 primers and the PCR products were evaluated. Then the purified products were sequenced on an Illumina NovaSeq platform (Anders, 2010; Wang et al., 2009).

Low-quality reads and contaminations were filtered out before data analysis using Cutadapt (v 1.9.1) (Martin, 2011). Adapter sequences were also removed during this step. The reference genome (HISAT2, v 2.0.1) was then aligned with the filtered data (Kim et al., 2015). Gene expression was detected by HTSEQ (v 0.6.1) and the differentially expressed genes (DEGs) analysis was performed by DESeq2 (v 1.6.3) (Anders and Huber, 2010). For the GO enrichment analysis, the DEGs were compared to all reference genes using GOseq (v 1.34.1) (Gene Ontology Consortium, 2004). Ingenuity Pathway Analysis (IPA) core analysis (Version 01–13, Ingenuity Systems, Redwood City, CA, USA) for molecular network analyses. Pathway enrichment analysis was carried out using KEGG (Kyoto Encyclopedia of Genes and Genomes) (Kanehisa and Goto, 2000). The Rich factor, P-value and DEGs number were shown in the enriched pathway. The ratio of differentially expressed gene numbers annotated in this pathway to the total gene numbers annotated in this pathway is defined as Rich factor. Greater Rich factor indicates greater intensity. Q value is a corrected P-value ranging from 0 to 1, with a lower value indicating greater intensity.

4.2.9 High-throughput 16S sequencing and analysis

Microbial genomic DNA extraction of fecal samples were carried out using TIANamp Stool DNA Kit (TIANGEN, China) according to the manufacturer's

instructions. DNA concentration and purity were measured by a Nanodrop Lite Spectrophotometer (Thermo Fisher Scientific, US). Extracted DNA was sent to Meiji company (Meiji, China). All qualified DNA was used to construct a library with primers (forward 338F: 5′- ACTCCTACGGGAGGCAGCAG -3′ and reverse 806R: 5′-GGACTACHVGGGTWTCTAAT -3′) targeting the V3-V4 region of the 16S rRNA gene. Purified amplicons were sequenced on an Illumina MiSeq PE300 platform (Illumina, San Diego, USA) based on the standard protocols by Majorbio Bio-Pharm Technology Co. Ltd. (Shanghai, China). Raw FASTQ files were de-multiplexed with an in-house perl script, quality-filtered with fastp (v 0.19.6) (Zhou., 2018), then merged with FLASH(v 1.2.11) (Magoč and Salzberg, 2011). The optimized sequences were then grouped into operational taxonomic units (OTUs) with 97% sequence similarity using UPARSE (v 11) (McDonald et al., 2012; Schumann, 2011). The most abundant sequence for each OTU was chosen as a representative sequence. The number of 16S rRNA gene sequences of each sample were rarefied to 20,000 to reduce the impact of sequencing depth on α and β diversity measurements. 16S Bioinformatic analysis of the gut microbiota was carried out using the Majorbio Cloud platform (https://cloud.majorbio.com). Rarefaction curves and α diversity index (including observed species, Chao index and Shannon index) were used by Mothur (v 1.10.1) based on OUTs. The percentage of variation explained by the treatment and its statistical significance was determined by the PERMANOVA test using Vegan package (v 2.5-3).

4.2.10 Motor coordination test

Before gavage exposure began, individual mice were trained for rotor-rod test for three consecutive days. At the end of the gavage exposure for 14 d, all mice were subjected to land foot spread test and rotor-rod test. Each mice had three trials for each test.

The landing foot spread test was used for testing nervous system effect of chemicals or drug according to the protocol of functional observatory battery testing of US EPA, as described in detail previously (Davuljigari et al., 2021; Ekuban et al., 2021; EPA, 1998). Briefly, mice were applied a food dye ink on the soles of the hindlimb and were held in vertically with the nose 15 cm above the bench. After dropped on the white paper, the distance of hindlimb was recorded. Wider distance between two hindlimb foot print indicate inability to coordinate landing thus nervous damage (Ekuban et al., 2021) . This test was performed three times and double-blinded.

Rotor-rod test was according to the protocol as described (Fan et al., 2010; Wu et al., 2020). Before test, mice were trained to adapt on staying on a rotating rod for 1 minute at 4 rpm, and then the rod was accelerated from 4 to 40 rpm progressively over a period of 5 mins. Duration a mouse can stay on the rotating rod was recorded as an indicator of motor coordination.

4.2.11 Statistical analyses

All results were expressed as mean ± standard deviation (SD). Analysis of variance (ANOVA) and Tukey's multiple-comparison test was used to evaluate statistical differences between biological endpoints of different treatments. All other analyses were performed using GraphPad Prism 8.0 (GraphPad Software, CA).

4.3 Results

4.3.1 Emulsifiers increased internal AA and metabolite GA concentration

Absorption of AA was rapid and can be readily detected in the plasma as quickly as 0.5 h after exposure and in the liver after 1 h. Metabolism of AA was also observed as AA concentration decreased in the plasma and liver while GA concentration increased over time (Fig. 4.2). Emulsifiers did not cause any change in AA concentration in plasma, but plasma GA concentration was significantly increased. AA_{TW} and AA_G both significantly increased plasma GA at 3 h, by 52 % and 84 %, respectively (Fig. 4.2 B). Concentration of AA in the liver was significantly decreased by emulsifiers in 1 h but the concentration was the same in all treatments at 3 h. Liver GA concentration showed the reverse pattern, where no difference was observed in 1 h but emulsifiers increased GA concentration at 3 h. At 3 h, AA_{TW} significantly increased liver GA by 38.5 %, and AA_G increased liver GA by 11.5 % (Fig. 4.2 D).

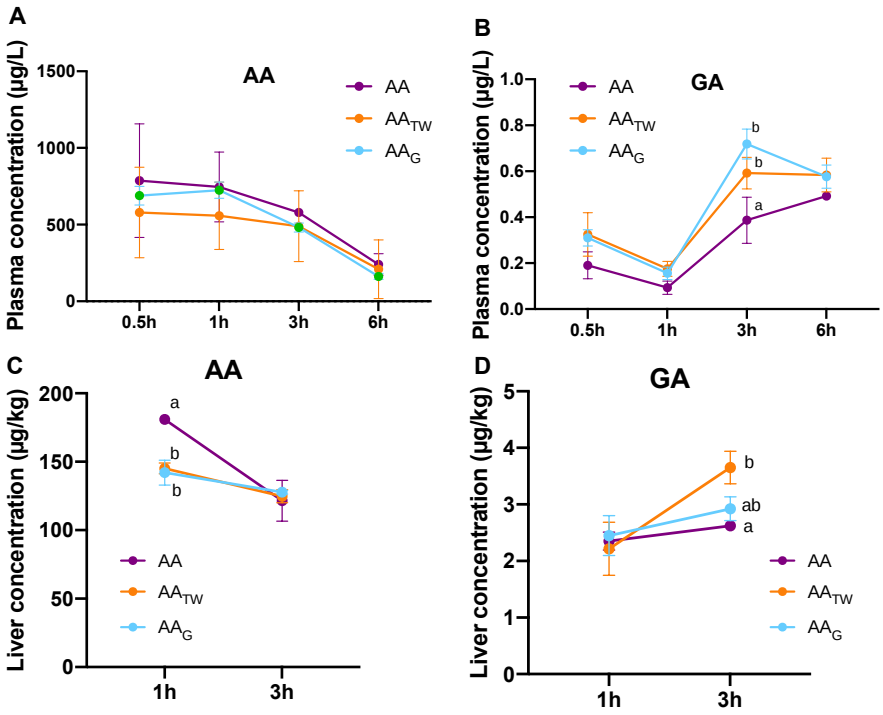

Figure 4.2 *Concentration of AA and its metabolite glycidamide (GA) after a single dose of gavage of AA (24 mg/kg) with or without emulsifiers (TW or G) in (A) and (C) plasma and (B) and (D) liver of rats respectively. Different letters represent statistically different values.*

4.3.2 Expression of genes of interest

Genes related to inflammation and gut barrier integrity were examined. TW alone had significant effect on expression of iNOS, Tlr2 and Tlr4 while G only had effect on iNOS (Figs. 4.3 A-C). AA_G led to significantly higher expression of proinflammatory biomarkers iNOS, TNFα and il-1β than AA. Relative to AA, AA_{TW} also caused significantly higher expression of another two genes Tlr2 and Tlr4 by 1.76 and 2 folds respectively, as well as PPARγ by 2.75 folds (Figs. 4.3 D, E).

Emulsifiers alone have no significant effect on the gene expression of tight junction proteins. However, Occludin and Claudin 1 in ileum were decreased when co-exposed with AA and emulsifiers. AA lowered another tight junction proteins Zo-1 expression, however there were no significant changes in Zo-1 expression in the AA_{TW} and AA_G groups as compared to AA. The mRNA level of Fabp2 in the ileum was lowered by 64.7 % and 50.8 % in the presence of TW and G, respectively, compared to the control group, and by 41.2 % and 50.0 % in the presence of AA_{TW} and AA_G, respectively, compared to the AA group.

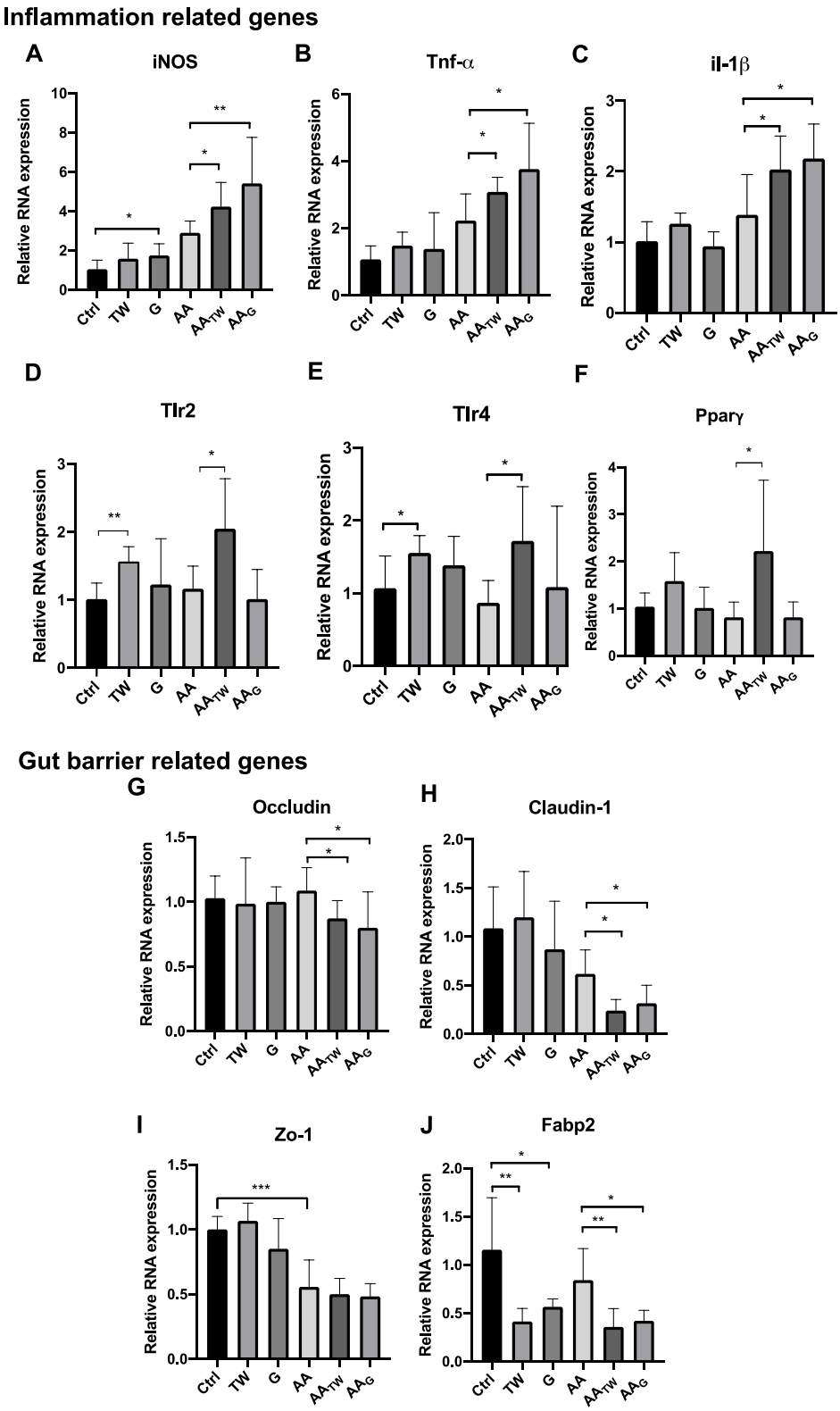

Figure 4.3 *Expression of genes related to inflammation and gut barrier integrity of mice ileum after exposure to 14 days emulsifiers, AA, AA_{TW} and AA_G. GADPH was used as an internal control. Asterisks indicate statistical significance *<0.05, **<0.01, ***<0.001.*

4.3.3 Ileum protein expression

Expression of proteins related to inflammation and gut barrier integrity in the ileum showed that emulsifiers could exacerbate toxicity of AA. The stress activated protein kinases (p38/SAPKs) and the extracellular signal regulated kinases (ERKs) are belong to MAPK pathways (Cuschieri and Maier, 2005). MAPKs are stimulated by Toll-like receptors (TLRs), which lead to increase inflammation (Rogero and Calder, 2018). Emulsifiers have no significant effect on protein levels of p-p38 and p-ERK. Compared with AA, AA_{TW} significantly increased the expression of p-p38, while AA_G increased the expression of p-ERK. Expression of Occludin and Claudin of ileum were not changed significantly by emulsifiers. Compared with AA, AA_{TW} and AA_G significantly decreased the expression of Claudin.

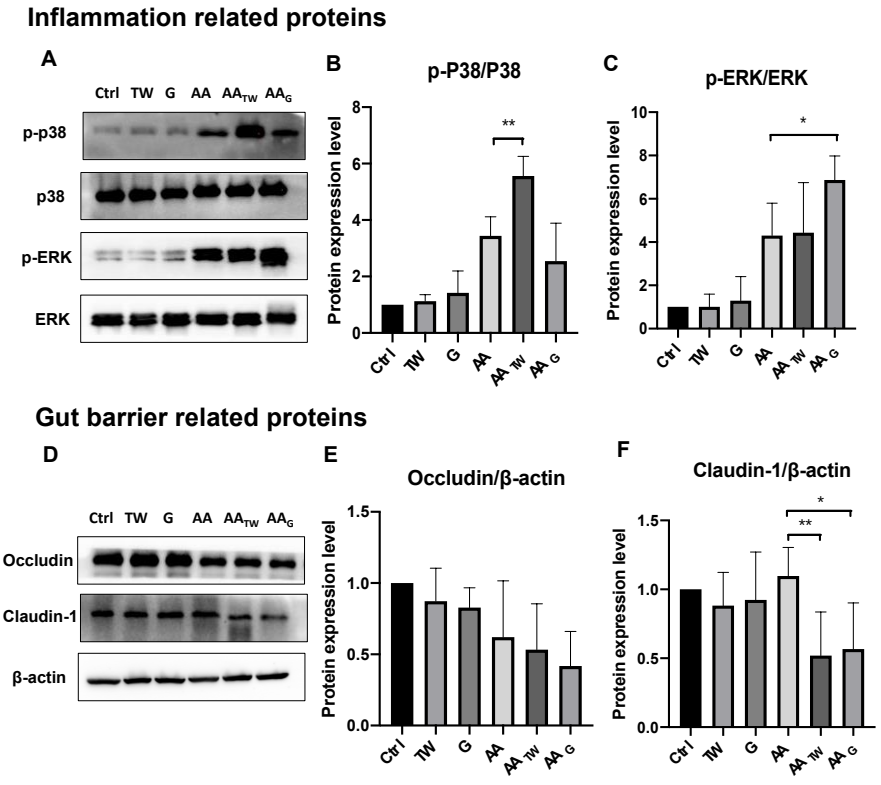

Figure 4.4 *Expression of phospho-p38 (p-p38) and phospho-ERK (p-ERK) using total p38 and total ERK as internal control (A-C) of mice ileum after exposure to 14 days emulsifiers, AA, AA_{TW} and AA_G. Expression of Occluding and Claudin-1 using β-actin as internal control (D-F)*

*of mice ileum after exposure to 14 days emulsifiers, AA, AA_{TW} and AA_G. Asterisks indicate statistical significance *<0.05, **<0.01, ***<0.001.*

4.3.4 Plasma protein levels

Plasma MCP-1 level was significantly higher in AA_{TW} and AA_G compared with AA (Fig.4.5 A). Compared with AA, there was no significant increase in level of Fabp2 in AA_{TW} and AA_G although a trend was observable (Fig.4.5 B).

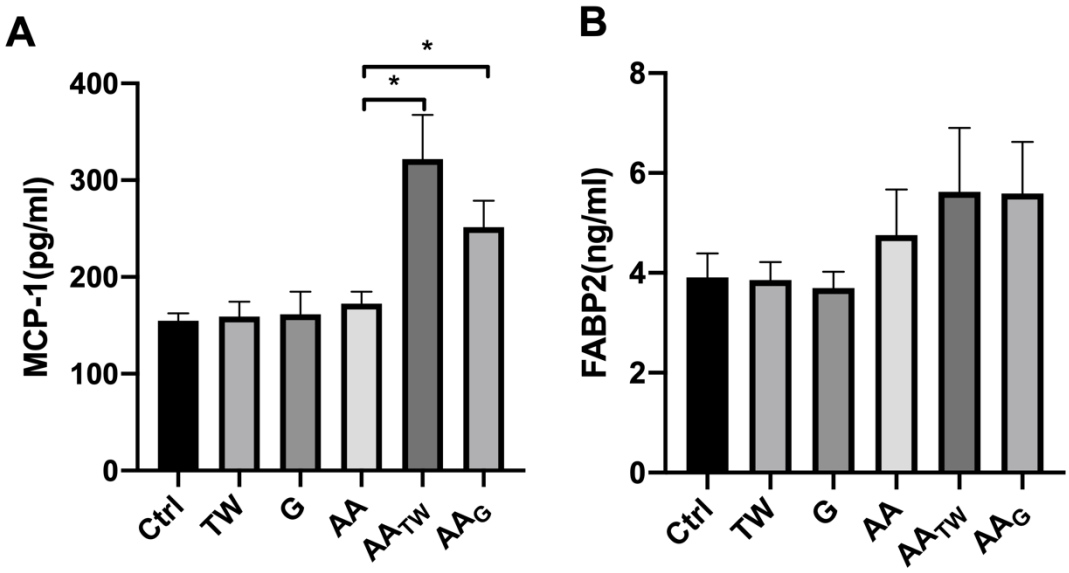

Figure 4.5 *Plasma (A) MCP-1 and (B) Fabp2 levels in mice after 14 days oral administration of emulsifiers, AA, AA_{TW} and AA_G. Asterisks indicate statistical significance *<0.05, **<0.01, ***<0.001.*

4.3.5 Histopathology

Liver of the control treatment was healthy and with ample deposit of glycogen (Fig. 4.6 A). In the TW treatment, there were minor infiltration of immune cells (Fig. 4.6 B, red arrow). More immune cell infiltration was observed in the AA treatment (Fig. 4.6 D). In the AA_{TW} treatment (Fig. 4.6 E), infiltration of immune cells were observed (Fig. 4.6 E, red arrow) and the presence of eosinophilic cytoplasm (Fig 4.6 E, black arrow) and fragmented nuclei (Fig. 4.6 E, green arrow). Similar signs of degradation of hepatocytes were observed in AA_G treatment (Fig. 4.6 F) but not as severe as $AA_{TW.}$

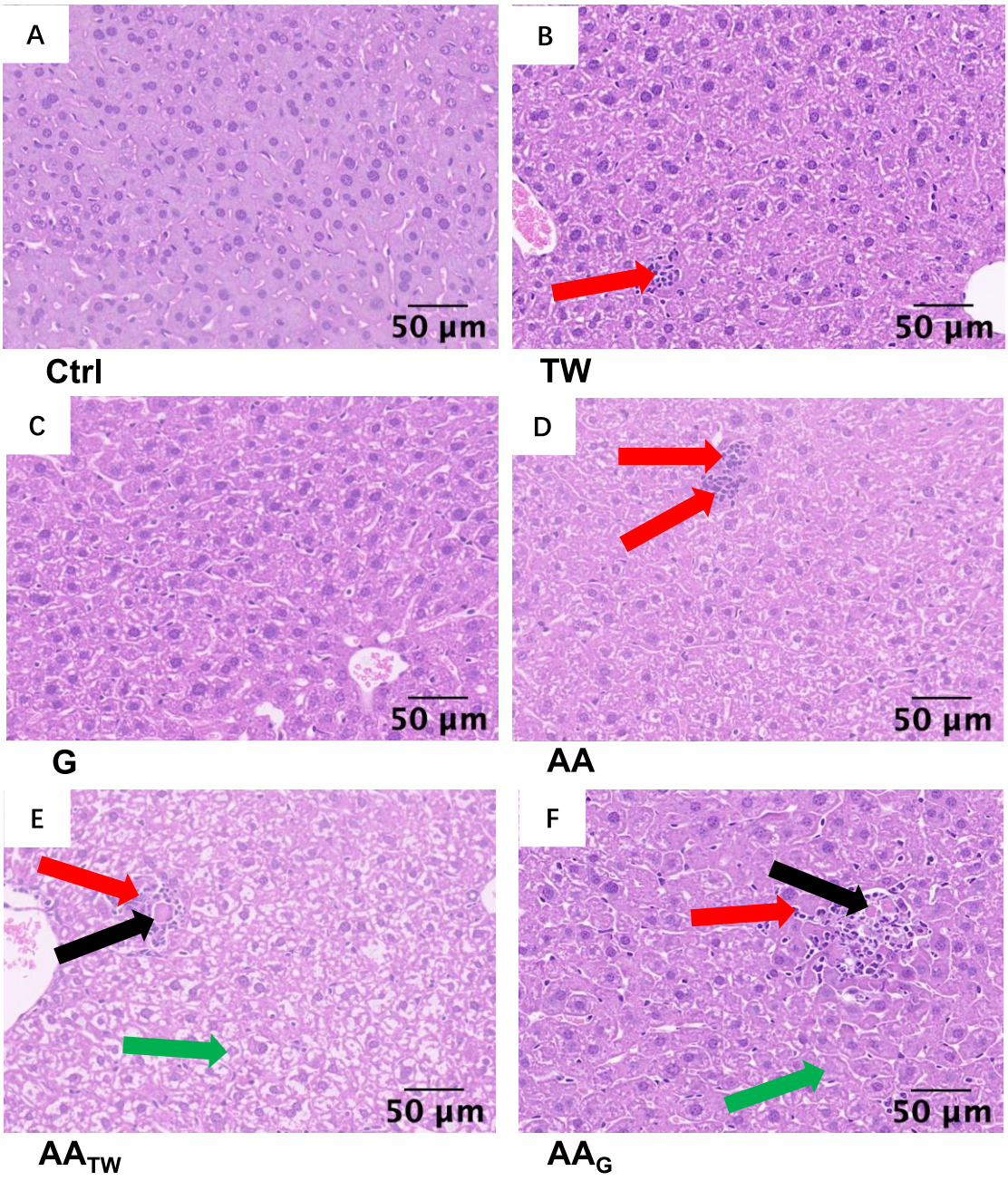

Figure 4.6 *Representative images of mice liver after 14-day oral administration of A) control treatment, B) Tween80 (TW), C) Glycerol monostearate (G), D) Acrylamide (AA), E) Acrylamide + TW (AA_{TW}) and F) Acrylamide + G (AA_G). Red arrows indicate infiltration of immune cells, black arrows indicate enhancement of eosinophilic cytoplasm, green arrows indicate fragmented nuclei. Scale bar = 50 µm.*

Healthy ileum with intact long villi structures was observed in control mice (Fig. 4.7 A). Emulsifiers alone also did not lead to change in the ileum (Figs. 4.7 B, C). In

AA, AA_{TW}, and AA_G treatments, damage in villi structures were observed (Figs. 4.7 D-F). Villi tips are partly damaged and villi length were much shorter than that of control. There were also severe fusing of villi structures in AA_{TW} (Fig. 4.7 E).

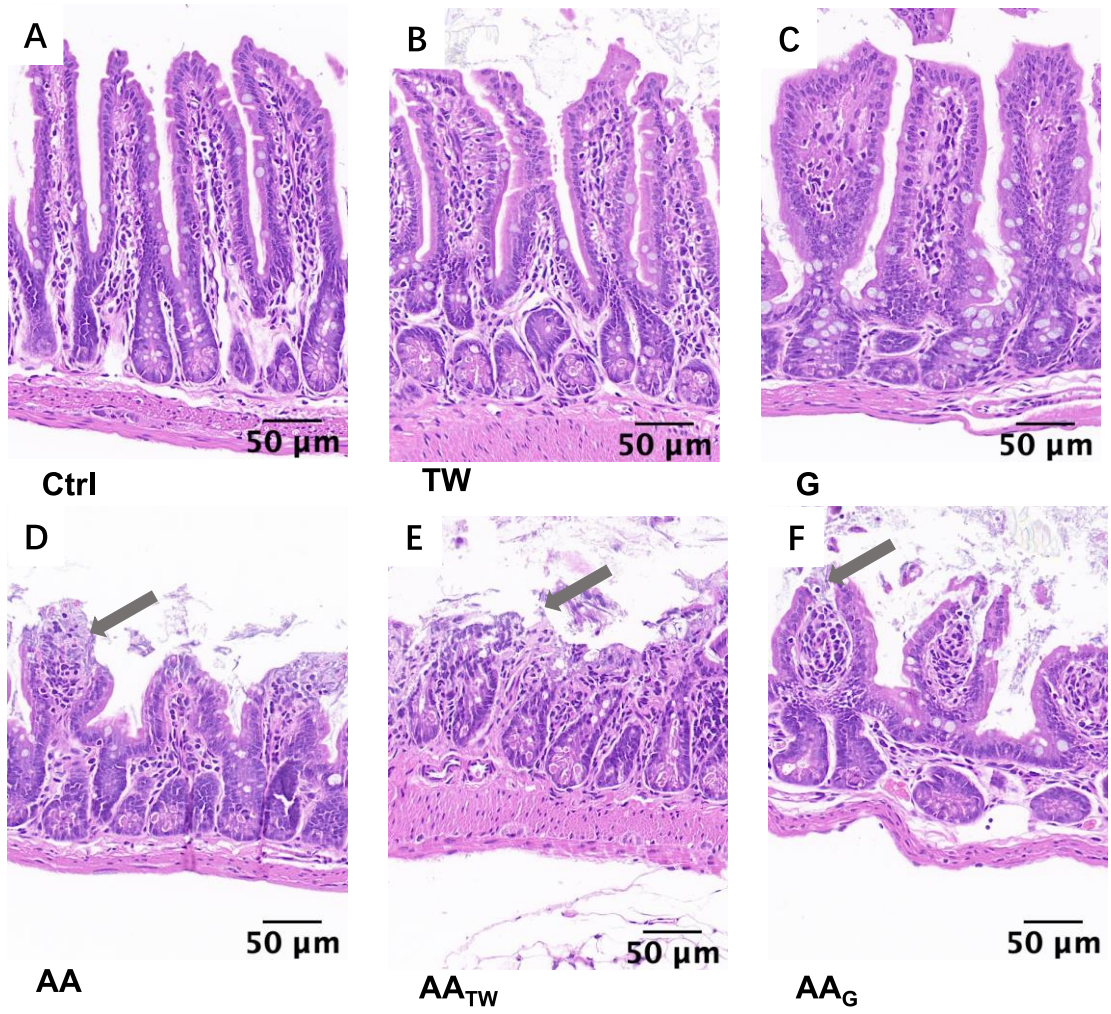

Figure 4.7 *Representative images of mice ileum after 14-day oral administration of control A) treatment, B) Tween80 (TW), C) Glycerol monostearate (G), D) Acrylamide (AA), E) Acrylamide + TW (AA_{TW}) and F) Acrylamide + G (AA_G). Grey arrows indicate damaged villi. Scale bar = 50 µm.*

4.3.6 Emulsifiers increased gut permeability

FITC-dextran level in serum is positively related to gut permeability. There was no significant difference in FITC-dextran concentration after 3 h of oral administration of TW or G. But TW significantly increased the permeability of FITC dextran through the gut after 14 days of gavage as serum dextran concentration was increased (Fig. 4.8). A similar increasing trend was observed for G at day 14 but the change was not significant.

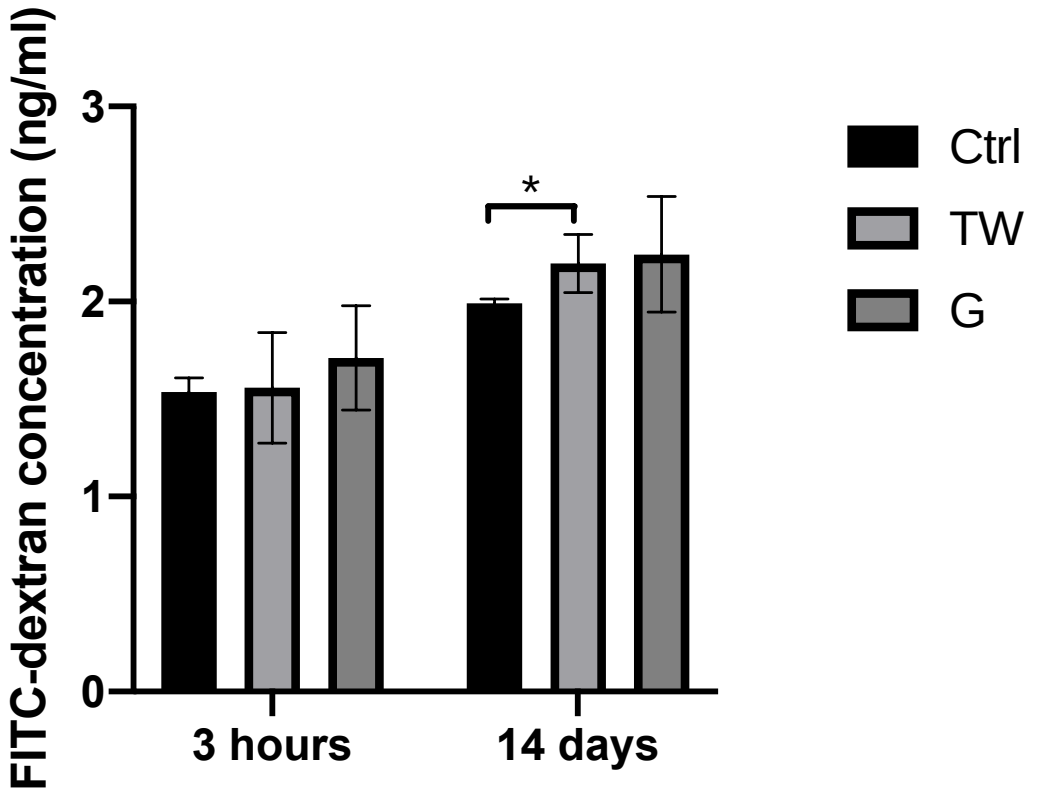

Figure 4.8 *FITC-dextran concentration of serum in the mice after 3 h and 14 days oral administration of emulsifiers. Asterisks indicate statistical significance *<0.05, **<0.01, ***<0.001.*

4.3.7 Transcriptomic changes in the ileum

Volcano plots were created to visualize the distribution of fold changes in expressed genes in the ileum between A) control (Control) and AA, B) AA and AA_{TW}, and C) AA and AA_G respectively (Fig. 4.9). In the three comparison groups, around 55

thousand genes were analyzed. There were 1,021 significant differentially expressed genes (DEGs) (453 down-regulated and 568 up-regulated) between Control and AA group (Fig.4.9 A). More DEGs were up-regulated than down-regulated and the fold change of up-regulation was also higher. Number of DEGs comparing AA and AA_{TW} and AA and AA_G were similar and were 454 and 472 respectively (Figs.4.9 B, C). Comparing AA and AA_{TW} the number of up-regulated and down-regulated DEGs were similar (243 vs 211) with slightly more down-regulated DEGs. Comparing AA and AA_G there were more down-regulated DEGs (267) than up-regulated ones (205).

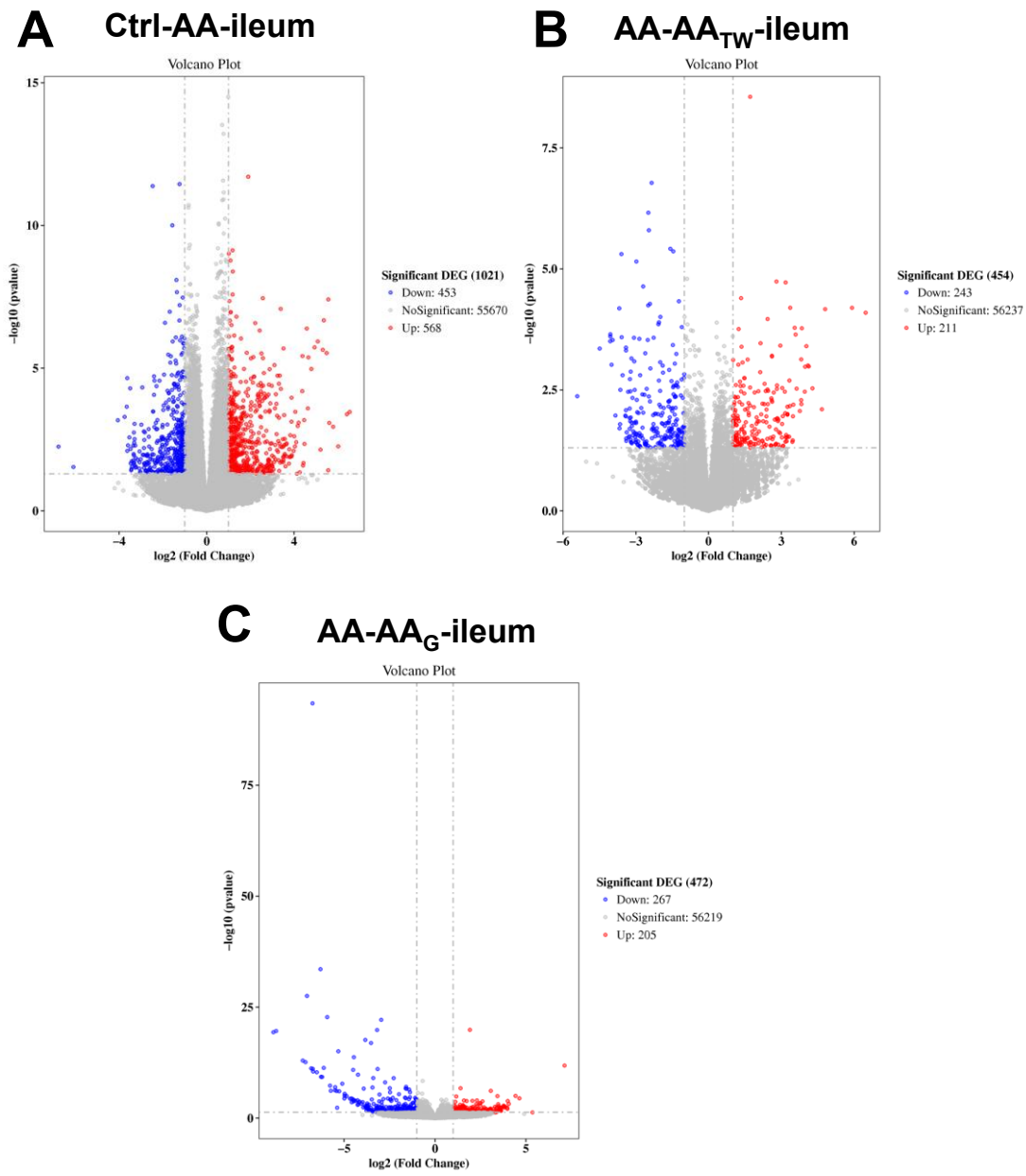

Figure 4.9 *Identification of the differentially expressed genes (DEGs) of mice ileum after exposure to 14 days, AA, AA_{TW} and AA_{G}. (A-C) Volcano plots of genes showing significantly different expression in ileum. X axis indicates fold change (log2) whereas Y axis shows p value (-log 10). Red dots or blue dots represent up-regulation or down-regulation respectively. Grey dots mean genes with no significant changes.*

Based on these DEGs, GO analysis for biological processes was performed (Fig. 4.10). The top 10 enriched pathways of these three pairs of comparison were mostly related to immune regulation (B cell receptor signaling pathway, positive regulation of

B cell activation, complement activation, adaptive immune response, immune response and phagocytosis). This showed that the primary response of the ileum to AA exposure was related to inflammation. Comparing AA against AA_{TW} or AA_{G} yielded other biological processes (fibrinolysis, organic acid metabolic process and exogenous drug catabolic process). This suggested that emulsifiers not only exacerbated inflammation caused by AA, they also led to other toxicities.

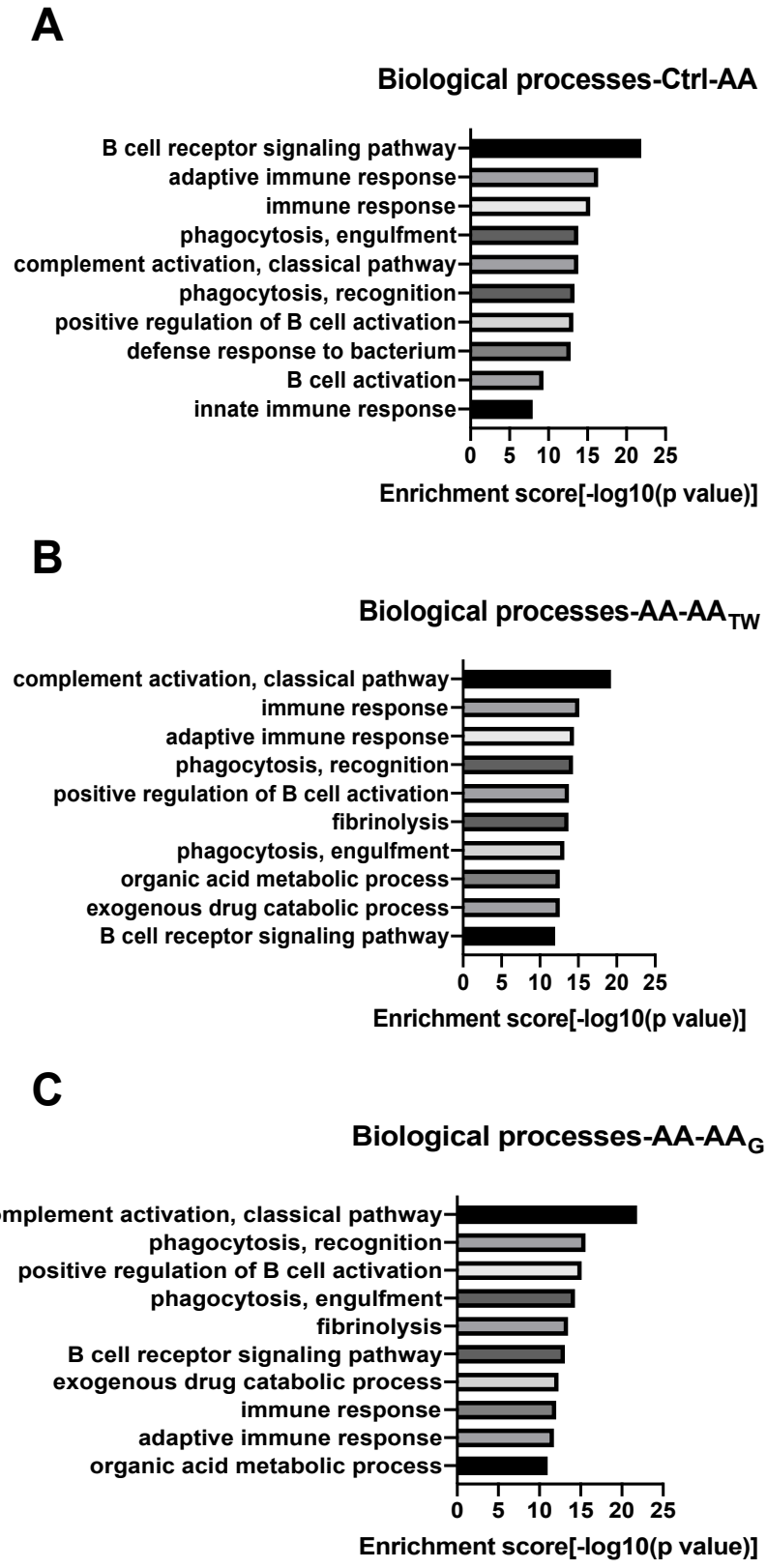

Figure 4.10 *Mice ileum biological processes of GO Ontology between (A) Control and AA, (B) AA and AA_{TW} and (C) AA and AA_{G}. The y-axis displays biological processes. The bars on the x-axis represent the enrichment score (log 10(p-value)) for each biological processes.*

Molecular networks analyses based on DEGs suggested that top three networks affected by AA were hematological system development and function, immune response, and gastrointestinal disease (Table 4.2). Using DEGs by comparing AA with AA_{TW} or AA_{G} showed the same top molecular network of hematological system development and function, suggesting that addition of emulsifiers primarily increased toxicity caused by AA. However, the second and third molecular network changed. When TW was added, inflammatory response, and lipid metabolism were perturbed. When G was added, organismal injury and abnormalities, and lipid metabolism were detected. These results suggested that addition of emulsifiers could increase the types of toxicity caused by AA.

Table 4.2 The top three molecular networks of mice ileum based on differentially expressed genes (DEGs) between Control and AA, AA and AA_{TW}, and AA and AA_G after 14-day exposure. DEGs are indicated in bold text.

Analysis	ID	Molecules in Network	Score	Focus Molecules	Top Diseases and Functions
Control-AA	1	BCR (complex), **CACNA1I**, **CD79A**, **CNR2**, **COCH**, **CXCL13**, **CXCR5**, **DEPP1**, ERK1/2, **FCMR**, **FCRL1**, **GAREM1**, **GCSAM**, **GDF15**, **GPR183**, **GUCY1A2**, **IL5RA**, **LAPTM5**, **LAT2**, **LPXN**, **MAP3K19**, NADPH oxidase, **NUDT5**, **PCSK1N**, **PRR7**, **RAC2,** Rap1, **RPL34**, Rsk, RXFP3, **SIGLEC10**, **TACSTD2**, **TNFSF8**	44	30	Hematological System Development and Function, Humoral Immune Response, Lymphoid Tissue Structure and Development
	2	**AICDA**, **AIRE**, **CCL19**, **CCL21**, **CD83**, **Chil3/Chil4**, **CLEC4E**, **COL9A3**, **CORO1A**, **CSN2**, **DLEU7**, **DOK3**, **Glycam1**, **Havcr1**, **HLA-DMB**, HLA-DR, **HSPB2**, Iga, **IL13RA2**, **IL17B**, **IL21**, **LILRB3**, **LTA**, **LTB**, **Madcam1**, NFAT (complex), NFkB (complex), **NIBAN3**, SAA, **SNN**, **SPIB**, **SRCAP**, **TDO2**, **TNFSF18**, **ZBTB32**	44	30	Cellular Development, Humoral Immune Response, Protein Synthesis
	3	**ACOD1**, Alpha Actinin, **Apol10a (includes others)**, **ATP6V0D2**, **BGLAP**, **BIN1**, **CSHL1**, **Cyp2d9 (includes others)**, **DSC3**, EGLN, **GATA4**, **H2-Eb2**, **HBB**, Histone h3, Histone h4, **HMX2**, **KRT14**, **KRT17**, **LEF1**, **LHX3**, **LRG1**, **Mup1 (includes others)**, **MYL4**, N-cor, **Orm1 (includes others)**, **PARVG**, **PLAG1**, **RIMS2**, RNA polymerase II, **RRAGD**, **S100A4**, **Serpina3g (includes others)**, **TBX6**, **TNFSF11**, **Trim43b (includes others)**	41	29	Gastrointestinal Disease, Inflammatory Disease, Inflammatory Response
$AA\text{-}AA_{TW}$	1	ADCY, Akt, ALT, **APCS**, **ASAH2**, **AZGP1**, **BST1**, **C5**, **C9**, Collagen Alpha1, **CPB2**, **CYP27B1**, **CYP2A6 (includes others)**, **Cyp2c70**, **CYP2F1**, **CYP3A5**, **CYP8B1**, **DRD1**, **F12**, **FYB2**, **GRM5**, **GYS2**, **IL17C**, **IL17F**, **KNG1**, Ldh (complex), **LEAP2**, **NR1I3**, **PLG**, **PTGDR**, **PTGDS**, **SCN1A**, **SLC10A1**, **SLCO1B3**, **UGT2B17**	53	30	Hematological System Development and Function, Lipid Metabolism, Molecular Transport
	2	**ADORA2B**, **AHSG**, **ALB**, amylase, **ARG2**, **CAMKV**, **DDN**, GOT, **HES5**, **HPX**, IL12 (complex), **ITIH1**, **ITIH2**, JAK1/2, **MAL**, MAP2K1/2, **MBL2**, MHC Class II (complex), MHC II, Mlc, **Mug1/Mug2**, Mup1 (includes others), NFkB (complex), PRKAA, RAS, **SERPINA1**, **SERPIND1**, **SLC17A7**, **SLC1A2**, **SLC2A5**, **SLC9A3**, **SPHK1**, **TDO2**, **TRIB3**, **TRIM38**	38	24	Amino Acid Metabolism, Cellular Compromise, Inflammatory Response
	3	**ABCB11**, ACADVL, ACOX1, ACSS1, **APOM**, **C8B**, **C9**, **CES3**, **Cyp2a12/Cyp2a22**, **Cyp2c54 (includes others)**, **CYP2C8**, **Cyp2d9 (includes others)**, **CYP3A5**, **CYP4A11**, **Cyp4a14**, EHHADH, **FAM151A**, **HAL**, **HGD**, **Igkv4-91**, IRF2BP2, **KNG1**, LEP, LY6D, **Mup1 (includes others)**, **Nat8f2**, NEDD9, **PAH**, PKD1, SCP2, **SLC22A25**, **SLC27A5**, **Spag6**, STAT5B, **Uox**	38	24	Energy Production, Lipid Metabolism, Small Molecule Biochemistry
$AA\text{-}AA_G$	1	**ABCB11**, Akt, **ANGPTL3**, **APOA2**, **APOA5**, **APOF**, **APOM**, **AZGP1**, **CPB2**, **CRP**, **CYP8B1**, **F12**, **F2**, **FGA**, **FGB**, **FGG**, **FYB2**, **GAD1**, **GRM5**, HDL, HDL-cholesterol, **KNG1**, **KRT17**, **LCAT**, LDL, LDL-cholesterol, **NR0B2**, **PIERCE1**, **PON1**, **PTGDS**, **SCN1A**, **SERPINC1**, **SERPIND1**, SYK/ZAP, VLDL-cholesterol	48	28	Cardiovascular Disease, Hematological Disease, Hematological System Development and Function
	2	**AHSG**, **APOH**, **CAMKV**, **CCL20**, Collagen type II, **CYP1A2, CYP2A6 (includes others)**, **DDN**, EGLN, **GAD2**, **GC**,**Hamp/Hamp2**, **HPX**, **ICAM5**, JAK1/2, **MAL**, MHC II, Mlc, **Mt2**, **Mup1 (includes others),** NFkB (complex), **NR1D1**, Nuclear factor 1, **SERPINA1**, **SERPINA3**, **SLC17A7**, **SLC1A2**, **SLC6A1**, **Slco1a1**, **TBR1**, TCF, **TDO2**, **TMPRSS6**, **UGT2B17**, Vegf	43	26	Hereditary Disorder, Neurological Disease, Organismal Injury and Abnormalities
	3	26s Proteasome, **AADAT**, **ACTA1**, **AKR1D1**, **BEST1**, **CASP14**, CG, **ELAVL2**, **ELOVL3**, **ENPP3**, FSH, **GATA4**, **GJB6**, Histone h3, **HMGCS2**, **HSD3B1**, **Hsd3b4 (includes others)**, **INSL5**, Insulin, **KCNK9**, **LCT,** Lh, LYPD3, **NR1D2**, **NR2E3**, **Nrxn3**, **OPN1SW**, **PAPPA**, **PPY**, **PVALB**, **RBFOX1**, RNA polymerase II, **SLC12A5**, Sos, **ZIC1**	43	26	Endocrine System Development and Function, Lipid Metabolism, Small Molecule Biochemistry

Using KEGG pathway analysis, nine of the top ten pathways affected by AA were linked to the regulation of immune system (Fig. 4.11). The top pathway was C5-Branched dibasic acid metabolism, which is part of carbohydrate metabolism (Ibrahim and Anishetty, 2012). Carbohydrate metabolism would be increased during inflammation (Wu et al., 2013) and may still be related to toxicity of AA to the immune system.

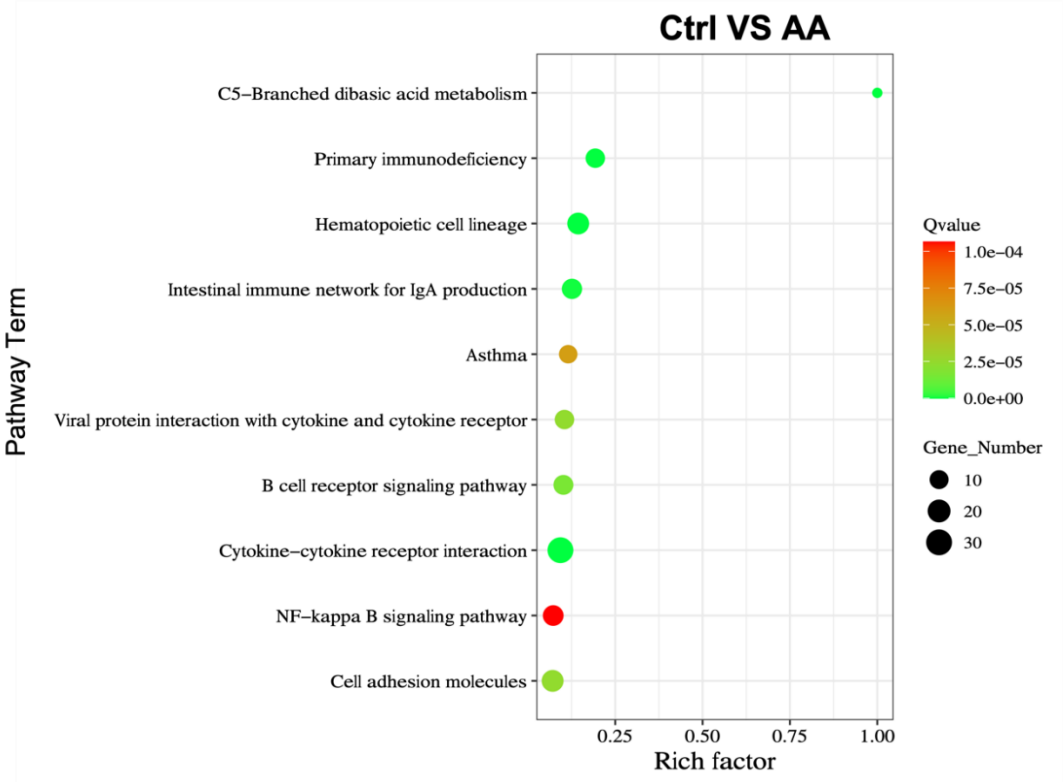

Figure 4.11 *KEGG pathway enrichment analysis of DEGs between Control and AA in ileum. The larger the Rich factor and the smaller the Q-value, the higher the significance.*

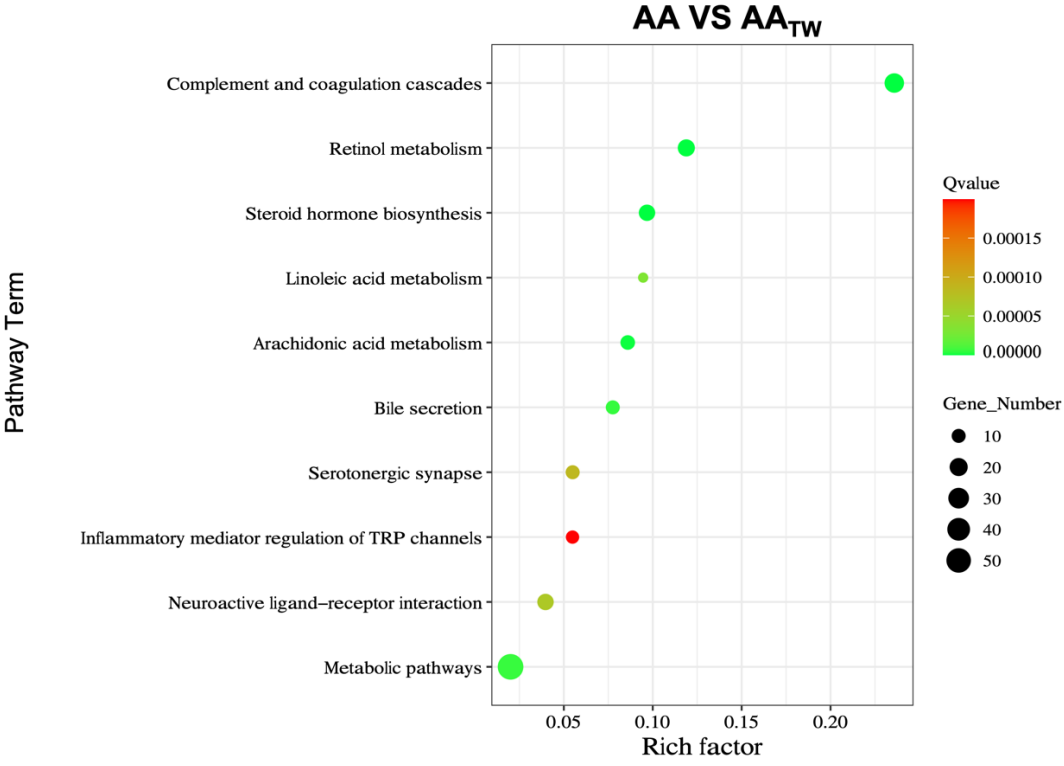

Figure 4.12 *KEGG pathway enrichment analysis of DEGs between AA and AA_{TW} in ileum. The larger the Rich factor and the smaller the Q-value, the higher the significance.*

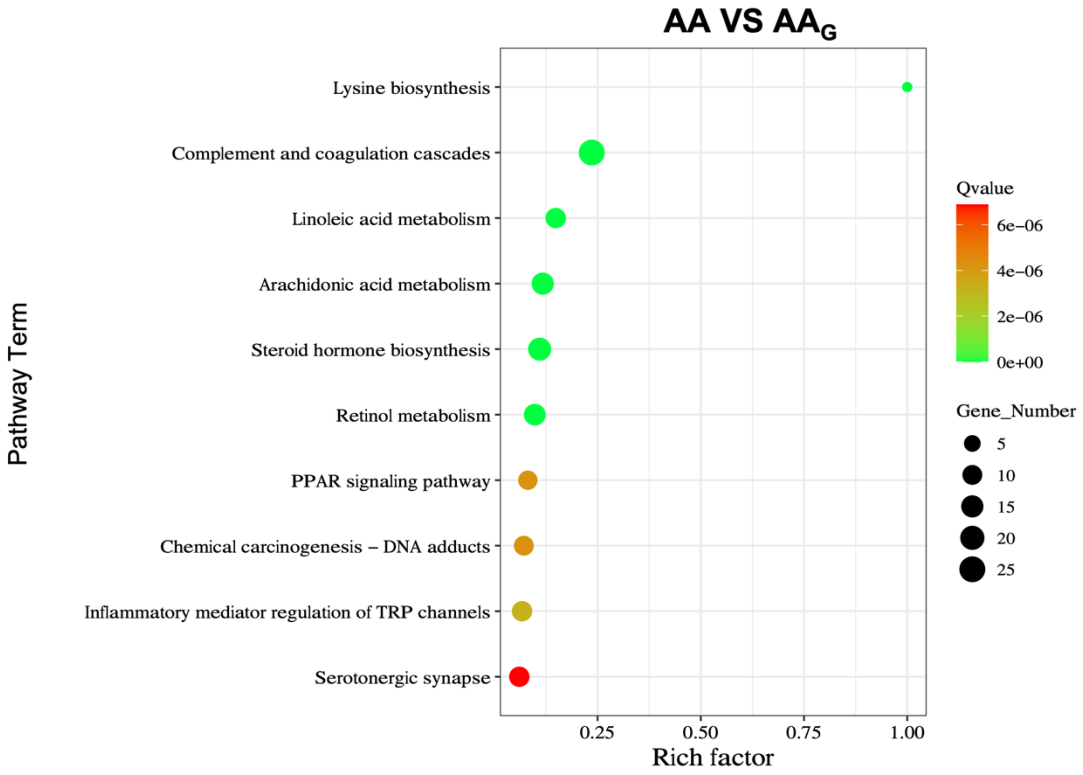

Figure 4.13 *KEGG pathway enrichment analysis of DEGs between AA and AA$_G$ in ileum. The larger the Rich factor and the smaller the Q-value, the higher the significance.*

Addition of TW led to shift in KEGG pathways impacted (Fig. 4.12). In the top 10 pathways, only two were related to immune system regulation (complement and coagulation cascades, and inflammatory mediator regulation of TRP channels.), six were related to obesity and lipid metabolism (retinol metabolism, steroid hormone biosynthesis, linoleic acid metabolism, arachidonic acid metabolism, bile secretion, and metabolic pathways), and two were connected to the nervous system (serotonergic synapse and neuroactive ligand-receptor interaction).

Addition of G led to shift in KEGG pathways impacted (Fig. 4.13). The top 10 KEGG pathways included two involved in immune system regulation (complement and coagulation cascades, inflammatory mediator regulation of TRP channels), six in obesity and lipid metabolism (lysine biosynthesis, linoleic acid metabolism, arachidonic acid metabolism, steroid hormone biosynthesis, retinol metabolism, PPAR

signaling pathway), one in carcinogenesis (chemical carcinogenesis - DNA adducts) and one related to the nervous system (serotonergic synapse). It is interesting that AA_{TW} and AA_G both influenced six identical pathways related to obesity and lipid metabolism, including retinol metabolism, steroid hormone biosynthesis, linoleic acid metabolism, and arachidonic acid metabolism.

Analyses results of GO biological processes, molecular networks and KEGG pathways all showed that AA_{TW} and AA_G not only interfered with immune system regulation but also had potential impact on the lipid metabolism and cause neurological damages. This confirms that emulsifiers not only reinforced toxic mechanism of AA (i.e. inflammation) in the ileum, they also created other toxic mechanisms.

4.3.8 Microbiota changes caused by AA and emulsifiers

4.3.8.1 α-diversity were not changed by AA and emulsifiers

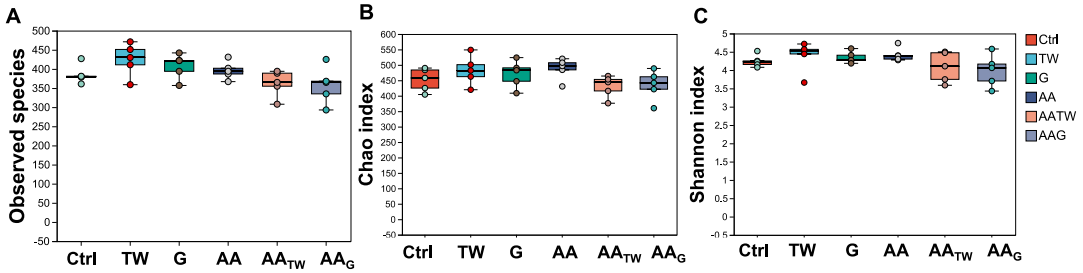

Figure 4.14 *Comparison of α-diversity analysis of intestinal microbiota after exposure to 14 days emulsifiers, AA, AA_{TW} and AA_G, (A) total observed species, (B) Chao 1 diversity index, (C) Shannon diversity index.*

Emulsifiers and AA did not increase the diversity and richness compared with control, no statistical difference was found in observed species, Chao1 and Shannon index.

4.3.8.2 Composition of gut microbiota was altered after the co-exposure of AA and emulsifiers.

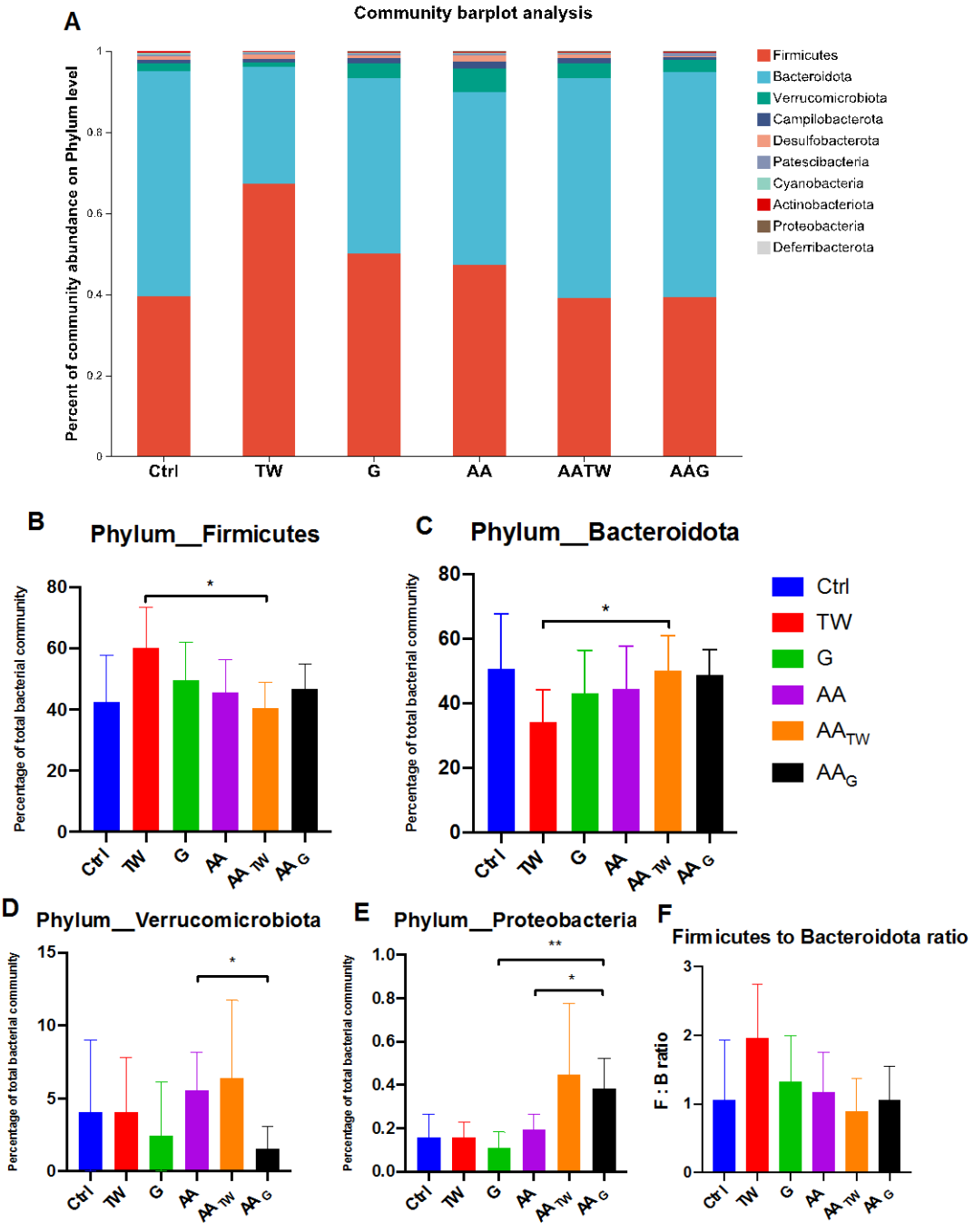

Figure 4.15 *Gut microbiota communities of various treatments at phylum level, (A) relative abundance of all detected phyla, relative abundance of (B) Firmicutes, (C) Bacteroidota, (D) Verrucomicrobia, (E) Proteobacteria; and (F) Firmicutes to Bacteroidota ratio. Asterisks indicate statistical significance *<0.05, **<0.01, ***<0.001.*

Phylum *Firmicutes*, *Bacteroidota* (*Bacteroidetes*) and *Verrucomicrobiota* were most abundant across six groups (Fig. 4.15A). TW and G have a tiny effect at the above phylum level except the abundance of *Firmicutes and Bacteroidota*. The *Firmicutes* had a high proportion of 60.1 % in the microbial community of TW group, while it was found lower in the specimens of AA_{TW} group (40.4 %). Co-exposure of TW, AA decreased the abundance of *Firmicutes* by 11.4 %. In comparison, the *Bacteroidota* had a low proportion of 34.0 % in bacterial community of TW group, while the percentage of it was higher in AA_{TW} group (50.1 %). Co-exposure of TW or G, AA increased the abundance of *Bacteroidota* by 13.2 % and 10 % respectively. But there was no significant difference in the *Firmicutes: Bacteroidetes* ratio (Fig. 4.15 F). *Verrucomicrobiota* in AA_G group decreased by 71.9 % compared to AA group (Fig. 4.15 D). Besides of the top three phylum, it was found that the abundance of Gram-negative *Proteobacteria* in AA_G group was higher than in G and AA group (Fig. 4.15 E).

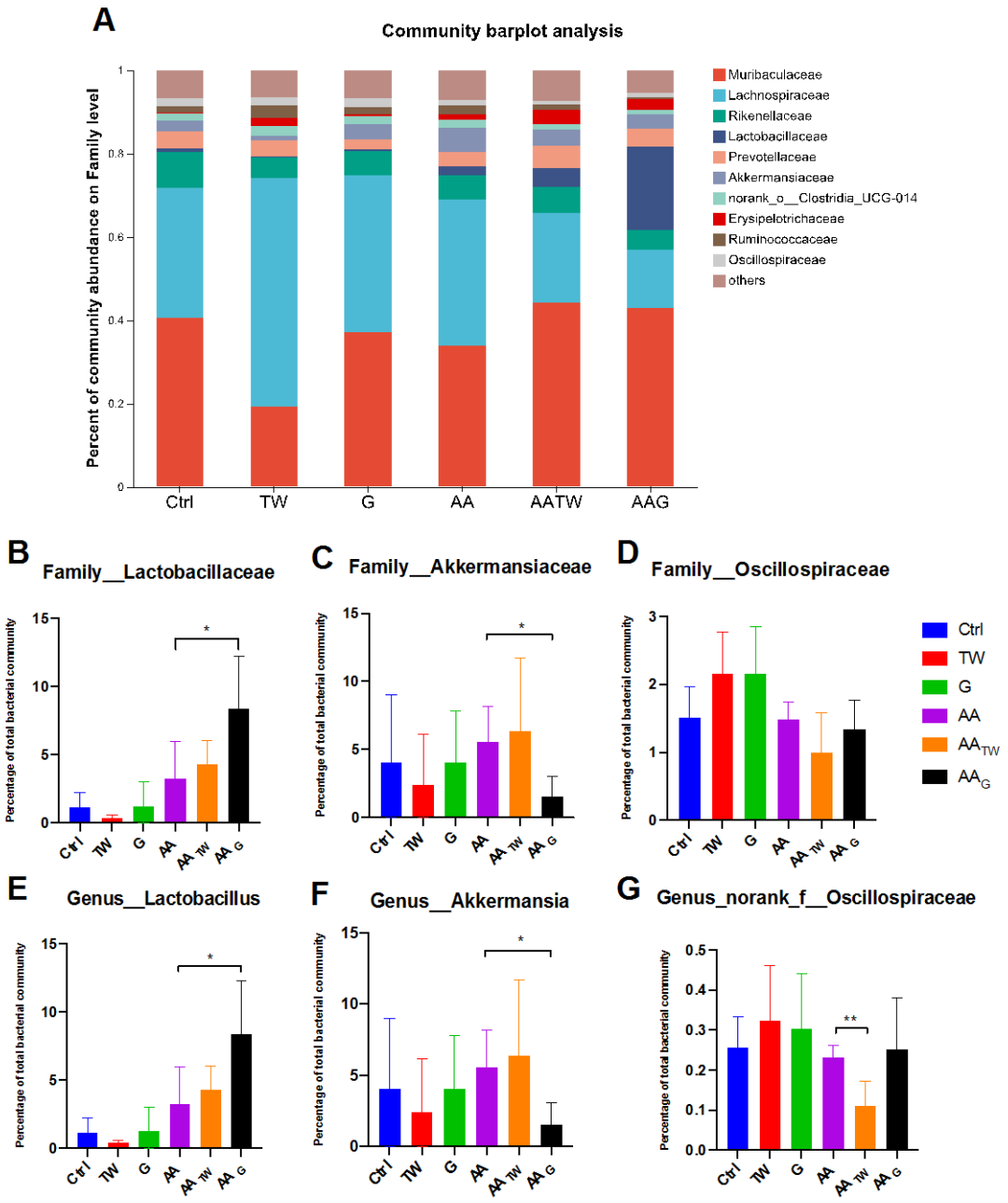

Figure 4.16 *Gut microbiota communities of various treatments at family level, (A) relative abundance of all detected families, relative abundance of (B) Lactobacillaceae, (C) Akkermansiaceae and (D) Oscillospiraceae; and relative abundance of the genus (E) Akkermansia, (F) Lactobacillus and (G) Oscillospiraceae. Asterisks indicate statistical significance *<0.05, **<0.01, ***<0.001.*

Differences in community among six groups were more obvious at the family level (Fig. 4.16 A). The abundance of *Lactobacillaceae* (Fig. 4.16 B) and *Akkermansiaceae* (Fig. 4.16 C) were not significantly affected by TW or G, however when compared to AA group, the abundance of *Lactobacillaceae* increased by 2.5-fold and that of *Akkermansiaceae* reduced by 71.9 % in the AA_G group. The relative abundance of *Oscillospiraceae* were increased in TW and G group (Fig. 4.16 D).

At genus level (Figs. 4.16 E-G), the trend of the genera followed that of their respective families. Besides, the proportion of *Oscillospiraceae* in AA_{TW} decreased by 51.9 % comparing to the AA group.

4.3.9 Co-exposure significantly increased daily weight gain

All animals survived the exposure and some treatments demonstrated growth in the exposure period (Fig. 4.17). Control, TW, G and AA_{TW} showed positive growth after 14 days. AA_G significantly increased the body weight at day 10 but reached a plateau after 10 days. The control treatment showed an average of 2.2 % increase in body weight over the exposure period. AA and AA_G treatments showed a similar increase in body weight of 3.0 % and 3.3 % respectively. Interestingly, AA_{TW} showed a significantly higher increase of body weight of 4.9 %, which is 2.2-fold higher than that of control and 1.6-fold higher than that of AA. All treatments had similar liver/ body weight ratio and colon weight/ length ratio (Figs. 4.17 C, D). This unusual increase in body weight has not been reported and indicate co-exposure of AA and emulsifiers such as TW could be a potential contributor to high weight gain.

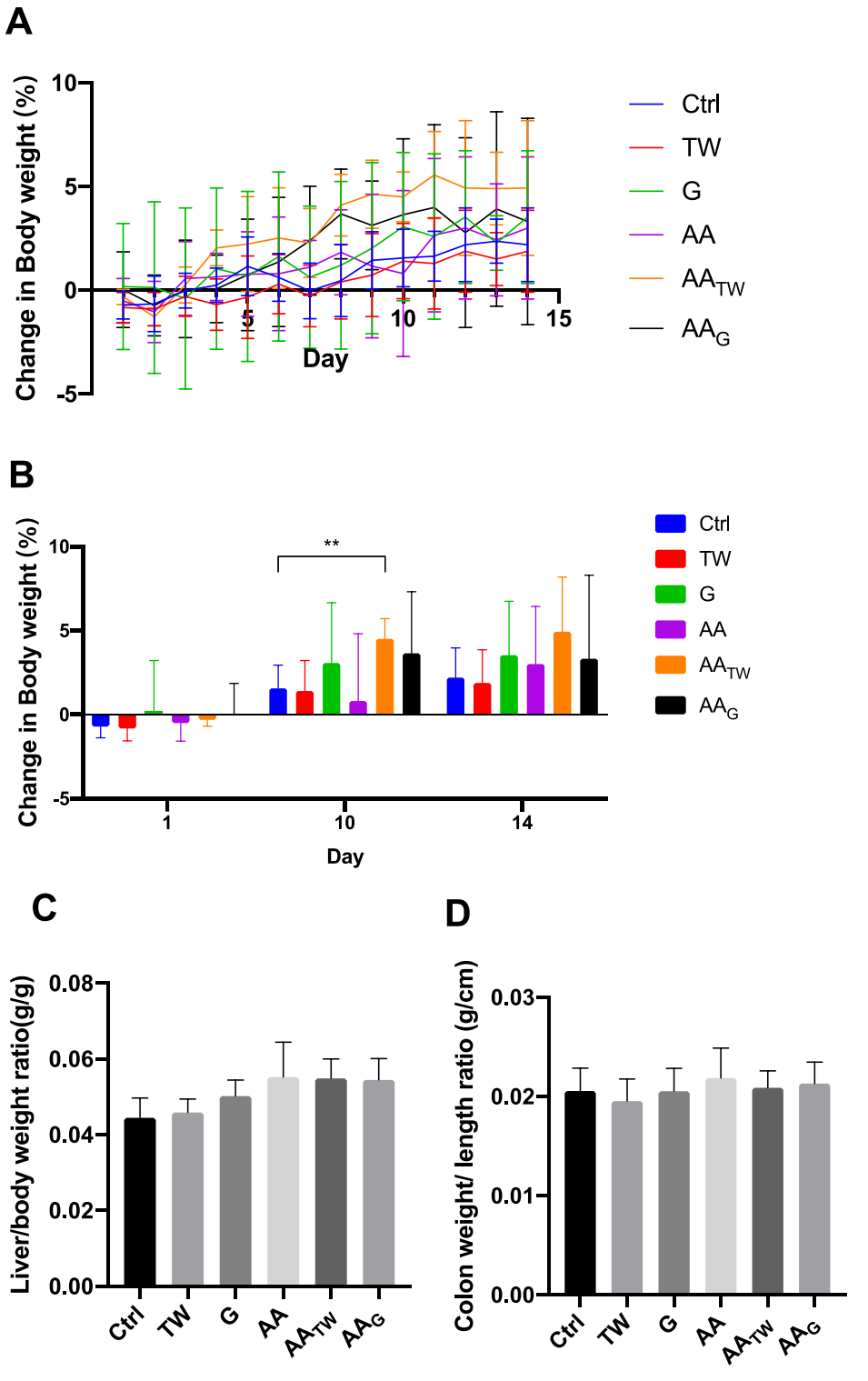

Figure 4.17 *Cumulative change in (A) percentage body weight over experimental period (mean ± SD) and (B) net change; (C) liver/body weight ratio and (D) colon weight/length ratio. Asterisks indicate statistical significance *<0.05, **<0.01, ***<0.001.*

4.3.10 Emulsifiers increases loss of coordinated motor function induced by AA

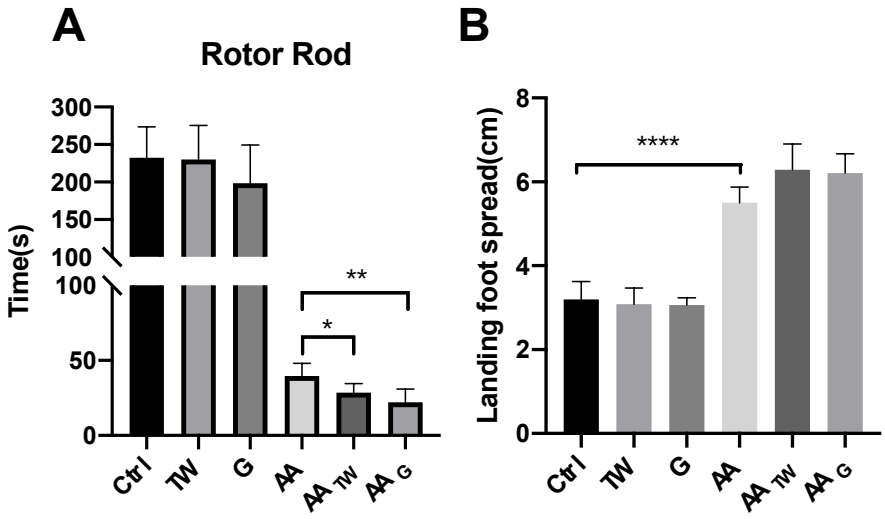

Figure 4.18 *Fine motor coordination comparison between mice of different treatments for 14 days as indicated by measurements of (A) time to fall on rotor rod and (B) landing hindlimb foot spread. Asterisks indicate statistical significance *<0.05, **<0.01, ***<0.001.*

Fine motor coordination was assessed by using the Rotor-Rod test and Landing Foot Spread Test. Toxicity of AA was pronounced as time to fall on rotor rod was decreased from 232.2 s in control to 39.8 s in AA (Fig. 4.18A). Addition of TW and G increased neurotoxicity of AA as rotor-rod performance of mice decreased significantly further from 39.8 s in AA to 28.5 s in AA_{TW} and 22.2 s in AA_G (Fig. 4.18A). AA significantly increased foot spread of landing hindlimb at the distances from 3.2 cm in control to 5.5 cm in AA. Addition of emulsifiers to AA did not change this endpoint (Fig. 4.18 B).

4.4 Discussion

Through this series of experiments, it was observed that emulsifiers could modify and enhance toxicity of AA in many ways.

Firstly, emulsifiers increased gut permeability, which could lead to increase uptake of AA. In the FITC-dextran experiment, we found out oral administration of TW for 2 weeks can significantly increase the permeability of intestine (Fig. 4.6). This is in accordance with an earlier study showing 1 % TW elevated gut permeability after 4 weeks administration (Nishimura et al., 2020). Although it has been shown previously that G can also increase absorption of phthalate esters (Gao et al., 2016), in my experiment G did not significantly increase absorption of FITC-dextran. However, TW or G treatments did not impact gene or protein expression of tight junction proteins (Figs. 4.3-4.4). This suggested that it is unlikely emulsifiers impact gut permeability through increase in paracellular absorption but instead influence transcellular absorption.

However, under co-exposure treatments (i.e. AA_{TW} and AA_{G}), tight junction proteins regulation were impacted. Gene expression of Claudin 1 and Zo-1 were impacted in both AA alone and co-exposure treatments (Fig. 4.3), whereas occluding was only impacted in co-exposure treatments. Similar findings were reported where co-exposure of G and MPEs (a phthalate mixture) down-regulated Zo-1 protein expression (Xia et al., 2021). Protein expression of claudin 1 was only impacted in co-exposure treatments while occluding showed a trend of decrease in both AA alone and co-exposure treatments but the changes were not significant (Fig. 4.4). In most of these cases, co-exposure treatments resulted in larger perturbation of tight junction protein regulation. These changes suggest that paracellular absorption was also impacted under co-exposure, leading to increase in gut permeability.

Research from the past suggested that when emulsifiers may meet the criteria of concentration, they may form micelles with other substances (Ahyayauch et al., 2010; Xia and Onyuksel, 2000). For example, TW can be incorporated into bacterial membranes, forms micelles that promote the transport of exterior protons into cells (Kimoto et al., 2002). G convert to 70 % triglycerides in enterocytes and can be found

in the human intestinal lumen as micelles or aggregates (Harris et al., 2013). Therefore, the absorption of AA may be increased by TW and G micelles. Intestine barrier prevents the translocation of endotoxins into blood. However, when the barriers were destroyed, not just intestine-derived contaminants AA but circulation-translocated bacteria can trigger inflammation.

Although AA concentrations in serum and liver were not increased by emulsifiers, concentration of GA was significantly increased. It has been reported that AA is metabolized either by direct conjugation with glutathione or oxidation into GA, which undergo further metabolism and are excreted in urine (Li et al., 2016a). A higher GA concentration caused by emulsifiers may indicate faster depletion of glutathione which would make the individual more vulnerable to oxidative damage caused by AA and GA toxicity.

It has been known AA can induce neurotoxicity (LoPachin, 2004). Our results showed emulsifiers increased loss of coordinated motor function induced by AA (Fig. 4.18). In co-exposure treatments, the serotonergic synapse pathway was disturbed (Figs. 4.12 and 4.13). 5-HT is a monoamine neurotransmitter that is essential for physiological functions such as motor function (Gershon, 2013). 5-HT has emerged as an important neurotransmitter in the gut-brain axis (Layunta et al., 2021). The development and long-term activities of both the enteric nervous system (ENS) and central nervous system (CNS) can be influenced by 5-HT, which can operate in neuroendocrine, endocrine, and/or paracrine ways (Margolis et al., 2021). It has been estimated that about 95% body serotonin (5-HT) was produced in the intestine (Terry and Margolis, 2017). The co-exposure treatments may have an effect on the production of 5-HT in intestine, disrupting the gut-brain axis and resulting in loss of coordinated motor function. Another explanation was that neurotoxicity was moderated through interaction with the microbiota. Microbiota have been reported to produce and degenerate tryptophan, a precursor of 5-HT and influence host 5-HT synthesis (Layunta et al., 2021). For

example certain species of *Akkermansiaceas* was reported to increase 5-HT level in colon and hippocampus (Yaghoubfar et al., 2020). Therefore the decrease of *Akkermansiaceas* caused by AA_G may inhibit motor function and intestinal inflammation by influence 5-HT.

In our results, addition of emulsifiers also aggravated inflammation caused by food contaminant AA. For example, emulsifiers increased expression of MCP-1, iNOS, TNFα and il-1β caused by AA (Fig 4.3). There were also larger areas of hepatocytes damage and immune cell infiltration in the co-exposure treatments (Fig 4.6). It was known that AA could induce inflammation. For example, it has been shown to increase the level of TNF-α and IL-1β (Amirshahrokhi, 2021). Emulsifier TW has also been suspected to induce inflammation, such as increasing expression of proinflammatory cytokine CXCL1 in colon of C57BL/6 WT mice after exposed to drinking water containing TW for 13 weeks (Viennois et al., 2017). One potential mechanism of co-exposure leading to higher inflammation maybe related to MAPK signal transduction pathway. MAPKs can be stimulated by Toll-like receptors (TLRs), which in turn lead to increased production of pro-inflammatory cytokines such as TNF-α and IL1β (Rogero and Calder, 2018). Significant up-regulation of Tlr 2 and Tlr4 was observed in the AA_{TW} treatment (Fig. 4.3). And AA_{TW} activated the expression of P38 while AA_G activated ERK (Fig. 4.4). This also explains the increased expression of downstream cytokines IL1β and TNF-α in both co-exposure treatments (Fig. 4.3).

It was unexpected that individuals of AA_{TW} and AA_G had high weight gain within the exposure period. As discussed previously, these two treatments also experienced the highest toxicity. Weight gain of these two treatments were over 2 times of that of the control at day 10 and were 51.6 -122.7 % at day 14. AA has been reported be able to induce obesity related biomarkers such as PPARγ in animals under high fat diet for 10 weeks (Lee and Pyo, 2019). Activation of upstream regulators of PPARγ by AA, such as p38 and ERKs of the MAPK, has been reported (Cuschieri and Maier, 2005).

In our study, AA led to activation of p-P38 and p-ERK. AA_{TW} and AA_{G} increased the expression of p-P38 and p-ERK respectively (Fig. 4.4). AA_{TW} also significantly increased the expression of PPARγ (Fig. 4.3). Therefore short term effect of addition of emulsifiers to AA was very similar to that of a chronic high fat diet. It was found that AA_{TW} and AA_{G} increased the abundance of bacteria *Proteobacteria* which is associated with weight gain (Xu et al., 2022), and decreased the abundance of bacteria *Verrucomicrobia* and *Akkermansia* which are associated with weight loss (Everard et al., 2013; Ulker and Yildiran, 2019). Therefore weight gain may be affected not just by the MAPK pathway, but also by gut microbiota.

Higher of *Firmicutes* to *Bacteroidota* ratio are related to obesity, proposing this ratio as an obesity biomarker (Magne et al., 2020). In our study, no changes were found in the *Firmicutes*: *Bacteroidota* ratio in the fecal samples of mice (Fig. 4.15). Several studies found no changes or even reported a decrease in the *Firmicutes/Bacteroidetes* ratio in obese animals and humans (Jumpertz et al., 2011; Patil et al., 2012; Schwiertz et al., 2010; Tims et al., 2013). The fact that, in most research, obese patients had lower bacterial diversity than lean people suggests that other compositional changes at the family, genus, or species level may be more vital than the *Firmicutes/Bacteroidetes* ratio (Aguirre and Venema, 2015). Therefore the family and genus level related to obesity is of concern.

In our results, AA_{TW} induced a lower abundance of genus *Oscillospiraceae* (Fig. 4.16 G), which may be linked to obesity. High abundance of *Oscillospiraceae* is associated with a low BMI and its abundance was positively correlated with human health (Chen et al., 2020; Yang et al., 2021). Nami and colleagues have shown TW decreased the abundance of *Oscillospiraceae (Naimi et al., 2021b),* whereas we have found only AA_{TW} decreased the abundance of *Oscillospiraceae.* The abundance of phylum *Verrucomicrobia*, family *Akkermansiaceae* (genus *Akkermansia*) were decreased in AA_{G} compared with AA (Figs. 4.15 and 4.16). The

phylum *Verrucomicrobia* is mainly found in the intestinal mucosa (Lindenberg et al., 2019). It plays a role in maintaining glucose homeostasis and intestinal health, including increasing immunity (Lindenberg et al., 2019). Besides, this phylum is thought to lower the risk of obesity and body weight (Ulker and Yildiran, 2019). *Akkermansia* is associates with decreased body mass and increased gut barrier function and health (Karcher et al., 2021). AA_{TW} and AA_G also increased the predominance of potentially inflammation promoting *Proteobacteria* (Fig. 4.15). *Proteobacteria* can induce inflammation by: impairing the gut mucosal barrier function (Jakobsson et al., 2015), by allowing lipopolysaccharide (LPS) and gut bacterial components to be transported to the systemic circulation (Shi et al., 2014). Increases in *Proteobacteria* also have been observed in obese humans or animals (Rizzatti et al., 2017). *Proteobacteria* also was the most consistently reported obesity-associated phylum (Xu et al., 2022). Besides, the abundance of beneficial bacterial *Lactobacillus* also be enhanced by AA_{TW} and AA_G (Fig. 4.16). *Lactobacillus* strain have beneficial effects on intestinal tissue integrity in inflammatory conditions, as well as actions against chemotherapeutic agent toxicity (Ichim et al., 2018). These beneficial defense system of bacterial appear to be activated by AA, especially AA_{TW} and AA_G. Based on these finding, it is possible AA_{TW} and AA_G promoted the obesity and inflammation via microbiota dysbiosis, which are associated with the increased abundance of pro-inflammatory bacterial and decreased abundance of weight-loss bacterial.

Research suggested that bacterial and its products may be involved in the low-grade inflammation associated with metabolic syndrome (Cani et al., 2007). For example, 1% TW of M-SHIME system increased the level of TLR4-agonist LPS, then TW-Treated M-SHIME transfer to mice also transmitted the low-grade inflammation and metabolic syndrome (Chassaing et al., 2017). Significant up-regulation of Tlr 2 and Tlr4 was observed in the AA_{TW} treatment (Fig. 4.3). We speculated AA_{TW} and AA_G may directly affect the microbiota, or indirectly influence TLR 4 and TLR2 to changes

microbiota and changes in the gut microbiota induced by AA_{TW} and AA_{G} can cause weight gain and other elements of the metabolic syndrome.

Transcriptomic analysis provided insight into overall changes when emulsifiers were added to AA. When looking at DEGs of AA relative to AA_{TW} or AA_{G}, different biological processes emerged (e.g. fibrinolysis) (Fig. 4.10). This may be related to metabolism of the emulsifiers used by gut microbiota. G is structurally constituted of the esterification products of glycerin and carboxylic acids, mainly including fatty acids (Yu et al., 2003). TW also could be converted to oleic acid (one types of fatty acids) by *Lactobacillus* sp. in the gut (Ziar and Riazi, 2022). Microbes can extract energy and carbon from fatty acids which might be supplied by TW and G (Sauer et al., 2008). While energy and carbon encouraged growth of both beneficial and harmful bacteria, overgrowth of some harmful bacterial (e.g., *Escherichia coli*, *Helicobacter pylori*, *Salmonella enteritidis* and *Staphylococcus aureus*) can cause fibrinolysis (Degen et al., 2007). Some microbes can use organic acids such as fatty acids as a source energy (Sauer et al., 2008), which also confirmed TW and G could supply energy for microbes.

Top 10 KEGG pathways impacted by AA exposure were all related to the immune system (Fig 4.11). In the co-exposure treatments, additional pathways related to obesity and lipid metabolism were affected. Some of these pathways are related to interaction with gut microbiota. Retinol metabolism was the KEGG pathway with the biggest rich factor in the comparison between AA and AA_{TW} (Fig 4.12). Retinol (Vitamin A) is critical nutrients obtained from food source, stored in the liver, and up taken and metabolism by intestinal epithelial cells (Gudas, 2022). Vitamin A play an important part in the developing nervous system, maintenance of epithelial surfaces, reproduction and immune competence (Blomhoff and Blomhoff, 2006). Epithelial cells metabolize vitamin A to retinoic acid (RA) to induce dendritic cells (DCs) to modulates immunity (Gudas, 2022). Disruption of vitamin A homeostasis will lead to obesity, diabetes, and metabolic disorders (Blaner, 2019). Overnutrition associated with obesity can impair

vitamin A metabolism and communication, resulting in weakened immune responses and increased susceptibility to respiratory viral infections (Penkert et al., 2020). Retinol production has been proposed to be complex, with potential interaction of bile acids, lipocalins, and lipopolysaccharides of gut microbiota and their metabolism(Srinivasan and Buys, 2019). Lysine biosynthesis is the most significant pathway in the comparison between AA and AA_G (Fig 4.13). Lysine is essential in animals and must obtained from food. Lysine play an important role including in the collagen, structural protein, in calcium homeostasis, and in fatty acid metabolism (Matthews, 2020). A deficiency or overload of lysine has been linked to some diseases. A deficiency in lysine can cause symptoms including anemia, altered connective tissue properties, impaired fatty acid metabolism, as well as systemic effects from protein-energy malnutrition (Hall and da Costa, 2018). On the other hand, an overload of lysine in plasma can be asymptomatic or cause some debilitating neurological disorders, such as ataxia, epilepsy, and psychomotor impairment (Hoffmann, 2006; Houten et al., 2013) Bacteria is one of organisms can synthesis lysine (Gillner et al., 2013). We found that both AA_{TW}-affected retinol and AA_G-affected lysine can be produced by bacteria. Addition of emulsifiers not just increase inflammation but may supply the energy to microbiota to influence the production of retinol or lysine, the disruption of these nutrient homeostasis may induce metabolic syndrome (De Siena et al., 2022).

An interesting finding of the KEGG pathway analysis was that the dependence pathway was one of the top 30 KEGG pathways to be altered when TW or G were added to the AA exposure (Tables S2-3). This is the pathway related to substance addiction and dependence. There were no studies suggesting that emulsifiers or AA toxicity to be related to this pathway. Further studies are required to confirm this observation.

In conclusion, emulsifiers increased the toxicity of AA to mice in terms of severity and types of toxicity. Emulsifiers elevated pro-inflammatory cytokines and

inflammation. They led to disruption of metabolic pathways, particularly lipids, and led to increased weight gain in mice. Neurotoxicity was increased. Gut microbiota was also changed in a different manner compared to AA or emulsifiers alone.

CHAPTER 5

Effect of acrylamide and in combination with emulsifiers on human fecal microbiota

5.1 Introduction

In the previous chapters I have demonstrated the mixture of AA and emulsifiers would interact and resulting in higher toxicity and more broad-spectrum toxicities. Results from Chapter 4 suggested that such results were at least in part related to interaction of the chemicals with fecal microbiota. Therefore it is important to examine such effects on human fecal microbiota. Recent research have reported various adverse effects of AA or food emulsifiers on human fecal microbiota. Researchers used 5 emulsifiers and 10 individual fecal samples for 48 h fermentation. Except soy lecithin, TW, rhamnolipids, carboxymethylcellulose and sophorolipids decreased microbiota diversity. Abundance of pathogenic *Escherichia/Shigella* and *Fusobacterium* were higher after rhamnolipids and sophorolipids exposure, but beneficial *Bacteroidetes* dropped (Miclotte et al., 2020).

Oral administration of AA dropped abundance of *Firmicutes* and elevated of abundance of *Bacteroidetes*, *Burkholderiales* and *Erysipelotrichales* in mice for 4 week's intervention. In addition, researchers indicated decreased *Firmicutes* to *Bacteroidetes* (F/B) ratio had been associated with weight loss (Wang et al., 2021).

In vitro fermentation investigations, which allow for dynamic sampling over time in reactors that replicate different parts of colon, have been created as techniques for studying human gut microbiota under extremely controlled settings. When compared to clinical trials or animal models, colonic fermentation models have advantages including low cost, higher reproducibility, no need for ethical permission, and, according to experiment, they can be carried out in less time. Colonic models allow for

physiologically simulated culture of human gut microbiota taken from fecal samples (Pham and Mohajeri, 2018). Numerous studies studying effects of various dietary emulsifiers on human microbiota have already been developed using in vitro gastrosimulator system, SHIME (Chassaing et al., 2017; Miclotte et al., 2021a; Miclotte et al., 2021b). Compared to other short term trial，SHIME can provide fecal microbiome enough time (10-20 days) to adjust the conditions present in each colon compartment. SHIME differs from other models by include upper digestive tract conditions, resulting in a series of five compartments replicating the upper (stomach, small intestine) and lower (ascending, transverse, and descending colon) digestive tracts. SHIME was developed to enable colonization of the mucosal microbiome. SHIME is flexible to be added or left away reactor compartments (Van de Wiele et al., 2015).

Thus, in this study we use a traditional *in vitro* fermentation and an *ex vivo* gastro-intestinal simulator SHIME to study synergistical effects on intestinal microbiota. Ability of food emulsifiers (TW or G) and AA to modulate microbial community was studied simulating an intake for 1 day and 21 days.

5.2 Materials and methods

5.2.1 24 h fecal fermentation sample preparation

For 24 h fecal fermentation, fecal sample was collected from a health female adult donor aged at 28. The volunteer was verified to not had taken any antibiotics, pre- or pro-biotics for at least 4 weeks before donation. Fecal samples were collected and divided in ten 50 mL sterilized tubes. In each tube, 1 g fecal sample were diluted with 9 mL PBS. Mixture was homogenized for 2 mins and centrifuged at 500 rpm for 5 mins. Supernatant from each tube was collected and combined for following experiments.

5.2.2 Minimum inhibitory concentration (MIC) assay

This MIC assay was used to identify suitable test concentration of AA and emulsifiers in subsequent experiments. Fecal supernatant samples of MIC assay were collected as described section 5.2.1. MIC values were performed by a serial dilution method. Serial 2-fold dilutions of AA (25 mM-400 mM) was conducted in different column of 96-well plates in brain heart infusion broth (BHI) medium with or without containing TW and G. Based on the MIC test of TW and G, concentrations below NOAEL: 0.1 % TW, 0.25% G and 0.025 % G, were selected for the subsequent co-exposure experiments (Fig. S5). BHI medium was made from powder (Qingdao Hope Biotechnology, China) dissolved in MilliQ water and autoclaved for 20 mins at 120 °C and stored at 4 °C. Bacterial concentration in fecal supernatants were adjusted with BHI broth medium to OD at 600 nm = 0.08-0.1 and 5ul of this mixture was added to wells of 96-well plate. The 96-well microplate was incubated at 37 °C for 24 h. MIC values were determined by Thermo Scientific Varioskan LUX Multimode Microplate Reader (OD at 600 nm). Results were obtained by six replicate wells of each concentration and three experimental repeats.

5.2.3 24 h fecal fermentation

Fecal fermentation was carried out as reported (Song et al., 2018). Ingredients of basal medium for fecal fermentation was as follow: glucose (5 g/L), peptone (2 g/L), yeast extract (2 g/L), $NaHCO_3$ (2 g/L), L-cysteine (0.5 g/L), bile salts (0.5 g/L), NaCl (0.1 g/L), K_2HPO_4 (0.04 g/L), KH_2PO_4 (0.04 g/L), $MgSO_4 \cdot 7H_2O$ (0.01 g/L), $CaCl_2 \cdot 6H_2O$ (0.01 g/L), hemin (50 mg/L), resazurin (1 mg/L), vitamin K1(10 mL/L) and MiliQ H_2O made up to 1 L. The pH of basal medium was adjusted to 6.8 with 1 M HCl. Medium was autoclaved for 20 mins at 120 °C before storing in 4 °C and used within 2 weeks. Supernatants were collected as described in section 5.2.1. Each fecal fermentation tube consists of 5.4 mL basal medium and 0.6 mL fecal supernatant. Food contaminants and emulsifiers were added into fecal fermentation medium to create appropriate test concentrations (Table 5.1). Samples were transferred into anaerobic environment on a shaking incubator at 200 rpm at 37 °C for 24 h. Anaerobic

environment was maintained in an anaerobic box containing anaerobic AnaeroGen™ 2.5 L sachet (Thermo Scientific, USA). The supernatant of fecal samples was divided amongst treatment in replicate tubes of 2 as shown in table 5.1. After fermentation of 24 h, all samples were centrifuged at 10,000 rpm for 10 mins at 4 °C to separate supernatant and sediment. The supernatants were collected for short chain fatty acids (SCFAs) analysis, and the sediment were collected for 16S sequencing.

Table 5.1 24h fecal fermentation treatments.

Treatments	Acronym
AA 25 mM	AAL
AA 25 mM + TW (0.1 %)	AAL_{TW}
AA 25 mM + G (0.25 %)	AAL_{GH}
AA 25 mM + G (0.025 %)	AAL_{GL}
AA 200 mM	AAH
AA 200 mM + TW (0.1 %)	AAH_{TW}
AA 200 mM + G (0.25 %)	AAH_{GH}
AA 200 mM + G (0.025 %)	AAH_{GL}

5.2.4 21 d SHIME experiment

Triple SHIME (Prodigest, Belgium) was set up according to manufacturer's instruction for AA, TW, and AA_{TW} treatments. Each SHIME system consisted of one combined stomach/small intestine chamber and one proximal colon (PC) chamber and one distal colon (DC) chamber (Fig. 5.1). Fecal sample was collected from one healthy female volunteer aged 27. The volunteer had verified to not have taken any antibiotics, pre- and pro-biotics for at least 4 weeks before donation. A 20 % (W/V) solution of fecal sample and anaerobic phosphate buffer was put in a stomacher bag and homogenized for 10 mins. Anaerobic phosphate buffer contained (per liter) 8.8 g K_2HPO_4, 6.8 g KH_2PO_4 and 0.1 g sodium thioglycolate, was adjusted to pH 7 and 15 mg/L sodium dithionite was added to buffer before use. Homogenate was centrifuged

at 590 g for 2 mins. Supernatant was inoculated with 5 % (v/v) in each colon chamber: 25 ml fecal sample was inoculated in 500 ml medium in proximal colon chamber and 40 ml fecal sample was inoculated in 800 ml growth medium in distal colon chamber. Throughout the experiment, contents in chambers were kept at 37 °C through water bath circulation system and mixture inside was stirred at 300 rpm constantly. The pH of proximal colon chamber content was controlled to be between 5.6-5.9 and pH of distal colon was controlled to be between 6.6-6.9 using 0.5 M NaOH and 0.5M HCl automatically.

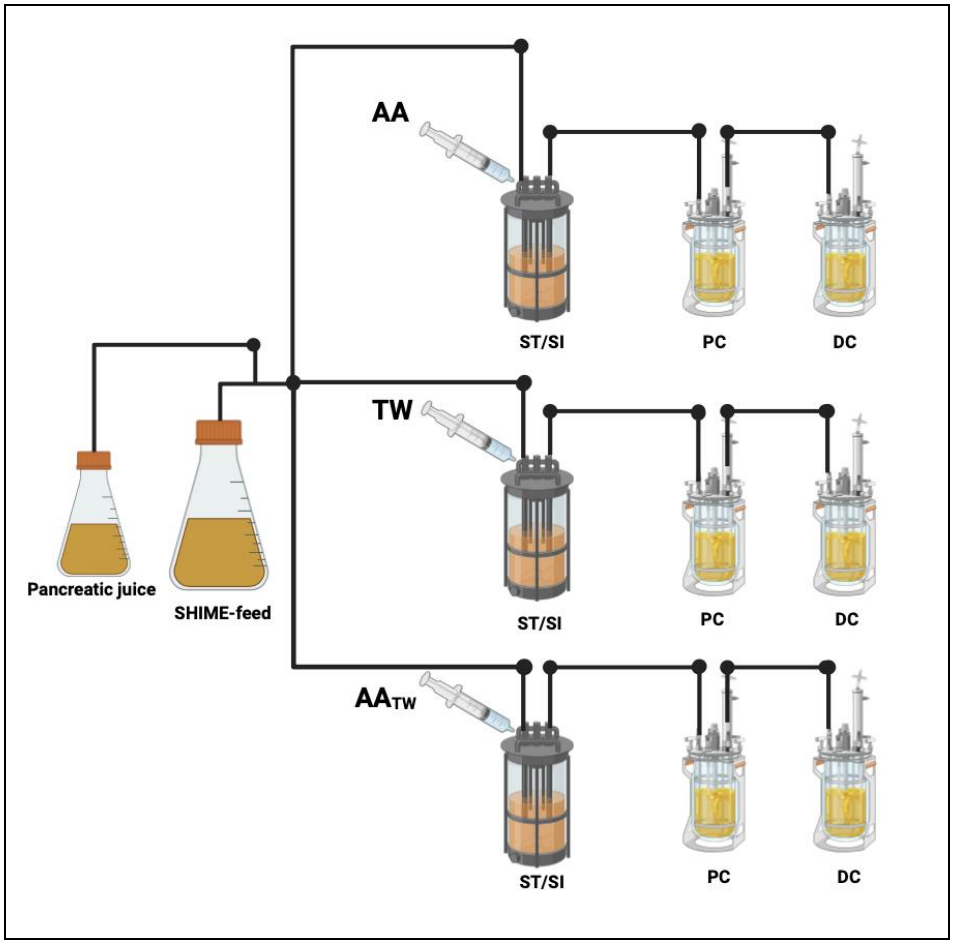

Figure 5.1 *SHIME experimental design.*

Feeding was carried out at 3 times a day and at 8 hr intervals. For every feed, 60 mL pancreatic juice (flow rate: 4 mL/min) and 140 mL growth medium (flow rate: 4.67 mL/min, pH 2) was pumped into stomach/small intestine chamber. Samples in

chambers were mixed thoroughly on stir bars. Pancreatic juice consisted of $NaHCO_3$ (12.5 g/L), Oxgall (6 g/1L) and Pancreatine (0.9 g/1L). Growth medium (PD-NM001B) was purchased directly from Prodigest (Prodigest, Belgium). This mixture was transferred to colon chambers at a flow rate: 3.5 mL/min until it is fully transferred. Before chemical exposure, microbiota was allowed to stabilize for 21 days in the SHIME setup. Proximal colon and distal colon chambers were maintained volume at 500 and 800 mL respectively after fecal sample incubation. Excess liquid were drained into a container containing 10 % bleach for later disposal. After stabilization, samples from proximal and distal colon chambers were collected set as baseline. Then 5 mL 100 mM AA, 0.1 % TW and 100 mM AA+ 0.1 % TW were injected in three stomach/small intestine chambers daily for 21 days. Luminal liquid was collected on day 1, day 3, day 7, day 10, day 14 and day 21, and stored at -80 °C for SCFA analysis and 16S sequencing.

5.2.5 Short chain fatty acids analysis

5ml supernatant samples were collected as described section 5.2.3 and 5.2.4. pH of the samples was adjusted to pH 2-3 by 1M HCl and then centrifuged at 5,000 rpm for 15 mins. Supernatant was passed through 0.45 μm PES filter and 1 mM 2-ethylbutyric acid was added as internal standard. A fused silica capillary column (30 × 0.32 mm, DB-FFAP 123-3232, Agilent Technologies Inc., USA) equipped with an Agilent 7980B GC system was used for GC separation as condition reported previously (Song et al., 2018). Flow rate of mobile phase N_2 gas was set at 0.6 mL/min, initial temperature of oven was set at 80 °C for 2 mins and then ramping gradually at 6 °C/min until 180 °C and maintained for 2 mins. Temperature of FID detector was set at 220 °C. Acetic acid, propionic acid, n-butyric acid, i-butyric acid, n-valeric acid, and i-valeric acid were measured and calibration curves were constructed between 1 and 50 mM range. All results were expressed as mean ± standard deviation (SD). Analysis of variance (ANOVA) and Tukey's multiple-comparison test was used to evaluate statistical

differences between biological endpoints of different treatments. All or analyses were performed using GraphPad Prism 8.0 (GraphPad Software, San Diego, CA).

5.2.6 High-throughput sequencing and bioinformatics analysis

Microbial genomic DNA extraction of samples collected as described section 5.2.3 and 5.2.4 were carried out using TIANamp Stool DNA Kit (TIANGEN, China) according to manufacturer's instructions. DNA concentration and purity were measured by a Nanodrop Lite Spectrophotometer (Thermo Fisher Scientific, US). Extracted DNA was sent to BGI company (BGI, China). Concentration of DNA in samples were higher than 50 ng, and with 260/280 ratio larger than 1.8. These sample DNA was used to construct a library with primers (forward 338F: 5′-ACTCCTACGGGAGGCAGCAG -3′ and reverse 806R: 5′-GGACTACHVGGGTWTCTAAT -3′) targeting V3-V4 region of 16S rRNA gene (BGI, China). PE300 system was used to sequence library (BGI, China). To obtain clean reads, raw data were filtered to remove adapter pollution, and then paired end reads with overlap (lower than 600 bp) were merged to tags. Regarding that, at 97 % sequence similarity, tags were clustered to optical transform unit (OTU) with USEARCH (v 7.0.1090). Tags of variable region were obtained with FLASH (v 1.2.11). Bioinformatics analysis was used to perform OTU and its abundance analysis, sample diversity analysis, differential analysis, and biomarker analysis. Microbiota at family level data were also analyzed with principal component analysis (PCA) (R package version 4.0.2) to visualize clustering patterns of microbiota data. Good's coverage estimator of all groups is above 95 %, showed sequencing depth fulfilled bacterial diversity.

5.3 Results and discussion

5.3.1 Addition of emulsifiers changed survival rate of fecal microbiota

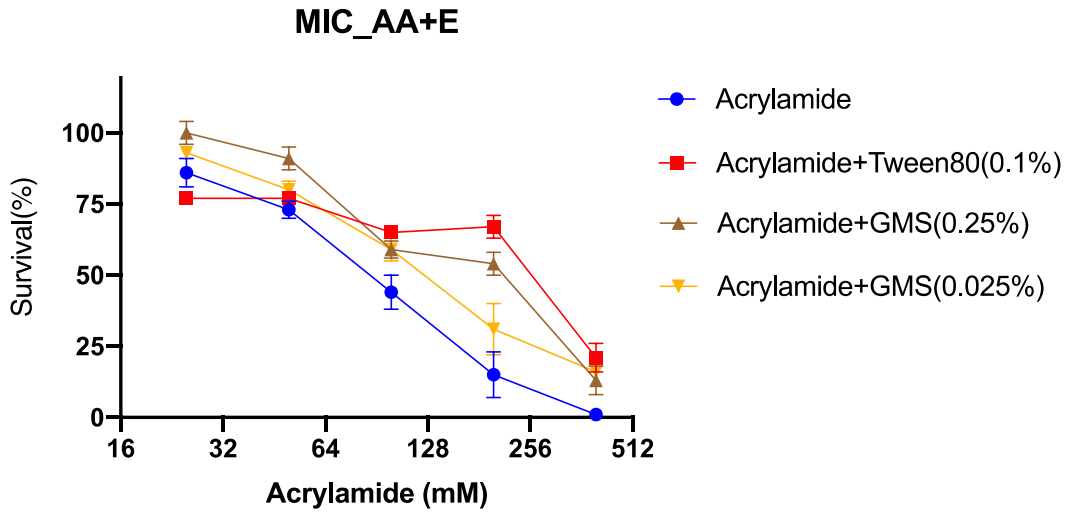

Figure 5.2 *Minimum inhibitory concentration (MIC) after 24 hours AA and emulsifiers co-exposure treatments.*

It was interesting that co-exposure treatments mostly resulted in higher survivorship of bacteria than AA alone. At 25 mM AA, addition of TW decreased survival rate of fecal microbiota while addition of G increased their survivorship. At point of 200 mM AA, both emulsifiers increased survivorship of bacteria. Higher G concentration also had stronger rescue effect on bacteria survivorship. We discovered that the total survival rate was lowered with increasing concentration for AA, AA_G, and AA_{TW}. Addition of G, bacteria had a higher survival rate than AA alone. The survival rate of AA_{TW} was only inferior to that of AA at a concentration of 25 mM. With increasing concentration, AA_{TW} became the group with the highest survival rate at 200mm. Therefore, we selected 25mM and 200mM concentration for following experiment. It was uncertain which bacteria increased their survival rate, however higher bacterial survival rate indicated that the emulsifiers provided the bacteria energy.

5.3.2 24 h fermentation effects

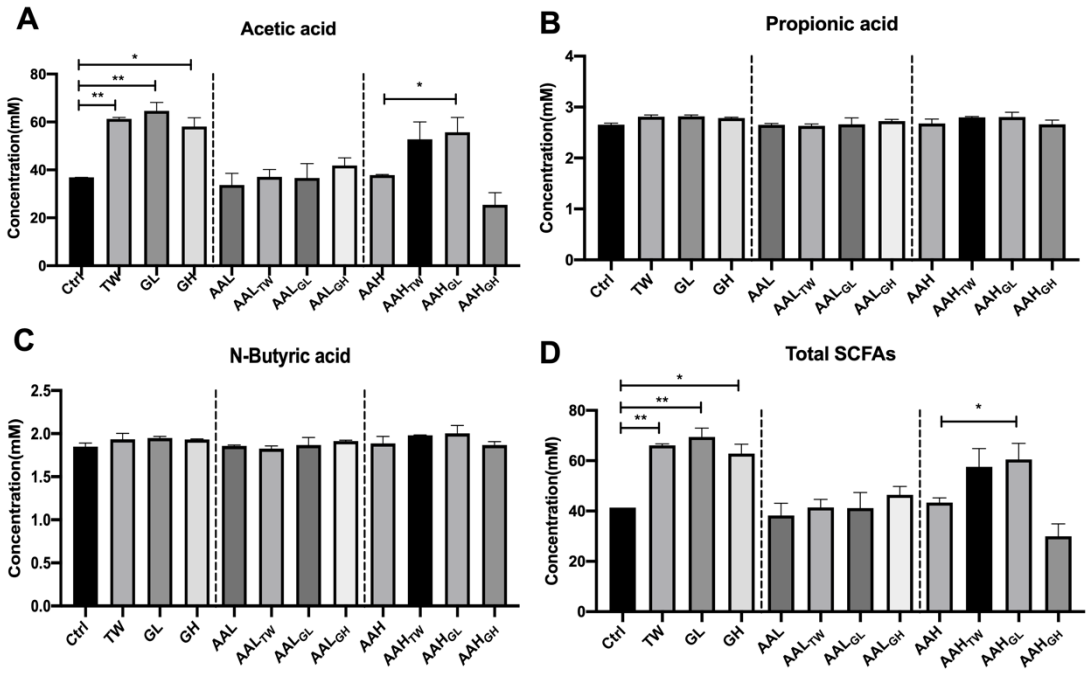

Figure 5.3 *Changes of concentrations (mM) of acetic acid (A), propionic acid (B), N-butyric acid (C) and total SCFAs (D) during 24 h fermentation of fecal samples with different treatments.*

Primary SCFA produced during fecal fermentation was found to be acetic acid. For all treatment groups, acetic acid content was the highest and contributed to over 90% of total SCFAs (Fig. 5.3). Addition of emulsifiers promoted acetic acid production. AA 200 mM with TW or GL showed increased acetic acid compared with AA 200 mM. Concentrations of propionic acid and n-butyric acid have not changed under all treatments. SCFAs were produced by anaerobic gut bacteria. Emulsifiers enhanced the production of acetic acid, which suggested that they can feed some bacteria. However, after adding AA, the production of SCFAs did not rise as aa concentration increased, which means AA could not be the energy source for those bacteria. AAH_{TW} and AAH_{GH} increased the level of acetic acid while AAH_{GL} decreased. These suggested that co-exposure not only affected the products of the bacterial related to emulsifiers, but also affected other bacteria. Addition of different emulsifiers also have various effect. The co-exposure effect on SCFAs was not simple additive.

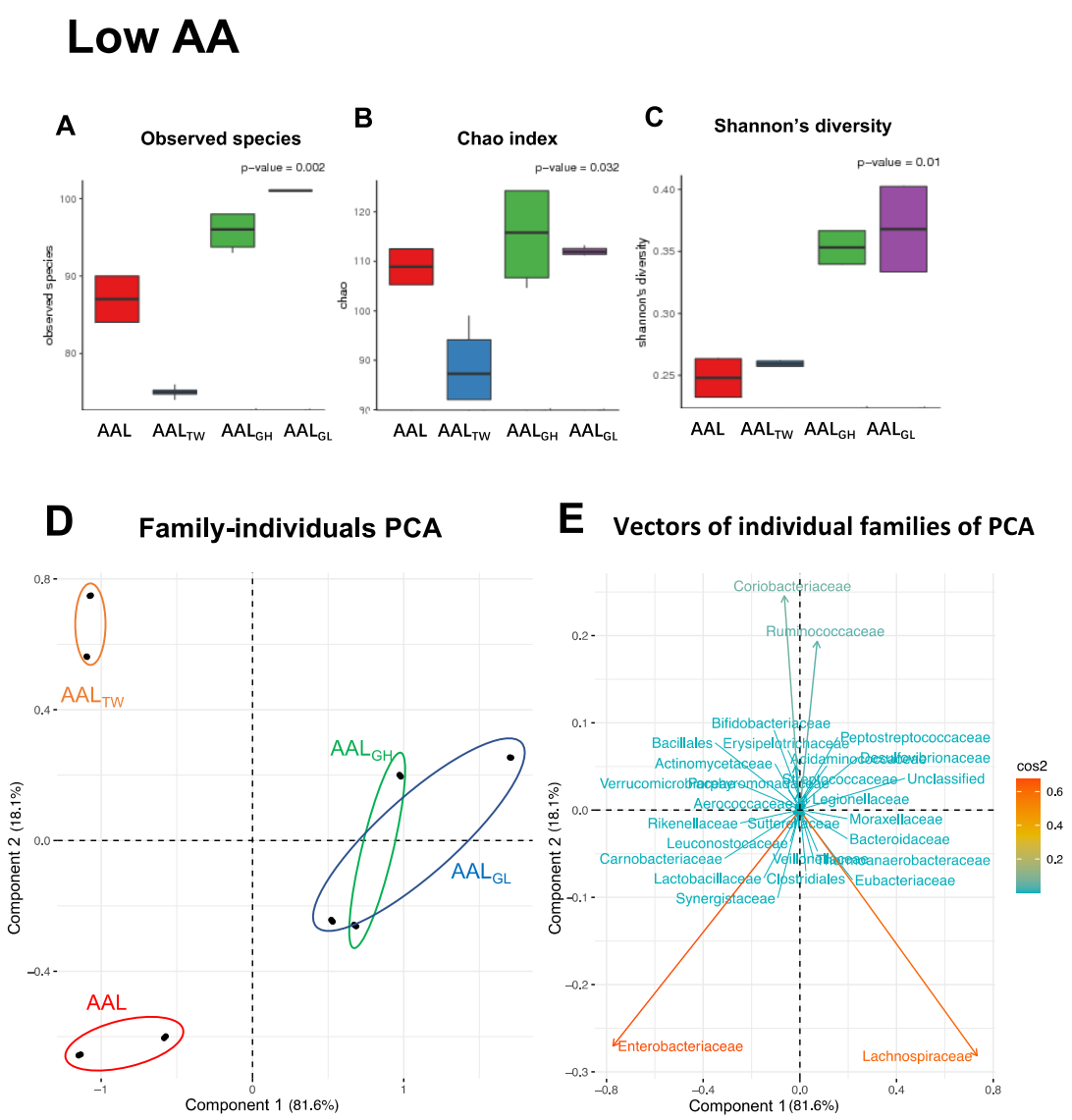

Figure 5.4 *Comparison of fecal microbiota after 24 hours emulsifiers alone, 25 mM AA alone and co-exposure of emulsifiers and 25 mM AA, (A) Observed species number of fecal bacteria, (B) Chao index, the higher Chao index, the higher community richness, (C) Shannon diversity index, the higher Shannon diversity index, the higher community diversity, (D) Principal component analysis (PCA) of microbiota community structure at family level of various treatments indicated by different colors, (E) Vector direction and strength of individual families and their contribution to PCA in (D). Colors are defined by the squared loadings (cos^2).*

Similar trends were observed in total observed species number and Chao index (Fig. 5.4): addition of G increased species number while addition of TW lowered species

number. Shannon diversity index was slightly different where addition of G increased the index, but TW had no significant effect.

PCA based on family level data showed treatment specific clustering of microbiota community (Fig. 5.4 D). Separation caused by addition of TW in vertical axis because of combined effects of family *Enterobacteriaceae*, family *Coriobacteriaceae* and family *Rumminococcaceae* (Fig. 5.4 E). There were no dominant family responsible for horizontal separation caused by addition of G, suggesting that the separation may be caused by small changes abundances of multiple families.

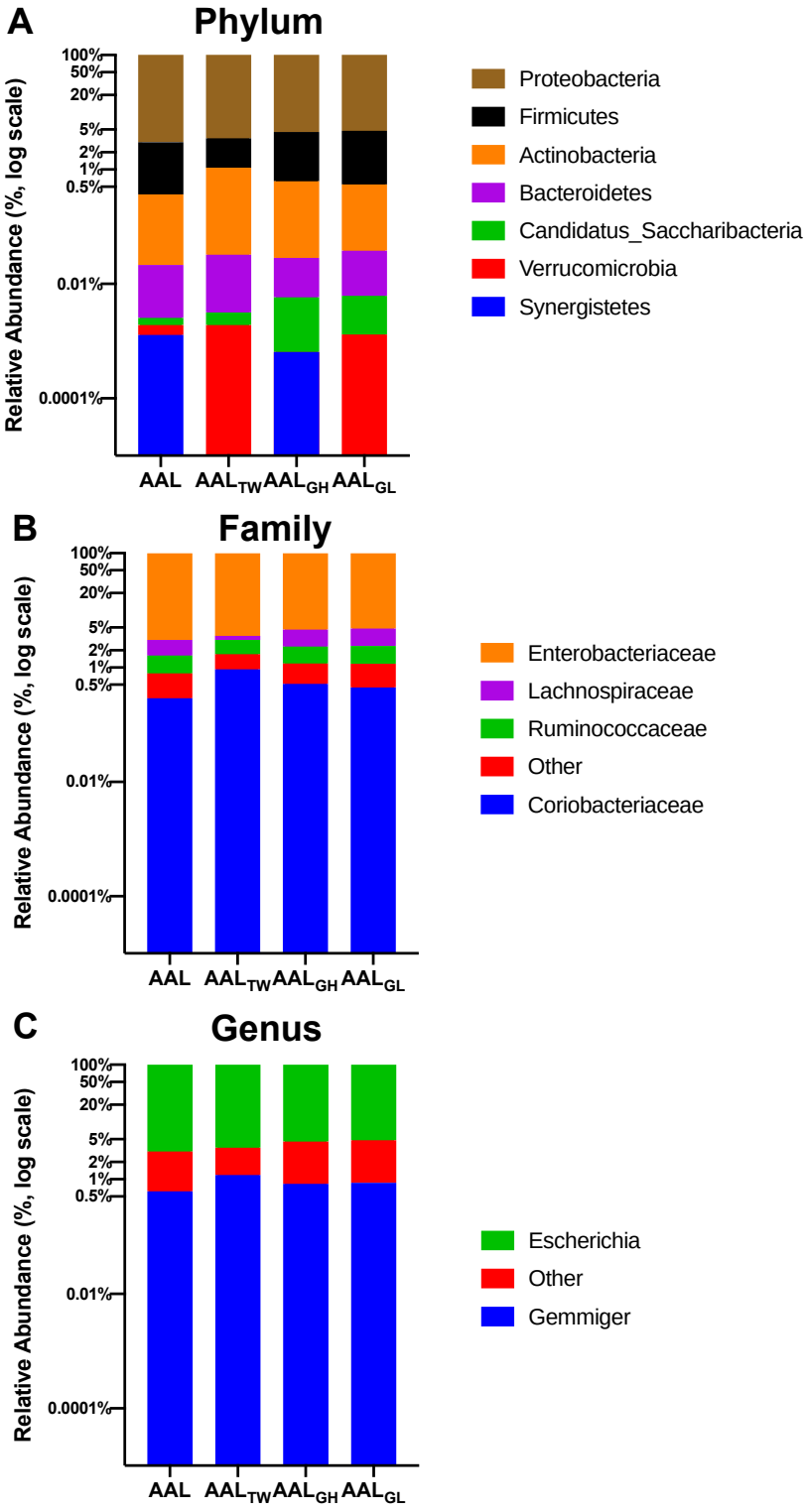

Figure 5.5 *Taxonomic distribution of fecal microflora at (A) phylum, (B) family, and (C) genus level in 24 hours 25 mM AA alone or in combination with TW, low G or High G treatment.*

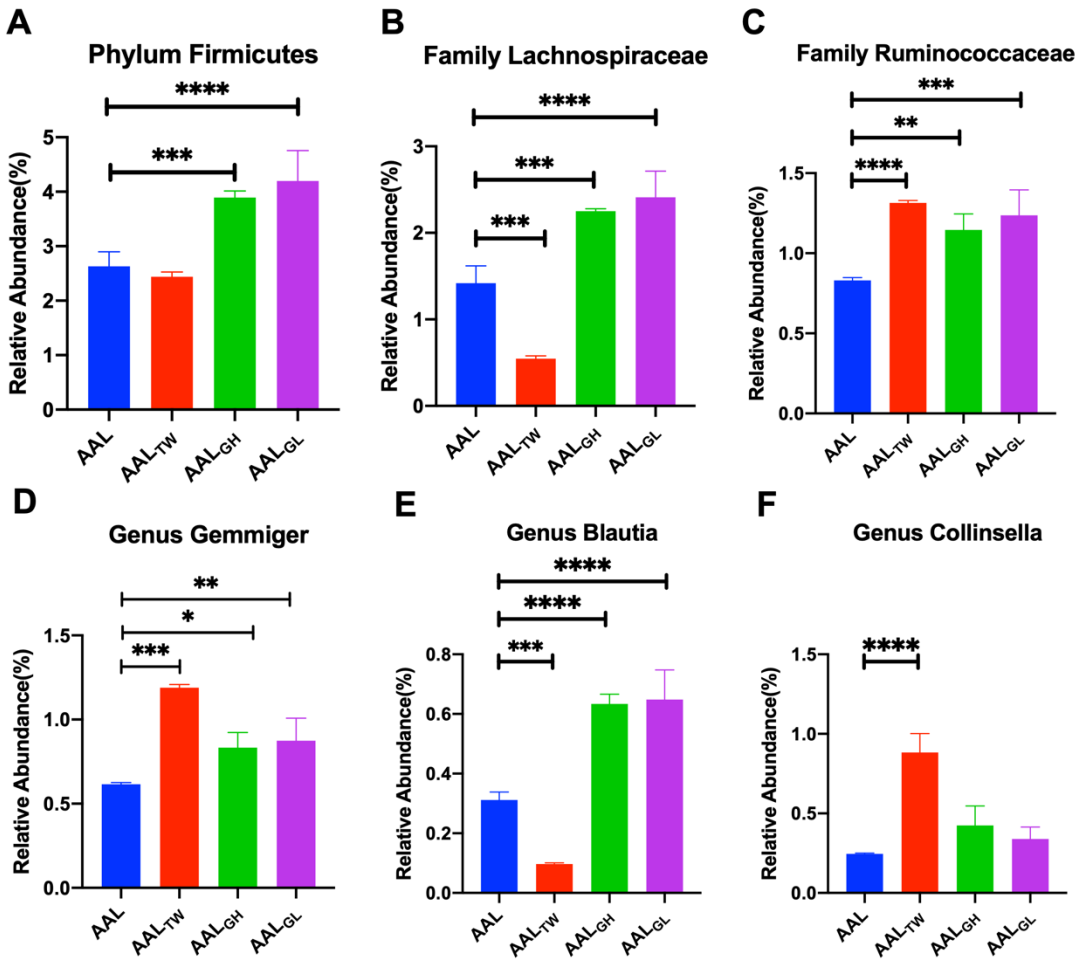

Figure 5.6 *Comparison of relative abundance of (A) Firmicutes, (B) Lachnospiraceae, (C) Ruminococcaceae, (D) Gemmiger, (E) Blautia and (F) Collinsella in 24 hours 25 mM AA alone or in combination with TW, low G or High G.*

Most of fecal microbiota detected in AA and combination of emulsifiers groups mainly fall into 2 phyla: *Proteobacteria* and *Firmicutes*, and 3 families: *Enterobacteriaceae*, *Lachnospiraceae*, and *Ruminococcaceae*, and two genera: *Escherichia* and *Gemmiger* (Fig. 5.5). Family *Enterobacteriaceae* and genus *Escherichia* are belonging to phylum *Proteobacteria*. The abundance of Family *Enterobacteriaceae* and genus *Escherichia* were higher than 95 %, but the difference between treatments was not significant. Family *Lachnospiraceae* and *Ruminococcaceae* are belonging to phylum *Firmicutes*. The top two phyla were *Proteobacteria* and *Firmicutes*. Irritable bowel syndrome has been reported to have

correlation with phylum *Firmicutes* and *Proteobacteria* (Rajilić–Stojanović et al., 2011).

At 25 mM AA exposure of 24 h group (Fig. 5.6), addition of TW decreased levels of family *Lachnospiraceae.* AA_{TW} increased the abundance of probiotic *Gemmiger* (Forbes et al., 2018) while decreased the abundance of probiotic *Blautia*. Besides, abundance of harmful bacteria *Collinsella* was greatly increased by $AA_{TW.}$ Addition of G enhanced abundance of *Firmicutes, Lachnospiraceae* and *Ruminococcaceae* as well as probiotic *Blautia.*

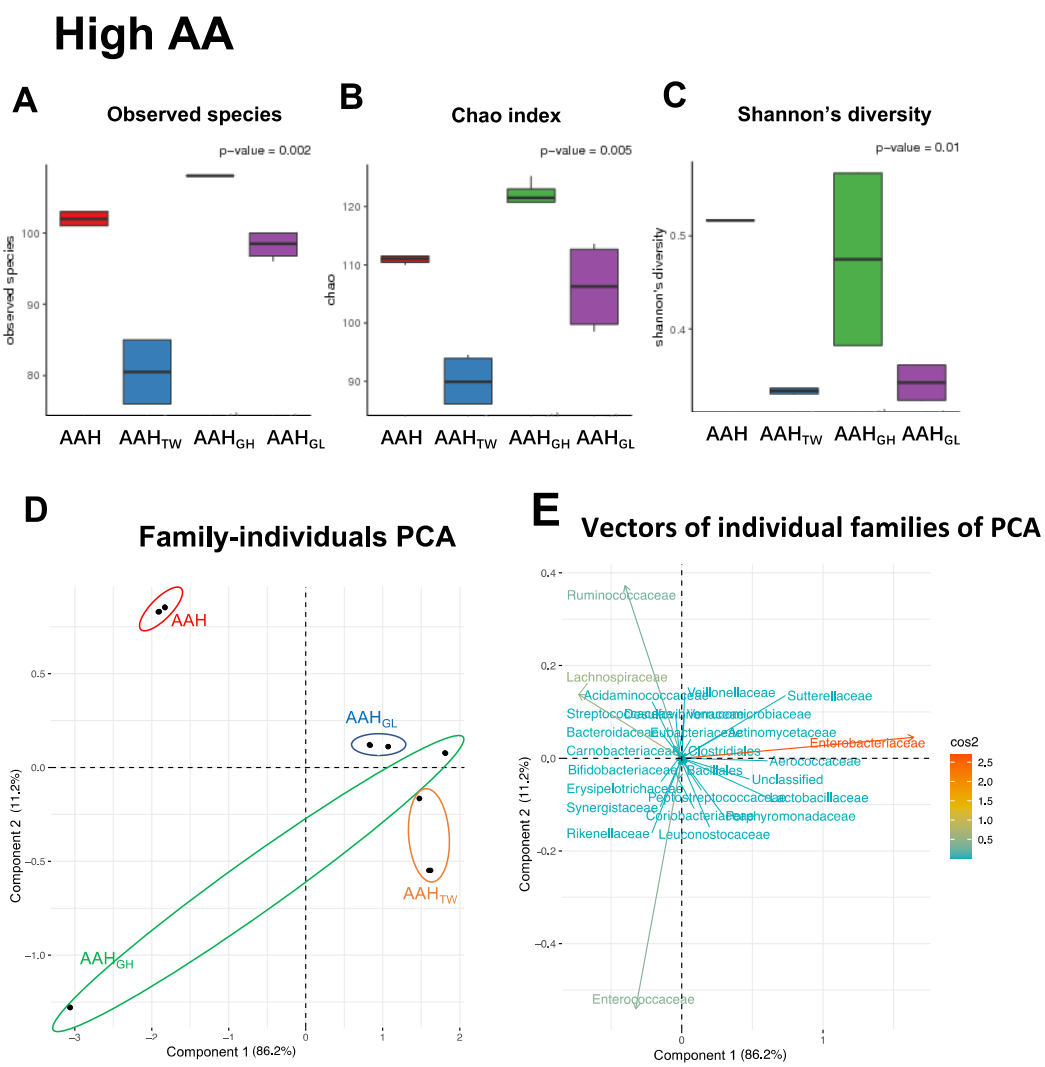

Figure 5.7 *Comparison of fecal microbiota after 24 hours emulsifiers alone, 200 mM AA alone and co-exposure of emulsifiers and 200 mM AA, (A) Observed species number of fecal bacteria, (B) Chao index, the higher Chao index, the higher community richness, (C) Shannon diversity index, the higher Shannon diversity index, the higher community diversity, (D) Principal component analysis (PCA) of microbiota community structure at family level of various treatments indicated by different colors, (E) Vector direction and strength of individual families and their contribution to PCA in (D). Colors are defined by the squared loadings (cos^2).*

At 200 mM AA (Fig. 5.7), addition of TW decreased total observed species, Chao index and Shannon index. High G increased total observed species and Chao index

whereas had unclear diversity. Low G had no effect on total observed species, Chao diversity index but significantly lower Shannon index.

PCA showed strong separation between AA treatment and those with emulsifiers. The emulsifiers groups were clustered together. The horizontal separation was driven by *Enterobacteriaceae* and separation for vertically was likely driven *Ruminococcaceae* and *Enterococcaceae*.

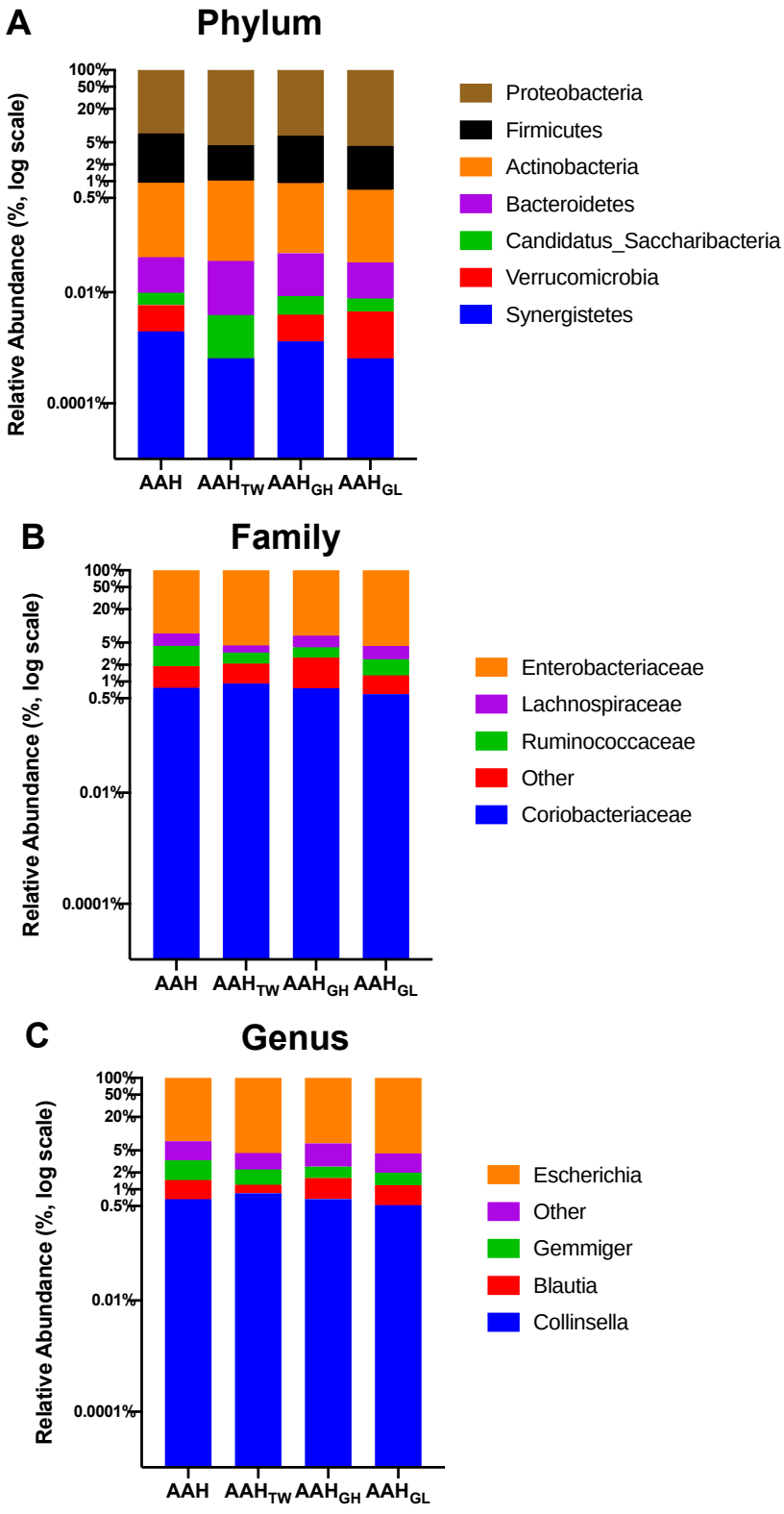

Figure 5.8 *Taxonomic distribution of fecal microflora at (A) phylum, (B) family, and (C) genus level in 24 hours 200 mM AA alone or in combination with TW, low G or High G treatment.*

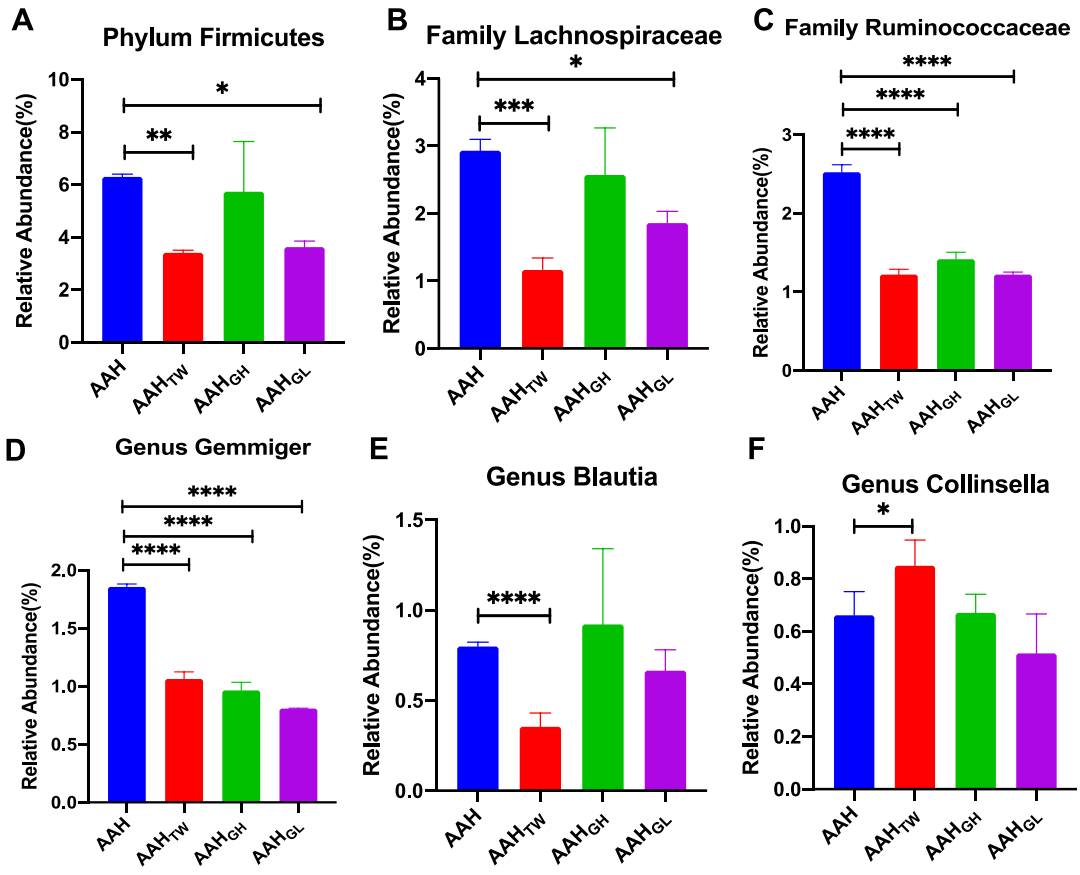

Figure 5.9 *Comparison of relative abundance of (A) Firmicutes, (B) Lachnospiraceae, (C) Ruminococcaceae, (D) Gemmiger, (E) Blautia and (F) Collinsella in 24 hours 200 mM AA alone or in combination with TW, low G or High G treatment.*

In 200mM AA exposure, AAH_{TW} and AAH_{GL} significantly reduced abundance of *Firmicutes* and *Lachnospiraceae* (Fig. 5.9). Addition of emulsifiers decreased abundance of *Ruminococcaceae* and Genus *Gemmiger*. Besides, AA_{TW} increased abundance of harmful bacteria *Collinsella* and decreased potential probiotic bacteria *Blautia* and *Gemmiger*.

Effects of emulsifier was different with different concentrations of AA. AAL_{GL} increased the abundance of *Firmicutes*, *Lachnospiraceae*, *Ruminococcaceae*, *Gemmiger*, *Blautia* and *Collinsella* while AAH_{GL} decreased abundance of them. While when GH was added to AAL or AAH, the trend of *Firmicutes*, *Lachnospiraceae*, *Ruminococcaceae* and *Gemmiger* were opposite. For co-exposure of TW, most

bacterial respond similarly to different AA concentration. Only the trends of AAL_{TW} and AAH_{TW} on *Ruminococcaceae* or *Gemmiger* were opposite.

The difference of various G concentrations on bacteria is minimal. Different concentration of G has similar effect on AAL. AAH_{GH} and AAH_{GL} had similar effect on microbiota. Compared with $AAH_{GL,}$ there were trends of AAH_{GH} on higher abundance of genera *Blautia* or *Collinsella* but the difference was not statistically significant.

Effect of emulsifiers on *Firmicutes* was mixed. It was unclear why *Firmicutes* were significantly decreased at AAH_{TW} and AAH_{GL} but not in AAH_{GH}. The changes of bacterium's abundance can lead to different outcome. The roles of the *Firmicute* in published paper have been inconsistent (Duncan et al., 2008; Kimura et al., 2013; Vrieze et al., 2012). *Firmicutes* is one kind of key metabolic function bacteria in human gut (Luo et al., 2021). Some papers indicated *Firmicutes* was positively correlated with metabolic syndrome also could contribute to bile acid and glucose metabolism (He et al., 2018; Vrieze et al., 2014).

TW showed more obvious effect on microbiota than G when combined with AA. At both concentrations of AA, co- exposure of TW showed the lowest species numbers, community richness and diversity, whereas co-exposure of G showed increased species numbers, community richness and diversity. Co-exposure of TW, AAL and AAH decreased the abundance of family *Lachnospiraceae* and probiotic genus *Blautia*. Family *Lachnospiraceae* is belonging to phylum *Firmicutes w*hich has shown prevent colitis (Surana and Kasper, 2017). *Blautia* is genus of containing probiotic bacteria also from family *Lachnospiraceae* and was reported of regulating human health, alleviating metabolic syndrome and biological transformation (Liu et al., 2021). On the contrary, AAL_{GH} and AAL_{GL} increased the abundance of family *Lachnospiraceae* and genus *Blautia*. But AAH_{GL} decreased *Lachnospiraceae*. Genus *Collinsella* is dominant part

of family *Coriobacteriaceae* and phylum *Actinobacteria. Collinsella* impacts host metabolism according to inhibiting liver glycogenesis, disrupting intestine cholesterol absorption and boosting triglyceride synthesis (Gomez-Arango et al., 2018). Administration of *Collinsella* decreased expression of tight junction protein ZO-1 in epithelial Caco-2 cell and increased permeability of intestine in mice (Chen et al., 2016). AAL_{TW} and AAH_{TW} resulted in increased abundance of genus *Collinsella*. The co-exposure of G and AA had no effect on the abundance of *Collinsella*.

As the concentration of AA increased, some beneficial bacteria, such as *Gemmiger* and *Ruminococcaceae*, also decreased. Endotoxin was negatively associated with *Ruminococcaceae* (Punzalan and Qamar, 2017). *Gemmiger* belong to family *Ruminococcaceae* and phylum *Firmicutes.* The genus *Gemmiger* was found to be higher abundance in heath people compared to patients with Crohn's disease (Forbes et al., 2018).

Based on the results, we found changes in fecal microbiota by emulsifiers aggravates effect in AA-induced gut community. The additive effect of TW is larger than G; Different concentration G have minor difference on these microbiota. Therefore, we selected TW for 21 days SHIME fermentation.

5.3.3 Effect of AA and emulsifiers over 21 days in SHIME

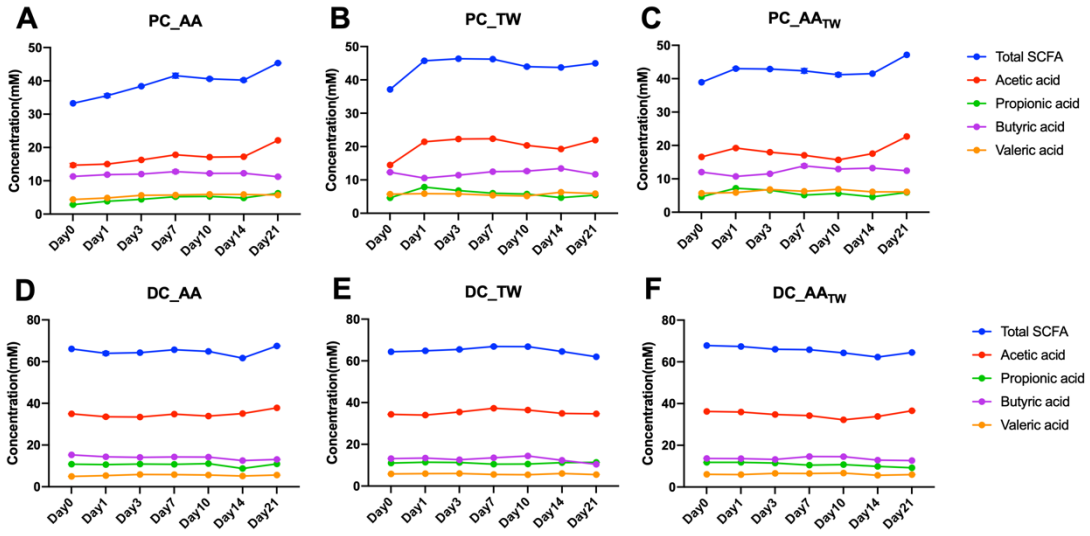

Figure 5.10 *Short chain fatty acid (SCFA) levels (mean ± SD) during and after treatment in PC and DC chambers from AA, TW, AA_{TW} treatment in terms of total SCFA, acetic acid, propionic acid, butyric acid and valeric acid.*

Total SCFA levels increased for all treatments in the PC across the experimental period, and its largely driven by the increase of acetic acid concentration (Fig. 5.10). There were fluctuations on levels of propionic acid, butyric acid and valeric acid in PC across the experimental period but no overall change could be observed. Total SCFA and acetic acid increase were gradual for AA and AA_{TW} treatments, but an earlier increase was observed in TW treatment in PC. Total SCFA, acetic acid, propionic acid, butyric acid, and valeric acid levels in DC fluctuated over the experiment, but no overall alteration was discovered. The overall differences were minor.

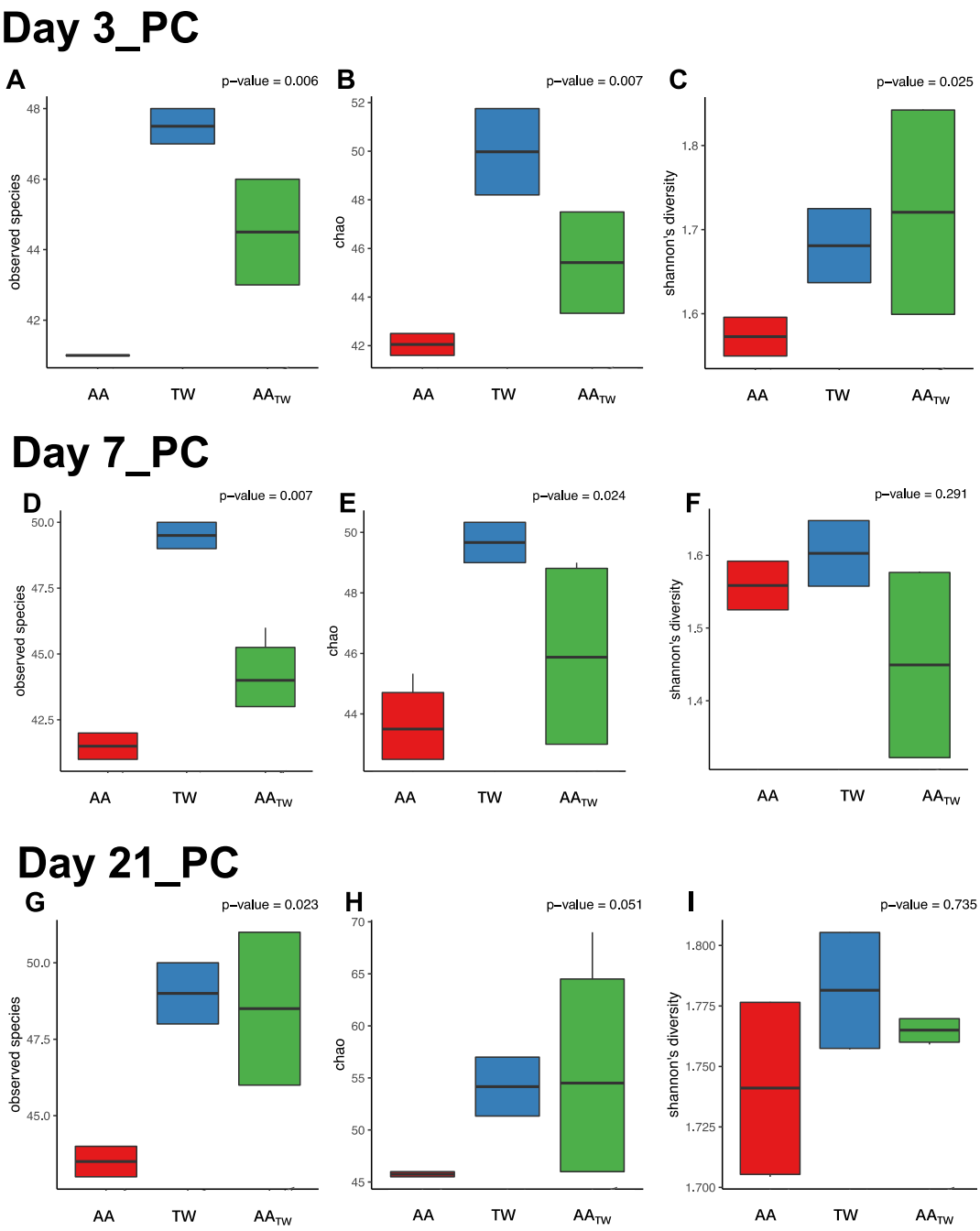

Figure 5.11 *Boxplots of total observed species in PC on (A) day 3, (D) day 7 and (G) day 21, Chao index at (B) day 3, (E) day 7 and (H) day 21, and Shannon diversity index at (C) day 3, (F) day 7 and (I) day 21. The higher Chao index, the higher community richness. The higher Shannon diversity index, the higher community diversity.*

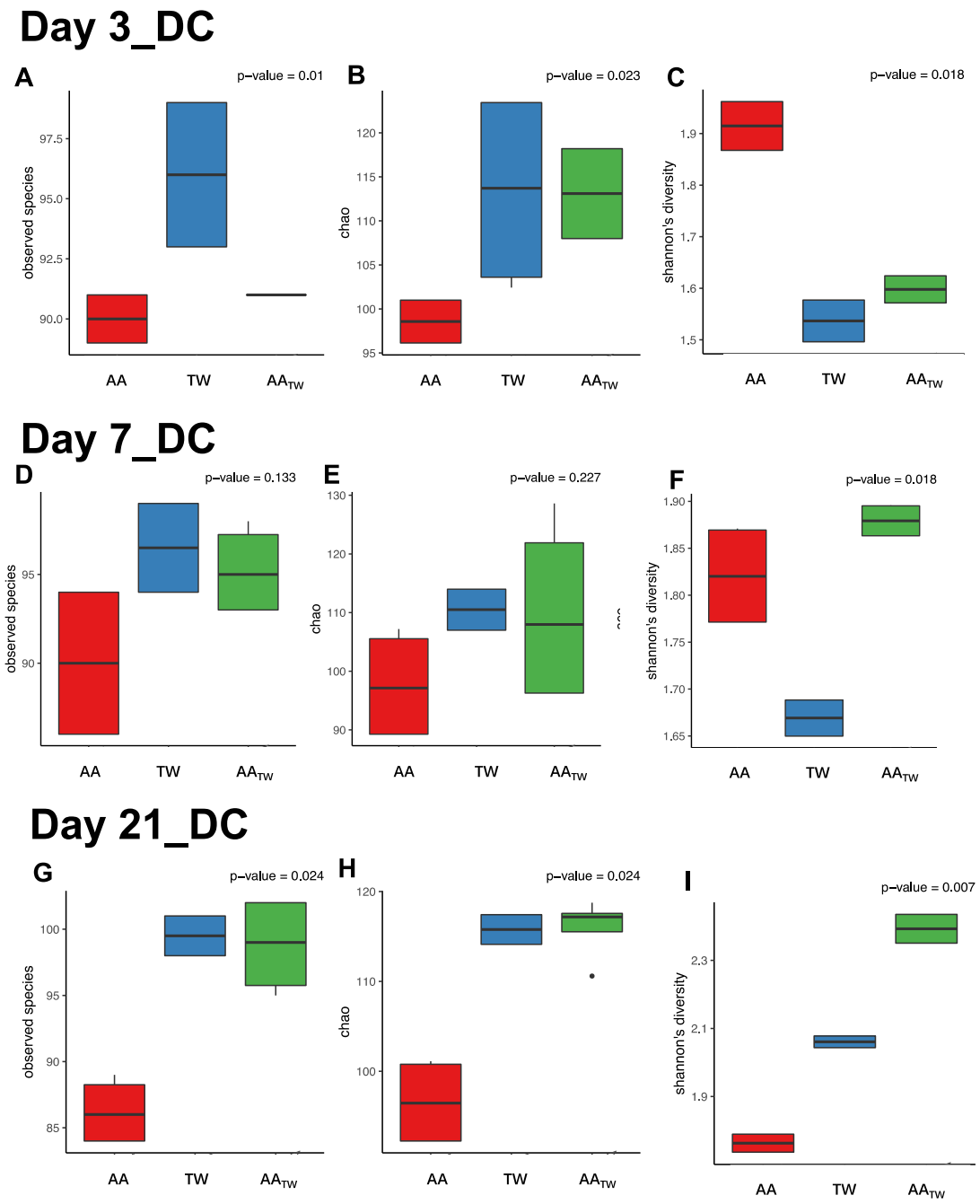

Figure 5.12 *Boxplots of total observed species in DC on (A) day 3, (D) day 7 and (G) day 21, Chao index at (B) day 3, (E) day 7 and (H) day 21, and Shannon diversity index at (C) day 3, (F) day 7 and (I) day 21. The higher Chao index, the higher community richness. The higher Shannon diversity index, the higher community diversity.*

In the PC, total observed species remained stable while species richness (Chao index) and diversity (Shannon's index) became more variable within treatments as

exposure continues (Fig. 5.11). Across the experimental period, there were large shifts of species diversity in all treatments, suggesting the community have not stabilized under the exposure treatments.

In the DC, total observed species increased slightly but the effect of treatments became more different and variability between samples increased with time (Fig. 5.12). AA treatment tend to have the lowest species richness and diversity. Interestingly, even though TW and AA_{TW} has similar species richness, TW has lower diversity, suggesting presence of highly dominant species compared with AA_{TW}. This trend was different from that in PC.

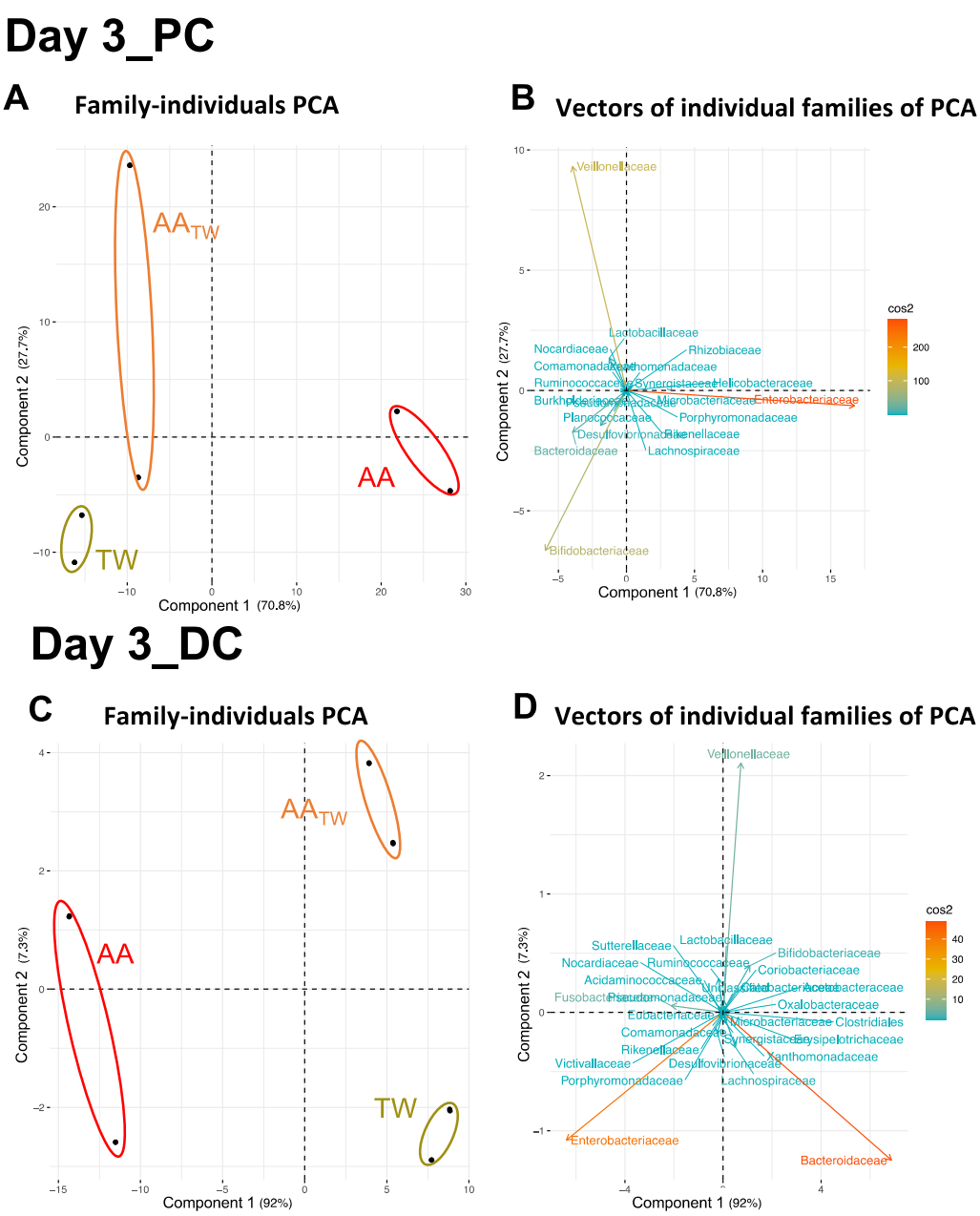

Figure 5.13 *Comparison of fecal microbiota after 3 days AA alone, TW alone and co-exposure of AA and TW in PC and DC chambers, (A&C) Principal component analysis (PCA) of microbiota community structure at family level of various treatments indicated by different colors, (B&D) Vector direction and strength of individual families and their contribution to PCA in (A&C). Colors are defined by the squared loadings (cos2).*

On day 3, differences in microbiota community between all three treatments have already developed in both PC and DC (Fig. 5.13). Differences in the microbial community was well explained by PCA (98.5 % in PC and 99.3 % in DC) (Fig. 5.13).

In PC chamber, the separation of treatments was mainly associated with abundance of *Enterobacteriaceae* (Fig. 5.13 B). For DC chamber, separation of AA_{TW} from AA treatment was driven by *Vellonellaceae* while clustering of TW was driven by *Bacteroidaceae* (Fig. 5.13 D).

The microbiota community of AA_{TW} was more similar to TW on day 3 (Fig. 5.13) but more similar to AA on day 7 (Fig. 5.14). In PC chamber, separation of AA_{TW} from AA treatment was driven by *Vellonellaceae* while clustering of TW was driven by *Bifidobacteriaceae* (Fig. 5.14 B). For DC chamber, the separation of treatments was mainly related to *Bacteroidaceae* (Fig. 5.14 D).

On day 21, the microbiota community of AA_{TW} was more similar to AA in PC chambers (Fig. 5.15). In PC chamber, separation of AA_{TW} from AA treatment was driven by *Enterobacteriaceae* while clustering of TW was driven by *Bifidobacteriaceae* (Fig. 5.15 B). For DC chamber, the separation of treatments was mainly related to *Bacteroidaceae* (Fig. 5.15 D).

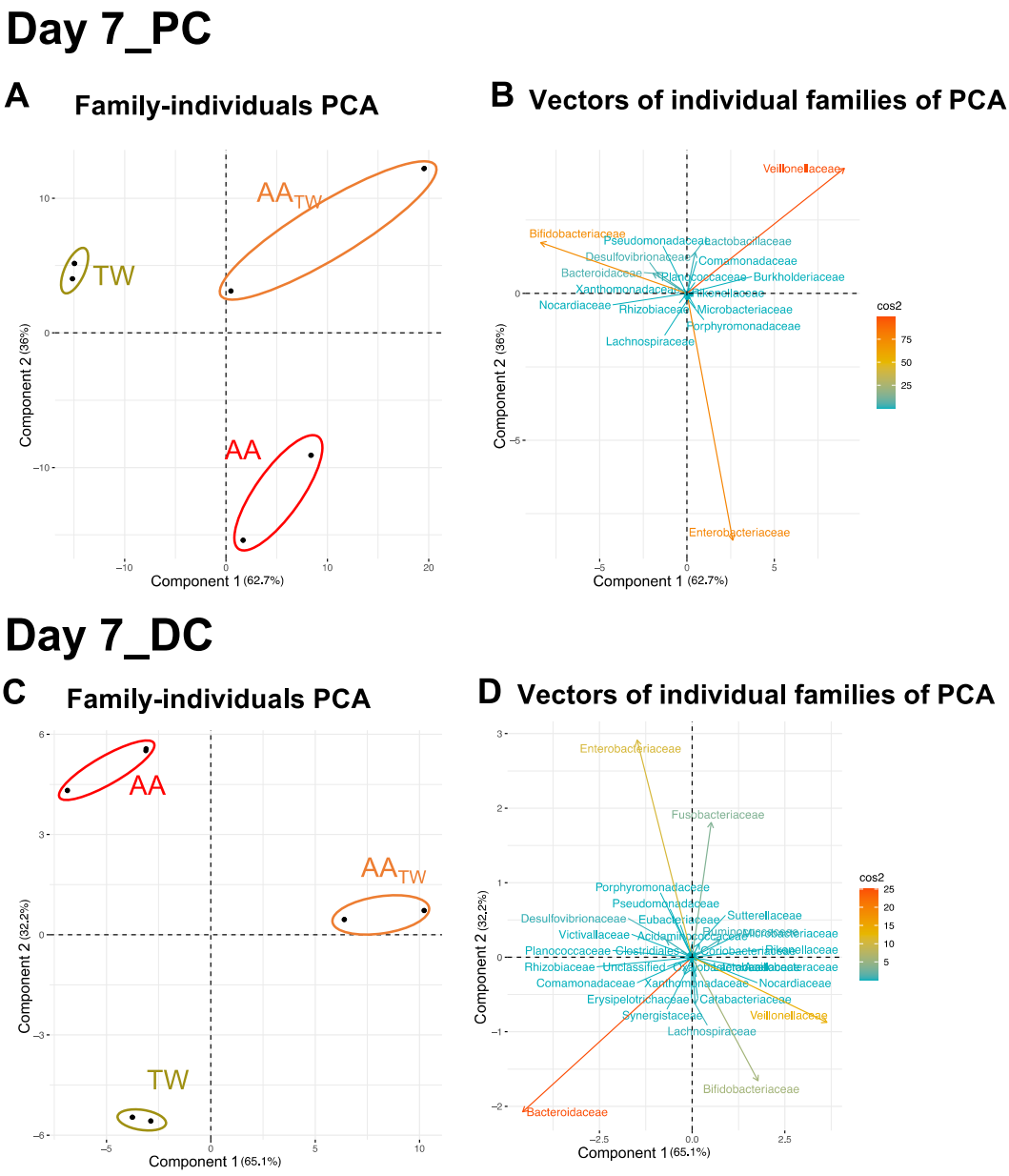

Figure 5.14 *Comparison of fecal microbiota after 7 days AA alone, TW alone and co-exposure of AA and TW in PC and DC chambers, (A&C) Principal component analysis (PCA) of microbiota community structure at family level of various treatments indicated by different colors, (B&D) Vector direction and strength of individual families and their contribution to PCA in (A&C). Colors are defined by the squared loadings (cos2).*

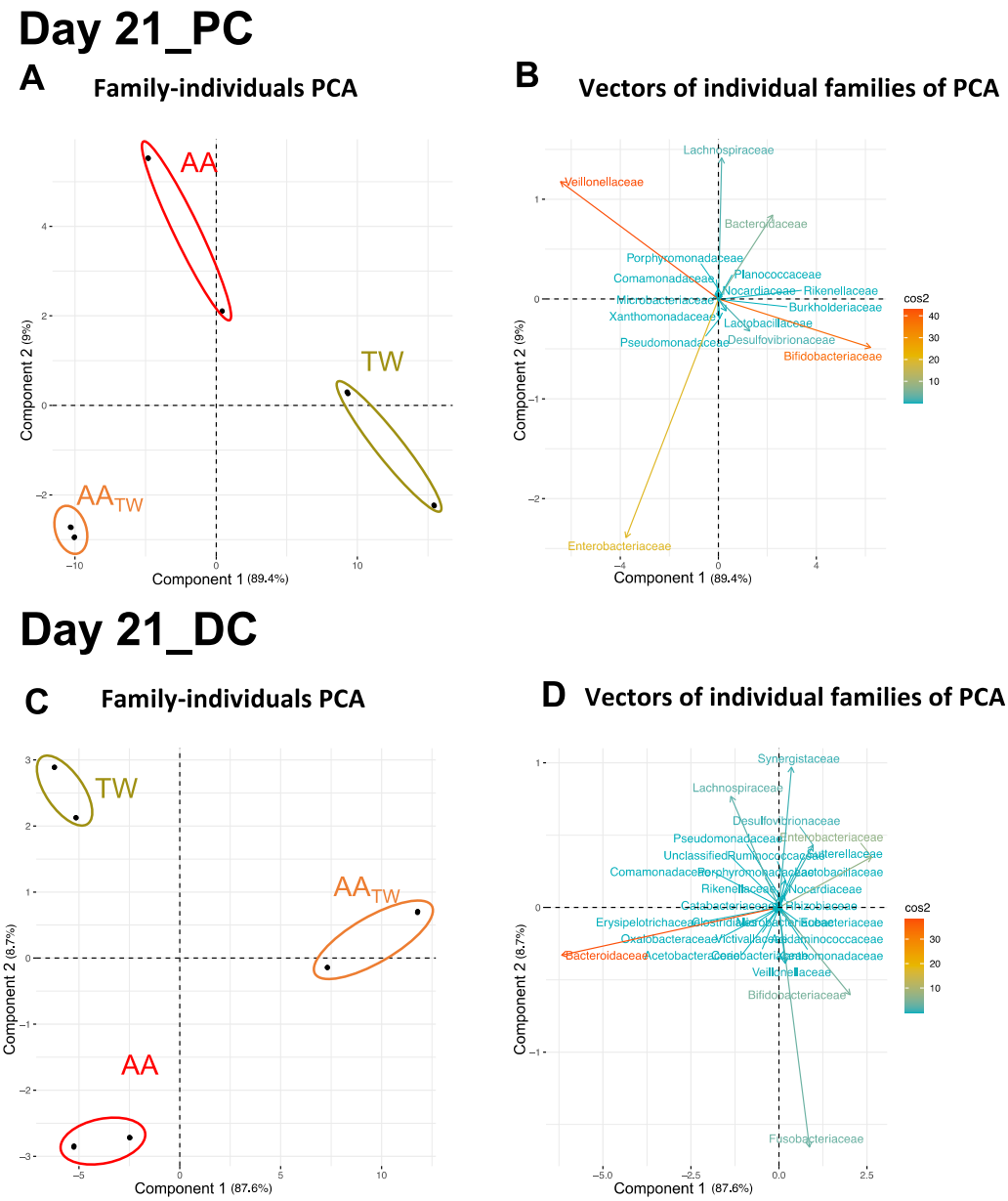

Figure 5.15 *Comparison of fecal microbiota after 21 days AA alone, TW alone and co-exposure of AA and TW in PC and DC chambers, (A&C) Principal component analysis (PCA) of microbiota community structure at family level of various treatments indicated by different colors, (B&D) Vector direction and strength of individual families and their contribution to PCA in (A&C). Colors are defined by the squared loadings (cos2).*

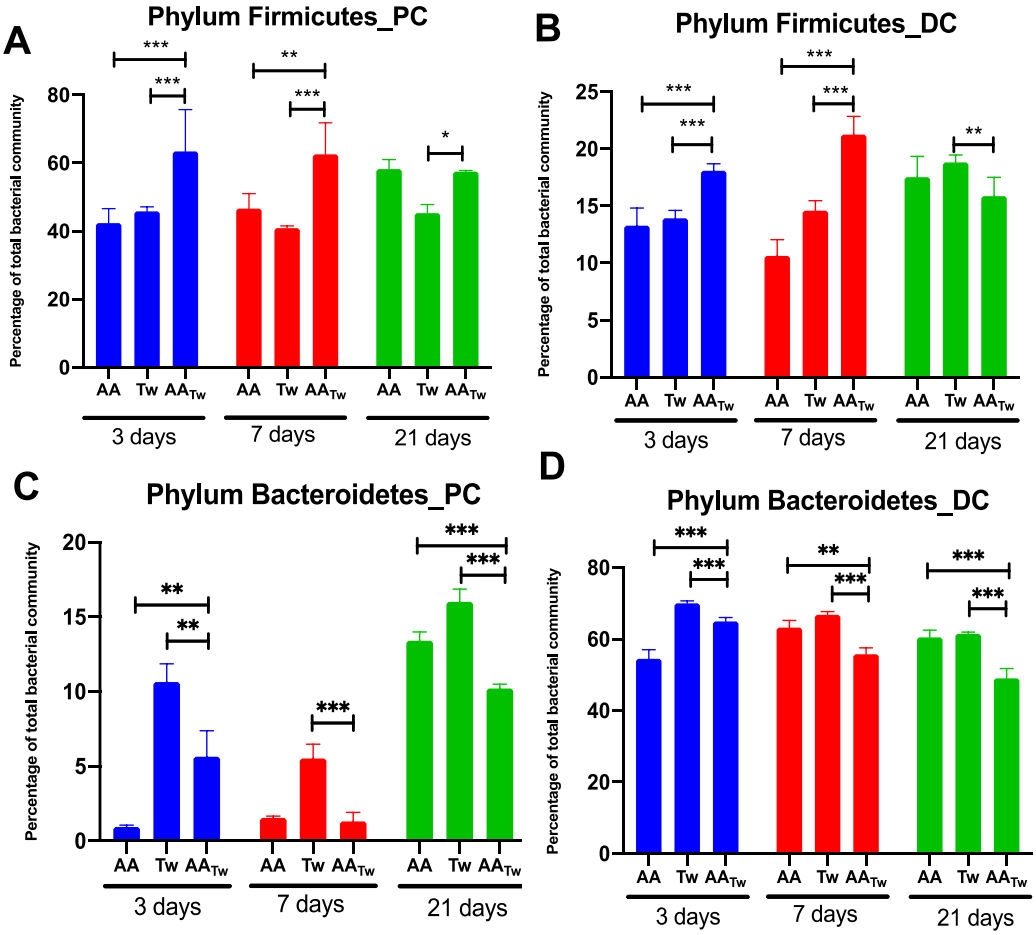

Figure 5.16 *Relative abundance of selected phyla on day 3, day 7 and day 21 of exposure: (A) Firmicutes in PC and (B) DC chambers; (C) Bacteroidetes in PC and (D) DC chambers.*

AA and TW had similar effect on the abundance of phylum *Firmicutes* (Figs. 5.16 A and B). AA_{TW} group induced a higher abundance of phylum *Firmicutes* than the other two treatments in PC and DC on day 3 and 7 but not on day 21. *Firmicutes* abundance became more similar between treatments on day 21. The abundance of *Firmicutes* in PC (40.9-63.4 %) is higher than in DC (10.6-21.3 %) chamber.

The relative abundance of *Bacteroidetes* was 0.9-16.0 % in PC chamber whereas went up to 70.0 % in the DC chambers (Figs. 5.16 C and D). At the first 7 days, the abundance of *Bacteroidetes* in AA was lower than 1.5 %, however on the day of 21, it raised to 13.4 % in PC. The trend of *Bacteroidetes* in TW was unstable in PC. AA_{TW}

group induced a lower abundance of phylum *Bacteroidetes* than the other two treatments in PC on day 7 and 21 but not on day 3. AA and TW have similar effect on the abundance of *Bacteroidetes* on day 7 and day 21. AA_{TW} had lower abundance of *Bacteroidetes* compared with AA and TW in DC chambers especially on day 7 and 21.

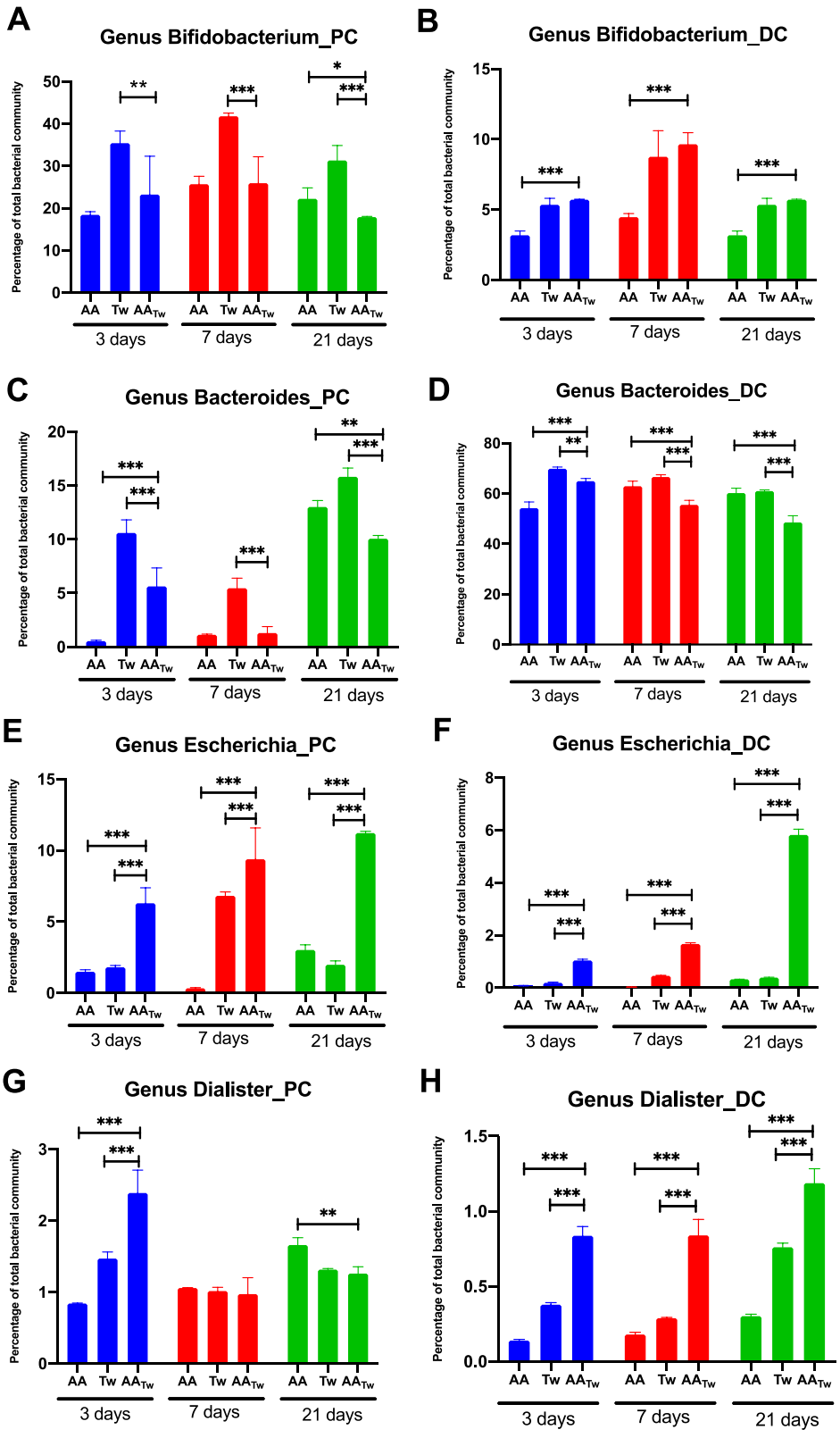

Figure 5.17 *Relative abundance of selected genera on day 3, day7 and day 21 of exposure: (A) Bifidobacterium in PC and (B) DC chambers; (C) Bacteroides in PC and (D) DC chambers; (E) Escherichia in PC and (F) DC chambers; (G) Dialister in PC and (H) DC chambers.*

Only TW increased the abundance of *Bifidobacterium* in PC (Fig. 5.17 A). Abundance of *Bifidobacterium* in AA and AA_{TW} were similar in PC on day 3 and day 7 but AA_{TW} resulted in decreased abundance of *Bifidobacterium* on 21 day (Fig. 5.17 A). Both TW and AA_{TW} had increased abundance of *Bifidobacterium* in DC chamber on days 3, 7 and 21 (Fig. 5.17 B). The effect of TW on the *Bifidobacterium* in PC and DC was not the similar. Role of *Bifidobacterium* in published studies have been mostly positive (Turroni et al., 2008). *Bifidobacterium* is a common probiotic bacterium that prevent gut from inflammation (Srutkova et al., 2015). However several studies also showed that *Bifidobacterium* was significantly more abundant in gut microbiota of IBD than healthy individuals (Scanlan et al., 2006; Seksik et al., 2003; Wang et al., 2014). It is uncertain if the addition of TW will turn the Bifidobacterium toward a positive or negative side.

Genus *Bacteroides* has similar trend as phylum *Bacteroidetes.* The relative abundance of *Bacteroides* was between 0.9-16.0 % in the PC chambers but went up to 70.0 % in the DC chambers (Figs. 5.17 C and D). On day 3 of the PC chamber, AA had the lowest abundance of *Bacteroides* and the abundance increased from day 7 to day 21. The abundance of *Bacteroides* in DC remained stable after AA treatment for 21 days. TW had the highest abundance of *Bacteroides* in PC and DC from day 3 to day 21. AA_{TW} had lower abundance of *Bacteroides* compared with AA and TW in PC and DC chambers especially on day 7 and 21. *Bacteroides* were known to help maintain a beneficial gut environment (Zafar and Saier Jr, 2021). However when it escaped the immune system of host, *Bacteroides* could produce some enterotoxin and cause infection such as bacteremia and abscess (Wexler, 2007). Lower abundance of *Bacteroides* was involved in the active phase of IBD patients (Zhou and Zhi, 2016). However, *Bacteroides* were higher abundance in obese patients with some metabolic disorders (Zeng et al., 2019).

A significant increase of bacteria *Escherichia* was observed in the AA_{TW} group throughout the experimental period and in both PC and DC chambers (Figs. 5.17 E and F). Compared to AA or TW, AA_{TW} increased the abundance of *Escherichia* by 3.7-fold and 5.6-fold respectively in PC on day 21 while AA_{TW} increased the abundance of *Escherichia* by 18.3-fold and 14.2-fold respectively in DC on day 21. Several *Escherichia* strains have been reported to be associated with a variety of intestinal and extraintestinal diseases (Kaper et al., 2004). Over-abundant of *Enterobacteriaceae* can increase gut permeability and induce endotoxemia to worsen liver function in cirrhosis (Quigley et al., 2013). In IBD, common changes include a decrease in key Gram-positive bacteria from within phylum *Firmicutes* and a raise in Gram-negative *Proteobacteria*, especially *Enterobacteriaceae* such as *Escherichia* associated with patient bowel lesions and shown to induce intestinal inflammation and inflammation-associated CRC in mice (Arthur et al., 2012; Merga et al., 2014; Partridge et al., 2019).

AA_{TW} strongly increased abundance of *Dialister* on day 3 of PC chambers and day 3, 7 and 21 of DC chambers. Especially, co-exposure of TW, AA increased the abundance of *Dialister* by 2.6-fold on day 21. *Dialister* has been reported it has a relationship with several diseases such as cancer, obesity, and depression due to production of acetate, lactate and propionate (Demirci, 2021).

Although direct comparison of microbial communities between 24 h fermentation batch and SHIME are not appropriate due to differences in microbial communities of donor, and different of experimental setup, there were commonalities in results of both set of experiment. Emulsifiers aggravated AA-induced changes in microbiota community that were potentially related to metabolic disorders and inflammatory bowel disease (IBD). The relative abundance of several important phyla of gut bacteria, such as *Firmicutes* and *Bacteroidetes* (a larger abundance of *Firmicutes* and a lower proportion of *Bacteroidetes*), was linked to metabolic syndrome (Ferrer et al., 2013). Previous study showed the relative abundance of *Firmicutes* was higher than 50 %

whereas the *Bacteroidetes* was lower than 50 % in ob/ob leptin-deficient obese mouse (Turnbaugh et al., 2006). At 24 h fermentation, AAL_{GL} and AAL_{GH} upregulated *Firmicutes* by 47.9 % and 60.0 % respectively (Fig. 5.6 A). However, the abundance of *Bacteroidetes* was not significantly changed (data no showed). On the 7 day of SHIME, AA_{TW} increased *Firmicutes* by 99.9 % (Fig. 5.16 B) whereas the abundance of *Bacteroidetes* dropped to 10.4 % in DC chamber (Fig. 5.16 D). On the 21 day of SHIME, AA_{TW} did not continue increasing the abundance of *Firmicutes* whereas *Bacteroidetes* decreased to 18.9 %. Although the total abundance of *Firmicutes* and *Bacteroidetes* in DC were not higher or lower than 50% respectively, co-exposure of emulsifiers lead to this trend, especially at day 7.

Blautia and family *Lachnospiraceae* were reported to alleviate metabolic syndrome (Liu et al., 2021). When TW was added to AAL and AAH, the abundance of family *Lachnospiraceae* and *Blautia* decreased (Figs. 5.6 and 5.9). *Collinsella* and *Escherichia* were reported to associated with IBD (Mirsepasi-Lauridsen et al., 2019; Swidsinski et al., 2002), and they were increased by AA_{TW}. For examples, AAL_{TW} and AAH_{TW} increased abundance of *Collinsella* in 24 h (Figs. 5.6 F and 5.9 F). AA_{TW} increased the abundance of *Escherichia* in PC and DC of SHIME (Figs. 5.17 E and F). The genus *Gemmiger* was found to be higher abundance in heath people compared to Crohn's disease patients (Forbes et al., 2018). Co-exposure with different emulsifiers, AAH decreased the abundance of beneficial *Gemmiger* (Fig. 5.9 D). Addition of emulsifiers, AA not just increased the harmful bacterial also decreased the beneficial. As time goes by, microbiota dysbiosis may be an initiator of obesity (Ley et al., 2006), aging (Mariat et al., 2009), irritable bowel syndrome (Jeffery et al., 2012) and colorectal cancer (Bamola et al., 2017). Therefore, balance of beneficial and pathogens bacterial is key role to maintain health host.

Acetate is an important bacterial metabolite. Following absorption into systemic circulation, acetate can serve as a substrate for synthesis of cholesterol in peripheral

tissues (Harris et al., 2012; Hijova and Chmelarova, 2007; Shoaie et al., 2013). Acetate also participates in the *de novo* synthesis of lipids in the liver in addition to acting as a substrate for the production of cholesterol (Sanz et al., 2010). Therefore acetate produced by microbiota seem to be closely associated to obesity and metabolic dysfunction (Chakraborti, 2015). In both the short term and long-term trial, acetate production was observed to increase in the co-exposure treatments. In the physiologically relevant, long term, and complex SHIME model, tested mixtures consistently increased SCFA production, with acetate being the molecule most affected in PC. The higher levels of acetate in co-exposure treatments were likely induced by higher abundance of *Firmicutes*. Increasing levels of acetate and *Firmicutes* may be lead to metabolic syndrome (Wang et al., 2020). However, another study indicated that exogenously administered acetic acid could work against obesity by controlling lipid metabolism of liver and skeletal muscles in type 2 diabetic rats (Yamashita, 2016). Further studies will be needed to better understand how the observed changes would impact the host.

The combination of food additives emulsifiers on fecal microbiota composition and function was complicated. Indeed, emulsifiers can influence the gut microbiome and host health by influencing the gut immune system, the intestinal epithelial barrier, or by directly influencing the gut microbiome and subsequently affecting the gut immune system and epithelial barrier. A growing body of evidence have shown that food emulsifiers can also induce low-grade inflammation (Jiang et al., 2018), and increase initiation of carcinogenesis (Viennois et al., 2017). Recently, Naimi et al. found that 8 out of 20 emulsifiers have significant impact on microbiota community diversity but effect of each emulsifier was different on human fecal microbiota using *ex vivo* bioreactor (Naimi et al., 2021b). These evidence suggested that wide application of food emulsifiers maybe associated with increasing incidence of gut inflammation, metabolic syndrome and possibly obesity.

Addition of TW and G caused both opposing and similar effects in the fecal microbiota. As a possible mechanism, TW and G have direct antimicrobial effects on certain bacterial membranes due to their hydrophobicity and detergent properties. It is still unknown why the presence of emulsifiers benefits some bacterial genera more than others. This benefit might have resulted from emulsifiers acting as a source of nutrition, from it changing the availability or consistency of SHIME-feed, or from the mixtures changing the interactions between the various species.

5.4 Conclusion

In conclusion, we understand the research have some limitations: 1) SHIME or any host-free microbiota batch lacks complexity of human systems; 2) an individual donor. However, these models have enabled us to conclude that our observation emulsifiers aggravate an effect in AA-induced microbiota community changes, associated with metabolic syndrome and IBD. These changes included changed the abundance of the metabolic syndrome related *Firmicutes* and *Bacteroidetes* (Figs. 5.6 and 5.16), decreased the abundance of alleviated metabolic syndrome genus *Blautia* and family *Lachnospiraceae* (Figs. 5.6 and 5.9). Increased acetate level may be associated with metabolic syndrome (Figs. 5.3 and 5.10). The pathogens bacterial *Collinsella* and *Escherichia* were increased by AA_{TW} (Figs. 5.6, 5.9 and 5.17), which were link to IBD. These microbiota changes suggest that the addition of emulsifiers enhanced the adverse effects of AA, so future experiments should focus on assessing *in vivo* impacts of mixtures exposed fecal microbiota, and the potential mechanism.

CHAPTER 6

General Discussion

This thesis set out to investigate if food emulsifiers could increase the toxicity of food contaminants, and if so, how. A number of test models were used to answer this research question and provide insight into how this could impact in humans. Through a series of experiments, there were strong evidence showing that food emulsifiers could increase toxicity of food contaminants.

6.1 Co-exposure with emulsifiers increased toxicity of process contaminants

Using simple human cell lines, I established that food emulsifier TW would increase toxicity of both process contaminants tested (Chapter 2). TW decreased IC50 and IC10 values of AA and BAP in all three cell lines tested. Similar results were obtained in zebrafish, a simple vertebrate biological model. In Chapter 3, it was observed that toxicity of AA and BAP was exacerbated by both emulsifiers, leading to increased perturbation of gut villi structures and liver necrosis. In Chapter 4, similar observations were also obtained where both emulsifiers increased toxicity of AA but TW had a stronger effect than G. More severe signs of hepatocyte damage were observed in AA_{TW} than AA_{G}.

6.2 Co-exposure with emulsifiers increased the uptake of food contaminants

One potential mechanism which emulsifiers can increase chemical toxicity was facilitation of chemical uptake (Gao et al., 2016). This could mean increased bioavailability (i.e. increase in fraction of chemical absorbed) and/or increase in the rate of uptake (i.e. speed of which chemical enters the body). Based on dose-response

relationships, increase of overall internal dose due to higher bioavailability would naturally translate into higher toxicity. Increase in the rate of uptake could also lead to rapid influx of chemicals locally, overwhelming biological defense leading to toxicity. Contaminant concentration was higher in emulsifier co-exposure treatments in all three tested cell lines (Chapter 2), zebrafish (Chapter 3) and mice (Chapter 4), suggesting that emulsifiers can lead to increased bioavailability of chemical contaminants. In the experiment with Calcein AM uptake in Caco-2 monolayer (Chapter 2), it was observed that slope of fluorescence increase intracellularly was steeper in cells exposed to emulsifiers. This suggested that emulsifiers could also increase the rate of chemical uptake. There are a number of possible explanations for these effects. Using Caco-2 monolayers (Chapter 2), it was found that emulsifiers could decrease tight junction protein expression and increase cell membrane permeability, suggesting barriers in transcellular and paracellular uptake were both compromised. Experiment on mice partially confirmed these results as tight junction protein gene and protein expression were also decreased by emulsifiers (Chapter 4). Increased uptake of FITC-dextran was observed in mice after short exposure to emulsifiers (Chapter 4) suggested that absorption through passive diffusion is increased. There was similar report of increased uptake of allergens (Harusato et al., 2022). It should be noted that all effects discussed in this passage was coming from exposure to emulsifier alone. Potential interactions with food contaminants had not been considered yet.

6.3 Co-exposure with emulsifiers increased gut inflammation

Co-exposure with emulsifiers also increased contaminant toxicity in ways other than increased contaminant uptake. These were evident in the animal studies (Chapters 3 and 4) where multiple inflammatory biomarkers were up-regulated in the combined treatments and more severe inflammation was observed in zebrafish and mice GI tract under histopathological investigations. Interaction of emulsifier and contaminants were either additive or synergistic as demonstrated in zebrafish (Chapter 3), where TW or G did not cause any inflammation of the liver, 3 mg/kg AA led to slight increase in lipid

accumulation but no inflammation, and the combination of AA and TW or G resulted in increase in inflammation and infiltration of immune cells. The similar histopathological changes were observed in mice (Chapter 4), where TW or G led to small infiltration of immune cells, 40 mg/kg AA led to more severe signs of degradation of hepatocytes and the combination of AA and TW or G resulted in disorganized hepatic cords and large areas of degradation of hepatocytes. Similar synergistic trends were observed in other immune biomarkers, such as gene expression of il-1β in zebrafish (Chapter 3) and Tnf-α in mice (Chapter 4).

It was that TW at high concentration (1.0 % v/v) via drinking water can lead to low-grade inflammation in wild-type mice and robust colitis in IL10 -/- mice (Chassaing et al., 2015). However in the current study of fish low concentration of emulsifiers were used (TW: 0.1 % w/w fish feed, G: 1 % w/w fish feed) and could already interact with food contaminants to increase toxicity. The concentration used in mice study for TW or GMS is 25 mg/kg bw/day or 200 mg/kg bw/day. 25 mg/kg bw/day TW is the acceptable daily intake (ADI) set by the Joint Food and Agriculture Organization of the United Nations (FAO)/World Health Organization (WHO) Expert Committee on Food Additives (JECFA) (EFSA Panel on Food Additives, 2015). While the daily intake of G is not limited, reported intake level of emulsifiers could be higher than 254 mg/kg bw/day in China (Gao et al., 2016). These mean the concentration of emulsifiers used in the mice study do exist in our life.

6.4 Potential effects of emulsifier co-exposure on metabolism and obesity

Transcriptome analyses of mice ileum comparing AA vs AA_{TW} and AA vs AA_{G} treatments showed more than 450 genes were significantly differentially expressed in each case (Chapter 4). Top KEGG pathways shifted from most related to immune diseases based on differentially expressed genes comparing AA and control to most related to obesity and lipid metabolism comparing AA and AA_{TW} or AA_{G}. Increased

gene expression of PPARγ was observed in mice after exposure to AA_{TW} (Chapter 4). These offered explanation to the observed weight increase of AA_{TW} which was double that of control and other treatments (Chapter 4).

AA were shown to cause obesity in C57BL/6J mice given an high-fat-diet via an activated MAPK pathway after 10 weeks (Lee and Pyo, 2019). TW caused low-grade inflammation and obesity/metabolic syndrome in wild-type C57Bl/6 mice (Chassaing et al., 2015). Interestingly, co-exposure with emulsifiers exhibited an effect on metabolism like combination of HFD such as increased gene expression of p-P38 and p-ERK (Chapter 4). These mean dietary of AA and emulsifiers have a potential to induce obesity and the mechanism require further investigation.

6.5 Co-exposure with emulsifiers increased alteration of gut microbiome

Addition of TW, both low AA and high AA decreased the number and diversity of intestinal bacterial species in 24h fermentation (Chapter 5), however the trend were inconsistency in 21 days SHIME fermentation (Chapter 5). The combination of AA and TW or G resulted in decrease in the number of species and diversity of intestinal bacterial species in mice but not significantly (Chapter 4). Using PCA analyses, it was observed that AA_{TW} increased separation from AA with fermentation time in DC chamber (Chapter 5). This suggested that addition of emulsifiers could change the number of species and diversity of microbiota community.

Co-exposure with TW also decreased beneficial bacterial and increased the harmful bacterial. AA_{TW} decreased the abundance of beneficial *Lachnospiraceae* and *Blautia*, and increased the abundance of harmful *Collinsella* in 24 h fermentation (Chapter 5). Similar changes were showed in the SHIME (Chapter 5), where AA_{TW} increased the abundance of harmful bacteria *Escherichia* and *Dialister*. Co-exposure with G increased most bacterial belong to metabolic function bacteria such as

Firmicutes in 24 h fecal fermentation. Because of fecal source difference, our studies of mice showed AA_{TW} and AA_G both increased the Gram-negative *Proteobacteria* (Chapter 4). AA_{TW} and AA_G both changed weight related bacterial in mice (Chapter 4), the bacterial species was different. AA_{TW} decreased the wight loss bacterial *Akkermansia*, however, AA_G decreased *Verrucomicrobia*. These means that co-exposure with emulsifiers increased alteration of gut microbiome. Interaction of emulsifiers and contaminants on microbial community were different, and the changes depended on the emulsifiers.

6.6 Co-exposure with emulsifiers increased neurotoxicity

AA was shown to cause neurotoxicity (LoPachin, 2004). It was observed to decrease performance of mice on rotor rod and landing hindlimb foot spread (Chapter 4). Performance on rotor-rod was the worst for individuals in AA_{TW} and AA_G (Chapter 4). Although not statistically significant, a trend was also observed where AA_{TW} and AA_G individuals have higher landing foot spread than the AA treatment. Emulsifiers increased loss of coordinated motor function induced by AA, which indicated neurotoxicity was increased. Transcriptome analyses of mice ileum comparing control and AA groups only mentioned inflammation. However serotonergic synapse pathway was involved when comparing AA and AA_{TW} or AA_G (Chapter 4). Our results also showed AA_G decreased the abundance of *Akkermansiaceas*. *Akkermansiaceas* was found to be able to increase 5-HT level in colon and hippocampus (Yaghoubfar et al., 2020). Therefore at 5-HT regulation maybe impacted at the co-exposure treatments. Low level of 5-HT maybe associated with a degrees of locomotor dysfunction (Ghosh and Pearse, 2015). Due to limited time available for my study, the brain was not analyzed in this research. Whether the increase in toxicity is simply due to increased uptake and/or increased the toxicity by affecting the gut-brain axis and 5-HT levels remains open to investigation.

6.7 Limitations and recommendations for further research

One of the most obvious limitations of my study is lack of chronic experiments. Much of my study had been impacted by Covid 19 and quarantine restrictions in the past 3 year. This led to the inability to carry out some of the planned studies due to lost in experiment time and difficulty in obtaining research animals and reagents. Due to time limitations, I could not carry out experiment on BAP.

Another key toxicity of AA is its carcinogenicity. Due to short exposure of the experiments, this toxicity cannot be investigated. Based on our results, there was no universal response to combined exposure of emulsifiers and contaminants. Therefore it may be necessary to carry out a chronic/life cycle test in order to understand if this mixture increases chance of carcinogenicity.

Previous study showed high-fat diet exacerbated effects of emulsifiers on adiposity and inflammation in mice (Lecomte et al., 2016). AA combined with high fat diet were also reported to activate MAPK to up-regulate adipogenesis biomarkers including peroxisome proliferator-activated receptors γ (PPARγ), CCAAT enhancer binding protein α (c/EBPα), and CCAAT enhancer binding protein β (c/EBPβ) (Lee and Pyo, 2019). It is therefore likely that AA and food emulsifier toxicity contributed to part of the positive association between ultra-processed food and obesity (Askari et al., 2020). Therefore, it will be interesting to combine use high fat diet and co-exposure of food emulsifier and AA in the future.

To investigate the mixture toxicity of food emulsifiers and food contaminants on microbiota, the present study used human fecal samples. Due to limitation of the instrument, SHIME system can only run three treatment groups simultaneously. Therefore limiting the experiment in Chapter 5. Future study should also focus on whether the alteration to the fecal microbiota is reversible. SHIME or any host-free microbiota batch lacks the complexity of human systems, and these batches were from

an individual donor. In order to study gut microbiota effect on the host, germ-free mice administered with external human microbiota is recommended. It is recommended to collect more fecal samples from 5-10 individuals. Furthermore, stool bank samples are recommended since it is difficult to repeat the experiment due to the inconsistent quality of feces.

The reason for this hypothesis is that emulsifiers are supposed to enhance absorption, and food contaminants often co-exist with emulsifiers in our everyday foods. What will happen if we eat it every day? The risks of toxicity related to exposure to AA were discussed in a Joint Expert Committee on Food Additives conference held in Rome in February 2005 (Joint FAO/WHO Expert Committee on Food Additives, 2006). JECFA only focused on NOAEL (no observed adverse effect level) of single chemical. But food emulsifiers, other food additives and contaminants co-exist in food. In this study emulsifiers enhanced toxicity of both lipid-soluble BAP but water-soluble AA. This raised question on whether single chemical based food safety evaluation is adequate to safeguard human health.

In conclusion, exposure of emulsifiers and food contaminants caused leaky gut by disrupt gut barriers to increase absorption of food contaminants, followed by over-absorption of contaminants and their mixtures, contributing to activate inflammation, weigh gain and microbiota dysbiosis. The propose of subject is to draw the attention of risk assessors to make an adequate evaluation of emulsifiers and improve the toxicity assessment of mixtures of food contaminants and emulsifiers.

Supplementary data

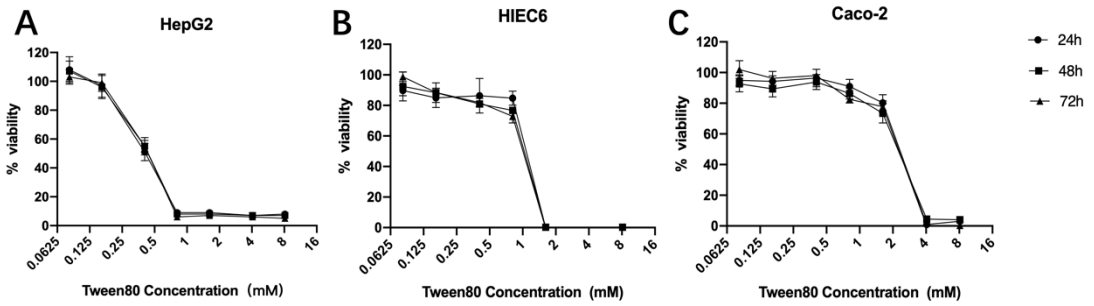

Figure S 1 *Effects of TW on cell viability. 48 h and 72 h cell viability of (A)HepG2, (B) HIEC6 and (C) Caco-2 treated with a serial concentration of TW. Error bars are standard deviations, n=3.*

There was dose-dependent decrease proliferation of three cell lines after TW treatment (Fig. S 1). Sensitivity of the three cell lines were different where HepG2 was the most sensitive and Caco-2 was the least sensitive. Notably, toxicity of TW did not change between 24 h to 72 h. The lowest NOAEL of TW was 162 µM in HepG2, 80 µM in HIEC6, 80 µM in Caco-2 cells at 72 h. In order to avoid the cytotoxicity caused by TW, 80 µM TW was chosen for the subsequent co-exposure experiments.

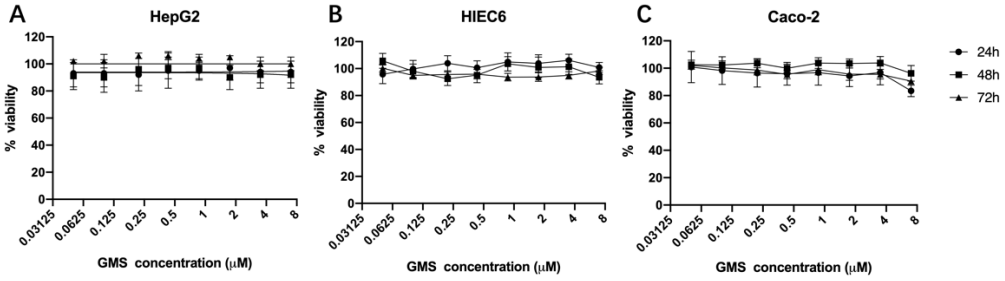

Figure S 2 *Effects of G on cell viability. 48 h and 72 h cell viability of (A) HepG2, (B) HIEC6 and (C) Caco-2 treated with a serial concentration of G. Error bars are standard deviations, n=3.*

For G, no significant decrease in cell viability was observed to all cell lines (Fig. S 2). Viability of three cell lines did not decrease with the time. Average cell viability of three cell lines is above 80 %. A slight but insignificant decrease of cell viability was observed only at 7 µM G for Caco-2. The NOAEL of G for all cell types were 7 µM. In order to avoid cytotoxicity caused by G, 3.5 µM G was chosen in the subsequent co-exposure experiments.

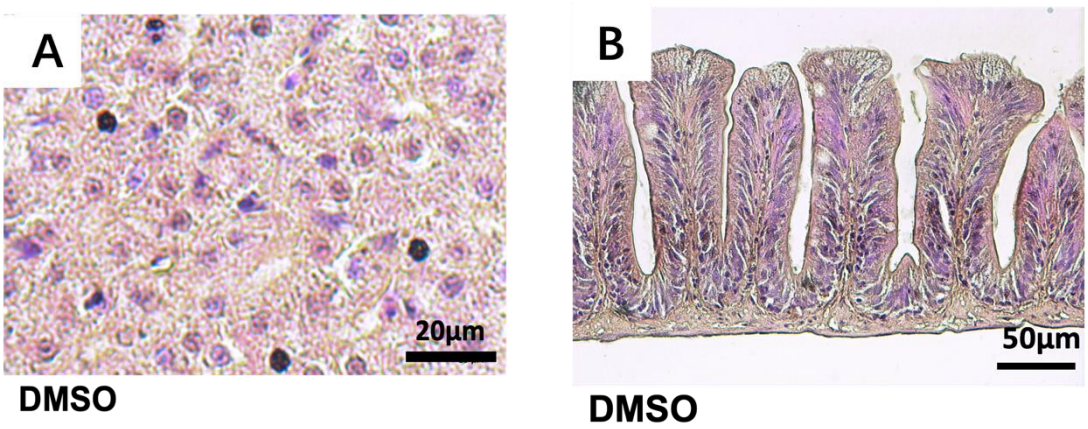

Figure S 3 *Photomicrographs H&E-stained paraffin sections showing liver (A) and gut (B) pathology in adult zebrafish after exposure to DMSO (vehicle control) fish feeds.*

DMSO have not significant effect on the liver and gut of zebrafish.

Table S 1 Classification of top 30 KEGG-enriched pathways between Control and AA in ileum of mice.

Classification of pathways	KEGG-enriched pathways
Immune system regulation	1. rheumatoid arthritis; 2. primary immunodeficiency; 3. inflammatory bowel disease; 4. autoimmune thyroid disease; 5. asthma; 6. allograft rejection; 7. Th17 cell differentiation; 8. Th1 and Th2 cell differentiation; 9. intestinal immune network for IgA production; 10. hematopoietic cell lineage; 11. Fc epsilon RI signaling pathway; 12. chemokine signaling pathway; 13. B cell receptor signaling pathway; 14. TNF signaling pathway; 15. NF-kappa B signaling pathway; 16. JAK-STAT signaling pathway; 17. viral protein interaction with cytokine and cytokine receptor; 18. cytokine-cytokine receptor interaction; 19. cell adhesion molecules.
Obesity and lipid metabolism	1. phenylalanine, tyrosine and tryptophan biosynthesis; 2. phenylalanine metabolism; 3 C5-Branched dibasic acid metabolism; 4. vitamin digestion and absorption; 5. arachidonic acid metabolism; 6. type I diabetes mellitus; 7. maturity onset diabetes of the young.
Infectious disease	1. malaria; 2. african trypanosomiasis; 3. staphylococcus aureus infection.
Environmental adaptation	1. circadian rhythm – fly.

Top30 enriched KEGG pathways were selected for the three pairs of comparisons (Tables S 1-3). In the comparisons of control and AA group, twenty two of the top pathways are linked to immune system regulation, seven associated with obesity and lipid metabolism and one related to stress adaptation (Table S 1).

The top 30 pathways in AA-AA_{TW} can be classified into 6 groups (Table S 2). 19 of 30 are linked to obesity and lipids. 4 of 30 are associated with substance dependence. 3 of 30 are related to nervous system. 2 of 30 are related to immune disease. 1 of 30 are related to infectious diseases. 1 of 30 are associated with cancer.

Table S 2 Classification of top 30 KEGG-enriched pathways between AA and AA_{TW} in ileum of mice.

Classification of pathways	KEGG-enriched pathways
Immune system regulation	1. complement and coagulation cascades; 2. inflammatory mediator regulation of TRP channels.
Obesity and lipid metabolism	1. tyrosine metabolism; 2. butanoate metabolism; 3. ascorbate and aldarate metabolism; 4. vitamin digestion and absorption; 5. cholesterol metabolism; 6. carbohydrate digestion and absorption; 7. bile secretion; 8. PPAR signaling pathway; 9. metabolic pathways; 10. biosynthesis of cofactors; 11. steroid hormone biosynthesis; 12. sphingolipid metabolism; 13. primary bile acid biosynthesis; 14. linoleic acid metabolism; 15. fatty acid elongation; 16. fatty acid degradation; 17. biosynthesis of unsaturated fatty acids; 18. arachidonic acid metabolism; 19. retinol metabolism.
Nervous system	1. serotonergic synapse; 2. glutamatergic synapse; 3. neuroactive ligand-receptor interaction.
Substance dependence	1. caffeine metabolism; 2. nicotine addiction; 3. cocaine addiction; 4. amphetamine addiction
Infectious disease	1. staphylococcus aureus infection.
Cancer	1. chemical carcinogenesis - DNA adducts.

The top 30 pathways in AA-AA_G groups can be classified into 7 groups (Table S 3). 17 of 30 are linked to obesity and lipids. 3 of 30 are associated with immune disease. 3 of 30 are related to infectious diseases.3 of 30 are related to nervous system.2 of 30 are associated with substance dependence. 1 of 30 are related to environmental adaptation. 1 of 30 are associated with cancer.

Table S 3 Classification of top 30 KEGG-enriched pathways between AA and AA_G in ileum of mice.

Classification of pathways	KEGG-enriched pathways
Immune system regulation	1. systemic lupus erythematosus; 2. complement and coagulation cascades; 3. inflammatory mediator regulation of TRP channels.
Obesity and lipid metabolism	1. tryptophan metabolism; 2. lysine biosynthesis; 3. histidine metabolism; 4. butanoate metabolism; 5. cholesterol metabolism; 6. bile secretion; 7. PPAR signaling pathway; 8. ovarian steroidogenesis; 9. metabolic pathways; 10. steroid hormone biosynthesis; 11. primary bile acid biosynthesis; 12. linoleic acid metabolism; 13. arachidonic acid metabolism; 14. retinol metabolism; 15. pantothenate and CoA biosynthesis; 16. taurine and hypotaurine metabolism; 17. beta-Alanine metabolism.
Nervous system	1. synaptic vesicle cycle; 2. serotonergic synapse; 3. neuroactive ligand-receptor interaction.
Substance dependence	1. caffeine metabolism; 2. nicotine addiction;
Infectious disease	1. malaria; 2. african trypanosomiasis; 3. staphylococcus aureus infection.
Cancer	1. chemical carcinogenesis - DNA adducts.
Environmental adaptation	1. circadian rhythm– fly.

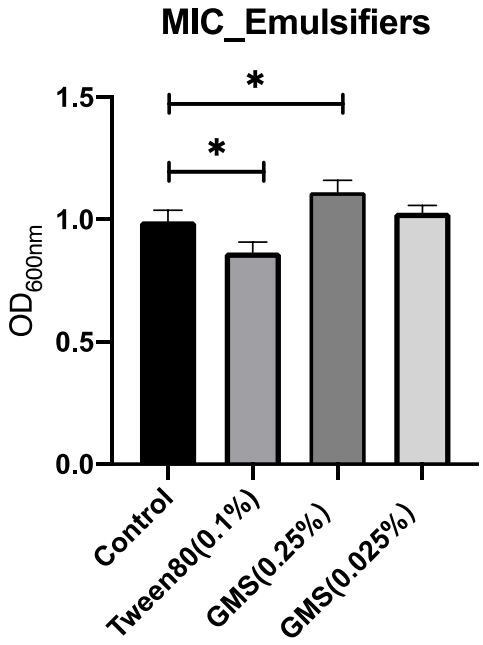

Figure S 4 *Minimum inhibitory concentration (MIC) after 24 hours emulsifiers treatment.*

As shown in figure S 4, 0.1%TW showed significant inhibitory effect against fecal microbiota while G but had no antibacterial activity. 0.25% G (GH) was more active than 0.025% G (GL) to increase viability of fecal bacterial.

References

Aguirre, M. and Venema, K., 2015. Does the gut microbiota contribute to obesity? Going beyond the gut feeling. Microorganisms 3, 213-235.

Ahyayauch, H., Bennouna, M., Alonso, A. and Goni, F.M., 2010. Detergent effects on membranes at subsolubilizing concentrations: transmembrane lipid motion, bilayer permeabilization, and vesicle lysis/reassembly are independent phenomena. Langmuir 26, 7307-7313.

Amirshahrokhi, K., 2021. Acrylamide exposure aggravates the development of ulcerative colitis in mice through activation of NF-κB, inflammatory cytokines, iNOS, and oxidative stress. Iranian Journal of Basic Medical Sciences 24, 312.

Anders, S., 2010. HTSeq: Analysing high-throughput sequencing data with Python http://www-huber. embl. de/users/anders. HTSeq/doc/index. html.

Anders, S. and Huber, W., 2010. Differential expression analysis for sequence count data. Nature Precedings, 1-1.

Arthur, J.C., Perez-Chanona, E., Mühlbauer, M., Tomkovich, S., Uronis, J.M., Fan, T.-J., Campbell, B.J., Abujamel, T., Dogan, B. and Rogers, A.B., 2012. Intestinal inflammation targets cancer-inducing activity of the microbiota. Science 338, 120-123.

Askari, M., Heshmati, J., Shahinfar, H., Tripathi, N. and Daneshzad, E., 2020. Ultra-processed food and the risk of overweight and obesity: a systematic review and meta-analysis of observational studies. International Journal of Obesity 44, 2080-2091.

Ayrton, A. and Morgan, P., 2001. Role of transport proteins in drug absorption, distribution and excretion. Xenobiotica 31, 469-497.

Bamola, V.D., Ghosh, A., Kapardar, R.K., Lal, B., Cheema, S., Sarma, P. and Chaudhry, R., 2017. Gut microbial diversity in health and disease: experience of healthy Indian subjects, and colon carcinoma and inflammatory bowel disease patients. Microbial Ecology in Health and Disease 28, 1322447.

Barta, C.A., Sachs-Barrable, K., Feng, F. and Wasan, K.M., 2008. Effects of monoglycerides on P-glycoprotein: modulation of the activity and expression in Caco-2 cell monolayers. Molecular Pharmaceutics 5, 863-875.

Bedell, M.A., Jenkins, N.A. and Copeland, N.G., 1997. Mouse models of human disease. Part I: techniques and resources for genetic analysis in mice. Genes & Development 11, 1-10.

Bischof, J.C., Padanilam, J., Holmes, W.H., Ezzell, R.M., Lee, R., Tompkins, R.G., Yarmush, M.L. and Toner, M., 1995. Dynamics of cell membrane permeability changes at supraphysiological temperatures. Biophysical Journal 68, 2608-2614.

Blaner, W.S., 2019. Vitamin A signaling and homeostasis in obesity, diabetes, and metabolic disorders. Pharmacology & Therapeutics 197, 153-178.

Blomhoff, R. and Blomhoff, H.K., 2006. Overview of retinoid metabolism and function. Journal of Neurobiology 66, 606-630.

Bonwick, G.A. and Birch, C.S., 2019. European Regulation of Process Contaminants in Food, Mitigating Contamination from Food Processing. The Royal Society of Chemistry, p. 225.

Bouma, M.-E., Rogier, E., Verthier, N., Labarre, C. and Feldmann, G., 1989. Further cellular investigation of the human hepatoblastoma-derived cell line HepG2: morphology and immunocytochemical studies of hepatic-secreted proteins. In Vitro Cellular & Developmental Biology 25, 267-275.

Branen, A.L., Davidson, P.M., Salminen, S. and Thorngate, J., 2001. Food additives. CRC Press, New York, USA.

Breschi, A., Gingeras, T.R. and Guigó, R., 2017. Comparative transcriptomics in human and mouse. Nature Reviews Genetics 18, 425-440.

Campbell, S.D., Goff, H.D. and Rousseau, D., 2002. Comparison of crystallization properties of a palm stearin/canola oil blend and lard in bulk and emulsified form. Food research international 35, 935-944.

Cani, P.D., Amar, J., Iglesias, M.A., Poggi, M., Knauf, C., Bastelica, D., Neyrinck, A.M., Fava, F., Tuohy, K.M. and Chabo, C., 2007. Metabolic endotoxemia initiates obesity and insulin resistance. Diabetes 56, 1761-1772.

Cani, P.D., Possemiers, S., Van de Wiele, T., Guiot, Y., Everard, A., Rottier, O., Geurts, L., Naslain, D., Neyrinck, A. and Lambert, D.M., 2009. Changes in gut microbiota control inflammation in obese mice through a mechanism involving GLP-2-driven improvement of gut permeability. Gut 58, 1091-1103.

Chakraborti, C.K., 2015. New-found link between microbiota and obesity. World Journal of Gastrointestinal Pathophysiology 6, 110.

Chassaing, B., Koren, O., Goodrich, J.K., Poole, A.C., Srinivasan, S., Ley, R.E. and Gewirtz, A.T., 2015. Dietary emulsifiers impact the mouse gut microbiota promoting colitis and metabolic syndrome. Nature 519, 92-96.

Chassaing, B., Van de Wiele, T., De Bodt, J., Marzorati, M. and Gewirtz, A.T., 2017. Dietary emulsifiers directly alter human microbiota composition and gene expression ex vivo potentiating intestinal inflammation. Gut 66, 1414-1427.

Chen, D., Liu, H., Wang, E., Yan, H., Ye, H. and Yuan, Y., 2018. Toxicogenomic evaluation of liver responses induced by acrylamide and glycidamide in male mouse liver. General Physiology and Biophysics 37, 175-184.

Chen, J., Wright, K., Davis, J.M., Jeraldo, P., Marietta, E.V., Murray, J., Nelson, H., Matteson, E.L. and Taneja, V., 2016. An expansion of rare lineage intestinal microbes characterizes rheumatoid arthritis. Genome Medicine 8, 1-14.

Chen, Y.-r., Zheng, H.-m., Zhang, G.-x., Chen, F.-l., Chen, L.-d. and Yang, Z.-c., 2020. High Oscillospira abundance indicates constipation and low BMI in the Guangdong Gut Microbiome Project. Scientific Reports 10, 9364.

Cornaire, G., Woodley, J., Hermann, P., Cloarec, A., Arellano, C. and Houin, G., 2004. Impact of excipients on the absorption of P-glycoprotein substrates in vitro and in vivo. International Journal of Pharmaceutics 278, 119-131.

Csáki, K.F., 2011. Synthetic surfactant food additives can cause intestinal barrier dysfunction. Medical Hypotheses 76, 676-681.

Cui, Q., Chen, F.-Y., Chen, H.-Y., Peng, H. and Wang, K.-J., 2019. Benzo [a] pyrene (BaP) exposure generates persistent reactive oxygen species (ROS) to inhibit the NF-κB pathway in medaka (Oryzias melastigma). Environmental Pollution 251, 502-509.

Cuschieri, J. and Maier, R.V., 2005. Mitogen-activated protein kinase (MAPK). Critical Care Medicine 33, S417-S419.

Davuljigari, C.B., Ekuban, F.A., Zong, C., Fergany, A.A., Morikawa, K. and Ichihara, G., 2021. Nrf2 activation attenuates acrylamide-induced neuropathy in mice. International Journal of Molecular Sciences 22, 5995.

De Siena, M., Raoul, P., Costantini, L., Scarpellini, E., Cintoni, M., Gasbarrini, A., Rinninella, E. and Mele, M.C., 2022. Food Emulsifiers and Metabolic Syndrome: The Role of the Gut Microbiota. Foods 11, 2205.

Degen, J., Bugge, T. and Goguen, J., 2007. Fibrin and fibrinolysis in infection and host defense. Journal of Thrombosis and Haemostasis 5, 24-31.

Demirci, M., 2021. Dialister in Microbiome of Cancer Patients: A Systematic Review and Meta-Analysis. Eurasian Journal of Medicine and Oncology.

Dimitrijevic, D., Shaw, A.J. and Florence, A.T., 2000. Effects of some non-ionic surfactants on transepithelial permeability in Caco-2 cells. Journal of Pharmacy and Pharmacology 52, 157-162.

Ding, X., Hu, X., Chen, Y., Xie, J., Ying, M., Wang, Y. and Yu, Q., 2021. Differentiated Caco-2 cell models in food-intestine interaction study: Current applications and future trends. Trends in Food Science & Technology 107, 455-465.

Domingo, J.L., 2012. Health risks of dietary exposure to perfluorinated compounds. Environment International 40, 187-195.

Domingo, J.L. and Nadal, M., 2015. Human dietary exposure to polycyclic aromatic hydrocarbons: A review of the scientific literature. Food and Chemical Toxicology 86, 144-153.

Duncan, S.H., Lobley, G., Holtrop, G., Ince, J., Johnstone, A., Louis, P. and Flint, H.J., 2008. Human colonic microbiota associated with diet, obesity and weight loss. International Journal of Obesity 32, 1720-1724.

Dunovská, L., Hajslova, J., Cajka, T., Holadova, K. and Hajkova, K., 2004. Changes of acrylamide levels in food products during technological processing. Czech Journal of Food Sciences 22, 283.

Ebrahimi, T., Rust, M., Kaiser, S.N., Slowik, A., Beyer, C., Koczulla, A.R., Schulz, J.B., Habib, P. and Bach, J.P., 2018. α1-antitrypsin mitigates NLRP3-inflammasome activation in amyloid β1–42-stimulated murine astrocytes. Journal of Neuroinflammation 15, 1-15.

Edagawa, M., Kawauchi, J., Hirata, M., Goshima, H., Inoue, M., Okamoto, T., Murakami, A., Maehara, Y. and Kitajima, S., 2014. Role of activating transcription factor 3 (ATF3) in endoplasmic reticulum (ER) stress-induced sensitization of p53-deficient human colon cancer cells to tumor necrosis factor (TNF)-related apoptosis-inducing ligand (TRAIL)-mediated apoptosis through up-regulation of death receptor 5 (DR5) by zerumbone and celecoxib. Journal of Biological Chemistry 289, 21544-21561.

EFSA Panel on Food Additives, 2015. Scientific Opinion on the re‐evaluation of polyoxyethylene sorbitan monolaurate (E 432), polyoxyethylene sorbitan monooleate (E 433), polyoxyethylene sorbitan monopalmitate (E 434), polyoxyethylene sorbitan monostearate (E 435) and polyoxyethylene sorbitan tristearate (E 436) as food additives. EFSA Journal 13, 4152.

Eissa, N., Hussein, H., Mesgna, R., Bonin, S., Hendy, G.N., Metz-Boutigue, M.-H., Bernstein, C.N. and Ghia, J.-E., 2018. Catestatin regulates epithelial cell dynamics to improve intestinal inflammation. Vaccines 6, 67.

Ekuban, F.A., Zong, C., Takikawa, M., Morikawa, K., Sakurai, T., Ichihara, S., Itoh, K., Yamamoto, M., Ohsako, S. and Ichihara, G., 2021. Genetic ablation of Nrf2 exacerbates neurotoxic effects of acrylamide in mice. Toxicology 456, 152785.

Elmén, L., Zlamal, J.E., Scott, D.A., Lee, R.B., Chen, D.J., Colas, A.R., Rodionov, D.A. and Peterson, S.N., 2020. Dietary Emulsifier Sodium Stearoyl Lactylate Alters Gut Microbiota in vitro and Inhibits Bacterial Butyrate Producers. Frontiers in Microbiology 11, 892.

EPA, U., 1998. Health effects test guidelines: OPPTS 870.6200 neurotoxicity screening battery. EPA 712-C-98-238.

European Commission, 2008. Regulation (EC) No 1333/2008 of the European Parliament and of the Council of 16 December 2008 on food additives, Official Journal of the European Communities, p. 18.

European Food Safety Authority, 2012. Update on acrylamide levels in food from monitoring years 2007 to 2010. EFSA Journal 10, 2938.

Everard, A., Belzer, C., Geurts, L., Ouwerkerk, J.P., Druart, C., Bindels, L.B., Guiot, Y., Derrien, M., Muccioli, G.G. and Delzenne, N.M., 2013. Cross-talk between Akkermansia muciniphila and intestinal epithelium controls diet-induced obesity. Proceedings of the National Academy of Sciences 110, 9066-9071.

Exon, J., 2006. A review of the toxicology of acrylamide. Journal of Toxicology and Environmental Health, Part B 9, 397-412.

Fan, Y., Shen, F., Frenzel, T., Zhu, W., Ye, J., Liu, J., Chen, Y., Su, H., Young, W.L. and Yang, G.Y., 2010. Endothelial progenitor cell transplantation improves long‐term stroke outcome in mice. Annals of Neurology 67, 488-497.

Farshori, P. and Kachar, B., 1999. Redistribution and phosphorylation of occludin during opening and resealing of tight junctions in cultured epithelial cells. The Journal of Membrane Biology 170, 147-156.

Ferrer, M., Ruiz, A., Lanza, F., Haange, S.B., Oberbach, A., Till, H., Bargiela, R., Campoy, C., Segura, M.T. and Richter, M., 2013. Microbiota from the distal guts of lean and obese adolescents exhibit partial functional redundancy besides clear differences in community structure. Environmental Microbiology 15, 211-226.

Fitzgerald, A., 2015. Emulsifiers: Properties, Functions, and Applications. Nova Science Publishers, Incorporated, NewYork, USA.

Florença, S.G., Ferreira, M., Lacerda, I. and Maia, A., 2021. Food myths or food facts? Study about perceptions and knowledge in a Portuguese sample. Foods 10, 2746.

Folmer, D.E., Doell, D.L., Lee, H.S., Noonan, G.O. and Carberry, S.E., 2018. A US population dietary exposure assessment for 4-methylimidazole (4-MEI) from foods containing caramel colour and from formation of 4-MEI through the thermal treatment of food. Food Additives & Contaminants: Part A 35, 1890-1910.

Forbes, J.D., Chen, C.-y., Knox, N.C., Marrie, R.-A., El-Gabalawy, H., de Kievit, T., Alfa, M., Bernstein, C.N. and Van Domselaar, G., 2018. A comparative study of the gut microbiota in immune-mediated inflammatory diseases—does a common dysbiosis exist? Microbiome 6, 1-15.

Francis, M.F., Cristea, M. and Winnik, F.M., 2004. Polymeric micelles for oral drug delivery: why and how. Pure and Applied Chemistry 76, 1321-1335.

Friberg, S., Sjoblom, J. and Larsson, K., 2003. Food emulsions. CRC Press, New York, USA.

Friedl, J.D., Steinbring, C., Zaichik, S., Le, N.-M.N. and Bernkop-Schnürch, A., 2020. Cellular uptake of self-emulsifying drug-delivery systems: polyethylene glycol versus polyglycerol surface. Nanomedicine 15, 1829-1841.

Fu, X., Jeselsohn, R., Pereira, R., Hollingsworth, E.F., Creighton, C.J., Li, F., Shea, M., Nardone, A., De Angelis, C. and Heiser, L.M., 2016. FOXA1 overexpression mediates endocrine resistance by altering the ER transcriptome and IL-8 expression in ER-positive breast cancer. Proceedings of the National Academy of Sciences 113, E6600-E6609.

Gao, H.-T., Xu, R., Cao, W.-X., Zhou, X., Yan, Y.-H.-M., Lu, L., Xu, Q. and Shen, Y., 2016. Food emulsifier glycerin monostearate increases internal exposure levels of six priority controlled phthalate esters and exacerbates their male reproductive toxicities in rats. Plos One 11, e0161253.

Garti, N., 2002. Food Emulsifiers: Structure–Reactivity Relationships, Design, and Applications, Physical properties of lipids. CRC Press, New York, USA, pp. 268-389.

Gauthier, R., Harnois, C., Drolet, J.-F., Reed, J.C., Vézina, A. and Vachon, P.H., 2001. Human intestinal epithelial cell survival: differentiation state-specific control mechanisms. American Journal of Physiology-Cell Physiology 280, C1540-C1554.

Gene Ontology Consortium, 2004. The Gene Ontology (GO) database and informatics resource. Nucleic Acids Research 32, D258-D261.

Gershon, M.D., 2013. 5-Hydroxytryptamine (serotonin) in the gastrointestinal tract. Current Opinion in Endocrinology, Diabetes, and Obesity 20, 14.

Ghosh, M. and Pearse, D.D., 2015. The role of the serotonergic system in locomotor recovery after spinal cord injury. Frontiers in Neural Circuits 8, 151.

Gillner, D.M., Becker, D.P. and Holz, R.C., 2013. Lysine biosynthesis in bacteria: a metallodesuccinylase as a potential antimicrobial target. JBIC Journal of Biological Inorganic Chemistry 18, 155-163.

Gomez-Arango, L.F., Barrett, H.L., Wilkinson, S.A., Callaway, L.K., McIntyre, H.D., Morrison, M. and Dekker Nitert, M., 2018. Low dietary fiber intake increases Collinsella abundance in the gut microbiota of overweight and obese pregnant women. Gut Microbes 9, 189-201.

Gudas, L.J., 2022. Retinoid metabolism: new insights. Journal of Molecular Endocrinology 69, T37-T49.

Halford, N.G. and Curtis, T., 2019. Acrylamide in Food. World Scientific, London, UK.

Hall, C.J. and da Costa, T.P.S., 2018. Lysine: biosynthesis, catabolism and roles. WikiJournal of Science 1, 1-8.

Harris, K., Kassis, A., Major, G. and Chou, C.J., 2012. Is the gut microbiota a new factor contributing to obesity and its metabolic disorders? Journal of Obesity 2012, 14.

Harris, K.L., Banks, L.D., Mantey, J.A., Huderson, A.C. and Ramesh, A., 2013. Bioaccessibility of polycyclic aromatic hydrocarbons: relevance to toxicity and carcinogenesis. Expert Opinion on Drug Metabolism & Toxicology 9, 1465-1480.

Harusato, A., Chassaing, B., Dauriat, C.J., Ushiroda, C., Seo, W. and Itoh, Y., 2022. Dietary Emulsifiers Exacerbate Food Allergy and Colonic Type 2 Immune Response through Microbiota Modulation. Nutrients 14, 4983.

Hasenhuettl, G.L. and Hartel, R.W., 2008. Food emulsifiers and their applications, Third ed. Springer, Cham, Switzerland.

He, Y., Wu, W., Wu, S., Zheng, H.-M., Li, P., Sheng, H.-F., Chen, M.-X., Chen, Z.-H., Ji, G.-Y. and Zheng, Z.-D.-X., 2018. Linking gut microbiota, metabolic syndrome and economic status based on a population-level analysis. Microbiome 6, 1-11.

Hijova, E. and Chmelarova, A., 2007. Short chain fatty acids and colonic health. Bratisl Lek Listy 108, 354.

Hoffmann, G.F., 2006. Cerebral organic acid disorders and other disorders of lysine catabolism. Inborn Metabolic Diseases: Diagnosis and Treatment, 293-306.

Hong, J.-M., Kim, J.E., Min, S.K., Kim, K.H., Han, S.J., Yim, J.H., Park, H., Kim, J.-H. and Kim, I.-C., 2021. Anti-inflammatory effects of antarctic lichen Umbilicaria antarctica methanol extract in lipopolysaccharide-stimulated RAW 264.7 macrophage cells and zebrafish model. BioMed Research International 2021, 1-12.

Houten, S.M., Te Brinke, H., Denis, S., Ruiter, J.P., Knegt, A.C., de Klerk, J.B., Augoustides-Savvopoulou, P., Häberle, J., Baumgartner, M.R. and Coşkun, T., 2013. Genetic basis of hyperlysinemia. Orphanet Journal of Rare Diseases 8, 1-8.

Howe, K., Clark, M.D., Torroja, C.F., Torrance, J., Berthelot, C., Muffato, M., Collins, J.E., Humphray, S., McLaren, K. and Matthews, L., 2013. The zebrafish reference genome sequence and its relationship to the human genome. Nature 496, 498-503.

Hsu, C.-Y., Wang, P.-W., Alalaiwe, A., Lin, Z.-C. and Fang, J.-Y., 2019. Use of lipid nanocarriers to improve oral delivery of vitamins. Nutrients 11, 68.

Hu, Y.-W., Ma, X., Huang, J.-L., Mao, X.-R., Yang, J.-Y., Zhao, J.-Y., Li, S.-F., Qiu, Y.-R., Yang, J. and Zheng, L., 2013. Dihydrocapsaicin attenuates plaque formation through a PPARγ/LXRα pathway in apoe−/− mice fed a high-fat/high-cholesterol diet. Plos One 8, e66876.

Huang, L., Xiao, L., Poudel, A.J., Li, J., Zhou, P., Gauthier, M., Liu, H., Wu, Z. and Yang, G., 2018. Porous chitosan microspheres as microcarriers for 3D cell culture. Carbohydrate Polymers 202, 611-620.

Huang, P.-S., Wen, M.-H., Xie, X., Xu, A., Lee, D.-F. and Chen, T.-Y., 2021. Generation of a homozygous knock-in human embryonic stem cell line expressing SNAP-tagged SOD1. Stem Cell Research 54, 102415.

Hussain, M.A., 2016. Food contamination: major challenges of the future. Multidisciplinary Digital Publishing Institute, Basel, Switzerland.

Ibrahim, M. and Anishetty, S., 2012. A meta-metabolome network of carbohydrate metabolism: Interactions between gut microbiota and host. Biochemical and Biophysical Research Communications 428, 278-284.

Ichim, T.E., Kesari, S. and Shafer, K., 2018. Protection from chemotherapy-and antibiotic-mediated dysbiosis of the gut microbiota by a probiotic with digestive enzymes supplement. Oncotarget 9, 30919.

Jakobsson, H.E., Rodríguez‐Piñeiro, A.M., Schütte, A., Ermund, A., Boysen, P., Bemark, M., Sommer, F., Bäckhed, F., Hansson, G.C. and Johansson, M.E., 2015. The composition of the gut microbiota shapes the colon mucus barrier. EMBO Reports 16, 164-177.

Jeffery, I.B., O'toole, P.W., Öhman, L., Claesson, M.J., Deane, J., Quigley, E.M. and Simrén, M., 2012. An irritable bowel syndrome subtype defined by species-specific alterations in faecal microbiota. Gut 61, 997-1006.

Jiang, Z., Zhao, M., Zhang, H., Li, Y., Liu, M. and Feng, F., 2018. Antimicrobial emulsifier–glycerol monolaurate induces metabolic syndrome, gut microbiota

dysbiosis, and systemic low‐grade inflammation in low‐fat diet fed mice. Molecular Nutrition & Food Research 62, 1700547.

Johnston, M., Wang, A., Catarino, M., Ball, L., Phan, V., MacDonald, J. and McKay, D., 2010. Extracts of the rat tapeworm, Hymenolepis diminuta, suppress macrophage activation in vitro and alleviate chemically induced colitis in mice. Infection and Immunity 78, 1364-1375.

Joint FAO/WHO Expert Committee on Food Additives, 1996. Toxicological evaluation of certain food additives and contaminants in foods. WHO food additives series, Geneva, Switzerland.

Joint FAO/WHO Expert Committee on Food Additives, 2006. Safety evaluation of certain contaminants in food. Food & Agriculture Org.

Jumpertz, R., Le, D.S., Turnbaugh, P.J., Trinidad, C., Bogardus, C., Gordon, J.I. and Krakoff, J., 2011. Energy-balance studies reveal associations between gut microbes, caloric load, and nutrient absorption in humans. The American Journal of Clinical Nutrition 94, 58-65.

Kamel, B.S. and Stauffer, C.E., 2013. Advances in baking technology. Springer, Cham, Switzerland.

Kanehisa, M. and Goto, S., 2000. KEGG: kyoto encyclopedia of genes and genomes. Nucleic Acids Research 28, 27-30.

Kaper, J.B., Nataro, J.P. and Mobley, H.L., 2004. Pathogenic escherichia coli. Nature Reviews Microbiology 2, 123-140.

Karcher, N., Nigro, E., Punčochář, M., Blanco-Míguez, A., Ciciani, M., Manghi, P., Zolfo, M., Cumbo, F., Manara, S. and Golzato, D., 2021. Genomic diversity and ecology of human-associated Akkermansia species in the gut microbiome revealed by extensive metagenomic assembly. Genome Biology 22, 209.

Khuda, S.E., Nguyen, A.V., Sharma, G.M., Alam, M.S., Balan, K.V. and Williams, K.M., 2022. Effects of emulsifiers on an in vitro model of intestinal epithelial tight junctions and the transport of food allergens. Molecular Nutrition & Food Research 66, 2100576.

Kim, D., Langmead, B. and Salzberg, S.L., 2015. HISAT: a fast spliced aligner with low memory requirements. Nature Methods 12, 357-360.

Kimoto, H., Ohmomo, S. and Okamoto, T., 2002. Enhancement of bile tolerance in lactococci by Tween 80. Journal of Applied Microbiology 92, 41-46.

Kimura, I., Ozawa, K., Inoue, D., Imamura, T., Kimura, K., Maeda, T., Terasawa, K., Kashihara, D., Hirano, K. and Tani, T., 2013. The gut microbiota suppresses insulin-mediated fat accumulation via the short-chain fatty acid receptor GPR43. Nature Communications 4, 1-12.

Kinth, P., Mahesh, G. and Panwar, Y., 2013. Mapping of zebrafish research: a global outlook. Zebrafish 10, 510-517.

Kohajdová, Z., Karovičová, J. and Schmidt, Š., 2009. Significance of emulsifiers and hydrocolloids in bakery industry. Acta Chimica Slovaca 2, 46-61.

Komoike, Y. and Matsuoka, M., 2019. In vitro and in vivo studies of oxidative stress responses against acrylamide toxicity in zebrafish. Journal of Hazardous Materials 365, 430-439.

Kortenkamp, A., Backhaus, T. and Faust, M., 2009. State of the Art Report on Mixture Toxicity—Final Report, Executive Summary. University of London School of Pharmacy, London, UK.

Krych, L., Hansen, C.H., Hansen, A.K., van den Berg, F.W. and Nielsen, D.S., 2013. Quantitatively different, yet qualitatively alike: a meta-analysis of the mouse core gut microbiome with a view towards the human gut microbiome. Plos One 8, e62578.

Kumagai, K., Tabu, K., Sasaki, F., Takami, Y., Morinaga, Y., Mawatari, S., Hashimoto, S., Tanoue, S., Kanmura, S. and Tamai, T., 2015. Glycoprotein nonmetastatic melanoma B (Gpnmb)-positive macrophages contribute to the balance between fibrosis and fibrolysis during the repair of acute liver injury in mice. Plos One 10, e0143413.

Layunta, E., Buey, B., Mesonero, J.E. and Latorre, E., 2021. Crosstalk between intestinal serotonergic system and pattern recognition receptors on the microbiota–gut–brain axis. Frontiers in Endocrinology 12, 748254.

Lecomte, M., Couëdelo, L., Meugnier, E., Plaisancié, P., Létisse, M., Benoit, B., Gabert, L., Penhoat, A., Durand, A. and Pineau, G., 2016. Dietary emulsifiers from milk and soybean differently impact adiposity and inflammation in association with modulation of colonic goblet cells in high‐fat fed mice. Molecular Nutrition & Food Research 60, 609-620.

Lee, H.-W. and Pyo, S., 2019. Acrylamide induces adipocyte differentiation and obesity in mice. Chemico-Biological Interactions 298, 24-34.

Lerner, A. and Matthias, T., 2015. Changes in intestinal tight junction permeability associated with industrial food additives explain the rising incidence of autoimmune disease. Autoimmunity Reviews 14, 479-489.

Ley, R.E., Turnbaugh, P.J., Klein, S. and Gordon, J.I., 2006. Human gut microbes associated with obesity. Nature 444, 1022-1023.

Li, D., Wang, P., Liu, Y., Hu, X. and Chen, F., 2016a. Metabolism of acrylamide: interindividual and interspecies differences as well as the application as biomarkers. Current Drug Metabolism 17, 317-326.

Li, M., Cui, J., Ngadi, M.O. and Ma, Y., 2015. Absorption mechanism of whey-protein-delivered curcumin using Caco-2 cell monolayers. Food Chemistry 180, 48-54.

Li, S., Yue, Y., Xu, W. and Xiong, S., 2013. MicroRNA-146a represses mycobacteria-induced inflammatory response and facilitates bacterial replication via targeting IRAK-1 and TRAF-6. Plos One 8, e81438.

Li, Y., Zhao, S., Nan, X., Wei, H., Shi, J., Li, A. and Gou, J., 2016b. Repair of human periodontal bone defects by autologous grafting stem cells derived from inflammatory dental pulp tissues. Stem Cell Research & Therapy 7, 1-9.

Lindenberg, F., Krych, L., Fielden, J., Kot, W., Frøkiær, H., Van Galen, G., Nielsen, D. and Hansen, A., 2019. Expression of immune regulatory genes correlate with the

abundance of specific Clostridiales and Verrucomicrobia species in the equine ileum and cecum. Scientific Reports 9, 12674.

Liu, L.M., Liang, D.Y., Ye, C.G., Tu, W.J. and Zhu, T., 2015. The UII/UT system mediates upregulation of proinflammatory cytokines through p38 MAPK and NF-κB pathways in LPS-stimulated Kupffer cells. PLos One 10, e0121383.

Liu, X., Mao, B., Gu, J., Wu, J., Cui, S., Wang, G., Zhao, J., Zhang, H. and Chen, W., 2021. Blautia—a new functional genus with potential probiotic properties? Gut Microbes 13, 1875796.

LoPachin, R.M., 2004. The changing view of acrylamide neurotoxicity. Neurotoxicology 25, 617-630.

Lu, Y., Wang, Y.-Y., Yang, N., Zhang, D., Zhang, F.-Y., Gao, H.-T., Rong, W.-T., Yu, S.-Q. and Xu, Q., 2014. Food emulsifier polysorbate 80 increases intestinal absorption of di-(2-ethylhexyl) phthalate in rats. Toxicological Sciences 139, 317-327.

Lugea, A., Salas, A., Casalot, J., Guarner, F. and Malagelada, J., 2000. Surface hydrophobicity of the rat colonic mucosa is a defensive barrier against macromolecules and toxins. Gut 46, 515-521.

Luo, M., Zhou, D.-D., Shang, A., Gan, R.-Y. and Li, H.-B., 2021. Influences of food contaminants and additives on gut microbiota as well as protective effects of dietary bioactive compounds. Trends in Food Science & Technology 113, 180-192.

Ma, J.-K., Saad Eldin, W.F., El-Ghareeb, W.R., Elhelaly, A.E., Khedr, M.H., Li, X. and Huang, X.-C., 2019. Effects of pyrene on human liver HepG2 cells: Cytotoxicity, oxidative stress, and transcriptomic changes in xenobiotic metabolizing enzymes and inflammatory markers with protection trial using lycopene. BioMed Research International 2019.

Magne, F., Gotteland, M., Gauthier, L., Zazueta, A., Pesoa, S., Navarrete, P. and Balamurugan, R., 2020. The firmicutes/bacteroidetes ratio: a relevant marker of gut dysbiosis in obese patients? Nutrients 12, 1474.

Magoč, T. and Salzberg, S.L., 2011. FLASH: fast length adjustment of short reads to improve genome assemblies. Bioinformatics 27, 2957-2963.

Margolis, K.G., Cryan, J.F. and Mayer, E.A., 2021. The microbiota-gut-brain axis: from motility to mood. Gastroenterology 160, 1486-1501.

Marhamati, M., Ranjbar, G. and Rezaie, M., 2021. Effects of emulsifiers on the physicochemical stability of Oil-in-water Nanoemulsions: A critical review. Journal of Molecular Liquids 340, 117218.

Mariat, D., Firmesse, O., Levenez, F., Guimarães, V., Sokol, H., Doré, J., Corthier, G. and Furet, J., 2009. The Firmicutes/Bacteroidetes ratio of the human microbiota changes with age. BMC Microbiology 9, 1-6.

Martin, M., 2011. Cutadapt removes adapter sequences from high-throughput sequencing reads. EMBnet. journal 17, 10-12.

Matthews, D.E., 2020. Review of lysine metabolism with a focus on humans. The Journal of Nutrition 150, 2548S-2555S.

McClements, D.J. and Gumus, C.E., 2016. Natural emulsifiers—Biosurfactants, phospholipids, biopolymers, and colloidal particles: Molecular and physicochemical basis of functional performance. Advances in Colloid and Interface Science 234, 3-26.

McDonald, D., Price, M.N., Goodrich, J., Nawrocki, E.P., DeSantis, T.Z., Probst, A., Andersen, G.L., Knight, R. and Hugenholtz, P., 2012. An improved Greengenes taxonomy with explicit ranks for ecological and evolutionary analyses of bacteria and archaea. The ISME journal 6, 610-618.

Merga, Y., Campbell, B.J. and Rhodes, J.M., 2014. Mucosal barrier, bacteria and inflammatory bowel disease: possibilities for therapy. Digestive Diseases 32, 475-483.

Mersch-Sundermann, V., Knasmüller, S., Wu, X.-j., Darroudi, F. and Kassie, F., 2004. Use of a human-derived liver cell line for the detection of cytoprotective, antigenotoxic and cogenotoxic agents. Toxicology 198, 329-340.

Miclotte, L., De Paepe, E., Li, Q., Van Camp, J., Raikovic, A. and Van de Wiele, T., 2021a. Differential Impact of rhamnolipids and TWEEN80 on composition and functionality of the gut microbiota in the SHIME system. BioRxiv, 2021.2012. 2015.472660.

Miclotte, L., De Paepe, E., Li, Q., Van Camp, J., Rajkovic, A. and Van de Wiele, T., 2021b. Long term exposure of human gut microbiota with high and low emulsifier sensitivity to soy lecithin in M-SHIME model. BioRxiv, 2021.2012. 2016.472798.

Miclotte, L., De Paepe, K., Rymenans, L., Callewaert, C., Raes, J., Rajkovic, A., Van Camp, J. and Van de Wiele, T., 2020. Dietary emulsifiers alter composition and activity of the human gut microbiota in vitro, irrespective of chemical or natural emulsifier origin. Frontiers in Microbiology 11, 577474.

Mirsepasi-Lauridsen, H.C., Vallance, B.A., Krogfelt, K.A. and Petersen, A.M., 2019. Escherichia coli pathobionts associated with inflammatory bowel disease. Clinical Microbiology Reviews 32, e00060-00018.

Naimi, S., Viennois, E., Gewirtz, A.T. and Chassaing, B., 2021a. Direct impact of commonly used dietary emulsifiers on human gut microbiota. Microbiome 9, 1-19.

Naimi, S., Viennois, E., Gewirtz, A.T. and Chassaing, B., 2021b. Direct impact of commonly used dietary emulsifiers on human gut microbiota. Microbiome 9, 1-19.

Neltner, T.G., Kulkarni, N.R., Alger, H.M., Maffini, M.V., Bongard, E.D., Fortin, N.D. and Olson, E.D., 2011. Navigating the US food additive regulatory program. Comprehensive Reviews in Food Science and Food Safety 10, 342-368.

Nerin, C., Aznar, M. and Carrizo, D., 2016. Food contamination during food process. Trends in Food Science & Technology 48, 63-68.

Nguyen, T.L.A., Vieira-Silva, S., Liston, A. and Raes, J., 2015. How informative is the mouse for human gut microbiota research? Disease Models & Mechanisms 8, 1-16.

Nusslein-Volhard, C. and Dahm, R., 2002. Zebrafish. Oxford University Press, New York, USA.

Pan, L., Sze, Y.H., Yang, M., Tang, J., Zhao, S., Yi, I., To, C.-H., Lam, C., Chen, D.F. and Cho, K.-S., 2022. Baicalein—A Potent Pro-Homeostatic Regulator of Microglia in Retinal Ischemic Injury. Frontiers in Immunology 13.

Pan, X., Wu, X., Yan, D., Peng, C., Rao, C. and Yan, H., 2018. Acrylamide-induced oxidative stress and inflammatory response are alleviated by N-acetylcysteine in PC12 cells: involvement of the crosstalk between Nrf2 and NF-κB pathways regulated by MAPKs. Toxicology Letters 288, 55-64.

Pappas, B., Yang, Y., Wang, Y., Kim, K., Chung, H.J., Cheung, M., Ngo, K., Shinn, A. and Chan, W.K., 2018. p23 protects the human aryl hydrocarbon receptor from degradation via a heat shock protein 90-independent mechanism. Biochemical Pharmacology 152, 34-44.

Park, J.C. and Im, S.-H., 2020. Of men in mice: the development and application of a humanized gnotobiotic mouse model for microbiome therapeutics. Experimental & Molecular Medicine 52, 1383-1396.

Partridge, D., Lloyd, K., Rhodes, J., Walker, A., Johnstone, A. and Campbell, B., 2019. Food additives: Assessing the impact of exposure to permitted emulsifiers on bowel and metabolic health–introducing the FADiets study. Nutrition Bulletin 44, 329-349.

Patil, D.P., Dhotre, D.P., Chavan, S.G., Sultan, A., Jain, D.S., Lanjekar, V.B., Gangawani, J., Shah, P.S., Todkar, J.S. and Shah, S., 2012. Molecular analysis of gut microbiota in obesity among Indian individuals. Journal of Biosciences 37, 647-657.

Penkert, R.R., Cortez, V., Karlsson, E.A., Livingston, B., Surman, S.L., Li, Y., Catharine Ross, A., Schultz‐Cherry, S. and Hurwitz, J.L., 2020. Vitamin A Corrects Tissue Deficits in Diet‐Induced Obese Mice and Reduces Influenza Infection After Vaccination and Challenge. Obesity 28, 1631-1636.

Perreault, N. and Beaulieu, J.-F., 1996. Use of the dissociating enzyme thermolysin to generate viable human normal intestinal epithelial cell cultures. Experimental Cell Research 224, 354-364.

Pham, V. and Mohajeri, M., 2018. The application of in vitro human intestinal models on the screening and development of pre-and probiotics. Beneficial Microbes 9, 725-742.

Punzalan, C. and Qamar, A., 2017. Probiotics for the treatment of liver disease, The Microbiota in Gastrointestinal Pathophysiology. Elsevier, pp. 373-381.

Putt, K.K., Pei, R., White, H.M. and Bolling, B.W., 2017. Yogurt inhibits intestinal barrier dysfunction in Caco-2 cells by increasing tight junctions. Food & function 8, 406-414.

Qin, X., Caputo, F.J., Xu, D.-Z. and Deitch, E.A., 2008. Hydrophobicity of mucosal surface and its relationship to gut barrier function. Shock 29, 372-376.

Rajilić–Stojanović, M., Biagi, E., Heilig, H.G., Kajander, K., Kekkonen, R.A., Tims, S. and de Vos, W.M., 2011. Global and deep molecular analysis of microbiota signatures in fecal samples from patients with irritable bowel syndrome. Gastroenterology 141, 1792-1801.

Rangan, C. and Barceloux, D.G., 2009. Food additives and sensitivities. Disease-a-Month 55, 292-311.

Rannug, A., 2020. How the AHR became important in intestinal homeostasis—a diurnal FICZ/AHR/CYP1A1 feedback controls both immunity and immunopathology. International Journal of Molecular Sciences 21, 5681.

Ridder, D.A., Wenzel, J., Müller, K., Töllner, K., Tong, X.-K., Assmann, J.C., Stroobants, S., Weber, T., Niturad, C. and Fischer, L., 2015. Brain endothelial TAK1 and NEMO safeguard the neurovascular unit. Journal of Experimental Medicine 212, 1529-1549.

Rizzatti, G., Lopetuso, L., Gibiino, G., Binda, C. and Gasbarrini, A., 2017. Proteobacteria: a common factor in human diseases. BioMed Research International 2017.

Roberts, C.L., Keita, Å.V., Duncan, S.H., O'Kennedy, N., Söderholm, J.D., Rhodes, J.M. and Campbell, B.J., 2010. Translocation of Crohn's disease Escherichia coli across M-cells: contrasting effects of soluble plant fibres and emulsifiers. Gut 59, 1331-1339.

Rogero, M.M. and Calder, P.C., 2018. Obesity, inflammation, toll-like receptor 4 and fatty acids. Nutrients 10, 432.

Roy, M.A., 2021. Investigating the developmental impacts of 3, 3'-dichlorobiphenyl (PCB-11) in zebrafish (Dario rerio). Doctoral Dissertations, 2326.

Rubinstein, A.L., 2006. Zebrafish assays for drug toxicity screening. Expert Opinion on Drug Metabolism & Toxicology 2, 231-240.

Santhanasabapathy, R., Vasudevan, S., Anupriya, K., Pabitha, R. and Sudhandiran, G., 2015. Farnesol quells oxidative stress, reactive gliosis and inflammation during acrylamide-induced neurotoxicity: behavioral and biochemical evidence. Neuroscience 308, 212-227.

Sanz, Y., Santacruz, A. and Gauffin, P., 2010. Gut microbiota in obesity and metabolic disorders. Proceedings of the Nutrition Society 69, 434-441.

Sauer, M., Porro, D., Mattanovich, D. and Branduardi, P., 2008. Microbial production of organic acids: expanding the markets. Trends in biotechnology 26, 100-108.

Scanlan, P.D., Shanahan, F., O'Mahony, C. and Marchesi, J.R., 2006. Culture-independent analyses of temporal variation of the dominant fecal microbiota and targeted bacterial subgroups in Crohn's disease. Journal of Clinical Microbiology 44, 3980-3988.

Schepens, M.A., Schonewille, A.J., Vink, C., van Schothorst, E.M., Kramer, E., Hendriks, T., Brummer, R.-J., Keijer, J., van der Meer, R. and Bovee-Oudenhoven, I.M., 2009. Supplemental calcium attenuates the colitis-related increase in diarrhea, intestinal permeability, and extracellular matrix breakdown in HLA-B27 transgenic rats. The Journal of Nutrition 139, 1525-1533.

Schumann, P., 2011. Peptidoglycan structure, Methods in microbiology. Elsevier, pp. 101-129.

Schwiertz, A., Taras, D., Schäfer, K., Beijer, S., Bos, N.A., Donus, C. and Hardt, P.D., 2010. Microbiota and SCFA in lean and overweight healthy subjects. Obesity 18, 190-195.

Seksik, P., Rigottier-Gois, L., Gramet, G., Sutren, M., Pochart, P., Marteau, P., Jian, R. and Dore, J., 2003. Alterations of the dominant faecal bacterial groups in patients with Crohn's disease of the colon. Gut 52, 237-242.

Settels, E., Bernauer, U., Palavinskas, R., Klaffke, H.S., Gundert-Remy, U. and Appel, K.E., 2008. Human CYP2E1 mediates the formation of glycidamide from acrylamide. Archives of Toxicology 82, 717-727.

Shah, P., Jogani, V., Bagchi, T. and Misra, A., 2006. Role of Caco‐2 cell monolayers in prediction of intestinal drug absorption. Biotechnology Progress 22, 186-198.

Sharon, G., Cruz, N.J., Kang, D.-W., Gandal, M.J., Wang, B., Kim, Y.-M., Zink, E.M., Casey, C.P., Taylor, B.C. and Lane, C.J., 2019. Human gut microbiota from autism spectrum disorder promote behavioral symptoms in mice. Cell 177, 1600-1618. e1617.

Shen, Y., Sun, Y., Wang, X., Xiao, Y., Ma, L., Lyu, W., Zheng, Z., Wang, W. and Li, J., 2022. Liver transcriptome and gut microbiome analysis reveals the effects of high fructose corn syrup in mice. Frontiers in Nutrition 9.

Shi, H., Liu, J. and Gao, H., 2021. Benzo (α) pyrene induces oxidative stress and inflammation in human vascular endothelial cells through AhR and NF-κB pathways. Microvascular Research 137, 104179.

Shi, K., Wang, F., Jiang, H., Liu, H., Wei, M., Wang, Z. and Xie, L., 2014. Gut bacterial translocation may aggravate microinflammation in hemodialysis patients. Digestive Diseases and Sciences 59, 2109-2117.

Shinji, S., Umezawa, K., Nihashi, Y., Nakamura, S., Shimosato, T. and Takaya, T., 2021. Identification of the myogenetic oligodeoxynucleotides (myoDNs) that promote differentiation of skeletal muscle myoblasts by targeting nucleolin. Frontiers in Cell and Developmental Biology 8, 616706.

Shoaie, S., Karlsson, F., Mardinoglu, A., Nookaew, I., Bordel, S. and Nielsen, J., 2013. Understanding the interactions between bacteria in the human gut through metabolic modeling. Scientific Reports 3, 1-10.

Snelson, M., Tan, S.M., Clarke, R.E., De Pasquale, C., Thallas-Bonke, V., Nguyen, T.-V., Penfold, S.A., Harcourt, B.E., Sourris, K.C. and Lindblom, R.S., 2021. Processed foods drive intestinal barrier permeability and microvascular diseases. Science Advances 7, eabe4841.

Song, A.-X., Mao, Y.-H., Siu, K.-C. and Wu, J.-Y., 2018. Bifidogenic effects of Cordyceps sinensis fungal exopolysaccharide and konjac glucomannan after ultrasound and acid degradation. International Journal of Biological Macromolecules 111, 587-594.

Sood, A. and Panchagnula, R., 2001. Peroral route: an opportunity for protein and peptide drug delivery. Chemical Reviews 101, 3275-3304.

Srinivasan, K. and Buys, E.M., 2019. Insights into the role of bacteria in vitamin A biosynthesis: Future research opportunities. Critical reviews in Food Science and Nutrition 59, 3211-3226.

Srutkova, D., Schwarzer, M., Hudcovic, T., Zakostelska, Z., Drab, V., Spanova, A., Rittich, B., Kozakova, H. and Schabussova, I., 2015. Bifidobacterium longum CCM 7952 promotes epithelial barrier function and prevents acute DSS-induced colitis in strictly strain-specific manner. Plos One 10, e0134050.

Stampfli, L. and Nersten, B., 1995. Emulsifiers in bread making. Food Chemistry 52, 353-360.

Surana, N.K. and Kasper, D.L., 2017. Moving beyond microbiome-wide associations to causal microbe identification. Nature 552, 244-247.

Swidsinski, A., Ladhoff, A., Pernthaler, A., Swidsinski, S., Loening–Baucke, V., Ortner, M., Weber, J., Hoffmann, U., Schreiber, S. and Dietel, M., 2002. Mucosal flora in inflammatory bowel disease. Gastroenterology 122, 44-54.

Terry, N. and Margolis, K.G., 2017. Serotonergic mechanisms regulating the GI tract: experimental evidence and therapeutic relevance. Gastrointestinal Pharmacology, 319-342.

Tims, S., Derom, C., Jonkers, D.M., Vlietinck, R., Saris, W.H., Kleerebezem, M., De Vos, W.M. and Zoetendal, E.G., 2013. Microbiota conservation and BMI signatures in adult monozygotic twins. The ISME journal 7, 707-717.

Touitou, E. and Barry, B.W., 2006. Enhancement in drug delivery. CRC Press, Boca Raton, Florida, USA.

Tsai, H.-C., Chang, F.-P., Li, T.-H., Liu, C.-W., Huang, C.-C., Huang, S.-F., Yang, Y.-Y., Lee, K.-C., Hsieh, Y.-C. and Wang, Y.-W., 2019. Elafibranor inhibits chronic kidney disease progression in NASH mice. BioMed Research International 2019.

Turnbaugh, P.J., Ley, R.E., Mahowald, M.A., Magrini, V., Mardis, E.R. and Gordon, J.I., 2006. An obesity-associated gut microbiome with increased capacity for energy harvest. Nature 444, 1027-1031.

Turner, J.R., 2009. Intestinal mucosal barrier function in health and disease. Nature Reviews Immunology 9, 799-809.

Turroni, F., Ribbera, A., Foroni, E., van Sinderen, D. and Ventura, M., 2008. Human gut microbiota and bifidobacteria: from composition to functionality. Antonie Van Leeuwenhoek 94, 35-50.

Ulker, I. and Yildiran, H., 2019. The effects of bariatric surgery on gut microbiota in patients with obesity: a review of the literature. Bioscience of Microbiota, Food and Health 38, 3-9.

US Food and Drug Administration, 2018. CFR-Code of Federal Regulations Title 21. US Food and Drug Administration, MD, USA.

US Food Drug and Administration, 2013. Overview of food ingredients, additives & colors. Retrieved March 21, MD, USA. https://www.fda.gov/food/food-ingredients-packaging/overview-food-ingredients-additives-colors.

Van de Wiele, T., Van den Abbeele, P., Ossieur, W., Possemiers, S. and Marzorati, M., 2015. The Simulator of the Human Intestinal Microbial Ecosystem (SHIME®),

in: K. Verhoeckx, P. Cotter, I. López-Expósito, C. Kleiveland, T. Lea, A. Mackie, T. Requena, D. Swiatecka and H. Wichers (Eds.), The Impact of Food Bioactives on Health: in vitro and ex vivo Models. Springer International Publishing, Cham, pp. 305-317.

Viennois, E. and Chassaing, B., 2018. First victim, later aggressor: How the intestinal microbiota drives the pro-inflammatory effects of dietary emulsifiers? Gut Microbes 9, 289-291.

Viennois, E., Merlin, D., Gewirtz, A.T. and Chassaing, B., 2017. Dietary emulsifier–induced low-grade inflammation promotes colon carcinogenesis. Cancer Research 77, 27-40.

Vineis, P., Robinson, O., Chadeau-Hyam, M., Dehghan, A., Mudway, I. and Dagnino, S., 2020. What is new in the exposome? Environment International 143, 105887.

Vrieze, A., Out, C., Fuentes, S., Jonker, L., Reuling, I., Kootte, R.S., van Nood, E., Holleman, F., Knaapen, M. and Romijn, J.A., 2014. Impact of oral vancomycin on gut microbiota, bile acid metabolism, and insulin sensitivity. Journal of Hepatology 60, 824-831.

Vrieze, A., Van Nood, E., Holleman, F., Salojärvi, J., Kootte, R.S., Bartelsman, J.F., Dallinga–Thie, G.M., Ackermans, M.T., Serlie, M.J. and Oozeer, R., 2012. Transfer of intestinal microbiota from lean donors increases insulin sensitivity in individuals with metabolic syndrome. Gastroenterology 143, 913-916. e917.

Wang, P.-X., Deng, X.-R., Zhang, C.-H. and Yuan, H.-J., 2020. Gut microbiota and metabolic syndrome. Chinese Medical Journal 133, 808-816.

Wang, W., Chen, L., Zhou, R., Wang, X., Song, L., Huang, S., Wang, G. and Xia, B., 2014. Increased proportions of Bifidobacterium and the Lactobacillus group and loss of butyrate-producing bacteria in inflammatory bowel disease. Journal of Clinical Microbiology 52, 398-406.

Wang, W.-D., Wu, J.-C., Hsu, H.-J., Kong, Z.-L. and Hu, C.-H., 2000. Overexpression of a zebrafish ARNT2-like factor represses CYP1A transcription in ZLE cells. Marine Biotechnology 2, 376-386.

Wang, Z., Gerstein, M. and Snyder, M., 2009. RNA-Seq: a revolutionary tool for transcriptomics. Nature Reviews Genetics 10, 57-63.

Wang, Z., Liu, H., Liu, J., Ren, X., Song, G., Xia, X. and Qin, N., 2021. Dietary Acrylamide Intake Alters Gut Microbiota in Mice and Increases Its Susceptibility to Salmonella Typhimurium Infection. Foods 10, 2990.

Wexler, H.M., 2007. Bacteroides: the good, the bad, and the nitty-gritty. Clinical Microbiology Reviews 20, 593-621.

Whitehurst, R.J., 2008. Emulsifiers in food technology. John Wiley & Sons, Oxford, UK.

World Health Organization, 2006. Safety evaluation of certain contaminants in food. World Health Organization, Geneve, Switzerland.

World Health Organization, 2009. Dietary exposure assessment of chemicals in food (Chapter 6). Principles and methods for the risk assessment of chemicals in food. Environmental Health Criteria 240. Geneve, Switzerland.

Wu, S., Stone, S., Nave, K.-A. and Lin, W., 2020. The integrated upr and erad in oligodendrocytes maintain myelin thickness in adults by regulating myelin protein translation. Journal of Neuroscience 40, 8214-8232.

Wu, Y., Wu, T., Wu, J., Zhao, L., Li, Q., Varghese, Z., Moorhead, J.F., Powis, S.H., Chen, Y. and Ruan, X.Z., 2013. Chronic inflammation exacerbates glucose metabolism disorders in C57BL/6J mice fed with high-fat diet. J Endocrinol 219, 195-204.

Xia, L.-Z., Yang, M., He, M., Jiang, M.-Z., Qin, C., Wei, Z.-J. and Gao, H.-T., 2021. Food emulsifier glycerin monostearate aggravates phthalates' testicular toxicity by disrupting tight junctions' barrier function in rats. Food Quality and Safety, Volume 5, fyab002.

Xia, W.J. and Onyuksel, H., 2000. Mechanistic studies on surfactant-induced membrane permeability enhancement. Pharmaceutical Research 17, 612-618.

Xu, Z., Jiang, W., Huang, W., Lin, Y., Chan, F.K. and Ng, S.C., 2022. Gut microbiota in patients with obesity and metabolic disorders—A systematic review. Genes & Nutrition 17, 1-18.

Yaghoubfar, R., Behrouzi, A., Ashrafian, F., Shahryari, A., Moradi, H.R., Choopani, S., Hadifar, S., Vaziri, F., Nojoumi, S.A. and Fateh, A., 2020. Modulation of serotonin signaling/metabolism by Akkermansia muciniphila and its extracellular vesicles through the gut-brain axis in mice. Scientific Reports 10, 22119.

Yamashita, H., 2016. Biological function of acetic acid–improvement in obesity and glucose tolerance by acetic acid in type 2 diabetic rats. Critical Reviews in Food Science and Nutrition 56, S171-S175.

Yang, J., Li, Y., Wen, Z., Liu, W., Meng, L. and Huang, H., 2021. Oscillospira-a candidate for the next-generation probiotics. Gut Microbes 13, 1987783.

Yang, Y., Zhang, L., Jiang, G., Lei, A., Yu, Q., Xie, J. and Chen, Y., 2019. Evaluation of the protective effects of Ganoderma atrum polysaccharide on acrylamide-induced injury in small intestine tissue of rats. Food & Function 10, 5863-5872.

Yousef, M. and El-Demerdash, F., 2006. Acrylamide-induced oxidative stress and biochemical perturbations in rats. Toxicology 219, 133-141.

Yu, C.-C., Lee, Y.-S., Cheon, B.-S. and Lee, S.-h., 2003. Synthesis of glycerol monostearate with high purity. Bulletin of the Korean Chemical Society 24, 1229-1231.

Zafar, H. and Saier Jr, M.H., 2021. Gut Bacteroides species in health and disease. Gut Microbes 13, 1848158.

Zeng, Q., Li, D., He, Y., Li, Y., Yang, Z., Zhao, X., Liu, Y., Wang, Y., Sun, J. and Feng, X., 2019. Discrepant gut microbiota markers for the classification of obesity-related metabolic abnormalities. Scientific Reports 9, 1-10.

Zhang, H., Yao, M., Morrison, R.A. and Chong, S., 2003. Commonly used surfactant, Tween 80, improves absorption of P-glycoprotein substrate, digoxin, in rats. Archives of Pharmacal Research 26, 768-772.

Zhang, Y., Chen, D., Yang, M., Qian, X., Long, C. and Zheng, Z., 2021. Comprehensive analysis of competing endogenous RNA network focusing on long noncoding RNA involved in cirrhotic hepatocellular carcinoma. Analytical Cellular Pathology 2021.

Zhao, M., Wang, P., Li, D., Shang, J., Hu, X. and Chen, F., 2017. Protection against neo-formed contaminants (NFCs)-induced toxicity by phytochemicals. Food and Chemical Toxicology 108, 392-406.

Zhao, M., Zhang, B. and Deng, L., 2022. The mechanism of acrylamide-induced neurotoxicity: current status and future perspectives. Frontiers in Nutrition 9.

Zheng, M., Lu, J., Lin, G., Su, H., Sun, J. and Luan, T., 2019. Dysbiosis of gut microbiota by dietary exposure of three graphene-family materials in zebrafish (Danio rerio). Environmental Pollution 254, 112969.

Zhou, Y. and Zhi, F., 2016. Lower level of bacteroides in the gut microbiota is associated with inflammatory bowel disease: a meta-analysis. BioMed Research International 2016.

Zhou., Y., Chen, Y., and Gu, J., 2018. Fastp: an Ultra-fast All-In-One FASTQ Preprocessor. Bioinformatics 34, i884-i890.

Zhu, Y.-T., Yuan, Y.-Z., Feng, Q.-P., Hu, M.-Y., Li, W.-J., Wu, X., Xiang, S.-Y. and Yu, S.-Q., 2021. Food emulsifier polysorbate 80 promotes the intestinal absorption of mono-2-ethylhexyl phthalate by disturbing intestinal barrier. Toxicology and Applied Pharmacology 414, 115411.

Ziar, H. and Riazi, A., 2022. Polysorbate 80 improves the adhesion and survival of yogurt starters with cholesterol uptake abilities. Saudi Journal of Biological Sciences 29, 103367.